



**MONASH** University

---

**Characterising and Treating  
a Refined Model of Allergic Airways Disease  
that mimics the key features of Human Asthma**

---

**Krupesh Patel**

BSc (Hons)

A thesis submitted for the degree of Doctor of Philosophy

**August 2018**

Department of Pharmacology

Monash University

## Copyright Notice

---

### ***Notice 2***

© Krupesh Patel (2018).

I certify that I have made all reasonable efforts to secure copyright permissions for third-party content included in this thesis and have not knowingly added copyright content to my work without the owner's permission.

## Abstract

---

### Background and Purpose

Asthma is a chronic respiratory airways disease, stemming from airway inflammation (AI) and airway remodelling (AWR), both contributing to airway hyperresponsiveness (AHR). Epithelial damage and related fibrosis have increasingly been identified as key contributors to asthma pathogenesis but are not targeted by currently-available asthma medication. Furthermore, these processes are poorly studied in currently-used animal models of chronic allergic airways disease (AAD). Therefore, this thesis first aimed to incorporate naphthalene (NA)-induced epithelial damage/repair into a well-established ovalbumin (OVA)-induced model of chronic AAD, which presents with AI, AWR, and AHR, to better mimic the pathogenesis of human asthma. It then aimed to use this refined model of chronic AAD to investigate the therapeutic efficacy of various treatment strategies - including an epithelial repair factor (trefoil factor 2; TFF2;  $0.5 \text{ mg}\cdot\text{mL}^{-1}$ ) and an antifibrotic (relaxin; RLX;  $0.8 \text{ mg}\cdot\text{mL}^{-1}$ ) in isolation and in combination; as well as a clinically-used corticosteroid (dexamethasone; DEX;  $0.5 \text{ mg}\cdot\text{mL}^{-1}$ ) in isolation and in combination with TFF2 and RLX (Aim2). Finally, it aimed to evaluate the therapeutic effects of amniotic epithelial stem cell (AEC)-derived exosomes (EXO;  $5 \mu\text{g}$  or  $25 \mu\text{g}$ ) alone and in combination with RLX ( $0.8 \text{ mg}\cdot\text{mL}^{-1}$ ) in comparison to  $1 \times 10^6$  AECs combined with RLX ( $0.8 \text{ mg}\cdot\text{mL}^{-1}$ ) (Aim-3); to determine the optimal therapeutic strategies that could reverse all three central components of disease pathology.

## **Abstract (cont.)**

---

### **Key Findings**

1. Superimposing epithelial damage onto established chronic AAD led to the maintenance of increased AI and AI-induced AWR, as well as exacerbated airway fibrosis and AHR.
2. Reversing aberrant collagen deposition/concentration – rather than other ECM proteins such as fibronectin or measures of AWR – was the key to normalizing chronic OVA+NA-induced deterioration of lung function
3. Reversing epithelial damage-induced AWR and airway fibrosis could normalise chronic AAD-induced AHR independently of AI.
4. Combining the anti-fibrotic effects of RLX with the epithelial-repair properties of TFF2 and anti-inflammatory effects of DEX; or with the tissue-reparative properties of AEC-EXO (25 g) offered optimal protection against chronic AAD-induced AI, AWR, fibrosis and AHR; and greater protection compared to that offered by DEX alone.
5. AEC-derived EXO alone dose-dependently and partially reduced AI, AWR and AHR associated with chronic AAD;
6. The combined effects of RLX and AEC-EXOs offered broader protection against chronic AAD pathogenesis compared to the combined effects of AECs + RLX.

## **Abstract (cont.)**

---

### **Conclusions and Impacts**

This thesis has reinforced the importance of airway epithelial damage as a contributor to airway fibrosis and AHR in the setting of chronic AAD/asthma; which augments the effects of AI on these parameters. It has also shown that therapeutic strategies that can target aberrant collagen concentration (fibrosis) and epithelial damage can effectively normalise chronic AAD-induced AHR without the need to influence AI. Such treatments/strategies may offer new hope for steroid-resistant asthma sufferers or may serve as adjunct therapies to clinically-used corticosteroids. Finally, it showed that combination strategies that could reverse all three central components of asthma (AI, AWR and AHR) including several measures of AWR provided optimal protection against the pathogenesis of chronic AAD/asthma; which may be used to treat mainstream or steroid-resistant asthma.

## Declaration

---

This thesis contains no material which has been accepted for the award of any other degree or diploma at any university or equivalent institution and that, to the best of my knowledge and belief, this thesis contains no material previously published or written by another person, except where due reference is made in the text of the thesis.

Signature:



Print Name: Krupesh Patel

Date: 29/08/2018

## Published Works Declaration

---

I hereby declare that this thesis contains no material which has been accepted for the award of any other degree or diploma at any university or equivalent institution and that, to the best of my knowledge and belief, this thesis contains no material previously published or written by another person, except where due reference is made in the text of the thesis.

This thesis includes **two** original papers published in peer-reviewed journals and **one submitted publication**. The core theme of the thesis is **to develop a refined experimental model of chronic allergic airways disease that better mimics human asthma; and to utilise this refined model to evaluate novel therapeutic strategies for treating the airway remodelling and airway remodelling-induced airway hyperresponsiveness associated with the disease**. The ideas, development and writing up of all the papers in the thesis were the principal responsibility of myself, the student, working within the **MRU0020 CLAYTON ResearchQ3** under the supervision of **A/Prof Chrishan S. Samuel** and **Dr. Simon G. Royce**.

The inclusion of co-authors reflects the fact that the work came from active collaboration between researchers and acknowledges input into team-based research.

## Published Works Declaration (cont.)

In the case of **chapters 3 to 5** my contribution to the work involved the following:

- Contributed to experimental design
- Carried out all experimental work
- Actively involved on preparing the manuscript for all 3 chapters

Thesis Chapter	Publication Title	Status	Nature and % of student contribution	Co-author name(s) Nature and % of Co-author's contribution*	Co-author(s), Monash student Y/N*
3	Characterization of a novel model incorporating airway epithelial damage and related fibrosis to the pathogenesis of asthma	Published	75%. Concept and collecting data and writing first draft	1)Chrishan Samuel, input into manuscript, 10% 2)Simon Royce, performed in vivo experiments and tissue analyses and input into manuscript, 15%	NA
4	Combining an epithelial repair factor and antifibrotic with a corticosteroid offers optimal treatment for allergic airways disease	Published	89%. Concept and collecting data and writing first draft	1)Chrishan Samuel, performed in vivo experiments and tissue analyses and input into manuscript, 5% 2)Simon Royce, performed in vivo experiments and tissue analyses and input into manuscript, 5% 3)Andrew Giraud, contribute TFF2, 1%	NA
5	Combining human amnion epithelial cell-derived exosomes with an anti-fibrotic offers optimal protection against allergic airways disease	Submitted	86%. Concept and collecting data and writing first draft	1)Chrishan Samuel, input into manuscript, 5% 2)Simon Royce, performed in vivo experiments and tissue analyses and input into manuscript, 5% 3)Rebecca Lim, isolated and characterised AECs and EXO and input into manuscript, 2% 4)Dandan Zhu, isolated and characterised AECs and EXO and input into manuscript, 2%	NA

*\*If no co-authors, leave fields blank*

I have not renumbered sections of submitted or published papers in order to generate a consistent presentation within the thesis.

Student signature:



Date: 29/08/2018

The undersigned hereby certify that the above declaration correctly reflects the nature and extent of the student's and co-authors' contributions to this work. In instances where I am not the responsible author I have consulted with the responsible author to agree on the respective contributions of the authors.

Main Supervisor signature:



Date: 29/08/2018

## Acknowledgements

---

While working on this project was an immense amount of fun to begin with, the personal demons that built up throughout the years exploded, making the writing up the most challenging and mentally exhausting experience I have ever had.

First and foremost, I need to thank my brilliant supervisors A/Prof Chrisan Samuel, and Dr Simon Royce. I know it has taken a lot longer to get to this point that expected but thank you both for giving me this incredible opportunity.

**Chrisan:** Thank you for giving me the chance to work with you back in 2012 as my PHA3990 supervisor, and for allowing me to continue working with you as part of my Honours and this PhD degree. You were always extremely generous with your time and were always available to answer any queries I had throughout the year. But most of all, thank you for never giving up on me, and for giving me the strength to continue.

**Simon:** Thank you for all the experiments and lab techniques you taught me over the years. I will always remember and cherish our moments in the lab. No matter how long and tiring the days in the lab were, you would always find a way to lighten things up.

**Mum, Dad, and Atisha:** There are no words to describe the support and love you have shown me throughout the PhD. Thank you for all the slack you cut me, and always being available to give me a lift to and from university, especially when I had crazy early starts or late nights.

**My best friends (Luke, Akarsh, Vince, and Vinay):** Thank you for always caring about me, and always being available when I just needed someone to talk to.

## **Acknowledgements (cont.)**

---

Especially in the last year and a half when things were at its worst I love you guys so much!

**The PhD team (Matt, Chao, John, Keshia, Eunice, Chau, Maggie, Richard, Ray, Emma, Kaki, May, Tommy, Yan, Vivian):** I will never forget each and every one of you. You have all helped me in your own special way, either academically or personally. Thank you for making this journey so fun.

**Stavros:** The idea of going to conferences without either of my supervisors was a nerve-racking idea. But thanks to you, it was made much better. Thanks for your company and always being there and introducing me to new people.

**Panel members:** Dr Brad Broughton, Dr Tracey Gaspari, and Dr Stavros Selemidis, thank you all for your constructive advice has allowed me to become a better PhD candidate.

**Collaborators:** Thank you to Prof Andrew Giraud, Dr Rebecca Lim, and Dr Dandan Zhu for their vital input into the various projects.

Finally, **Stumpy!** I offer you one last salute. Thank you for your service. I will never forget you.

## Table of Contents

---

Copyright notice.....	ii
Abstract.....	iii
Declaration.....	vi
Published work declaration.....	vii
Acknowledge.....	ix
Table of contents.....	xi
List of Tables.....	xx
List of Figures.....	xxi
Abbreviations.....	xxiii
Lists of Publications.....	xxvi
List of Conferences and Presentations.....	xxviii
<b>Chapter 1 – Introduction.....</b>	<b>1</b>
1.0 Introduction.....	2
1.1 Pathophysiology of asthma.....	5
1.1.1 Airway inflammation.....	6
1.1.1.1 Allergen sensitization.....	6
1.1.1.2 Early-phase allergic reaction.....	7
1.1.1.3 Late-phase allergic reaction.....	9
1.1.1.4 Chronic allergic reaction.....	10
1.1.2 Airway Remodelling.....	11
1.1.2.1 Epithelial damage.....	11
1.1.2.2 Goblet cell metaplasia.....	13
1.1.2.3 Subepithelial fibrosis.....	14
1.1.2.4 Airway smooth muscle hypertrophy and hyperplasia.....	18

## Table of Contents (cont.)

---

1.1.2.5 Angiogenesis.....	20
1.1.3 Airway Hyperresponsiveness.....	20
1.2 Current therapies.....	22
1.2.1 $\beta$ 2-adrenergic receptor agonists.....	23
1.2.2 Corticosteroids.....	23
1.2.3 Other therapies.....	25
1.2.4 Disadvantages of current therapies.....	27
1.2.5 Emerging therapies for AWR.....	26
1.2.5.1 Trefoil factor family 2.....	28
1.2.5.2 Relaxin.....	30
1.2.5.3 Histone de-acyetylase inhibitor.....	31
1.2.5.4 Stem cell therapy.....	32
1.2.5.5 Stem cell-derived exosomes.....	34
1.3 Animal models.....	35
1.3.1 Mouse models of chronic AAD.....	35
1.3.1.1 Ovalbumin-induced chronic AAD.....	35
1.3.1.2 House-dust mite-induced chronic AAD.....	39
1.3.2 Mouse models of epithelial damage.....	39
1.3.1.1 Naphthalene-induced epithelial damage.....	41
1.3.1.2 Other models of epithelial damage.....	43
1.4 Aims and hypothesis.....	44
1.4.1 Aim 1.....	45
1.4.2 Aim 2.....	45
1.4.3 Aim 3.....	45
1.5 References.....	46

## Table of Contents (cont.)

---

<b>Chapter 2 – General Methods</b> .....	<b>77</b>
2.0 General Methods.....	78
2.1 Materials.....	78
2.1.1 Serelaxin.....	78
2.1.2 Trefoil factor 2.....	78
2.1.3 Dexamethasone.....	78
2.1.4 Human amniotic stem cells.....	79
2.1.5 Human amniotic stem cell-derived exosomes.....	79
2.2 Animals.....	79
2.3 Animal models.....	80
2.3.1 Ovalbumin-induced mouse model of allergic airways disease.....	80
2.3.2 Naphthalene-induced mouse model of epithelial damage.....	80
2.3.3 Combined mouse models of allergic airways disease that incorporates epithelial damage.....	83
2.4 Treatment strategies.....	83
2.4.1 Intranasal administration.....	83
2.4.1.1 Serelaxin.....	83
2.4.1.2 Trefoil factor 2.....	84
2.4.1.3 Dexamethasone.....	84
2.4.1.4 Human aniotic epithelial cells.....	84
2.4.1.5 Human aniotic epithelial cells-derived exosomes.....	87
2.5 Invasive plethysmography.....	87
2.6 Broncho-alveolar lavage.....	90
2.6.1 Total inflammatory cell count.....	90

## Table of Contents (cont.)

---

2.6.2 Differential inflammatory cell count.....	91
2.6.2.1 Data analysis.....	92
2.7 Tissue collection.....	92
2.8 Protein analysis.....	92
2.8.1 Protein extraction from animal tissue.....	92
2.8.2 Bradford protein assay.....	93
2.8.3 Gelatin zymography.....	94
2.9 Hydroxyproline assay.....	95
2.10 Lung histopathology.....	97
2.10.1 Haematoxylin and eosin.....	97
2.10.2 Masson trichrome.....	98
2.10.3 Alcian blue-periodic acid Schiff.....	98
2.10.4 Immunohistochemistry.....	99
2.11 Morphometry .....	101
2.11.1 Haematoxylin and eosin.....	101
2.11.2 Masson trichrome.....	102
2.11.3 Alcian blue-periodic acid Schiff.....	102
2.11.4 Immunohistochemistry.....	103
2.11.4.1 Annexin V.....	103
2.11.4.2 Thymic stromal lymphopoietin.....	103
2.11.4.3 Fibronectin.....	104
2.11.4.4 Transforming growth factor- $\beta$ .....	104
2.11.4.5 $\alpha$ -Smooth muscle actin.....	105
2.12 Statistical analysis.....	105
2.13 References.....	107

## Table of Contents (cont.)

---

<b>Chapter 3 – Characterization a refined model of allergic airway disease.....</b>	<b>110</b>
3.0 Abstract.....	111
3.1 Introduction.....	111
3.2 Materials and methods.....	112
3.2.1 Animals.....	112
3.2.2 Establishing the combined models of AAD.....	112
3.2.3 Invasive plethysmography.....	112
3.2.4 Bronchoalveolar lavage .....	114
3.2.5 Tissue collection.....	114
3.2.6 Lung histopathology.....	114
3.2.7 Histological evaluation of inflammation.....	114
3.2.8 Immunohistochemistry.....	114
3.2.9 Morphometric analysis.....	114
3.2.10 Hydroxyproline assay.....	114
3.2.11 Statistical analysis.....	116
3.3 Results.....	117
3.3.1 Individual vs combined effects of OVA-induced AAD and NA-induced epithelial damage on AI.....	117
3.3.2 Individual vs combined effects of OVA-induced AAD and NA-induced epithelial damage on remodelling.....	117
3.3.2.1 Epithelial denudation.....	117
3.3.2.2 Epithelial thickening.....	117
3.3.2.3 Goblet cell metaplasia.....	117
3.3.3 Individual vs combined effects of OVA-induced AAD and NA-induced epithelial damage on airway fibrosis.....	117
3.3.3.1 Subepithelial collagen thickening.....	117

## Table of Contents (cont.)

---

3.3.3.2 Total lung collagen concentration.....	118
3.3.4 Individual vs combined effects of OVA-induced AAD and NA-induced epithelial damage on AHR.....	118
3.3.5 Individual vs combined effects of OVA-induced AAD and NA-induced epithelial damage on other parameters of epithelial damage and fibrosis.....	118
3.3.5.1 Epithelial apoptosis.....	118
3.3.5.2 TGF- $\beta$ 1 expression.....	118
3.4 Discussion.....	118
3.5 References.....	123
<b>Chapter 4 – Treating a refined model of allergic airway disease with an epithelial repair factor, an antifibrotic, and a corticosteroid.....</b>	<b>125</b>
4.0 Abstract.....	126
4.1 Introduction.....	127
4.2 Materials and methods.....	128
4.2.1 Animals.....	128
4.2.2 Induction and treatment of chronic AAD incorporating epithelial damage.....	128
4.2.3 Invasive plethysmography.....	128
4.2.4 Bronchoalveolar lavage .....	128
4.2.5 Tissue collection.....	128
4.2.6 Lung histopathology.....	128
4.2.7 Histological evaluation of airway inflammation.....	130
4.2.8 Immunohistochemistry.....	130

## Table of Contents (cont.)

---

4.2.9 Morphometric analysis.....	131
4.2.10 Hydroxyproline assay.....	132
4.2.11 Gelatin zymography.....	133
4.2.12 Statistical analysis.....	133
4.3 Results.....	133
4.3.1 Individual versus combined effects of RLX, TFF2 and DEX on airway inflammation.....	133
4.3.2 Individual versus combined effects of RLX, TFF2 and DEX on airway remodelling.....	133
4.3.2.1 Goblet cell metaplasia.....	133
4.3.2.2 Epithelial damage.....	133
4.3.2.3 Epithelial thickness.....	133
4.3.3 Individual versus combined effects of RLX, TFF2 and DEX on airway fibrosis.....	133
4.3.3.1 Subepithelial ECM thickness.....	133
4.3.3.2 Total lung collagen concentration.....	134
4.3.3.3 Subepithelial fibronectin expression.....	134
4.3.3.4 TGF- $\beta$ 1 expression.....	134
4.3.3.5 Myofibroblast differentiation.....	134
4.3.3.6 Gelatinase expression and activity.....	135
4.3.4 Individual versus combined effects of RLX, TFF2 and DEX on dynamic airway compliance.....	136
4.4 Discussion and conclusion.....	136
4.5 References.....	138

## Table of Contents (cont.)

---

<b>Chapter 5 – Treating a refined model of allergic airways disease with an antifibrotic, and human amnion epithelial cell-derived exosomes.....</b>	<b>140</b>
5.0 Abstract.....	141
5.1 Introduction.....	142
5.2 Methods.....	146
5.2.1 Animals.....	146
5.2.2 Establishing the refined models of AAD.....	146
5.2.3 Invasive plethysmography.....	147
5.2.4 Tissue collection.....	149
5.2.5 Lung histopathology.....	149
5.2.6 Histological evaluation of airway inflammation.....	150
5.2.7 Immunohistochemistry.....	150
5.2.8 Morphometric analysis.....	151
5.2.9 Hydroxyproline assay.....	152
5.2.10 Statistical analysis.....	152
5.3 Results.....	153
5.3.1 Individual versus combined effects of EXO and RLX on airway inflammation.....	153
5.3.2 Individual versus combined effects of EXO and RLX on airway remodelling.....	156
5.3.2.1 Goblet cell metaplasia.....	156
5.3.2.2 Epithelial damage.....	159
5.3.2.3 Epithelial thickness.....	162
5.3.3 Individual versus combined effects of EXO and RLX on airway fibrosis.....	162
5.3.3.1 Subepithelial ECM thickness.....	162

## **Table of Contents (cont.)**

---

5.3.3.2 Total lung collagen concentration.....	165
5.3.3.3 TGF- $\beta$ 1 expression.....	167
5.3.3.4 Myofibroblast differentiation.....	170
5.3.4 Individual versus combined effects of EXO and RLX on airway resistance.....	173
5.4 Discussion and conclusion.....	175
5.5 References.....	184
<b>Chapter 6 – Discussion and conclusion.....</b>	<b>188</b>
6.0 Discussion and conclusion.....	189
6.1 Main findings.....	189
6.2 Limitations.....	196
6.5 Conclusion.....	199
6.6 References.....	200
<b>Appendix 1.....</b>	<b>203</b>
<b>Appendix 2.....</b>	<b>214</b>
<b>Appendix 3.....</b>	<b>226</b>

## List of Tables

---

Table 1-1: Matrix metalloproteinases family.....	16
Table 1-2: Summary of the features of human asthma that have been successfully replicated into animal models of asthma.....	42
Table 2-1: List of various antibodies used for immunohistochemical staining.....	100
Table 4-i: List of key target and ligands.....	127
Table 4-1: Summary of the individual versus combined effects of RLX, TFF2, and DEX in the OVA + NA model.....	135
Table 5-1: Table 5-1. Summary of the individual vs combined effects of EXO ± RLX vs. AECs + RLX in the OVA+NA model.....	177
Table 6-1: Summary of the various individual and combined therapies investigated.....	195

## List of Figures

---

Figure 1-1: Schematic illustration of the chronic inflammatory cycle involved in airway inflammation present in asthma.....	8
Figure 1-2: Pathogenesis of asthma.....	21
Figure 1-3: Mouse model of chronic allergic airways disease.....	37
Figure 1-4: Mouse model of epithelial damage.....	40
Figure 2-1: Schematic illustration of experimental models and treatments for Aim 1.....	81
Figure 2-2: Schematic illustration of experimental models and treatments for Aim 2.....	85
Figure 2-3: Schematic illustration of experimental models and treatments for Aim 3.....	88
Figure 3-1: Schematic illustration of how the AAD and epithelial damage models were combined.....	113
Figure 3-2: Determination of airway inflammation score from H&E-stained airways and BAL differential cell count.....	115
Figure 3-3: Determination of airway epithelial denudation, epithelial thickening and subepithelial collagen thickness from Masson trichrome-stained sections.....	116
Figure 3-4: Determination of goblet cell number from Alcian blue periodic acid Schiff-stained sections.....	119
Figure 3-5: Determination of airway resistance from dose-response to methacholine.....	120
Figure 3-6: Determination of epithelial apoptosis and TGF- $\beta$ 1 expression in immunohistochemically-stained sections.....	121
Figure 3-7: The proposed sequence of events that occur in the OVA – NA model.....	122
Figure 4-1: Individual versus combined effects of RLX, TFF2, and DEX on peribronchial inflammation and goblet cell metaplasia.....	129

## List of Figures (cont.)

---

Figure 4-2: Individual versus combined effects of RLX, TFF2, and DEX on TSLP-associated epithelial damage and the extent of airway epithelial thickness.....	130
Figure 4-3: Individual versus combined effects of RLX, TFF2, and DEX on subepithelial ECM thickness, lung collagen concentration and subepithelial fibronectin deposition.....	131
Figure 4-4: Individual versus combined effects of RLX, TFF2, and DEX on epithelial TGF- $\beta$ 1 expression and subepithelial myofibroblast accumulation.....	132
Figure 4-5: Individual versus combined effects of RLX, TFF2, and DEX on lung MMP-9 and MMP-2 expression and activity.....	134
Figure 4-6: Individual versus combined effects of RLX, TFF2, and DEX on cDyn.....	135
Figure 5-1: Schematic illustration of experimental model models and treatments.....	148
Figure 5-2: Individual vs. combined effects of EXO + RLX vs. AECs + RLX on peribronchial inflammation.....	154
Figure 5-3: Individual vs. combined effects of EXO + RLX vs. AECs + RLX on goblet cell metaplasia.....	157
Figure 5-4: Individual vs. combined effects of EXO + RLX vs. AECs + RLX on TSLP-associated epithelial damage.....	160
Figure 5-5: Individual vs. combined effects of EXO + RLX vs. AECs + RLX on the extent of airway epithelial and subepithelial thickness.....	163
Figure 5-6: Individual vs. combined effects of EXO + RLX vs. AECs + RLX on lung collagen concentration, as a measure of fibrosis.....	166
Figure 5-7: Individual vs. combined effects of EXO + RLX vs. AECs + RLX on epithelial TGF- $\beta$ 1 expression.....	168
Figure 5-8: Individual vs. combined effects of EXO + RLX vs. AECs + RLX on subepithelial myofibroblast accumulation.....	171
Figure 5-9: Individual vs. combined effects of EXO + RLX vs. AECs + RLX on airway resistance (AHR) .....	174

## Abbreviations

$\alpha$ -SMA	alpha-smooth muscle actin
AAD	allergic airways disease
AB-PAS	alcian blue-periodic acid Schiff
AEC	amniotic epithelial stem cells
AHR	airway hyperresponsiveness
AI	airway inflammation
AJCs	adherens junction cells
AngII	angiotensin II
ANOVA	analysis of variance
ATP	adenosine triphosphate
AWR	airway remodelling
BAL	bronchoalveolar lavage
BALF	bronchoalveolar lavage fluid
BMSC	bone marrow-derived stem cells
BSA	bovine serum albumin
BW	body weight
CaCl <sub>2</sub>	calcium chloride
cAMP	cyclic adenosine monophosphate
CC10	Clara cell 10 protein
CD23	cluster of differentiation 23
CD40	cluster of differentiation 40
CDH1	e-cadherin gene
CHI3L1	chitinase-3-like protein 1
Cl <sub>2</sub>	chlorine gas
CO	corn oil
CXCR4	chemokine receptor type 4
DAB	Dimethylaminoazobenzene
DEX	Dexamethasone
DMSO	dimethyl sulfoxide
DNA	deoxyribonucleic acid
DPX	distyrene, plasticizer (tricresyl phosphate), and xylene
ECM	extracellular matrix
EXO	Exosomes
FCS	fetal calf serum
Fc $\epsilon$ RI	high-affinity IgE receptor type 1
Fc $\epsilon$ RII	high-affinity IgE receptor type 2
FCS	fetal calf serum
gob-5	mouse calcium ion-activated chlorine ion channels
h	Hour
hAEC	human amniotic stem cells
HCl	hydrochloric acid
hCLCA1	human calcium ion-activated chlorine ion channels

HCIO	hypochlorous acid
HDAC	histone de-acetylase
HDACi	histone de-acetylase Inhibitor
HDM	house dust mite
H&E	haematoxylin and eosin
IgE	immunoglobulin E
IL-4	interleukin 4
IL-5	interleukin 5
IL-8	interleukin 8
IL-9	interleukin 9
IL-10	interleukin 10
IL-13	interleukin 13
IL-33	interleukin 33
i.n.	Intranasal
i.p.	intraperitoneal
kDa	kilodalton
Kg	kilogram
LTB4	leukotrienes B4
LTC4	cystine leukotriene 4
MCh	methylcholine
mM	millimolar
MMP-2	matrix metalloproteinases 2, gelatinase A
MMP-9	matrix metalloproteinases 9, gelatinase B
mg	milligram
mg·mL <sup>-1</sup>	milligram per millilitre
mg/kg	milligram per kilogram
mRNA	messenger ribonucleic acid
miRNA	micro ribonucleic acid
MUC5A2	mucin glycoprotein 5A2
NA	naphthalene
NKCC1	sodium potassium chloride co-transporter channels
nm	nanometre
OVA	ovalbumin
PAF	platelet-activating factor
PBS	phosphate buffer saline
PDE	phosphodiesterases
PDGF	platelet-derived growth factor
PGD2	prostaglandin D2
PKA	protein kinase A
RLN2	relaxin gene 2
RLN3	relaxin gene 3
RLX	relaxin/serelaxin
rpm	revolutions per minute
RXFP1	relaxin family peptide 1
SABA	short acting $\beta$ 2-adrenoreceptor

SAL	Saline
SDS	sodium dodecyl sulphate
SEM	standard error of mean
Smad2	Smad family member 2
TFF2	trefoil factor family 2
TGF- $\beta$	transforming growth factor beta
T <sub>H</sub> 2	T-helper type 2 cell
TIMP	tissue inhibitors of metalloproteinases
TNF- $\alpha$	tumour-necrosis factor- $\alpha$
TSLP	thymic stromal lymphopietin
$\mu\text{g/g}$	microgram per gram
$\mu\text{m}$	Micrometre
v/v	volume to volume
VEGFA	vascular endothelial growth factor A
w/v	weight to volume

## List of Publications

---

### 2014

Royce, S.G.\*, Patel K.P.\*, Samuel, C.S. (2014) Characterization of a novel model incorporating airway epithelial damage and related fibrosis to the pathogenesis of asthma. *Laboratory Investigations* **94**(12):1326-39 (*Refer to Chapter 3*)

#### **\*co-first authors**

Royce, S.G., Lim, C.X, Patel, K.P., Wang, B., Samuel, C.S., Tang, M.L. (2014) Intranasally administered serelaxin abrogates airway remodelling and attenuates airway hyperresponsiveness in allergic airways disease. *Clinical Experimental and Allergy* **44**(11):1399-408. (*Refer to Appendix 1*)

### 2015

Royce, S.G., Shen, M., Patel, K.P., Huuskes, B.M., Ricardo, S.D., Samuel, C.S. (2015) Mesenchymal stem cells and serelaxin synergistically abrogate established airway fibrosis in an experimental model of chronic allergic airways disease. *Stem Cell Research* **15**(3):495-505. (*Refer to Appendix 2*)

### 2016

Patel K.P., Giraud, A.S., Samuel, C.S., Royce, S.G. (2016) Combining an epithelial repair factor and anti-fibrotic with a corticosteroid offers optimal treatment for allergic airways disease. *British Journal of Pharmacology* **173**(12):2016-2029.

(*Refer to Chapter 4*)

## List of Publications (cont.)

---

Royce, S.G., Tominaga A.M., Shen, M., **Patel, K.P.**, Huuskes, B.M., Lim R., Ricardo, S.D., Samuel, C.S. (2016) Serelaxin improves the therapeutic efficacy of RFXP1-expressing human amnion epithelial cells in experimental allergic airway disease. *Clinical science (London)* 130(23):2151-2165. (*Refer to Appendix 3*)

## **2018**

Royce S.G.\*, **Patel K.P.\***, Mao W.Y.\*, Zhu D., Lim R. and Samuel C.S. (2017) Serelaxin enhances the therapeutic effects of human amnion epithelial cell-derived exosomes in experimental models of lung disease. *Manuscript Submitted. (Adapted in Chapter 5)*

**\*co-first authors**

## List of Conferences and Presentations

---

### 2014

**Patel, K.P.**, Samuel, C.S., Royce, S.G. Characterisation of a novel model of the contribution of airway epithelial damage and fibrosis to the pathogenesis of asthma. 2nd Airway, Inflammation and Remodelling Meeting 2014 **April 10<sup>th</sup> – 11<sup>th</sup>, Melbourne, Australia (Poster Presentation)**

### 2015

**Patel, K.P.**, Samuel, C.S., Royce, S.G. Incorporating airway epithelial damage onto established chronic allergic airways disease exacerbates airway fibrosis and related airway hyperresponsiveness. TSANZSRS 2015 Annual Science Meeting. March 27<sup>th</sup> – April 1<sup>st</sup>, Gold Coast, Australia **(Poster Presentation)**

### 2016

**Patel, K.P.**, Samuel, C.S., Royce, S.G. Combining an epithelial repair factor and anti-fibrotic with a corticosteroid offers optimal treatment for the pathogenesis of allergic disease incorporating epithelial damage. TSANZSRS 2016 Annual Science Meeting. April 1<sup>st</sup> – 6<sup>th</sup>, Perth, Australia **(Oral Presentation)**

**Patel, K.P.**, Samuel, C.S., Royce, S.G. Combining an epithelial repair factor and anti-fibrotic with a corticosteroid offers optimal treatment for allergic airways disease. European Respiratory Society International Congress 2016. September 3<sup>rd</sup> – 7<sup>th</sup>, London, United Kingdom **(Poster Discussion Presentation)**

## List of Conferences and Presentations (cont.)

---

**Patel, K.P.**, Samuel, C.S., Royce, S.G. Pharmacological targeting of epithelial repair and fibrosis associated with chronic allergic disease. AWTRS & MEPSA 2016. November 7<sup>th</sup> – 9<sup>th</sup>, Melbourne, Australia (***Oral and Poster Presentation***)

---

**CHAPTER 1:**  
**INTRODUCTION**

---

## 1.0 INTRODUCTION

Airways are important in facilitating the movement of air from outside the body to the lungs and to facilitate the diffusion of oxygen into the blood stream. However, when exposed to environmental stimuli such as allergens, pollutants and occupational drugs or chemicals; or non-allergic stimuli such as cold air or excessive exercise, these triggers can induce inflammatory responses and mediators into the airways. Eventually, these inflammatory mediators can trigger several remodelling processes which lead to tightening of the muscles around the airways, obstruction and narrowing of the airways and ultimately the difficulty in breathing associated with asthma. The word asthma comes from the Greek word *ἀσθμα*, meaning short breath, gasp for breath. There are two key clinical features that are present to various degrees in patients that suffer from asthma. Firstly, there is excessive variation in the lung function of a patient suffering from asthma, compared to an unaffected person. Secondly, there are various respiratory symptoms such as, chest tightness, coughing, shortness of breath, and wheezing. These can vary over time and may be present or absent at any point of the pathogenesis of asthma (Melbye *et al.*, 1994; Anderson, 2008; Bateman *et al.*, 2017).

Around the world approximately 325 million people are affected by this respiratory disease. By 2025, it is believed that a further ~100 million people will be suffering from this debilitating disease (Masoli *et al.*, 2004; Australian Centre for Asthma Monitoring, 2011). Asthma also contributes to one in every 250 deaths worldwide. These deaths are mostly preventable, if not for the

suboptimal treatment options that are currently available. Prevalence rates can differ greatly between countries, from 0.7% in Macau to 18.4 % in Scotland (Burney, 1996; Asher *et al.*, 1998; Beasley, 1998; Masoli *et al.*, 2004). Asthma is the most prevalent chronic disease affecting children and is also highly prevalent in older adults.

Clinical studies have shown that pre-pubescent males are more at risk at developing asthma (Dodge & Borrow, 1980), while both genders are equally at risk during puberty (de Marco *et al.*, 2000). Only after puberty, are females more susceptible than males to develop asthma (de Marco *et al.*, 2000).

In Australia, the prevalence of asthma in adults is greater than 1/10, higher than most countries in the world (AIHW, 2011). Australia also has the highest death rate associated with asthma (Australian Centre for Asthma Monitoring, 2011) and the number of Australian women that die from asthma is double that of Australian men (Australian Centre for Asthma Monitoring, 2011). Additionally, there is a higher prevalence of asthma in the indigenous population within Australia (Australian Centre for Asthma Monitoring, 2011). With such a high number of sufferers, it also causes an immense financial impact, costing Australia approximately \$28 billion in 2015 – which is about \$11,740 per asthma sufferer (Asthma Australia, 2015).

The causes that lead to the development of asthma can be divided into two groups. Firstly there are environmental factors that include allergens, pathogens, micro-organisms, tobacco smoke and/or air pollution (Holgate,

2008) (Figure 1- 1). Secondly, there are many genetic factors that can lead to the development of asthma (Holgate, 2008) (Figure 1-1). Being a heterogeneous disorder (Zhang Y, et al., 2012), there are multiple genes that (when mis-regulated) can affect different cellular processes leading to the development of asthma (Zhang Y, et al., 2012); such as the CHI3L1 gene which may lead to airway remodelling, while the dysregulation of the IL33 gene has been observed in childhood asthma (Zhang Y, et al., 2012). Processes that can be disrupted include many aspects of airway inflammation and airway remodelling (see further details below) (Zhang Y, et al., 2012).

Around the world, different countries have different definitions and grading for asthma severity. In Australia, asthma severities are divided into three categories: mild, moderate, and severe (Chung et al., 2014). Mild asthma is characterised as patients that exhibit occasional respiratory symptoms and require the use of a therapeutic controller no more than twice a week. Moderate asthma is characterised as patients that exhibit respiratory symptoms and require the use of a therapeutic controller on most days. Moderate asthma patients also exhibit symptoms during the night time and while walking (less than once a week). Severe asthma is characterised as patients that exhibit occasional respiratory symptoms daily and require the use of a therapeutic controller three or four times a day. Severe asthma patients also exhibit symptoms during the night time and while walking (more than once a week), as well as requiring usually hospital and emergency admissions, and often have a history of life-threatening asthma attacks (National Asthma Campaign (Australia), 1998; Colice, 2004).

There are multiple risk factors that can not only increase a person's chance of developing asthma, but they can also affect the phenotype of asthma. Tobacco smoking or air pollution is linked with severe asthma (Chaudhuri *et al.*, 2006; Comhair *et al.*, 2011). Obesity can affect the development of severe asthma in various ways depending on age of onset and degree of allergic inflammatory (Dixon *et al.*, 2011; Holguin *et al.*, 2011). The combination of tobacco smoke and obesity has even been linked to corticosteroid insensitivity (Peter-Golden *et al.*, 2006; Lazarus *et al.*, 2007). In the workplace, exposure to various harmful chemicals and toxins can bring about late onset, severe asthma (Plana *et al.*, 2010). Several co-morbidities including gastro-oesophageal reflux disease, obstructive sleep apnoea, recurrent respiratory infections, and severe sinus disease seem to result in more frequent exacerbations in adults with severe asthma (Sterk *et al.*, 2005).

### 1.1 PATHOPHYSIOLOGY OF ASTHMA

There are three central components involved in the pathogenesis of asthma: airway inflammation (AI), airway remodelling (AWR) and airway hyperresponsiveness (AHR; the clinical end-point of asthma) (Royce *et al.*, 2012; Tang *et al.*, 2009; **Figure 1-2**).

### 1.1.1 Airway Inflammation (AI)

#### 1.1.1.1 Allergen Sensitization

Airway inflammation (AI) begins with the sensitization of the airways to specific allergens that have been inhaled. These allergens either bind to immature dendritic cells that are present on the epithelium, or travel past damaged epithelial cells into the airway wall where they then bind to submucosal dendritic cells. Uptake and processing of the allergen by the dendritic cells initiate maturation and migration of these cells. Maturation of dendritic cells involve several processes; the main one being the production of major histocompatibility complex (MHC) class II molecule, which are present on the cell surface, and a peptide derived from the allergen. The dendritic cells also migrate from the submucosa into the regional lymph node. Following migration, mature dendritic cells present allergen-derived peptides to naïve T-cells, stimulating their differentiating into a T-helper type 2 ( $T_H2$ ) cell phenotype (Figure 1-1). This process is facilitated by the early release of interleukin (IL)-4, which are produced by basophils, eosinophils, mast cells, natural killer T cells and/or T cells (Marshall, 2004; Sokol et al., 2014) (Figure 1-1). These newly differentiated  $T_H2$  cells release IL-4 and IL-13, which facilitate the binding of B-cells to CD28- and CD40-binding ligands present on the  $T_H2$  cell surface, stimulating the production of specific immunoglobulin (Ig)-E to the allergen. The IgE diffuse out of these B-cells, into the lymphatic vessel, where they enter the blood circulation for systemic distribution. Finally, the IgE enter the interstitial fluid binding to high-affinity IgE receptors (FcεRI) present on the surface of mast

cells, priming the mast cell to respond to later re-exposure of the airway to the allergen.

#### 1.1.1.2 Early-Phase Allergic Reaction

Within minutes after allergen re-exposure, mast-cell-derived cytokines are released in the site of injury. This process is initiated when the allergen binds to two or more allergen-specific IgE present on the mast-cell surface, leading to mast-cell activation. Activated mast-cells undergo several complex responses mediated by FcεRI, leading to the release of three classes of biologically active substances (Kraft, 2007; Marshall, 2004; Rivera & Gilfillan, 2006): (i) cytoplasmic granules, (ii) lipid-derived mediators, and (iii) gene-transcription-mediated factors.

Cytoplasmic granules refer to a variety of factors including: biological amines (such as histamine) (Galli et al., 2005; Rivera & Gilfillan, 2006); serglycin proteoglycans (such as heparin and chondroitin sulphate); serine proteases (such as tryptase, chymases, carboxypeptidases) (Caughey, 2011) and some cytokines (tumour-necrosis factor (TNF)-α) and growth factors (vascular endothelial growth factor A (VEGFA)) (Bradding & Holgate, 1996; Galli et al., 2005; Rivera & Gilfillan, 2006; Saito et al., 2001). Lipid-derived mediators are synthesised from metabolised arachidonic acid via cyclooxygenase and lipoxygenase pathways leading to the release of prostaglandin D2 (PGD2), leukotrienes B4 (LTB4) and cysteine leukotriene 4 (LTC4) and in some cases platelet-activating factor (PAF) (Finkelman & Vercelli, 2007; Boyce, 2008). Cytoplasmic granules and lipid-derived mediators are important drivers of early-

**Figure 1-1**

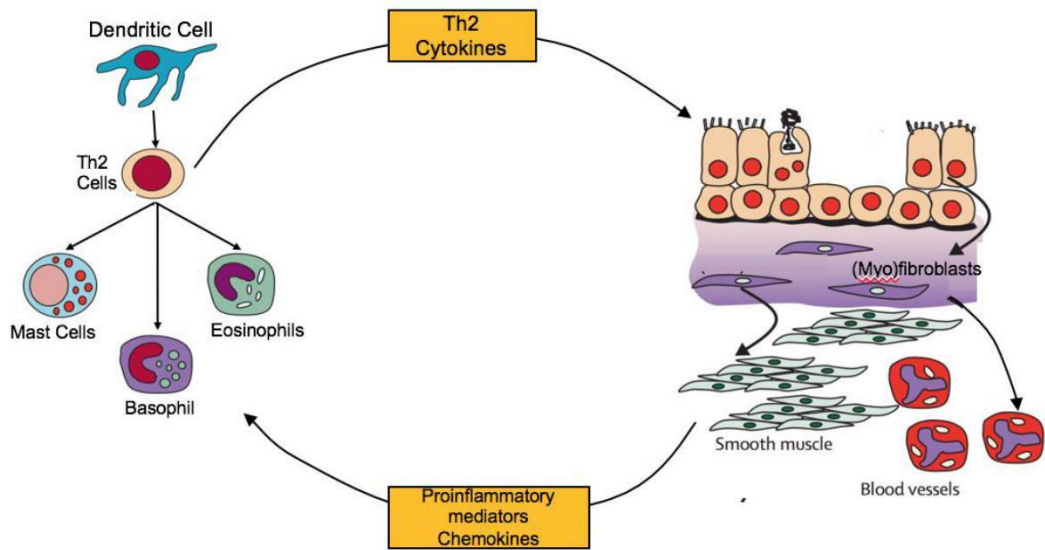


**Figure 1-1: Schematic illustration of the chronic inflammatory cycle involved in airway inflammation present in asthma.**

Dendritic cells present allergens to  $T_H2$  cells and cause the activation of effector cells. The cytokines produced during this process damage the epithelium and then stimulate the production of various growth factors. As a result of this process, characteristic remodelling process occur with the production of proinflammatory mediators and chemokines. As such, a cycle is established, wherein wound injury (through the release of toxic cytokines from inflammatory cells) occurs concurrently with wound healing (remodelling processes). Figure adapted from Holgate ST, 2008.

phase allergic reactions, and result in symptoms such as coughing due to contraction of bronchial smooth muscle leading to exacerbated airway flow obstruction in lower airways (Lalloo et al., 1996); itching due to reddening of skin caused by vasodilation and sneezing and tear formation as a result of increased vascular permeability leading to tissue swelling (Sarin S et al., 2006).

The production of inflammatory factors such as cytokines, chemokines, and growth factors are up-regulated at a transcriptional level during early-phase allergic reactions but play an important role in late-phase allergic reactions.

#### 1.1.1.3 Late-Phase Allergic Reaction

Late-phase allergic reactions develop 2-6 hours after allergen re-exposures and often peak after 6-9 hours. While not all sensitised patients develop late-phase allergic reactions, other patients exhibit no clinical discrimination between the end of early-phase and the start of late-phase allergic reactions. This allergic reaction phase involves the slow release of cytokines, chemokines and growth factors synthesised from activated mast-cells (Galli et al., 2005; Kraft, 2007; Rivera & Gilfillan, 2006). These mast-cell products have the potential to directly or indirectly recruit other immune cells (TNF- $\alpha$ , LTB<sub>4</sub>, IL-8), activate innate immune cells (TNF- $\alpha$  and IL-5) and affect dendritic, T- and B-cell biology (IL-10, TNF- $\alpha$ , transforming growth factor (TGF)- $\beta$ 1 and histamine) (Galli et al., 2005; Galli et al., 2008); while some products released by mast cells can also have anti-inflammatory or immunosuppressant actions (IL-10, TGF- ) (Galli et al., 2008; Sayed et al., 2008). Activated mast-cell derived products, the main one being thymic stromal lymphopoietin (TSLP), can also affects epithelial,

fibroblasts, smooth muscle, nerve and vascular endothelial cells (Schleimer et al., 2007).

Lastly, it is believed that some of the features observed in late-phase allergic reactions are considered to be long-term consequences of activated mast cell and antigen-stimulated T-cell products (Galli et al., 2005).

#### 1.1.1.4 Chronic Airway Inflammation

Inflammation becomes chronic when it persists due to repetitive and continuous allergen exposure. Chronic AI is associated with changes to structural cells, and in most cases, substantially altered lung function. While early- or late-phase allergic reactions can be clinically-studied in volunteers, chronic inflammation requires the use of human biopsy samples, or experimental animal models of allergic lung disorders. As such, it is not known how early- and late-phase inflammation progresses into chronic inflammation. Studies have shown that inflammation associated the viral infections (the main one being rhinovirus) can exacerbate symptoms associated with asthma (Gern & Busse, 2002), while inflammation associated with atopic dermatitis (Leung et al., 2004) and/or allergic rhinitis (Pawankar, 2004) can exacerbate altered airway epithelial function.

Chronic AI can induce structural changes that can affect all the layers of the airways. In the airway epithelium, chronic inflammation can give rise to an increase the presence of mucus-secreting cells (goblet cells), increase cytokine and chemokine production in epithelial cells as well as exacerbate epithelial injury (Doherty & Broide, 2007; Holgate, 2007; Mauad et al., 2007; Schleimer et

al., 2007). In the submucosal region, chronic inflammation can increase myofibroblast activation resulting in an increase in extracellular matrix protein (ECM) deposition beneath epithelial basement membrane (lamina reticularis) (Doherty & Broide, 2007; Holgate, 2007; Mauad et al., 2007). Chronic AI can also induce smooth muscle hypertrophy and hyperplasia as well as increase in pulmonary vasculature (neovascularisation) (Mauad et al., 2007).

### **1.1.2 Airway Remodelling (AWR)**

Genetic factors (via AI-independent and to a lesser degree, AI-dependent mechanisms) (Baron et al., 2011; Holgate, 2008) also lead to the development of AWR. AWR refers to the structural changes that occur in and around the trachea, bronchi and bronchioles and include processes such as epithelial damage/thickening, goblet cell metaplasia, subepithelial collagen deposition (fibrosis), smooth muscle hypertrophy, and angiogenesis, as further detailed below (Holgate, 2008; Royce et al., 2012; **Figure 1-2**).

#### **1.1.2.1 Epithelial Damage**

Epithelial damage is a process which has been **increasingly studied** as a key cause of AWR (Carroll et al., 1993), and which has been shown to correlate with the development of AHR (Bergeron et al., 2010; Boulet et al., 1997).

The airway epithelium is an important physical barrier that is responsible for protecting the internal environment of the lungs from pathogenic organisms and harmful substances that may be inhaled into the lungs from the external

environment (Holgate, 2000). The cells in the epithelial layer are able to form a physical barrier comprised of proteins that allow adjacent cells (regardless whether they are the same type of cell or not) to stick together, called apical junctional complexes (AJC) (Hammad & Lambrecht 2015). There are two types of AJCs: (i) tight junctions – these are intercellular junctions that appear near the top of adjacent cells, and (ii) adherens junctions – these junctions form a tight bond between adjacent cell to allow a passage of ions and water-soluble substances to pass through the epithelial layer (Tamura & Tsukita 2014).

One means of protection involves the use of mucociliary cells that are able to physically expel pathogens that have been trapped in the mucosal layer which coats the external surface of the epithelium (further explained in section 1.1.2.2). The epithelium can also release a number of cytokines and chemokines that result in the recruitment of inflammatory cells, which aid in the clearance in pathogens that have infiltrated the airway (Kim & Leung 2012; Parker et al., 2014; Lappalainen et al., 2005) However, the excessive activation of an epithelial-induced inflammatory response may result in development of chronic AI (refer to section 1.1.1.4). Recently, it has been established that the dysfunction of AJCs can lead to the destabilization of the airway epithelial layer, resulting in the infiltration of inhaled allergens into the submucosa, which has been associated with the pathogenesis of asthma (Georas & Rezaee, 2014; Loxham et al., 2014).

Inherent genetic mutations (Zhang Y, et al., 2012) or disruptions (in some cases of corticosteroid use) can lead to the susceptibility of epithelial damage. E-cadherin, a cell-adhesion molecule located between epithelial cells

(Ierodiakonou et al., 2011), is important for keeping the cells of the bronchial epithelium together (Ierodiakonou et al., 2011). When there is a single-nucleotide polymorphisms to the CDH1 gene, it leads to a reduction in e-cadherin levels resulting in reduced adhesion between the epithelial cells (Ierodiakonou et al., 2011). This is followed by denudation (shedding of epithelial lining) of the epithelium which leads to re-epithelialisation (reparative healing), alterations in the cell types that make up the epithelium and aberrant wound healing (Bergeron et al., 2010). As the epithelium is sensitive to the influence of the T<sub>H</sub>2 mediators and inflammatory cells described above, any alterations to this layer will have detrimental effects (Holgate, 2007). The epithelial layer protects against a number of inflammatory processes, and its destruction will lead to an increase in AI (Polito et al., 1998). Hence, processes such as goblet cell metaplasia and subepithelial fibrosis eventually contribute to the onset of AHR, and correlate to asthma severity (Bergeron et al., 2010; Holgate, 2000). Furthermore, damage to the epithelium leads to re-epithelialisation, which further exacerbates airway fibrosis. Most of these effects are mediated by factors released by eosinophils (Kay et al., 2004; Leigh et al., 2002). Studies have shown that there is an association between the extent of epithelial damage and asthma severity (Bergeron et al., 2010; Holgate, 2000).

#### 1.1.2.2 Goblet Cell Metaplasia (GCM)

Goblet cells are mucous secretory cells that play an important role in protecting the airway epithelium and represent a measure of AI-induced AWR. In the airways of healthy individuals, goblet cells secrete a variety of mucous-

associated glycoproteins (the main one being MUC5B), into the airway lumen in order to trap any harmful substances that may have been inhaled. These trapped substances are then expelled from the airway with the help of ciliated epithelial cells in a process called mucociliary clearance. However, in patients that suffer from asthma, there is an increased number of goblet cells resulting in excessive mucous secretion (especially the MUC5A2 glycoprotein), which can impair mucociliary clearance and in extreme cases, result in the death of asthma-sufferers.

There are several mechanisms that are believed to lead to GCM, which are initiated from T<sub>H</sub>2-induced cytokine signalling. T<sub>H</sub>2 cells secrete cytokines such as IL-4, IL-5, IL-9 and IL-13, which play separate but related roles in the development of GCM. While it is unknown exactly how these cytokines stimulate GCM, the ability of IL-9 to induce MUC5A2 production in epithelial cells is believed to be the first step in the differentiation process. T<sub>H</sub>2 cells also induce the over-expression of calcium ion-activated chlorine ion channels (hCLCA1 in humans, gob-5 in mice), which has been associated with GCM in cell cultured-based experiments (Hauber, et al., 2006). It has also been observed that goblet cells have upregulated sodium potassium chloride co-transporter channels (NKCC1) in human asthma.

#### 1.1.2.3 Subepithelial Fibrosis

Subepithelial fibrosis (or scarring) results from aberrant wound healing to the damaged airways and refers to the deposition of aberrant extracellular matrix proteins (ECM; primarily consisting of collagen) in the lamina reticularis

basement membrane. If improperly regulated, it progresses around the airways in response to continual disease progression, and further exacerbates the development of AHR (independently of AI). As such, subepithelial fibrosis is a major hallmark of chronic allergic asthma (Ammit, 2005; Bergeron et al., 2010).

The deposition of ECM proteins begins with the release of TGF- $\beta$  (primarily TGF- $\beta$ 1) from various inflammatory cells including eosinophils, fibroblasts, lymphocytes and mast cells (in response to the development of AI, refer to section 1.1.1.2), as well as epithelial cells (in response to epithelial damage, refer to section 1.1.2.1) (Batra V et al., 2004). The presence of TGF- $\beta$ 1 stimulates the differentiation of matrix-producing fibroblasts, which are recruited by inflammatory cells to sites of injury, into activated myofibroblasts, the latter containing properties of smooth muscle cells and hence, being characterised by their expression of  $\alpha$ -smooth muscle actin ( $\alpha$ -SMA) (Batra V et al., 2004); and which synthesise large amounts of ECM proteins when activated (Branton & Kopp, 1999). Myofibroblast-mediated ECM and collagen deposition occurs as part of the wound healing response to tissue injury, but often leads to fibrosis progression when myofibroblast activation is sustained upon repeated stimuli or injury to the airways.

The main enzymes involved in removing excess ECM proteins are matrix metalloproteinases (MMPs; Table 1-1). Produced by epithelial and inflammatory cells (Yao et al., 1998), MMPs are zinc-dependant endopeptidases responsible for degrading collagen I, IV, V, VII, X, XI, and XVI fibres as well as gelatin, elastin, fibronectin, and other ECM components (Lagente et al., 2005). The main MMPs

**Table 1-1: Matrix metalloproteinases family.**

Name	Molecular weight latent/active (kDa)	Substrates
<u>Interstitial collagenases</u>		
MMP-1 (collagenase-1)	52/41	Collagen I, II, III, VII, VIII, X, aggrecan, gelatin, proMMP-2, pro-MMP-9
MMP-8 (collagenase-2)	85/64	Collagen I, II, III, VII, VIII, X, aggrecan, gelatin
MMP-13 (collagenase-3)	65/55	Collagen I, II, III, aggrecan, gelatin
MMP-18 (collagenase-4)	53/42	
<u>Gelatinases</u>		
MMP-2 (Gelatinase-A)	72/66	Collagen I, II, III, IV, V, VII, X, XI, XIV, gelatin, elastin, fibronectin, aggrecan
MMP-9 (Gelatinase-B)	92/85	Collagen IV, V, VII, X, XIV, gelatin, pro-MMP-9, proMMP-13, elastin, aggrecan
<u>Stromelysins</u>		
MMP-3 (Stromelysin-1)	57/45, 28	Collagen II, III, IV, IX, X, XI, elastin, pro-MMP-1, proMMP-7, pro-MMP-8, pro-MMP-9, pro-MMP-13
MMP-10 (Stromelysin-2)	56/47, 24	Collagen III, IV, V, gelatin, fibronectin
MMP-11 (Stromelysin-3)	58/28	Fibronectin, laminin, gelatin, aggrecan
<u>Membrane-type MMPs</u>		
MMP-14 (MT1-MMP)	66/60	Pro-MMP-2, pro-MMP-13, collagen I, II, III, gelatin, aggrecan, fibronectin, laminin
MMP-15 (MT2-MMP)	68/62	Pro-MMP-2, gelatin, fibronectin, laminin
MMP-16 (MT3-MMP)	64/55	Pro-MMP-2

MMP-17 (MT4-MMP)	57/53	Unknown
MMP-24 (MT5-MMP)	63/45	Pro-MMP-2
MMP-25 (MT6-MMP)	Unknown	Gelatin

Others

MMP-7 (matrilysin-2)	28/19	Collagen II, III, IV, IX, X, XI, elastin, pro-MMP-1, proMMP-7, pro-MMP-8, pro-MMP-9, pro-MMP-13, gelatin, aggrecan, fibronectin, laminin
MMP-26 (matrilysin)	28/unknown	Collagen IV, gelatin, fibronectin
MMP-12 (metalloelastase)	54/45, 22	Elastin
MMP-19	57/45	Tenascin, gelatin, aggrecan
MMP-20 (enamelysin)	54/22	Enamel, gelatin
MMP-21	70/53	Unknown
MMP-23	Unknown	Unknown
MMP-27	Unknown	Unknown
MMP-28 (epilysin)	Unknown/58, 55	Unknown

**Table 1-1: Matrix metalloproteinases family.**

A total of 28 MMPs have been described with 24 of them having been identified in vertebrates. While MMPs taxonomy was first built according to their substrate specificity, it is also classified based on their structural similarities. Adapted from Gueders et al., 2006.

involved in collagen degradation in the lungs of asthmatics are the gelatinases, MMP-2 (gelatinase A) and MMP-9 (gelatinase B); which can cleave various collagens and gelatin, the latter which is then cleared from the body (Gueders et al., 2006). The activity of these MMPs are regulated at several levels including that by tissue inhibitors of metalloproteinases (TIMPs). The pathogenesis of chronic allergic asthma is associated with excessive TGF- $\beta$ 1 production, myofibroblast differentiation, TIMP expression but significantly reduced MMP activity; resulting in excessive ECM deposition, ultimately leading to scarring and stiffening of the airways, which compromises airway/lung function (Branton & Kopp, 1999). In the clinical setting, subepithelial reticular basement membrane thickening is present in all stages of asthma (Elias et al., 1999; Boulet et al., 1997). The subepithelial layer in healthy individuals is around 4-5 $\mu$ m, compared to 7-23 $\mu$ m exhibited in people that suffer from chronic asthma (Homer & Elias, 2000). Since thickening of the subepithelial layer also occurs in children, it suggests that subepithelial ECM thickening can occur early in the development of AWR (Payne et al., 2003).

#### 1.1.2.4 Airway Smooth Muscle Hypertrophy and Hyperplasia

The increase in airway smooth muscle is commonly used as an indicator of the development of AWR. The increase in airway smooth muscle mass is due to either hypertrophy (increase in cell size) and or hyperplasia (increase in cell number) (Bentley & Hershenson, 2008; Kaminska et al., 2009). It has also been reported that airway smooth muscle thickening may be a better indicator of asthma severity compared to AI or subepithelial thickening (Bentley &

Hershenson, 2008; Druilhe et al., 2008; Kaminska et al., 2009). However, while the mechanisms involved in airway smooth muscle enlargement are uncertain, there are hypotheses that support either smooth muscle hypertrophy or hyperplasia contributing to asthma severity (Burgess et al., 2009).

**In support of airway smooth muscle hypertrophy**, epithelial damage-induced subepithelial thickening is not limited to the lamina reticularis basement membrane (Bergeron et al., 2010; Hirst et al., 2004). There is often an increase in ECM deposition within the airway smooth muscle layer as well (Bergeron et al., 2010; Druilhe et al., 2008; Hirst et al., 2004), resulting in airway smooth muscle hypertrophy due to the increased TGF- $\beta$ 1 activity and smooth muscle stretch (Druilhe et al., 2008; Hirst et al., 2004).

**In support of airway smooth muscle hyperplasia**, it has been reported that there is an increase in cytokines such TGF- $\beta$ 1 and heparin-binding epidermal growth factor (Bentley & Hershenson, 2008; Hassan et al., 2010). While controversial, it is also believed that the increase in Ki-67 and other nuclear antigens involved in cellular proliferation may play a role in airway smooth muscle hyperplasia (Hassan et al., 2010).

Smooth muscle hypertrophy and/or hyperplasia leads to the development of airway obstruction, which brings about the onset of some of the symptoms mentioned previously as well as other structural changes associated with AWR (Bergeron et al., 2010; Hirst et al., 2004).

#### 1.1.2.5 Angiogenesis

Angiogenesis refers to the development of new blood vessels that protrude off pre-existing blood vessels (Li et al., 1997; Ribatti et al., 2009). Studies have shown that this process increases in cases of mild (Li et al., 1997) and severe asthma (Ribatti et al., 2009). Angiogenesis is triggered by both AI and AWR stimuli. AI and AWR can lead to the production of VEGF, which is the main growth factor that promotes angiogenesis of the airways (Mura et al., 2004; Ribatti et al., 2009). VEGF can be synthesised by alveolar epithelial cells, bronchial epithelial cells, smooth muscle cells, fibroblasts and alveolar macrophages; (Ribatti et al., 2009). AWR-induced subepithelial collagen deposition, results in a reduction in MMP-9 (gelatinase B), which is not only important for collagen deposition, but can also inhibit angiogenesis (Lee et al., 2006; Ribatti et al., 2009). This process has been shown to stimulate and exacerbate the progression of AWR and AI (Bergeron et al., 2010; Li et al., 1997; Ribatti et al., 2009).

#### 1.1.3 Airway Hyperresponsiveness (AHR)

It is important to note that the AWR that results from AI, can further exacerbate AI; and that both AI and AWR lead to the development of AHR (Meurs et al., 2008) (**Figure 1-2**), which refers to the excessive response of the airways to bronchoconstriction (Meurs et al., 2008; O'Byrne et al., 2009). AHR is the final pathophysiological process that is involved in the development of asthma and is an important indicator of asthma severity. While the mechanisms leading to

Figure 1-2

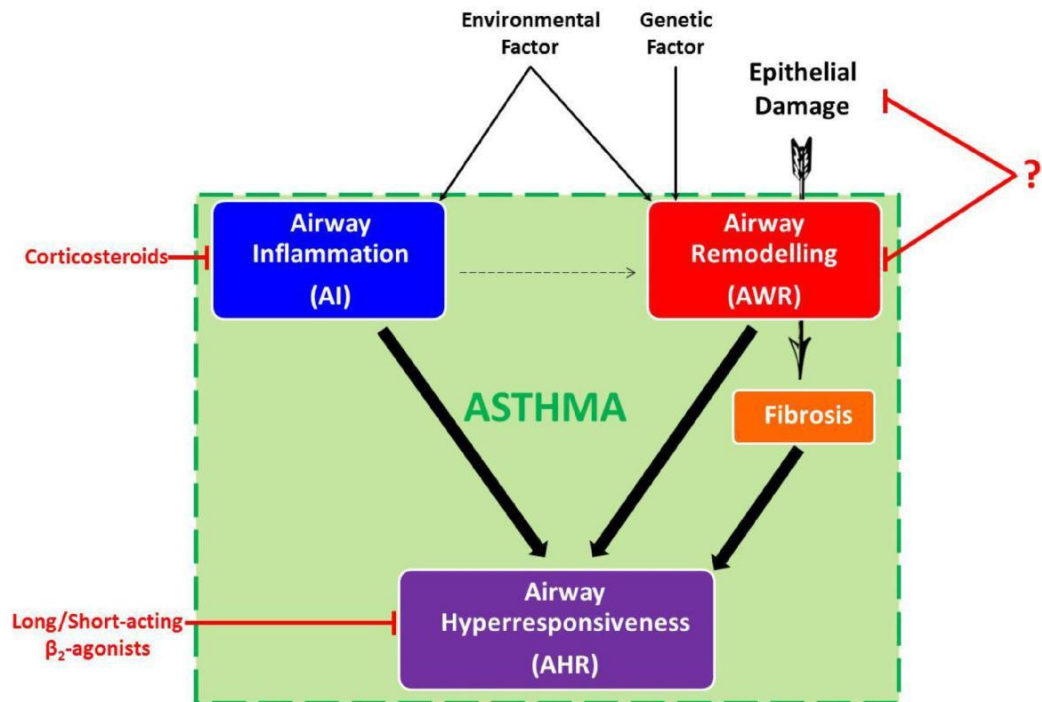


Figure 1-2: Pathogenesis of Asthma

The pathogenesis of human asthma is triggered due to environmental and genetic factors. This leads to the development of airway inflammation (AI) and airway remodelling (AWR), which both contribute to the progression of airway hyperresponsiveness (AHR). These three features form the central features of asthma.

Epithelial damage has been increasingly studied as a novel trigger of the development on AWR and subsequent airway fibrosis.

Current therapies involve the use of corticosteroids; which are used to reverse damage associated with AI and AI-induced AWR; and long and short acting  $\beta_2$  agonists; which suppress episodes of AHR. However, there are no therapies that specifically treat epithelial damage or AWR.

AHR are yet to be fully defined, it is known that selective (pathogen, allergens, and/or micro-organisms) and/or non-selective (cold weather) environmental factors, AI and/or AWR can all contribute to AHR. Inflammatory cells such as mast cells and eosinophils can lead to increased reactivity and narrowing of the airways (Kay et al., 2004). Likewise, structural changes in the airways (AWR) such as thickening of the basement membrane and increased smooth muscle mass are thought to directly contribute to AHR independently of AI (Holgate ST et al., 2009).

This project will specifically attempt to address some of the contributors associated with epithelial damage and fibrosis to the development of AHR. The extent of AHR development can be accessed via the measurement of airway reactivity, in response to increasing concentrations of known bronchoconstrictors.

## **1.2 CURRENT THERAPIES**

Current asthma therapies work by either suppressing episodes of AHR (Sears et al., 1990) or inhibiting AI-induced damage (Barnes, 2010; Barnes et al., 2003; AIHW, 2011). Asthma treatments primarily involve combination therapies. Treatments vary depending on the severity of symptoms and asthma attacks (Barnes, 2010). Currently, a combination of  $\beta$ 2-adrenergic receptor agonists and corticosteroids are used to treat asthma and its symptoms (Barnes, 2010) (**Figure 1-2**).

### **1.2.1 2-Adrenergic Receptor Agonists**

$\beta$ 2-adrenoreceptor agonists have been used since the early 1960's as effective agent for relaxing the airway smooth muscle in response to episodes of AHR (Ortega VE, 2014). However, in the 1960's and 1970's, there were a substantial number of asthma-related mortalities, which were associated with the unregulated use of a high-dose short-acting  $\beta$ 2-agonist (SABA), isoproterenol, and the less selective SABA, fenoterol (Pearce et al., 1990; Stolley PD, 1972).

While  $\beta$ 2-adrenoreceptor agonists have been shown to cause bronchial smooth muscle relaxation, the exact mechanism of action is not completely understood. They bind to Gs-coupled  $\beta$ 2-adrenoceptors on the airway smooth muscle cells, which allows for the dissociation of the  $\alpha$ -subunit from the  $\beta\gamma$ -subunit (Johnson, 1999). The free  $\alpha$ -subunit can then stimulate adenylyl cyclase subtype VI to convert adenosine triphosphate (ATP) into cyclic adenosine monophosphate (cAMP) allowing for the activation of inactive protein kinase A (PKA) into activated PKA (Billington et al., 1999). While it is not completely understood how, it is believed that activated PKA plays a role in the release of calcium from the sarcoplasmic reticulum, resulting in airway smooth muscle relaxation (Kume et al., 1994).

### **1.2.2 Corticosteroids**

Since the 1950's, corticosteroids have been the mainstay of systemic asthma treatment (Carryer et al., 1950; Crompton G, 2006). However, due to the number of side-effects relating to their route of administration, corticosteroids started being delivered via inhalation from the early 1970's (Brown et al., 1972;

Chatterjee et al., 1972; Clark, 1972; Cameron, 1973; Hodson et al., 1974; Vilsvik & Scand, 1974).

Inhaled corticosteroids work by targeting the intracellular glucocorticosteroid receptors of airway epithelial cells (Gibson et al., 2001; Ketchell et al., 2002).

Corticosteroids enter the epithelial cells via diffusion and bind to glucocorticosteroid subtype  $\alpha$  receptors (GR $\alpha$ ) (Rhen & Cidlowski, 2005). These corticosteroid-GR $\alpha$  units, form homodimers and then bind to glucocorticosteroid response element in the promoter region of steroid - responsive genes. This activation can lead to either: (i) transregression: the inhibition of the downstream effects of proinflammatory factors, such as AP-1 and NF- $\kappa$ B; or (ii) transactivation: the development of corticosteroids-induced systemic side effects, likely through DNA binding (Barnes & Adcock, 2003, Ito et al., 2001). This can result in an increase in  $\beta$ 2-adrenoreceptors and the promotion of the secretion of anti-inflammatory proteins such as leukoprotease inhibitors, and mitogen-activated protein kinase phosphate-1 (MKP-1) (Barnes, 2006; Clark, 2003). Corticosteroids can also inhibit multiple genes that encode for adhesion molecules, chemokines, cytokines, inflammatory enzymes and receptors (Barnes & Adcock, 2003).

Using corticosteroids at high concentrations, or for an extended period of time can also lead to adverse side-effects. Local adverse effects generally associated with inhaled corticosteroid use include coughing (Bryant & Pepys, 1976; Shim & Williams, 1987), dysphonia (Hanania et al., 1995), hoarseness and pharyngeal discomfort (Babu & Samuel, 1988), oropharyngeal candidiasis (Milne & Crompton, 1974; Vogt, 1979; Salzman & Pyszczynski, 1988; Toogood, 1990),

perioral dermatitis (Dubus et al., 2001), thirst (Dubus et al., 2001), and tongue hypertrophy (Dubus et al., 2001; Linder et al., 1995). They can also cause systemic adverse side-effects such as adrenocortical suppression (Hanania et al., 1995; Maxwell, 1990), bruising and skin thinning (Capwell & Reynolds, 1990), glaucoma (Garbe et al., 1997), osteoporosis (by interfering with calcium and phosphate metabolism) (Toogood et al., 1988; Packe et al., 1992), and posterior subcapsular cataracts (Cumming et al., 1997).

### **1.2.3 Other Therapeutics:**

In order to reduce the dosage (and therefore side-effects) of corticosteroids being administered, they have been used in conjunction with other, already established therapeutics (AIHW, 2011):

*Theophylline* (a methylxanthine drug) has been clinically used for more 70 years for its modest bronchodilatory and anti-inflammatory properties (AIHW, 2011). The exact mechanism of action of theophylline is not fully understood (Barnes, 2008). It is believed that one mechanism by which theophylline acts by passing through the plasma membrane of the airway smooth muscle to inhibit intracellular phosphodiesterases (PDEs) III and IV (Poolson et al., 1978). PDEs III and IV converts cAMP into AMP (Rabe et al., 1995), thus reducing the cAMP available for  $\beta$ 2-adrenoceptor-stimulated bronchodilation (refer to section 1.2.1). Theophylline has also been shown to have anti-inflammatory effects in the airways. Low dose theophylline treatment is associated with reduced eosinophil infiltration into the airways (Lim et al., 2001; Sullivan et al., 1994). However, the anti-inflammatory effects of theophylline are not as potent to that

induced by clinically-used corticosteroids (Barnes PJ, 2008). Additionally, there is currently no long-term data on the effects of theophylline (Barnes & Pauwels, 1994). The use of theophyllines is also associated with frequent adverse side-effects when its plasma concentration exceeds 20mg/l (Barnes & Pauwels, 1994). Common side-effects are abdominal discomfort, cardiac arrhythmias, headache, nausea, restlessness, and vomiting, primarily due to PDE inhibition (Nicholson et al., 1991). Theophylline use has also been associated with behavioural issues and learning difficulties in children (Rachelefsky et al., 1986).

*Omalizumab*, while being derived from murine origins, are recombinant humanised IgG antibodies, with 5% murine residues (Presta et al., 1993; Spector, 2004). Omalizumab selectively binds to the two Cε3 domain on the main branch of the IgE antibody to form trimeric or hexameric, IgE/anti-IgE complexes (Pelaia et al., 2008). By blocking IgE signalling, omalizumab prevents IgE from forming complexes with FcεRI and FcεRII/CD23, thus preventing the activation of the IgE-dependant pathway in the development of AI (Chang et al., 2007; Presta et al., 1994). Omalizumab is also associated with very few adverse side-effects, with occurrence rates reported at around 0.09% (Cox et al., 2007). While these side-effects are local and limited to the site of administration, it is generally associated with headaches, nausea, and tiredness (Holgate et al., 2005). While it has been reported that omalizumab use has been associated with an increased risk of getting cancer, studies have shown that it does not increase cancer occurrence (Busse et al., 2012; Long et al., 2007).

*Leukotrienes* are biologically active compounds that originate from leukocytes that have been shown to be involved in the development of both acute and chronic AHR) (Al Heialy et al., 2011; Royce et al., 2009). This has led to the development of leukotriene antagonists, which are able to block the receptors that leukotrienes bind to and activate (Holgate et al., 1996). As a therapeutic, they are generally used in patients that are aspirin-sensitive (AIHW, 2011). However, they have a reduced and variable effect in suppressing AI compared to the effects of corticosteroids (AIHW, 2011).

#### **1.2.4 Disadvantages of Current Treatments:**

There are several short-comings associated with these current treatments for asthma. In the case of short- and long-acting  $\beta$ -agonists, even though they relieve AHR transiently, they do not suppress the processes that are involved in AI or AWR, which are the two main processes contributing to AHR (Sears et al., 1990). This means that the development of AI and/or AWR-induced AHR continues to occur in the presence of  $\beta$ -agonist use, further compromising bronchial tissue functionality and integrity (Sears et al., 1990).

In the case of corticosteroids, there are several asthmatic patients, particularly those with severe disease symptoms that have been found to be resistant to their effects (Barnes et al., 2003; Sher et al., 1994; Walsh et al., 2003). Additionally, corticosteroids only have limited effects on AWR (as AI influences AWR development to a moderate degree) (Royce et al., 2013). Hence, there is currently no effective treatment that specifically targets AWR and its role in stimulating the development of AHR (Royce et al., 2013).

As such, more research must be done in order to better understand the pathogenesis of asthma to help develop novel therapies that better target all three major components of asthma. In particular, this project will focus on **i)** epithelial damage - which has been **increasingly studied** as a key cause of AWR and subsequently AHR (Cho, 2011; Hirota et al., 2011; Karagiannis et al., 2012); and **ii)** fibrosis -which is a hallmark of AWR associated with asthma (Leigh et al., 2002; Royce et al., 2013; Temelkovski et al., 1998); and how they both contribute to the development of AHR.

#### **1.2.5 Emerging Therapies for AWR:**

As most of the available therapies used to treat asthma focus on suppressing AI, more research needs to focus on potential therapies to treat AWR, epithelial damage and subsequent fibrosis. **Our lab has a keen interest in several emerging therapies, which have been detailed below.**

##### **1.2.5.1 Trefoil Factor Family 2**

The trefoil factor family (TFF1-3) are a group of peptide-hormones found in mucus-secretory tissues in humans, and to a greater extent in the gastrointestinal tract lining, where they appear to play an important role in epithelial repair and cytoprotection. More specifically, TFF2 is found in the highest concentration in the epithelium of the stomach; and recent studies have shown that TFF2 is increased in expression in the lung epithelium of mice with chronic allergic airways disease (AAD), compared to that observed in normal healthy mice (Royce et al., 2013). Adding to this, a functional genomic study

made reference to TFF2 as the third highest out of eleven genes that were increased in asthma sufferers (Kuperman et al., 2005); confirming its relevance in the setting of asthma. Due to its reparative effects, it is believed that exogenous administration of TFF2 to the lungs may help in the repair of the damaged epithelium associated with asthma. Recently completed studies in an experimental model of chronic AAD (which mimics several features of human asthma) demonstrated the therapeutic significance of TFF2 in the chronically inflamed lung tissue, where it was found to markedly inhibit sub-epithelial collagen deposition and AHR; based on its ability to reverse markers of epithelial damage (epithelial thickening and goblet cell metaplasia) (Royce et al., 2013). In addition to its ability to mediate epithelial repair and cytoprotection, TFF2 has been demonstrated to have anti-fibrotic and anti-AWR effects via its stimulation of the CXCR4 receptor, which results in a reduction in PDGF expression (Hofman et al., 2007; Royce et al., 2013).

#### 1.2.5.2 Relaxin

In 1926, relaxin was first discovered as a reproductive hormone (Sherwood, 2004), responsible for the softening of the pelvic ligaments in preparation for child birth (Sherwood, 2004). In humans, there are now three relaxin genes that have been discovered: RLN1, RLN2, and RLN3 (Bathgate et al., 2013; Royce et al., 2014), with the product of the RLN2 gene, H2 relaxin being the major stored and circulating form. Interest in H2 relaxin grew enormously when it was discovered that it possessed anti-fibrotic (Seibold et al., 2000) and other organ-protective properties.

Outside asthma, fibrosis is a hallmark of several diseases, and studies have shown that H2 relaxin can reduce fibrosis in many animal models of organ damage affecting the heart (Samuel, 2005; Samuel et al., 2006; Samuel and Hewitson, 2006), kidneys (Samuel and Hewitson, 2006), liver (Williams et al., 2001; Bennett et al., 2014) and lungs (Moore et al., 2008; Mookerjee et al., 2006); where it has been shown to consistently reduce TGF- 1- and myofibroblast-induced collagen synthesis and deposition, while promoting collagen-degrading MMP activity.

Relaxin also contains anti-apoptotic, anti-inflammatory, vasodilatory and wound healing properties, that make it an appealing therapy for lung diseases characterised by AWR and fibrosis (Samuel et al., 2007; Royce et al., 2014). With regards to AAD, H2 relaxin has been shown to effectively treat the allergic airways by: inhibiting the infiltration of pro-inflammatory cells into the lungs (Bani et al., 1997; Masini et al., 1994); promote dilation of alveolar blood capillaries (Bani et al., 1997); and reduce the thickness of the air–blood barrier (Bani et al., 1997). In experimental models of chronic AAD, H2 relaxin, administered subcutaneously (Kenyon et al., 2003; Royce et al., 2009) or intranasally (Royce et al., 2014) has also been shown to reverse several markers of AWR, including epithelial thickening and fibrosis, in addition to AHR. These effects of H2 relaxin were found to be mediated by its ability to inhibit Smad2 phosphorylation (where Smad2 is an intracellular protein that promotes TGF- 1 signal transduction) and hence, the pro-fibrotic effects of promotes TGF- 1 on myofibroblast differentiation (Royce et al., 2014); and myofibroblast contractility

(Huang et al., 2011), leading to reduced myofibroblast-mediated ECM/collagen deposition. H2 relaxin has also been found to promote lung MMP-2 and MMP-9 levels (Royce et al., 2009) in mice with chronic AAD, which would favour increased gelatinase-induced collagen degradation.

#### 1.2.5.3 Histone De-acetylase Inhibitors

Histones are a family of proteins that are involved in the DNA condensation into chromatin. When activated, there are acetylated in order to uncoil that specific area of the DNA strand and expose a certain gene that is required for transcription and subsequent protein synthesis. Histone de-acetylase (HDAC) Inhibitors (HDACi) work by hyperacetylating histone proteins which leave genes on the DNA to undergo transcription. Such genes that are exposed to HDACi play roles in the regulation of apoptosis, cellular proliferation and inflammation (Dokmanovic et al., 2007; Frew et al., 2009; Rasheed et al., 2008).

Current research has shown that apart from having a broad range of anti-inflammatory actions, HDACi have also been shown to have anti-remodelling and anti-fibrotic actions. Choi and colleagues (2005) were able to show that HDACi were able to reduce AI and AHR in an acute model of allergic airways disease. They believed this was possibly due to HDACi being able to inhibit T cell recruitment, and therefore, subsequent production of TH2 cytokines (Choi et al., 2005). HDACi have also been shown to reduce airway fibrosis by inhibiting TGF- $\beta$ -induced differentiation of fibroblasts (into myofibroblasts) (Hemmatzad et al., 2009; Kaimori et al., 2010). Of relevance to AAD, the HDACis valproic acid

(Royce et al. 2011) and trichostatin A (Royce et al., 2012) have been shown to reduce airway inflammation and subepithelial collagen deposition, and attenuate AHR; suggesting that they may have therapeutic potential in the setting of asthma.

#### 1.2.5.4 Stem Cell Therapy

In recent years, there has been a surge of interest in the potential therapeutic use of stem cells as a treatment for several world incurable diseases including various lung diseases (Alkhouri et al., 2014; Yang & Jia, 2014). Stem cells are specialised progenitor cells that either have capacity to differentiate into many different cell types found in the body or mediate therapeutic effects in the absence of differentiating into other cell types. While there are a number of different sources for various stems cells, which can be isolated and identified via *in vitro* and *in vivo* methods, these sources fall under two categories: embryonic or foetal stem cells, and adult stem cells. Despite the pluripotency and versatility of stem cells sourced from embryos or foetuses, many researchers opt to use adult stem cells as they view them as a more ethical source for providing different types of stem cells.

While stem cells have exhibited a potent effect in an acute setting of asthma, they seem to be less response when used in chronic asthma. It has been shown that the exacerbated levels of airway fibrosis in the chronic setting (which is not as pronounced in the acute setting) hinder stem cell survival and accessibility to sites of damage (Cheng et al., 2014; Lei et al., 2015). As such, an anti-fibrotic agent may need to be used with stem cell treatment so that a more favourable

environment can be fostered for the stem cells to illicit their reparative responses.

Our lab was interested in the response of either human adult bone marrow-derived mesenchymal stem cells (BMSC) (Royce et al., 2015) or human embryonic amniotic epithelial stem cells (AEC) (Royce et al., 2016), in the absence or presence of the anti-fibrotic effects of H2 relaxin. When administered to mice subjected to a 9-week model of chronic AAD, once-weekly from weeks 9-11, the BMSCs alone ( $1 \times 10^6$  cell/mouse) demonstrated modest anti-inflammatory and anti-remodelling/anti-fibrotic effects, and as a result did not significantly suppress AHR (Royce et al., 2015). In comparison,  $1 \times 10^6$  AECs/mouse alone were able to normalise epithelial thickness, and partially diminished airway fibrosis and AHR by ~40–50% in the same murine model of chronic AAD. However, when BMSCs or AECs were combined with H2 relaxin, this resulted in significantly reduced airway inflammation and the normalization of epithelial thickness, airway fibrosis and AHR back to that measured in uninjured control mice (Royce et al., 2015; Royce et al., 2016); confirming that the anti-fibrotic effects of H2 relaxin were able improve the therapeutic effects of BMSCs or AECs. Furthermore, H2 relaxin was found to directly promote BMSC or AEC proliferation by binding to RXFP1 which was expressed by these cells (Royce et al., 2016).

#### 1.2.5.5 Stem Cell-derived Exosomes

In addition to the presence of fibrosis limiting the viability and accessibility of stem cell-based therapies as effective treatments for chronic diseases, another potential limitation associated with stem cells is the finding that many of them appear to be cleared from the damaged organ within 4-7 days of administration. To this extent, it has been proposed that many stem cells likely mediate their therapeutic and reparative effects through secreted vesicles known as exosomes, which contain bioactive substances such as proteins, mRNAs and microRNAs; long after stem cells have been cleared post-administration. These membrane bound vesicles (exosomes) are approximately 30-100nm in length, have a floatation density of 1.13-1.19g/ml and contain DNA, mRNAs, miRNAs, proteins, and lipids (Heijnen et al., 1999; van Niel et al., 2001; Wolfers et al., 2014) that constitute the reparative contents of their parental stem cells. Interest in the use of stem cell-derived exosomes has been growing, as they provide us with potentially viable alternative to the use of stem cells. Exosomes are a non-living entity, and as such are easier to keep stable and store. Exosomes, once extracted can be stored frozen, and thawed immediately for use when required, whereas stem cells need to be stored in liquid nitrogen over long periods and require culture-induced expansion in preparation for their therapeutic use, which exposes these cells to the toxic effects of DMSO. Also, the volume of stem cells that can be administered in the setting of a mouse model of human asthma is restricted to approximately 1-2 million cells, whereas the therapeutic potential of 10-100 million stem cells can be administered in the form of exosomes. Therefore, exosomes offer various manufacturing and regulatory advantages over cell-based therapies.

### **1.3 ANIMAL MODELS**

The limited availability of human tissue and primary cells from the human airways has led many investigators to explore the potential of experimental models that can mimic the processes of human asthma (Cates et al., 2007). It is important to note, however, that only two non-human animals can develop asthma: horses (equine) and cats (felines) (Norris Reiner et al., 2004). Therefore, the experimental form of asthma that is induced in other laboratory animals including rodents is AAD (Royce et al., 2013). Widely used in mice, AAD models can also be established in sheep (Palmieri et al., 2006) and primates (Biagini et al., 1986) as the respiratory tract of these species resemble human anatomy. Although all these models exhibit several features of human asthma, none of these undergo the full spectrum of features seen in human disease.

#### **1.3.1 Mouse Models of Chronic AAD:**

##### **1.3.1.1 Ovalbumin-Induced Chronic AAD**

The ovalbumin (OVA)-induced mouse model of chronic AAD is regarded as the 'gold-standard' model for studying the pathogenesis of asthma (Hirota et al., 2011; Shin et al., 2009). OVA is a water-soluble glycoprotein found in egg white, which act as an allergen in animals, stimulating an inflammatory reaction when administered (Honma et al., 1996).

The primary role of this model is to induce an asthma-like state through the course of two separate phases (Royce et al., 2013; Temelkovski et al., 1998). Initially there is a sensitisation phase, which involves the mice becoming

sensitised to OVA on day 0 and day 14 (Royce et al., 2013; Temelkovski et al., 1998; **Figure 1-3A**); or saline as a control (**Figure 1-3B**). This is followed by a chronic challenge phase, which involves the mice being exposed to OVA or saline over a chronic period of time (i.e. for 30 minutes a day, three times a week for a 6-week period) to induce an allergic response (Kumar et al., 2008; Temelkovski et al., 1998).

There are three key variables that affect the extent of damage observed in mice associated with AAD which has been explored extensively by Kumar and his colleagues (2008). Firstly, the strain of mice dictates the protocol of the sensitisation and chronic challenge phases (Kumar et al., 2008). Two commonly used strains are the BALB/c and C57BL/6 strains (Foster et al., 1996; Kumar et al., 2008; Kuperman et al., 1998). Both exhibit AI to a similar degree; however, AI and AHR occur to a greater degree in BALB/c compared to C57BL/6 mice (Kumar et al., 2008). Secondly, the method of sensitising the mice can also differ (Kumar et al., 2008). The allergen can either be administered alone, or in conjunction with a substance (e.g. adjuvants) that promotes inflammatory responses (Kumar et al., 2008). The number of administrations can differ between one and three, but generally within a three-week period (between

**Figure 1-3**

**A) OVA-INDUCED MOUSE MODEL OF ALLERGIC AIRWAYS DISEASE**



**B) SALINE CONTROL**

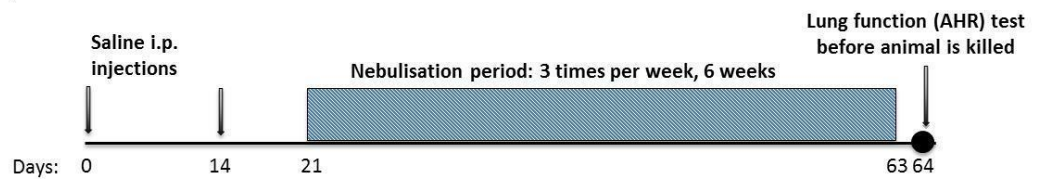


**Figure 1-3: Mouse Model of chronic Allergic Airways Disease**

**A)** Ovalbumin-induced Mouse Model of Allergic Airways Disease: On day 0 and 14, mice are subjected to an intraperitoneal (i.p.) injection of 0.02% w/v OVA. From day 21-63, mice are nebulised with 2.5%w/v OVA for 30min, 3 times a week, for 6 weeks. By day 64, invasive plethysmography will show that there is an increase in AHR, and tissue samples will show that there is an increase in eosinophils, neutrophils, monocytes and lymphocytes in and around the airways as well as an increase in epithelial thickening, goblet cell metaplasia and subepithelial fibrosis. **B)** Control mice for this model are sensitised and challenged with saline instead of OVA.

days 0-21) (Kumar et al., 2008). Also, the route of administration of the allergen can differ depending on the allergen used (Kumar et al., 2008). Usually the allergen is administered via intraperitoneal (i.p.) injection, intratracheal injection or intranasal delivery (Kumar et al., 2008). Lastly, the method of chronically challenging the mice can also differ (Kumar et al., 2008). The allergen can be administered via intranasal or inhalation methods (Kumar et al., 2008). However, there is a large variability as to the concentration of allergen used, and the number of times a week and number of weeks the mice are exposed to the allergen (Kumar et al., 2008).

Currently there are several experimental models of OVA-induced AAD that have different time frames (Locke et al., 2007; Foster et al., 2008). Acute and subacute models of AAD, which can be established over 3-4 days and 7 days, respectively, undergo AI and some AWR, but do not present with airway fibrosis, which is a well-established hallmark of asthma (Locke et al., 2007; Maes et al., 2010). On the other hand, chronic models of AAD exhibit AI, several features of AWR including fibrosis, as well as an increase in the expression of pro-fibrotic factors (Locke et al., 2007). As such, the chronic models tend to provide a better representation of AAD as opposed to the acute and subacute models (Locke et al., 2007). OVA-treated mice undergo AI, several features of AWR (epithelial thickening, goblet cell metaplasia, smooth muscle thickening), fibrosis, and AHR (Royce et al., 2013; Table 1-2). However, they do not undergo epithelial damage which has been increasingly studied as a key cause of asthma (Cates et al.,

2007). To address this latter deficiency, other models have been established (see section 1.3.2).

#### 1.3.1.2 House Dust Mite-Induced Chronic AAD

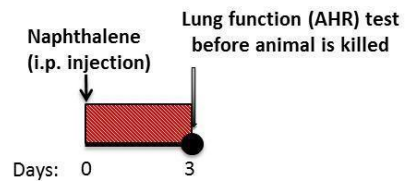
A relatively new model of chronic AAD is the house dust mite (HDM)-induced model of AAD. This model stimulates the development of AAD via an intratracheal injection or an intranasal delivery of a HDM allergen (Cates et al., 2007; Sarpong et al., 2003). HDM (*Dermatophagoides pteronyssinus*) (Cates et al., 2007) causes a cascade of inflammatory reactions to occur in the airways that ultimately lead to an increase in circulating IgE levels that are specific to HDM (Cates et al., 2007; Sarpong et al., 2003). It is believed that the AAD that develops as a result of this allergen is a better representation of human asthma as HDM (unlike OVA) is a bona fide allergen for humans that triggers asthma (Cates et al., 2007; Sarpong et al., 2003). However, more research needs to be done in order to refine this model as the sensitization/chronic challenge phases for this model are not defined (Birrell et al., 2010; Cates et al., 2007), can be variable and don't necessarily produce the degree of AWR and fibrosis seen in the OVA model.

#### 1.3.2 Mouse Models of Epithelial Damage:

As mentioned previously, epithelial damage has been increasingly studied as a new cause of the development of AWR and subsequently AHR (Holgate, 2000). However, epithelial damage have not been consistently reproduced in the commonly used models of AAD that are used to study the pathogenesis of

**Figure 1-4**

**A) NAPHTHALENE-INDUCED MOUSE MODEL OF EPITHELIAL DAMAGE**



**B) CORN OIL CONTROL**

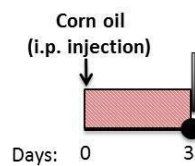


**Figure 1-4: Mouse Model of Epithelial Damage**

**A)** Naphthalene-induced Mouse Model of Epithelial Damage: On day 0, mice are i.p. injected with a 200mg/kg dose of NA. Three days post-injury, mice are subjected to invasive plethysmography, and tissue samples will show that there is an increase in epithelial damage and subepithelial fibrosis. **B)** control mice receive corn oil, the vehicle for NA.

asthma (Cates et al., 2007). Hence, new models have been established in order to study the role of epithelial damage and how it stimulates the development of AWR and AHR. There are currently several acute experimental animal models of epithelial damage, each using a different toxin to cause epithelial damage (Bates et al., 2008; Hedge et al., 1979; Karagiannis et al., 2012).

#### 1.3.2.1 Naphthalene-Induced Epithelial Damage

Naphthalene (NA) is a cytotoxic agent that is able to selectively target and destroy Clara cells in a dose-dependent manner (Hirota et al., 2011; Karagiannis et al., 2012; Van Winkle et al., 1995). Clara cells are located on the bronchial epithelium (Elizur et al., 2007; Gail et al., 1983) and are responsible for the secretion of various products into the bronchial lining that are important for the protection of the epithelium (such as surfactant proteins) (Elizur et al., 2007; Singh et al., 1997) as well as inhibiting inflammatory reactions mediated via T<sub>H</sub>2 responses (such as club-cell-specific 10kDa protein - CC10) (Elizur et al., 2007; Singh et al., 1997). NA works by being converted into reactive toxic metabolites via the actions of cytochrome P450 proteins located in the endoplasmic reticulum of Clara cells. (Buckpitt et al., 2002; Hirota et al., 2011; Karagiannis et al., 2012).

Thus, the destruction of these cells leads to the development of lesions which cause epithelial damage, aberrant wound healing and subsequently fibrosis. This model requires the mice to receive one i.p. injection of NA which is given at day

**Table 1-2: Summary of the features of human asthma that have been successfully replicated into animal models of asthma**

Characteristics of Human Asthma	Chronic Models of AAD		Acute Models of Epithelial Damage		
	OVA	HDM	NA	L-lysine	Cl <sub>2</sub>
AI	✓	✓			
Epithelial Damage			✓	✓	✓
Epithelial Thickening	✓	✓			
Goblet Cell Metaplasia	✓	✓			
Subepithelial Fibrosis	✓	✓	✓	✓	✓
AHR	✓	✓	✓	✓	✓

**Table 1-2: Summary of the features of human asthma that have been successfully replicated into animal models of asthma**

Chronic models of AAD with allergen such as OVA or HDM exhibit AI, epithelial thickening, goblet cell metaplasia, subepithelial fibrosis, and AHR; but lack epithelial damage as part of their pathology. On the other hand, chemicals/toxins such as NA, L-lysine, and Cl<sub>2</sub> can induce epithelial damage, resulting in subepithelial fibrosis, and AHR; but lack AI and other features of AWR (epithelial thickening and goblet cell metaplasia) as part of their pathology.

0 (Karagiannis et al., 2012; Van Winkle et al., 1995; **Figure 1-4A**). The mice will then undergo the processes mentioned above by 3 days post-injury (Elizur et al., 2007; Karagiannis et al., 2012). The control for this model is corn oil, as that is the vehicle used for NA (Karagiannis et al., 2012; Van Winkle et al., 1995; **Figure 1-4B**). The mice that undergo this model exhibit epithelial denudation, re-epithelialization, goblet cell metaplasia, fibrosis and AHR (Karagiannis et al., 2012). However, this model does not generally undergo AI which often underlies the development of asthma (**Table 1-2**).

#### 1.3.2.2 Other Models of Epithelial Damage

L-lysine is an amino acid that can mimic catatonic protein of immune cells (Bates et al., 2008; Bates et al., 2006; Hirota et al., 2011) and has been shown to disrupt the functioning of the tight junction proteins that link the epithelial cells together. It was also shown that this disruption, which ultimately affects the functioning of the epithelial layer, is sufficient to cause the development of AHR (**Table 1-2**). Additionally, Chlorine gas ( $\text{Cl}_2$ ) has also been used to study epithelial damage (Chester et al., 1977; Hedge et al., 1979; Martin et al., 2003), especially since it was used in chemical warfare during the Second World War (Chester et al., 1977). Current studies mainly use chlorine gas models utilized to mimic what happens to workers who have had accidental exposure to  $\text{Cl}_2$  at manufacturing plants (Chester et al., 1977). However, there are some experimental models that look at how chlorine gas causes epithelial damage, leading to AWR and AHR (Hedge et al., 1979; Martin et al., 2003; **Table 1-2**).  $\text{Cl}_2$  is able to dissolve into the water on the mucosal lining of the lungs in order to produce hydrochloric acid

(HCl) and hypochlorous acid (HClO) (Hedge et al., 1979). Both these acids when dissolved react with sulfhydryl (-H-S-) and disulphide bonds (-S-S-) in sulphur containing proteins of the epithelium (Hedge et al., 1979). Cl<sub>2</sub> administration has also shown been the cause AI in human studies; however, the AI-related changes are triggered by a massive increase in the number on neutrophils into the lungs (Bougault et al., 2009). As such, it would not be an appropriate fit for an eosinophilic driven allergic asthma study, as it requires a large increase in eosinophils, not neutrophils. Studies have also shown that Cl<sub>2</sub> cytotoxicity capacity is 10-30 time more potent than HCl (Hedge et al., 1979). Cl<sub>2</sub> is administered via inhalation, and the concentration of Cl<sub>2</sub> as well as time of exposure seems to differ between studies (Chester et al., 1977; Hedge et al., 1979; Martin et al., 2003).

#### 1.4 AIMS AND HYPOTHESIS

Epithelial damage has been increasingly studied as a novel aetiology leading to the pathogenesis of asthma (contributing to the development of AWR and subsequently AHR), however this is not accurately addressed in current models used to study the pathogenesis of asthma (as not all the features of human asthma are replicated). As such, a novel model needs to be developed to address this new finding, which forms the basis of this PhD project. Therefore, it is believed that superimposing epithelial damage (i.e. in the form of NA-induced damage) onto the 'gold-standard' chronic OVA-induced model of AAD, will exhibit a wider spectrum of features that are associated with human asthma (i.e. AI, airway epithelial damage, AWR/fibrosis and AHR); that may be used in the

future as a better representative experimental model of human asthma. This newly developed model can then be evaluated to study various treatment strategies for asthma associated with AI, AWR (incorporating epithelial damage) and AHR; namely, TFF2, H2 relaxin, AEC-derived exosomes and combinations of TFF2 and H2 relaxin, AECs and H2 relaxin or AEC-derived exosomes and relaxin; in comparison to a currently-used corticosteroid (i.e. dexamethasone).

#### **1.4.1 Aim 1**

To superimpose the NA-induced model of epithelial damage onto the 9-week OVA-induced mouse model of chronic AAD at three distinct time-points to determine: (i) how closely these combined models represent the features of human asthma and (ii) the contributions of AI vs. epithelial damage to fibrosis and AHR;

#### **1.4.2 Aim 2**

To treat the optimal refined model (from Aim-1, which best mimics the pathology of human asthma) with TFF2, H2 relaxin, dexamethasone (a corticosteroid) or the combined effects of TFF2 and H2 relaxin; and

#### **1.4.3 Aim 3**

To treat the optimal refined model (from Aim-1, which best mimics the pathology of human asthma) with either 5µg or 25µg of human AEC-derived exosomes, in the absence or presence of H2 relaxin; and in comparison to  $1 \times 10^6$  AECs combined with H2 relaxin.

## 1.5 REFERENCES

Al Heialy S, McGovern TK, Martin JG (2011). Insights into asthmatic airway remodelling through murine models. *Respirology*. **16**(4): 589-597.

Alkhouri H, Poppinga WJ, Tania NP, Ammit A, Schuliga M (2014). Regulation of pulmonary inflammation by mesenchymal cells. *Pulm Pharmacol Ther*. **29**(2):156-165.

Allen JE, Bischof RJ, Sucie Chang HY, Hirota JA, Hirst SJ, Inman MD, et al. (2009). Animal models of airway inflammation and airway smooth muscle remodelling in asthma. *Pulm Pharmacol Ther*. **22**(5): 455-465.

Ammit AJ (2005). The role of mRNA stability in airway remodelling. *Pulm Pharmacol Ther*. **18**(6): 405-415.

Australian Centre for Asthma Monitoring (2011). *Asthma in Australia 2011*. AIHW Asthma Series no. 4. Cat. no. ACM 22. Canberra: AIHW.

Babu S, Samuel P (1988). The effect of inhaled steroids on the upper respiratory tract. *J Laryngol Otol*. **102**(7):592-594.

Bani D, Ballati L, Masini E, Bigazzi M, Sacchi TB. (1997). Relaxin counteracts asthma-like reaction induced by inhaled antigen in sensitised guinea pigs. *Endocrin*. **138**(5):1909-1915.

Barnes PJ (2006). Corticosteroid effects on cell signalling. *Eur Respir J.* **27**(2):413-426.

Barnes PJ (2010). New therapies for asthma: is there any progress? *Trends Pharmacol Sci.* **31**(7): 335-343.

Barnes PJ, Pauwels RA (1994). Theophylline in the management of asthma: time for reappraisal? *Eur Respir J.* **7**(3):579-591.

Barnes PJ, Adcock IM (2003). How Do Corticosteroids Work in Asthma? *Ann Intern Med.* **139**:359-370.

Baron RM, Choi AJS, Owen CA, Choi AMK (2011). Genetically manipulated mouse models of lung disease: potential and pitfalls. *Am J Physiol Lung Cell Mol Physiol.* **302**:L485-L497.

Bates JH, Cojocaru A, Haverkamp HC, Rinaldi LM, Irvin CG (2008). The synergistic interactions of allergic lung inflammation and intratracheal cationic protein. *Am J Respir Crit Care Med.* **177**(3):261-268.

Bates JH, Wagers SS, Norton RJ, Rinaldi LM, Irvin CG (2006). Exaggerated airway narrowing in mice treated with intratracheal cationic protein. *J Appl Physiol.* **100**:500-506.

Bathgate, R. A., Halls, M. L., van der Westhuizen, E. T., Callander, G. E., Kocan, M., & Summers, R. J. (2013). Relaxin family peptides and their receptors. *Physiol Rev.* **93**:405–480.

Batra V, Musani AI, Hastie AT, Khurana S, Carpenter KA, Zangrilli JG, Peters SP (2004). Bronchoalveolar lavage fluid concentrations of transforming growth factor (TGF)-beta1, TGF-beta2, interleukin (IL)-4 and IL-13 after segmental allergen challenge and their effects on alpha-smooth muscle actin and collagen III synthesis by primary human lung fibroblasts. *Clin Exp Allergy.* **34**(3):437-444.

Bennett RG, Heimann DG, Singh S, Simpson RL, Tuma DJ (2014). Relaxin decreases the severity of established hepatic fibrosis in mice. *Liver Int.* **34**(3):416-426.

Bentley JK, Hershenson MB (2008). Airway smooth muscle growth in asthma: proliferation, hypertrophy, and migration. *Proc Am Thorac Soc.* **5**(1):89-96.

Bergeron C, Pagé N, Joubert P, Barbeau B, Hamid Q, Chakir J (2003). Regulation of procollagen I ( $\alpha$ 1) by interleukin-4 in human bronchial fibroblasts: a possible role in airway remodelling in asthma. *Clin Exp Allergy.* **33**(10):1389-1397.

Bergeron C, Tulic MK, Hamid Q (2010). Airway remodelling in asthma: from benchside to clinical practice. *Can Respir J.* **17**(4):e85-93.

Biagini RE, Moorman WJ, Lewis TR, Bernstein IL (1986). Ozone enhancement of platinum asthma in a primate model. *Am. Rev. Respir.* **4**:719-725.

Birrell MA, Van Oosterhout AJ, Belvisi MG (2010). Do the current house dust mite-driven models really mimic allergic asthma? *The European respiratory journal: official journal of the European Society for Clinical Respiratory Physiology.* **36**(5):1220-1221.

Boulet LP, Laviolette M, Turcotte H, Cartier A, Dugas M, Malo JL, et al. (1997). Bronchial subepithelial fibrosis correlates with airway responsiveness to methacholine. *CHEST.* **112**(1):45-52.

Boyce JA (2008). Eicosanoids in asthma, allergic inflammation, and host defense. *Curr Mol Med.* **8**(5):335-349.

Bradding P, Holgate ST (1996). The mast cell as a source of cytokines in asthma. *Ann N Y Acad Sci.* **796**:272-281.

Branton MH, Kopp JB (1999). TGF-beta and fibrosis. *Microbes Infect.* **1**(15):1349-1365.

Brown HM, Storey G, George WH (1972). Beclomethasone dipropionate: a new steroid aerosol for the treatment of allergic asthma. *Br Med J.* **1**(5800):585-590.

Bryant DH, Pepys J (1976). Bronchial reactions to aerosol inhalant vehicle. *Br Med J.* **1**(6021):1319-1320.

Buckpitt A, Boland B, Isbell M, Morin D, Shultz M, Baldwin R, et al. (2002).

Naphthalene-induced respiratory tract toxicity: metabolic mechanisms of toxicity.

*Drug Metab Rev.* **34**(4):791-820.

Burgess JK, Ceresa C, Johnson SR, Kanabar V, Moir LM, Nguyen TT, Oliver BG, Schuliga M, Ward J (2009). Tissue and matrix influences on airway smooth muscle function. *Pulm Pharmacol Ther.* **22**(5):379-387.

Busse W, Buhl R, Fernandez Vidaurre C, Blogg M, Zhu J, Eisner MD, Canvin J (2012). Omalizumab and the risk of malignancy: results from a pooled analysis. *J Allergy Clin Immunol.* **129**(4):983-989.

Cameron SJ, Cooper EJ, Crompton GK, Hoare MV, Grant IW (1973). Substitution of beclomethasone aerosol for oral prednisolone in the treatment of chronic asthma. *Br Med J.* **4**(5886):205-207.

Capewell S1, Reynolds S, Shuttleworth D, Edwards C, Finlay AY (1990). Purpura and dermal thinning associated with high dose inhaled corticosteroids. *BMJ.* **300**(6739):1548-1551.

Carroll N, Elliot J, Morton A, James A (1993). The structure of large and small airways in nonfatal and fatal asthma. *Am Rev Respir Dis.* **147**(2):405-410.

Carryer HM, Koelsche GA, Prickman LE, Maytum CK, Lake CF, Williams HL (1950). The effect of cortisone on bronchial asthma and hay fever occurring in subjects sensitive to ragweed pollen. *J Allergy Clin Immunol.* **21**(4):282-287

Cates EC, Fattouh R, Johnson JR, Llop-Guevara A, Jordana M (2007). Modeling responses to respiratory house dust mite exposure. In: Sjobring U, Taylor UD. *Models of Exacerbations in Asthma and COPD*, edn, Vol. 14. Canada: Karger. 42-67.

Caughey GH (2011). Mast cell proteases as protective and inflammatory mediators. *Adv Exp Med Biol.* **716**:212-234.

Chang TW, Wu PC, Hsu CL, Hung AF (2007). Anti-IgE antibodies for the treatment of IgE-mediated allergic diseases. *Adv Immunol.* **93**:63-119.

Chatterjee SS, Ross AE, Carroll K, Harris DM, Butler AG (1972). Respiratory function on asthmatic patients using beclomethasone dipropionate administered by pressurised aerosol. *Curr Med Res Opin.* **1**(3):173-181.

Chaudhuri R, Livingston E, McMahon AD, Lafferty J, Fraser I, Spears M, McSharry CP, Thomson NC (2006). Effects of smoking cessation on lung function and airway inflammation in smokers with asthma. *Am J Respir Crit Care Med.* **174**(2):127-133.

Cheng T, Liu Q, Zhang R, Zhang Y, Chen J, Yu R, Ge G (2014). Lysyl oxidase promotes bleomycin-induced lung fibrosis through modulating inflammation. *J Mol Cell Biol.* **6**(6):506-515.

Chester EH, Kaimal J, Payne CB, Kohn PM (1977). Pulmonary injury following exposure to chlorine gas. *CHEST.* **72**(2):247-250.

Cho JY (2011). Recent advances in mechanisms and treatments of airway remodelling in asthma: a message from the bench side to the clinic. *Korean J Intern Med.* **26**(4):367-383.

Clark AR (2003). MAP kinase phosphatase 1: a novel mediator of biological effects of glucocorticoids? *J Endocrinol.* **178**(1):5-12.

Clark TJ (1972). Effect of beclomethasone dipropionate delivered by aerosol in patients with asthma. *Lancet.* **1**(7765):1361-1364.

Colice GL (2004). Categorizing asthma severity: an overview of national guidelines. *Clin Med Res.* **2**(3):155-163.

Comhair SA, Gaston BM, Ricci KS, Hammel J, Dweik RA, Teague WG, Meyers D, Ampleford EJ, Bleecker ER, Busse WW, Calhoun WJ, Castro M, Chung KF, Curran-Everett D, Israel E, Jarjour WN, Moore W, Peters SP, Wenzel S, Hazen SL, Erzurum SC; National Heart Lung Blood Institute Severe Asthma Research Program (2011). Detrimental effects of environmental tobacco smoke in relation to asthma severity. *PLoS One*. **6**(5):e18574.

Cox L, Platts-Mills TA, Finegold I, Schwartz LB, Simons FE, Wallace DV; American Academy of Allergy, Asthma & Immunology; American College of Allergy, Asthma and Immunology (2007). American Academy of Allergy, Asthma & Immunology/American College of Allergy, Asthma and Immunology Joint Task Force Report on omalizumab-associated anaphylaxis. *J Allergy Clin Immunol*. **120**(6):1373-1377.

Crompton G (2006). A brief history of inhaled asthma therapy over the last fifty years. *Prim Care Respir J*. **15**(6):326-331.

Cumming RG1, Mitchell P, Leeder SR (1997). Use of inhaled corticosteroids and the risk of cataracts. *N Engl J Med*. **337**(1):8-14.

de Marco R, Locatelli F, Sunyer J, Burney P (2000). Differences in incidence of reported asthma related to age in men and women. A retrospective analysis of the data of the European Respiratory Health Survey. *Am J Respir Crit Care Med*. **162**(1):68-74.

Dixon AE, Pratley RE, Forgione PM, Kaminsky DA, Whittaker-Leclair LA, Griffes LA, Garudathri J, Raymond D, Poynter ME, Bunn JY, Irvin CG (2011). Effects of obesity and bariatric surgery on airway hyperresponsiveness, asthma control, and inflammation. *J Allergy Clin Immunol.* **128**(3):508-515.e1-2.

Dodge RR, Burrows B (1980). The prevalence and incidence of asthma and asthma-like symptoms in a general population sample. *Am Rev Respir Dis.* **122**(4):567-575.

Doherty T, Broide D (2007). Cytokines and growth factors in airway remodelling in asthma. *Curr Opin Immunol.* **19**(6):676-680.

Druilhe A, Zahm JM, Benayoun L, El Mehdi D, Grandsaigne M, Dombret MC, Mosnier I, Feger B, Depondt J, Aubier M, Pretolani M (2008). Epithelium expression and function of retinoid receptors in asthma. *Am J Respir Cell Mol Biol.* **38**(3):276-282.

Dubus JC, Guerra MT, Bodiou AC (2001) Cockroach allergy and asthma. *Allergy.* **56**(4):351-352.

Elias JA, Zhu Z, Chupp G, Homer RJ (1999). Airway remodelling in asthma. *J Clin Invest.* **104**(8):1001-1006.

Elizur A, Adair-Kirk TL, Kelley DG, Griffin GL, deMello DE, Senior RM (2007). Clara cells impact the pulmonary innate immune response to LPS. *Am J Physiol Lung Cell Mol Physiol.* **293**(2): L383-L392.

Evans MJ, Van Winkle LS, Fanucchi MV, Plopper CG (1999). The attenuated fibroblast sheath of the respiratory tract epithelial-mesenchymal trophic unit. *American journal of respiratory cell and molecular biology* 21(6): 655-657.

Fahy JV (2002). Goblet cell and mucin gene abnormalities in asthma. *CHEST.* **122**(6 suppl):320S-326S.

Finkelman FD, Vercelli D (2007). Advances in asthma, allergy mechanisms, and genetics in 2006. *J Allergy Clin Immunol.* **120**(3):544-550.

Foster PS, Hogan SP, Ramsay AJ, Matthaei KI, Young IG (1996). Interleukin 5 deficiency abolishes eosinophilia, airways hyperreactivity, and lung damage in a mouse asthma model. *J Exp Med.* **183**(1):195-201.

Gail DB, Lenfant CJ (1983). Cells of the lung: biology and clinical implications. *Am Rev Respir Dis.* **127**(3):366-387.

Galli SJ, Kalesnikoff J, Grimaldeston MA, Piliponsky AM, Williams CM, Tsai M (2005). Mast cells as "tunable" effector and immunoregulatory cells: recent advances. *Annu Rev Immunol.* **23**:749-786.

Galli SJ, Tsai M, Piliponsky AM (2008). The development of allergic inflammation. *Nature*. **454**(7203):445-454.

Garbe E, LeLorier J, Boivin JF, Suissa S (1997). Inhaled and nasal glucocorticoids and the risks of ocular hypertension or open-angle glaucoma. *JAMA*. **277**(9):722-727.

Georas SN, Rezaee F (2014). Epithelial barrier function: at the front line of asthma immunology and allergic airway inflammation. *J Allergy Clin Immunol*. **134**(3):509-520.

Gern JE, Busse WW (2002). Relationship of viral infections to wheezing illnesses and asthma. *Nat Rev Immunol*. **2**(2):132-138.

Gibson PG1, Saltos N, Fakes K (2001). Acute anti-inflammatory effects of inhaled budesonide in asthma: a randomised controlled trial. *Am J Respir Crit Care Med*. **163**(1):32-36.

Gueders MM, Foidart JM, Noel A, Cataldo DD (2006). Matrix metalloproteinases (MMPs) and tissue inhibitors of MMPs in the respiratory tract: potential implications in asthma and other lung diseases. *Eur J Pharmacol*. **533**(1-3):133-144.

Hammad H, Lambrecht BN (2015). Barrier Epithelial Cells and the Control of Type 2 Immunity. *Immunity*. **43**(1):29-40.

Hanania NA, Chapman KR, Kesten S (1995). Adverse effects of inhaled corticosteroids. *Am J Med*. **98**(2):196-208.

Hassan M, Jo T, Risse PA, Tolloczko B, Lemière C, Olivenstein R, Hamid Q, Martin JG. Airway smooth muscle remodelling is a dynamic process in severe long-standing asthma. *J Allergy Clin Immunol*. **125**(5):1037-1045.

Hauber H, Foley SC, Hamid Q (2006). Mucin overproduction in chronic inflammatory lung disease. *Can Respir J*. **13**(6):327-335

Hedge JR, Morrissey WL (1979). Acute chlorine gas exposure. *JACEP*. **8**:59-63.

Heijnen HF, Schiel AE, Fijnheer R, Geuze HJ, Sixma JJ (1999). Activated platelets release two types of membrane vesicles: microvesicles by surface shedding and exosomes derived from exocytosis of multivesicular bodies and alpha-granules. *Blood*. **94**(11):3791-3799.

Hirota JA, Hackett TL, Inman MD, Knight DA (2011). Modeling asthma in mice: what have we learned about the airway epithelium? *Am J Respir Cell Mol Biol*. **44**(4):431-438.

Hirst SJ, Martin JG, Bonacci JV, Chan V, Fixman ED, Hamid QA, et al. (2004). Proliferative aspects of airway smooth muscle. *J Allergy Clin Immunol.* **114**(2 Suppl): S2-S17.

Hodson ME, Batten JC, Clarke SW, Gregg I (1974). Beclomethasone dipropionate aerosol in asthma. Transfer of steroid-dependent asthmatic patients from oral prednisone to beclomethasone dipropionate aerosol. *Am Rev Respir Dis.* **110**(4):403-408.

Hoffmann, W., Jagla, W., & Wiede, A. (2001). Molecular medicine of TFF-peptides: from gut to brain. *Histol Histopathol.* **16**:319–334.

Holgate ST (2000). Epithelial damage and reponse. *Clin Exp Allergy.* **30**(Suppl 1):37-41.

Holgate ST (2007). The epithelium takes centre stage in asthma and atopic dermatitis. *Trends Immunol.* **28**(6):248-251.

Holgate ST (2008). Pathogenesis of asthma. *Clin Exp Allergy.* **38**(6):872-97.

Holgate ST, Arshad HS, Roberts GC, Howarth PH, Thurner P, Davies DE (2009). A new look at the pathogenesis of asthma. *Clin Sci (Lond).* **118**(7):439-450

Holgate ST, Bradding P, Sampson AP (1996). Leukotriene antagonists and synthesis inhibitors: New directions in asthma therapy. *J Allergy Clin Immunol.* **98**(1):1-13.

Holgate ST, Djukanović R, Casale T, Bousquet J (2005). Anti-immunoglobulin E treatment with omalizumab in allergic diseases: an update on anti-inflammatory activity and clinical efficacy. *Clin Exp Allergy.* **35**(4):408-416.

Holgate ST, Holloway J, Wilson S, Bucchieri F, Puddicombe S, Davies DE (2004). Epithelial-mesenchymal communication in the pathogenesis of chronic asthma. *Ann Am Thorac Soc.* **1**(2):93-98.

Holguin F, Bleecker ER, Busse WW, Calhoun WJ, Castro M, Erzurum SC, Fitzpatrick AM, Gaston B, Israel E, Jarjour NN, Moore WC, Peters SP, Yonas M, Teague WG, Wenzel SE (2011). Obesity and asthma: an association modified by age of asthma onset. *J Allergy Clin Immunol.* **127**(6):1486-1493.e2.

Holloway, Beghé, Holgate (1999). The genetic basis of atopic asthma. *Clin Exp Allergy.* **29**(8):1023-1032.

Homer RJ1, Elias JA (2000). Consequences of long-term inflammation. Airway remodelling. *Clin Chest Med.* **21**(2):331-343.

Honma K, Kohno Y, Saito K, Shimojo N, Horiuchi T, Hayashi H, et al. (1996). Allergenic epitopes of ovalbumin (OVA) in patients with hen's egg allergy: inhibition of basophil histamine release by haptenic ovalbumin peptide. *Clin Exp Immunol* 103: 446-453.

Huang X, Gai Y, Yang N, Lu B, Samuel C, Thannickl VJ, Zhou. (2011). Relaxin regulates myofibroblast contractility and protects against lung fibrosis. *Am J Path.* **179**(6):2751-2765.

Ierodiakonou D, Postma DS, Koppelman GH, Boezen HM, Gerritsen J, Ten Hacken N, et al. (2011). E-cadherin gene polymorphisms in asthma patients using inhaled corticosteroids. *Eur Respir J.* **38**(5):1044-1052.

Kaminska M, Foley S, Maghni K, Storness-Bliss C, Coxson H, Ghezzi H, Lemièrre C, Olivenstein R, Ernst P, Hamid Q, Martin J (2009). Airway remodelling in subjects with severe asthma with or without chronic persistent airflow obstruction. *J Allergy Clin Immunol.* **124**(1):45-51

Karagiannis TC, Li X, Tang MM, Orłowski C, El-Osta A, Tang MLK, et al. (2012). Molecular model of naphthalene-induced DNA damage in the murine lung. *Hum Exp Toxicol.* **31**(1):42-50.

Kay AB, Phipps S, Robinson DS (2004). A role for eosinophils in airway remodelling in asthma. *Trends Immunol.* **25**(9):477-482.

Ketchell RI, Jensen MW, Lumley P, Wright AM, Allenby MI, O'connor BJ (2002). Rapid effect of inhaled fluticasone propionate on airway responsiveness to adenosine 5'-monophosphate in mild asthma. *J Allergy Clin Immunol.* **110**(4):603-606.

Kim BE, Leung DY (2012). Epidermal barrier in atopic dermatitis. *Allergy Asthma Immunol Res.* **4**(1):12-6.

Kraft M (2007). Part III: Location of asthma inflammation and the distal airways: clinical implications. *Curr Med Res Opin.* **23**(Suppl 3):S21-27.

Kumar RK, Herbert C, Foster PS (2008). The 'classical' ovalbumin challenge model of asthma in mice. *Curr Drug Targets.* **9**:485-494.

Kume H, Hall IP, Washabau RJ, Takagi K, Kotlikoff MI (1994). Beta-adrenergic agonists regulate KCa channels in airway smooth muscle by cAMP-dependent and -independent mechanisms. *J Clin Invest.* **93**(1):371-379.

Kuperman D, Schofield B, Wills-Karp M, Grusby MJ (1998). Signal Transducer and Activator of Transcription Factor 6 (Stat6)-deficient Mice Are Protected from Antigen-induced Airway Hyperresponsiveness and Mucus Production. *J Exp Med.* **187**(6): 939-948.

Kuperman DA, Lewis CC, Woodruff PG, Rodriguez MW, Yang YH, Dolganov GM, Fahy JV, Erle DJ (2005). Dissecting asthma using focused transgenic modeling and functional genomics. *J Allergy Clin Immunol.* **116**(2):305-311.

Lagente V, Manoury B, Nénan S, Le Quément C, Martin-Chouly C, Boichot E (2005). Role of matrix metalloproteinases in the development of airway inflammation and remodelling. *Braz J Med Biol Res.* **38**(10):1521-1530.

Laloo UG, Barnes PJ, Chung KF (1996). Pathophysiology and clinical presentations of cough. *J Allergy Clin Immunol.* **98**(5 Pt 2):S91-S97.

Lappalainen U, Whitsett JA, Wert SE, Tichelaar JW, Bry K (2005). Interleukin-1beta causes pulmonary inflammation, emphysema, and airway remodelling in the adult murine lung. *Am J Respir Cell Mol Biol.* **32**(4):311-318.

Lazarus SC, Chinchilli VM, Rollings NJ, Boushey HA, Cherniack R, Craig TJ, Deykin A, DiMango E, Fish JE, Ford JG, Israel E, Kiley J, Kraft M, Lemanske RF Jr, Leone FT, Martin RJ, Pesola GR, Peters SP, Sorkness CA, Szeffler SJ, Wechsler ME, Fahy JV; National Heart Lung and Blood Institute's Asthma Clinical Research Network (2007). Smoking affects response to inhaled corticosteroids or leukotriene receptor antagonists in asthma. *Am J Respir Crit Care Med.* **175**(8):783-790.

Lei L, Zhong XN, He ZY, Zhao C, Sun XJ (2015). IL-21 induction of CD4+ T cell differentiation into Th17 cells contributes to bleomycin-induced fibrosis in mice. *Cell Biol Int.* **39**(4):388-399.

Leigh R, Ellis R, Wattie J, Southam DS, De Hoogh M, Gauldie J, et al. (2002). Dysfunction and remodelling of the mouse airway persist after resolution of acute allergen-induced airway inflammation. *Am J Respir Cell Mol Biol.* **27**(5):526-535.

Leung DY, Nicklas RA, Li JT, Bernstein IL, Blessing-Moore J, Boguniewicz M, Chapman JA, Khan DA, Lang D, Lee RE, Portnoy JM, Schuller DE, Spector SL, Tilles SA (2004). Disease management of atopic dermatitis: an updated practice parameter. Joint Task Force on Practice Parameters. *Ann Allergy Asthma Immunol.* **93**(3 Suppl 2):S1-S21.

Li X, Wilson JW (1997). Increased Vascularity of the Bronchial Mucosa in Mild Asthma. *Am J Respir Crit Care Med.* **156**:229-233.

Lim S, Tomita K, Caramori G, Jatakanon A, Oliver B, Keller A, Adcock I, Chung KF, Barnes PJ (2001). Low-dose theophylline reduces eosinophilic inflammation but not exhaled nitric oxide in mild asthma. *Am J Respir Crit Care Med.* 2001 Jul 15;164(2):273-6.

Linder N, Yaron M, Handsher R, Kuint J, Birenbaum E, Mazkereth R, Lubin D, Mendelson E, Safrir O, Reichman B (1995). Early immunization with inactivated poliovirus vaccine in premature infants. *J Pediatr.* **127**(1):128-130.

Locke NR, Royce SG, Wainwright JS, Samuel CS, Tang ML (2007). Comparison of airway remodelling in acute, subacute, and chronic models of allergic airways disease. *Am J Respir Cell Mol Biol.* **36**(5):625-632.

Long A, Rahmaoui A, Rothman KJ, Guinan E, Eisner M, Bradley MS, Iribarren C, Chen H, Carrigan G, Rosén K, Szeffler SJ (2014). Incidence of malignancy in patients with moderate-to-severe asthma treated with or without omalizumab. *J Allergy Clin Immunol.* **134**(3):560-567.

Loxham M, Davies DE, Blume C (2014). Epithelial function and dysfunction in asthma. *Clin Exp Allergy.* **44**(11):1299-1313.

Maes T, Provoost S, Lanckacker EA, Cataldo DD, Vanoirbeek JA, Nemery B, et al. (2010). Mouse models to unravel the role of inhaled pollutants on allergic sensitization and airway inflammation. *Respiratory research* **11**:7.

Marshall GD (2004). Neuroendocrine mechanisms of immune dysregulation: applications to allergy and asthma. *Ann Allergy Asthma Immunol.* **93**(2 Suppl 1):S11-17.

Martin JG, Campbell HR, Iijima H, Gautrin D, Malo JL, Eidelman DH, et al. (2003). Chlorine-induced injury to the airways in mice. *Am J Respir Crit Care Med.* **168**(5): 568-574.

Mauad T, Bel EH, Sterk PJ (2007). Asthma therapy and airway remodelling. *J Allergy Clin Immunol.* **120**(5):997-1009.

Maxwell DL (1990). Adverse effects of inhaled corticosteroids. *Biomed Pharmacother.* **44**(8):421-427.

Meurs H, Gosens R, Zaagsma J (2008). Airway hyperresponsiveness in asthma: lessons from in vitro model systems and animal models. *Eur Respir J* **32**(2):487-502.

Milne LJ, Crompton GK (1974). Beclomethasone dipropionate and oropharyngeal candidiasis. *Br Med J.* **3**(5934):797-798.

Mookerjee I, Tang MLK, Solly N, Tregear GW, Samuel CS (2005). Investigating the role of relaxin in the regulation of airway fibrosis in animal models of acute and chronic allergic airway disease. *Ann NY Acad Sci.* **1041**:194–196.

Moore B, Murphy RF, Agrawal DK (2008). Interaction of TGF-beta with immune cells in airway disease. *Curr Mol Med.* **8**:427–436.

Nicholson CD, Challiss RA, Shahid M (1991). Differential modulation of tissue function and therapeutic potential of selective inhibitors of cyclic nucleotide phosphodiesterase isoenzymes. *Trends Pharmacol Sci.* **12**(1):19-27.

Norris Reiner CR, Decile KC, Berghaus RD, Williams KJ, Leutenegger CM, Walby WF, et al. (2004). An Experimental Model of Allergic Asthma in Cats Sensitised to House Dust Mite or Bermuda Grass Allergen. *Int Arch Allergy Immunol.* **135**(2):117-131.

O'Byrne PM, Gauvreau GM, Brannan JD (2009). Provoked models of asthma: what have we learnt? *Clinical and experimental allergy: journal of the British Society for Allergy and Clinical Immunology.* **39**(2):181-192.

Oettgen HC, Geha RS (1999). IgE in asthma and atopy: cellular and molecular connections. *J Clin Invest.* **104**(7):829-835.

Ortega VE (2014). Pharmacogenetics of beta2 adrenergic receptor agonists in asthma management. *Clin Genet.* **86**(1):12-20.

Packe GE, Douglas JG, McDonald AF, Robins SP, Reid DM (1992). Bone density in asthmatic patients taking high dose inhaled beclomethasone dipropionate and intermittent systemic corticosteroids. *Thorax.* **47**(6):414-417.

Palmieri TL, Enkhbaatar P, Bayliss R, Traber LD, Cox RA, Hawkins HK, et al. (2006). Continuous nebulised albuterol attenuates acute lung injury in an ovine model of combined burn and smoke inhalation. *Crit Care Med.* **34**(6):1719-1724.

Parker LC, Stokes CA, Sabroe I (2014). Rhinoviral infection and asthma: the detection and management of rhinoviruses by airway epithelial cells. *Clin Exp Allergy*. **44**(1):20-28.

Pawankar R (2004). Allergic rhinitis and asthma: the link, the new ARIA classification and global approaches to treatment. *Curr Opin Allergy Clin Immunol*. **4**(1):1-4.

Pawankar R (2005). Mast cells in allergic airway disease and chronic rhinosinusitis. *Chem Immunol Allergy*. **87**:111-129.

Payne DN, Rogers AV, Adelroth E, Bandi V, Guntupalli KK, Bush A, Jeffery PK (2003). Early thickening of the reticular basement membrane in children with difficult asthma. *Am J Respir Crit Care Med*. **167**(1):78-82.

Pearce N, Grainger J, Atkinson M, Crane J, Burgess C, Culling C, Windom H, Beasley

R (1990). Case-control study of prescribed fenoterol and death from asthma in New Zealand, 1977-81. *Thorax*. **45**(3):170-175.

Pelaia G, Renda T, Romeo P, Busceti MT, Maselli R (2008). Omalizumab in the treatment of severe asthma: efficacy and current problems. *Ther Adv Respir Dis*. **2**(6):409-421.

Polito AJ, Proud D (1998). Epithelial cells as regulators of airway inflammation. *J Allergy Clin Immunol*. **102**(5):714-718.

Polson JB, Krzanowski JJ, Goldman AL, Szentivanyi A (1978). Inhibition of human pulmonary phosphodiesterase activity by therapeutic levels of theophylline. *Clin Exp Pharmacol Physiol.* **5**(5):535-539.

Presta LG, Lahr SJ, Shields RL, Porter JP, Gorman CM, Fendly BM, Jardieu PM (1993). Humanization of an antibody directed against IgE. *J Immunol.* **151**(5):2623-2632.

Presta L, Shields R, O'Connell L, Lahr S, Porter J, Gorman C, Jardieu P (1994). The binding site on human immunoglobulin E for its high affinity receptor. *J Biol Chem.* **269**(42):26368-26373.

Rabe KF, Magnussen H, Dent G (1995). Theophylline and selective PDE inhibitors as bronchodilators and smooth muscle relaxants. *Eur Respir J.* **8**(4):637-642.

Rachelefsky GS, Wo J, Adelson J, Mickey MR, Spector SL, Katz RM, Siegel SC, Rohr AS (1986). Behavior abnormalities and poor school performance due to oral theophylline use. *Pediatrics.* **78**(6):1133-1138.

Rhen T, Cidlowski JA (2005). Antiinflammatory action of glucocorticoids--new mechanisms for old drugs. *N Engl J Med.* **353**(16):1711-1723.

Ribatti D, Puxeddu I, Crivellato E, Nico B, Vacca A, Levi-Schaffer F (2009).

Angiogenesis in asthma. *Clin Exp Allergy.* **39**(12):1815-1821.

Rivera J, Gilfillan AM (2006). Molecular regulation of mast cell activation. *J Allergy Clin Immunol.* **117**(6):1214-1225.

Royce SG, Cheng V, Samuel CS, Tang ML (2012). The regulation of fibrosis in airway remodelling in asthma. *Mol Cell Endocrinol.* **351**(2):167-175.

Royce SG, Dang W, Ververis K, De Sampayo N, El-Osta A, Tang MLK & Karagiannis TC. (2011). Protective effects of valproic acid against airway hyperresponsiveness and airway remodelling in a mouse model of allergic airways disease. *Epigenetics.* **6**(12):1463-1470.

Royce SG, Dang W, Yuan G, Tran J, El-Osta A, Karagiannis TC, Tang ML. (2012). Effects of the histone deacetylase inhibitor, trichostatin A, in a chronic allergic airways disease model in mice. *Arch Immunol Ther Exp (Warsz).* **60**(4):295-306.

Royce SG, Lim C, Muljadi RC, Samuel CS, Ververis K, Karagiannis TC, Giraud AS, Tang ML (2013). Trefoil factor-2 reverses airway remodelling changes in allergic airways disease. *Am J Respir Cell Mol Biol.* **48**(1):135-144.

Royce SG, Lim CXF, Patel KP, Wang B, Samuel CS, Tang MLK. (2014). Intranasally administered serelaxin abrogates airway remodelling and attenuates airway hyperresponsiveness in allergic airways disease. *Clin Exp Allergy.* **44**:1399-1408.

Royce SG, Moodley Y, Samuel CS. (2013). Novel therapeutic strategies for lung disorders associated with airway remodelling and fibrosis. *Pharmacology & Therapeutics*. **141**:250-260.

Royce SG, Sedjahtera A, Samuel CS, Tang ML (2013). Combination therapy with relaxin and methylprednisolone augments the effects of either treatment alone in inhibiting subepithelial fibrosis in an experimental model of allergic airways disease. *Clin Sci (Lond)*. **124**(1):41-51.

Royce SG, Shen M, Patel KP, Huuskes BM, Ricardo SD, Samuel CS (2015). Mesenchymal stem cells and serelaxin synergistically abrogate established airway fibrosis in an experimental model of chronic allergic airways disease. *Stem Cell Res*. **15**(3):495-505.

Royce SG, Tang ML (2009). The effects of current therapies on airway remodelling in asthma and new possibilities for treatment and prevention. *Curr Mol Pharmacol*. **2**(2):169-181.

Royce SG, Tominaga AM, Shen M, Patel KP, Huuskes BM, Lim R, Ricardo SD, Samuel CS (2016). Serelaxin improves the therapeutic efficacy of RXFP1-expressing human amnion epithelial cells in experimental allergic airway disease. *Clin Sci (Lond)*. **130**(23):2151-2165.

Royce, SG, Li X, Tortorella S, Goodings L, Chow BS, Giraud A S, Tang MLK, Samuel CS (2013). Mechanistic insights into the contribution of epithelial damage to

airway remodelling: novel therapeutic targets for asthma. *Am J Respir Cell Mol Biol.* **50**(1):180-192.

Saito H, Howie K, Wattie J, Denburg A, Ellis R, Inman MD, Denburg JA (2001). Allergen-induced murine upper airway inflammation: local and systemic changes in murine experimental allergic rhinitis. *Immunology.* **104**(2):226-234.

Salzman GA, Pyszczynski DR (1988). Oropharyngeal candidiasis in patients treated with beclomethasone dipropionate delivered by metered-dose inhaler alone and with Aerochamber. *J Allergy Clin Immunol.* **81**(2):424-428.

Sarin S, Undem B, Sanico A, Togias A (2006). The role of the nervous system in rhinitis. *J Allergy Clin Immunol.* **118**(5):999-1016.

Sarpong SB, Zhang LY, Kleeberger SR (2003). A novel mouse model of experimental asthma. *Int Arch Allergy Immunol.* **132**(4): 346-354.

Samuel CS (2005). Relaxin: antifibrotic properties and effects in models of disease. *Clin. Med. Res.* **3**:241–249.

CS, Du XJ, Bathgate RAD, Summers RJ (2006). ‘Relaxin’ the stiffened heart and arteries: the therapeutic potential for relaxin in the treatment of cardiovascular disease. *Pharmacol. Ther.* **112**:529–552.

Samuel CS, Hewitson TD (2006). Relaxin in cardiovascular and renal disease. *Kidney Int.* **69**:1498–1502.

Samuel, C. S., Hewitson, T. D., Unemori, E. N., & Tang, M. L. (2007). Drugs of the future: the hormone relaxin. *Cell Mol Life Sci.* **64**:1539–1557.

Schleimer RP, Kato A, Kern R, Kuperman D, Avila PC (2007). Epithelium: at the interface of innate and adaptive immune responses. *J Allergy Clin Immunol.* **120**(6):1279-1284.

Sears MR, Taylor DR, Print CG, Lake DC, Li Q, Flannery EM, et al. (1990). Regular inhaled beta-agonist treatment in bronchial asthma. *The Lancet.* **336**(8728):1391-1396.

Seibold JR, Korn JH, Simms R, Clements PJ, Moreland LW, Mayes MD, Furst DE, Rothfield N, Steen V, Weisman M, Collier D, Wigley FM, Merkel PA, Csuka ME, Hsu V, Rocco S, Erikson M, Hannigan J, Harkonen WS, Sanders ME (2000). Recombinant human relaxin in the treatment of scleroderma. A randomised, double-blind, placebo-controlled trial. *Ann. Intern. Med.* **132**:871– 879.

Sher ER, Leung DY, Surs W, Kam JC, Zieg G, Kamada AK, et al. (1994). Steroid-resistant asthma. Cellular mechanisms contributing to inadequate response to glucocorticoid therapy. *J Clin Invest.* **93**(1):33-39.

Sherwood OD (2004). Relaxin's physiological roles and other diverse actions.

Endocr Rev, **25**:205–234.

Shim C, Williams MH Jr (1987). Cough and wheezing from beclomethasone aerosol. Chest. **91**(2):207-209.

Shin YS, Takeda K, Gelfand EW (2009). Understanding asthma using animal models. Allergy Asthma Immunol Res **1**(1):10-18.

Singh G, Katyal SL (1997). Clara cells and Clara cell 10 kD protein (CC10). Am J Respir Cell Mol Biol. **17**(2):141-143.

Sokol K, Sur S, Ameredes BT (2014). Inhaled environmental allergens and toxicants as determinants of the asthma phenotype. Adv Exp Med Biol. **795**:43-73.

Spector S (2004). Omalizumab: efficacy in allergic disease. Panminerva Med. **46**(2):141-148.

Sterk PJ, Masclee AA, Spinhoven P, Schmidt JT, Zwinderman AH, Rabe KF, Bel EH (2005). Risk factors of frequent exacerbations in difficult-to-treat asthma. Eur Respir J. **26**(5):812-818.

Stolley PD (1972). Asthma mortality. Why the United States was spared an epidemic of deaths due to asthma. *Am Rev Respir Dis.* **105**(6):883-890.

Sullivan P, Bekir S, Jaffar Z, Page C, Jeffery P, Costello J (1994). Anti-inflammatory effects of low-dose oral theophylline in atopic asthma. *Lancet.* **343**(8904):1006-1008.

Tang ML, Samuel CS, Royce SG (2009). Role of relaxin in regulation of fibrosis in the lung. *Ann N Y Acad Sci.* **1160**:342-347.

Temelkovski J, Hogan SP, Shepherd DP, Foster PS, Kumar RK (1998). An improved murine model of asthma: selective airway inflammation, epithelial lesions and increased methacholine responsiveness following chronic exposure to aerosolised allergen. *Thorax.* **53**(10):849-856.

Toogood JH (1990). Complications of topical steroid therapy for asthma. *Am Rev Respir Dis.* **141**(2 Pt 2):S89-S96.

Toogood JH, Crilly RG, Jones G, Nadeau J, Wells GA (1988). Effect of high-dose inhaled budesonide on calcium and phosphate metabolism and the risk of osteoporosis. *Am Rev Respir Dis.* **138**(1):57-61.

van Niel G, Raposo G, Candalh C, Boussac M, Hershberg R, Cerf-Bensussan N, Heyman M (2001). Intestinal epithelial cells secrete exosome-like vesicles. *Gastroenterology.* **121**(2):337-349.

van Winkle LS, Buckpitt AR, Nishio SJ, Isaac JM, Plopper CG (1995). Cellular response in naphthalene-induced Clara cell injury and bronchiolar epithelial repair in mice. *Am J Physiol.* **269**(6):L800-L818.

Vilsvik JS, Schaanning J (1974). Beclomethasone dipropionate aerosol in adult steroid-dependent obstructive lung disease. *Scand J Respir Dis.* **55**(3):169-175.

Vogt FC (1979). The incidence of oral candidiasis with use of inhaled corticosteroids. *Ann Allergy.* **43**(4):205-210.

Walsh GM, Sexton DW, Blaylock MG (2003). Corticosteroids, eosinophils and bronchial epithelial cells: new insights into the resolution of inflammation in asthma. *J Endocrinol.* **178**(1):37-43.

Williams EJ, Benyon RC, Trim N, Hadwin R, Grove BH, Arthur MJ, Unemori EN, Iredale JP, (2001). Relaxin inhibits effective collagen deposition by cultured hepatic stellate cells and decreases rat liver fibrosis in vivo. *Gut.* **49**:577–583.

Wolfers J, Lozier A, Raposo G, Regnault A, Théry C, Masurier C, Flament C, Pouzieux S, Faure F, Tursz T, Angevin E, Amigorena S, Zitvogel L (2001). Tumor-derived exosomes are a source of shared tumor rejection antigens for CTL cross-priming. *Nat Med.* **7**(3):297-303.

Yang J, Jia Z (2014). Cell-based therapy in lung regenerative medicine. *Regen Med Res.* **2**(1):7.

Yao PM, Delclaux C, d'Ortho MP, Maitre B, Harf A, Lafuma C (1998). Cell-matrix interactions modulate 92-kD gelatinase expression by human bronchial epithelial cells. *Am J Respir Cell Mol Biol.* **18**(6):813-822.

Zhang Y, Mofatt MF, Cookson WOC. (2012). Genetic and genomic approach to asthma: new insights of origins. *Curr Opin Pulm Med.* **18**(1):6-13.

---

**CHAPTER 2:**  
**GENERAL METHODS**

---

## **2.0 GENERAL METHODS**

The general reagents and materials used in this thesis are detailed in this chapter and unless otherwise specified, all reagents used were of analytical grade. The detailed methodologies described in this chapter have been utilised and abbreviated in Chapters 3-5.

### **2.1 MATERIALS**

#### **2.1.1 Serelaxin**

Recombinant H2 relaxin (also referred to as serelaxin) was generously provided by Corthera Inc (San Carlos, CA, USA; a subsidiary of Novartis International AG, Basel, Switzerland). For simplicity, recombinant H2 relaxin/serelaxin will be abbreviated as 'RLX' throughout thesis (as highlighted in Chapter 1).

#### **2.1.2 Trefoil Factor 2**

Glycosylated human recombinant trefoil factor (TFF)2 was generously provided by Prof. Andrew Giraud (Murdoch Children's Research Institute, University of Melbourne, Parkville, Victoria, Australia).

#### **2.1.3 Dexamethasone**

Dexamethasone sodium phosphate was purchased from Hospira Australia Pty Ltd, Mulgrave, Victoria, Australia.

#### **2.1.4 Human Amniotic Stem Cells**

Human amniotic stem cells (hAECs; from term placentas and frozen at 5 million to 22.5 million cells/vial) were obtained from Dr Rebecca Lim (Hudson Institute of Medical Research, Clayton, Victoria, Australia).

#### **2.1.5 Human Amniotic Stem Cell-derived Exosomes**

hAEC-derived exosomes were also obtained from Dr Rebecca Lim (Hudson Institute of Medical Research).

### **2.2 ANIMALS**

All animals utilised in this thesis were six-to-eight week old female Balb/c mice, which were obtained from Monash University Animal Services (Clayton, Victoria, Australia). Mice were transported to the Department of Pharmacology Mouse Room and allowed to acclimatise one week before they were subjected to any experimentation; and were housed a controlled environment and maintained on a fixed lighting schedule (12 hours of light/dark cycle) with free access to rodent lab chow (Barastock Stockfeeds, Pakenham, Victoria, Australia) and water. All described experiments were approved by the Monash University Animal Ethics Committee, which adheres to the Australian code of practice for the care and use of laboratory animals for scientific purposes; under ethics number Monash Animal Research Platform (MARP)/2012/085.

## **2.3 ANIMAL MODELS**

### **2.3.1 Ovalbumin-induced Mouse Model of Allergic Airway Disease**

The 9-week ovalbumin (OVA)-induced model of chronic allergic airways disease (AAD) was established as previously described (Kumar et al., 2008; Temelkovski et al., 1998). Six-to-eight week old female Balb/c wild type mice were sensitised with two intraperitoneal (i.p.) injection of 10µg, Grade V OVA (Sigma-Aldrich, St Louis, MO, USA) and 1mg of aluminium potassium sulfate (Sigma-Aldrich) in 500µl of saline, on days 0 and 14. Mice were then challenged with an aerosol of 2.5% (w/v) OVA in saline solution, delivered using an Omron NE-U07 nebuliser (Omron Electronics, Shimogyo-ku, Kyoto, Japan) for 30 minutes, three days a week for six weeks (from day 21-63) (**Figure 2-1A**). Vehicle-treated mice received 500µl of saline on days 0 and 14 and were challenged with saline aerosol from day 21-63 (Temelkovski et al., 1998) (**Figure 2-1B**).

### **2.3.2 Naphthalene-induced Mouse Model of Epithelial Damage**

The 3-day naphthalene (NA)-induced model of acute epithelial damage was established to sub-groups of mice, as described before (Royce, 2014a). Six-to-eight week old female Balb/c wild type mice were administered a single dose of 200mg/ml of NA (Sigma-Aldrich) dissolved in corn oil (Sigma-Aldrich) equivalent to 200µl per 20g body weight (BW) and delivered by i.p. administration on day 64 (**Figure 2-1C**). Vehicle-treated mice received a single i.p injection of corn oil on day 64 (**Figure 2-1D**).

Figure 2-1:

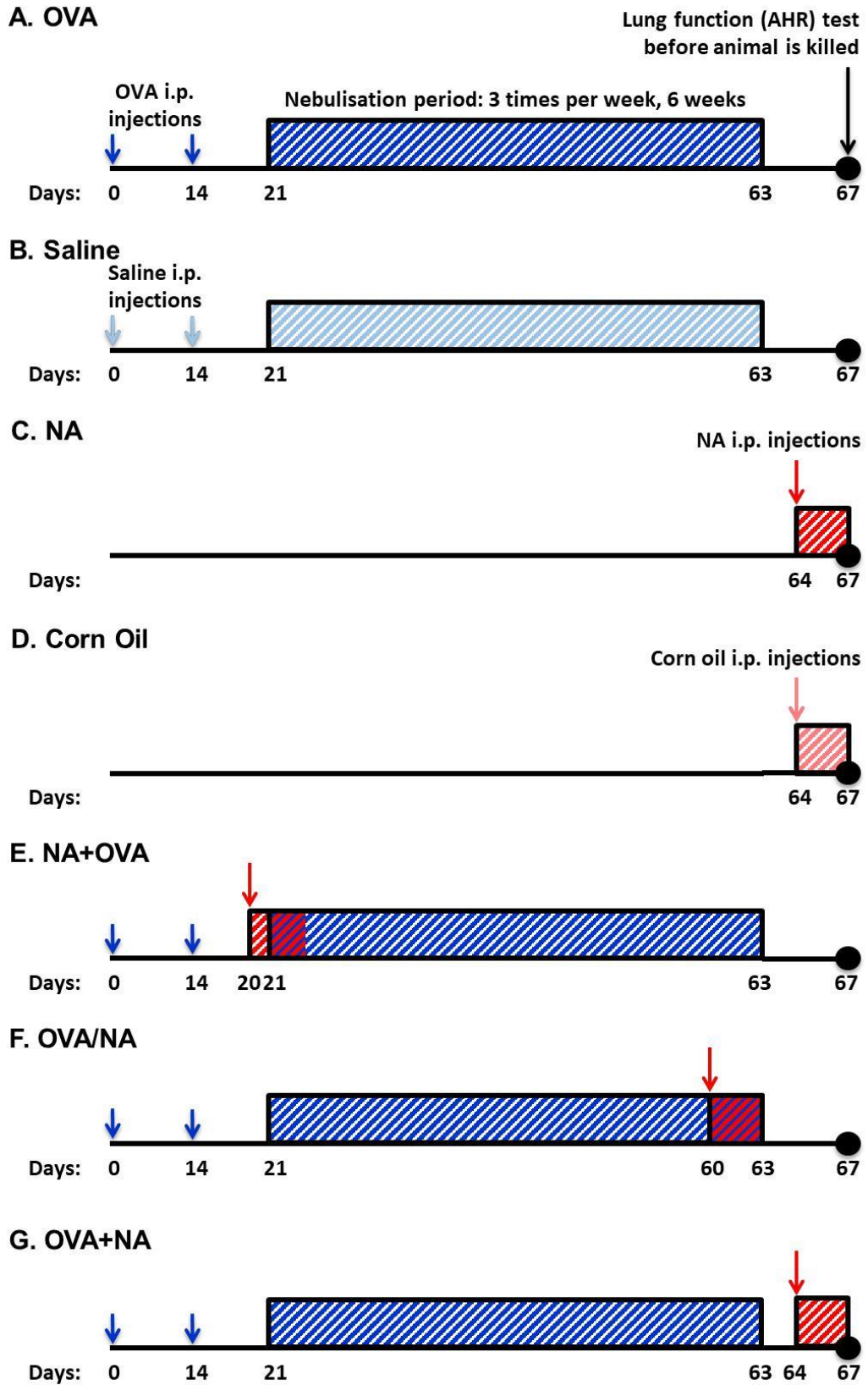


**Figure 2-1: Schematic illustration experimental models and treatments for Aim 1**

**A)** On day 0 and 14, mice are subjected to an i.p. injection of 0.02% w/v OVA. From day 21-63, mice are nebulised with 2.5%w/v OVA for 30min, 3 times a week, for 6 weeks (OVA). **B)** Control mice for this model are sensitised and challenged with saline (vehicle for OVA) between days 0-63 (Saline).

**C)** On day 64, mice are i.p. injected with a 200mg/kg dose of NA (NA). **D)** Control mice for this model receive corn oil (vehicle for NA) on day 64 (CO).

Mice undergoing one of the combined models were sensitised and challenged with OVA as per A). An i.p. injected with a 200mg/kg dose of NA was administered either **E)** prior to OVA nebulisations (day 20, NA+OVA); **F)** during the end of the OVA nebulisations (day 60, OVA/NA); or **G)** after OVA nebulisations (day 64, OVA+NA).

### **2.3.3 Combined Mouse Models of Allergic Airways Disease that incorporates Epithelial Damage**

The 3-day NA-induced model of epithelial damage was superimposed onto the 9-week OVA-induced model of AAD at three separate time-points: i) prior to (day 20 (**Figure 2-1E**), ii) during the end of (day 60) (**Figure 2-1F**), or iii) after (day 64) the 6-week challenge period with aerosolised OVA (**Figure 2-1G**) (refer to Chapter From Chapter 4 onwards, all references to a combined mouse model of AAD that incorporated epithelial damage refers to the administration of NA after the 6-week challenge period with aerosol OVA (on day 64) (**Figure 2-1G**).

## **2.4 TREATMENT STRATEGIES**

### **2.4.1 Intranasal administration**

Mice were briefly anaesthetised using isoflurane (Baxter, Deerfield, IL, USA), held in a supine before having 50µl of one or more of the treatment options described below, pipetted onto to nostrils, which the mice inhale.

#### **2.4.1.1 Serelaxin**

Intranasal administration of 50µl of 0.8mg/kg/day (**Figure 2-2B**) a level that is within the normal physiological range of serum relaxin in pregnant rodents (Mookerjee et al., 2009; Hossain et al., 2011) and mice (Mookerjee et al., 2009; Hewitson et al., 2010 Pini et al., 2010) which is known to prevent/reduce organ fibrosis in numerous disease models regardless of etiology (review in Samuel et al. 2007). In 2014 Royce and colleagues showed that the same dose of relaxin

could be delivered Intranasally and have the same effect (Royce et.al, 2014, Royce et.al, 2015).

#### 2.4.1.2 Trefoil Factor 2

Intranasal administration of 50µl of 0.5mg/kg/day of TFF2 was used (**Figure 2-2C**), based on previous studies that successfully used to demonstrate the therapeutic effects of TFF2 (Thim et al., 1993, Royce, et. al, 2014a)

#### 2.4.1.3 Dexamethasone

Dexamethasone is commonly used in various animal models (Royce et al., 2014b, Essilfie et al., 2012) as it is also used in clinical setting to treat AI in patients that suffer from asthma. In a clinical setting, patients receive a dose between 0.3-0.6mg/kg/day (Shefrin & Goldman, 2009, **Figure 2-2E**). Intranasal administration of 50µl of 0.5mg/kg/day of dexamethasone was used, based on previous studies showing that this concentration and dosage of dexamethasone was adequate to reduce inflammation in the airway (Essilfie et al., 2012).

#### 2.4.1.4 Human amniotic epithelial cells

For the hAEC, cells from 2-3 vials were pooled (to obtain cells from 2-3 donors to limit donor-dependant variability) and recovered overnight in Dulbecco's modified Eagle's medium F-12 media containing 10% fetal calf serum (FCS). On the morning of each schedule treatment,  $1 \times 10^6$  hAECs were re-suspended in 50µl of phosphate-buffered saline (PBS), ready for administration.

Figure 2-2:

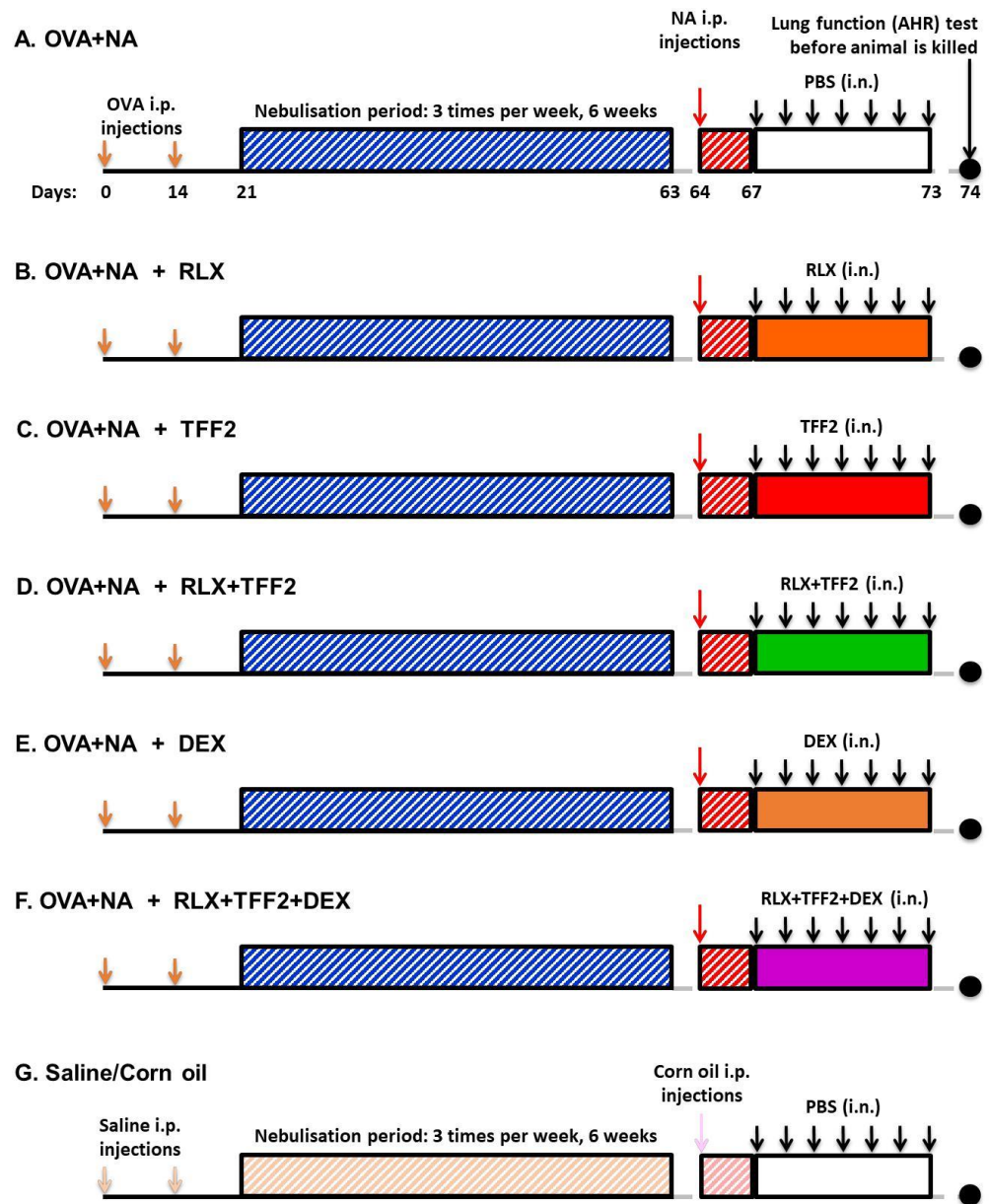


**Figure 2-2: Schematic illustration of experimental models and treatments for**

**Aim 2**

On day 0 and 14, mice are subjected to an i.p. injection of 0.02% w/v OVA. From day 21-63, mice are nebulised with 2.5%w/v OVA for 30min, 3 times a week, for 6 weeks.

On day 64, mice are i.p. injected with a 200mg/kg dose of NA. Three days post-injury, mice received daily i.n. administrations of either **A**) saline (vehicle for all drug treatments; injury control), **B**) RLX ( $0.8 \text{ mg}\cdot\text{mL}^{-1}$ ), **C**) recombinant human glycosylated TFF2 ( $0.5 \text{ mg}\cdot\text{mL}^{-1}$ ), **D**) RLX and TFF2, **E**) DEX ( $0.5 \text{ mg}\cdot\text{mL}^{-1}$ ) or **F**) RLX, TFF2 and DEX. On day 74, all mice were subjected to invasive plethysmography, and tissue samples taken for further analysis.

**G**) Control mice for this model are sensitised and challenged with saline (vehicle for OVA) between days 0-63, receive corn oil (vehicle for NA) on day 64, and received daily i.n. administrations of saline between days 67-73.

#### 2.4.1.5 Human amniotic epithelial cells-derived exosomes

Exosomes (EXO) were isolated from several pooled amnions and characterised as described before (Tan et al., 2018). EXO were then dissolved in saline for therapeutic administration as detailed below. Proteomic pathway clustering analysis including proteins significantly enriched by EXO and RNA sequencing analysis of EXO were recently reported (Tan et al., 2018).

## 2.5 INVASIVE PLETHYSMOGRAPHY

Mice are anaesthetised using by i.p injection of 200µg/g of Ketamine (Parnell Laboratories, Alexandria, NSW, AU) and 10 µg/g of Xylazine (Troy Laboratories, Smithfield, NSW, AU) before being subjected to a tracheostomy. This involves a small incision to be made to the neck; the trachea is revealed by blunt dissection (pushing apart) of the surrounding muscle; a small incision is made in the trachea; and the tracheostomy cannula (tube) is inserted into the trachea and tied off with suture. The other end of the tracheostomy cannula is then attached to the plethysmography machine, Buxco® FinePointe Series RC (Buxco Electronics) which ventilated the mice by delivering 0.01ml/g bodyweight at a rate of 120 strokes/min in a mouse plethysmography chamber. Mice then receive acetyl methacholine via a nebuliser (10µl per dose; for 3 minutes per dose). The nebulised Acetyl methacholine is breathed in via the tracheostomy cannula and then breathed straight out again with each breath. AHR measurements are then taken by flow and pressure sensors in the plethysmography machine (in

Figure 2-3:

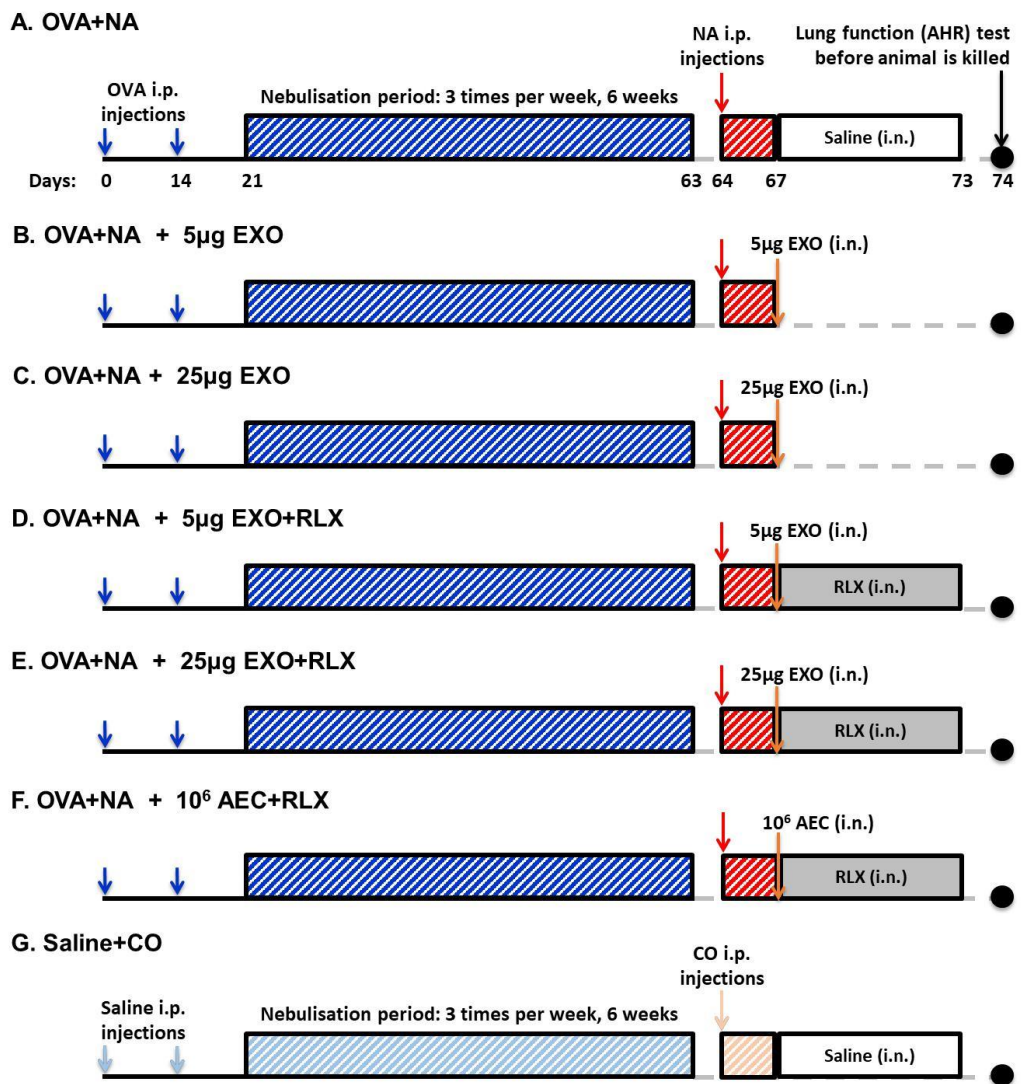


**Figure 2-3: Schematic illustration experimental models and treatments for Aim 3**

On day 0 and 14, mice are subjected to an i.p. injection of 0.02% w/v OVA. From day 21-63, mice are nebulised with 2.5%w/v OVA for 30min, 3 times a week, for 6 weeks.

On day 64, mice are i.p. injected with a 200mg/kg dose of NA. Three days post-injury, mice received i.n. administrations of either A) saline (daily, vehicle for all drug treatments; injury control), B) 5µg of AEC-derived EXO, C) 25µg of AEC-derived EXO, D) 5µg of AEC-derived EXO and RLX ( $0.8 \text{ mg} \cdot \text{mL}^{-1}$ , daily), F) 25µg of AEC-derived EXO and RLX, or G)  $10^6$  AEC and RLX. On day 74, all mice were subjected to invasive plethysmography, and tissue samples taken for further analysis.

H) Control mice for this model are sensitised and challenged with saline (vehicle for OVA) between days 0-63, receive corn oil (vehicle for NA) on day 64, and received daily i.n. administrations of saline between days 67-73.)

response to increasing doses of acetyl methacholine); which is attached to a computer which measure a variety of respiratory markers including airway resistance and dynamic airway compliance. Results were expressed as i) maximal resistance and minimal compliance, after each dose on MCh minus baseline (PBS alone) resistance and compliance, respectively.

## **2.6 BRONCHO-ALVEOLAR LAVAGE**

Following invasive plethysmography, the lungs of the mice were lavaged three times with 500µl of cold PBS and pooled in ice-cold 20% (v/v) FCS in PBS. The samples were centrifuged (Eppendorf centrifuge 5810R; Sigma-Aldrich, Castle Hill, NSW, Australia) at 12000rpm for 10 minutes at 4°C, after which, the supernatant was aliquoted out and stored at -20°C, while the pellet of inflammatory cells were washed in 5% (v/v) FCS/PBS.

### **2.6.1 Total Inflammatory Cell Count**

Total viable cell counts were performed automatically using Invitrogen™ Countess automated cell counter (Thermo Fisher Scientific, Eugene, OR, USA). 10µl of each sample of inflammatory cells in 5% (v/v) FCS/PBS was combined with 10µl of trypan blue, before being pipetted onto an Invitrogen™ Countess chambered slide (Thermo Fisher Scientific, Eugene, OR, USA). The number of

total, alive and dead cells, and subsequent percentage viability were quantified using a Invitrogen™ Countess automated cell counter.

### 2.6.2 Differential Inflammatory Cell Count

Slides, filters, and sample wells were fastened and inserted into the slide holders. 50µl of each inflammatory cell sample in 5% (v/v) FCS/PBS were loaded into each sample well and were spun at 6000RPM for five minutes. After the cells were spun onto the slides, the fasteners for each slide were slowly opened and empty sample wells and filter paper carefully removed, to not disturb the smeared cells on the slide. Cytospin smears ( $2 \times 10^4$  cells) were then fixed with propanol and left to dry overnight before undergoing modified Wright's stain (Hema-Tek, Bayer Diagnostics, Leverkusen, Germany).

Since cytopsin smears were fixed in propanol and not paraffin wax, slides didn't undergo the dewaxing process as specified in section 2.10. Instead, slides were incubated in DiffQuick solution I and DiffQuick solution II for 5-10 minutes before being briefly rinsed in running tap water for a minute, followed by rinses in 75% ethanol of 3 minutes, absolute ethanol (twice), and then xylene (twice) for 5 minutes each. Once complete, slides were mount with a resinous mounting medium (DPX; Ajax Finechem, Taren Point, NSW, Australia). After the mountant dried, slides were scanned using Aperio Scanscope CS (Leica Biosystems Imaging Inc, Heidelberg, Nussloch, Germany) Aperio eSlide Manager (Leica Biosystems Imaging Inc) and analysed using Aperio ImageScope (Leica Biosystems Imaging Inc).

### 2.6.2.1 Data Analysis

Five to six random pictographs were selected from the smear of inflammatory cells. Using Aperio ImageScope (v12.3.2.8013, Leica Biosystems, Nussloch, Germany) software, these regions were boxed, and the cells were differentiated as being either eosinophils, neutrophils, lymphocytes, or monocytes and quantified. Any cell found in the region that did not fall under these categories were ignored. Once a total of 100 cells were quantified from each region, the data corresponding for each cell was averaged and expressed as a percentage. Each percentage was multiplied to the specimen's total cell count (determined in section 2.6.1), to reveal an approximate number of each of the inflammatory cells in the BALF samples collected.

## 2.7 TISSUE COLLECTION

Lung tissue was weighed (total lung weight), and then separated into individual lobes for various analysis including hydroxyproline analysis, histological analysis and MMP zymography.

## 2.8 PROTEIN ANALYSIS

### 2.8.1 Protein Extraction from Animal Tissue

Protein were extracted from the collected lung tissue using a method described by Woessner (Woessner Jr. 1995). Tissue were homogenised in buffer

made up of 0.25% (w/v) Triton-X-100 in 10mM CaCl<sub>2</sub> (20ml/grams of- wet weight tissue), using a TP18-10 Ultra-Turrax homogeniser (Janke und Kunkel-Straße, Staufen, Germany). Homogenates from each sample were then centrifuged at 3,300g for 30 minutes at 4°C and the supernatants were subsequently aspirated from the pallets (containing 85-90% of the total protein). Pellets were re-suspended in 0.1M CaCl<sub>2</sub> and then heated at 60°C in a water bath for 4 minutes with gentle shaking. Thereafter, the samples were cooled on ice for at least 5 minutes and centrifuged at 16,000g for 5 minutes at 4°C. The supernatant (the contained most of the protein) was collected and concentrated using Millipore molecular sieve concentrator (Millipore Corporation, Bedford, MA, USA) with a 10kDa molecular weight cut off, by centrifugation (at 51,000G for 30 minutes at 2°C, using Eppendorf centrifuge 5810R). Therefore, the sieves were topped with 500µl of 0.5M Tris-HCl (pH 6.8) followed by centrifuging at 51,000g for 5-10 minutes at 4°C, to equilibrate the extracts in Tris-HCl buffer, while concentrating the protein content of the extracts. The concentrated supernatant was then collected and protein content concentration for each sample was determined by the Bio-Rad protein assay dye reagent concentration method which is based on the principle of the Bradford protein assay (described in section 2.9.3). This comprises to two separate methods – either SDS-page or Tris-HCl.

### **2.8.2 Bradford protein assay**

Protein concentrations were quantified by the principle of Bradford protein assay; using a protein assay dye reagent concentrate (Bio-Rad). Protein

concentrations were determined from the concentrated supernatant extracted from lung tissue using a standard curve of 0µg, 2.5µg, 5µg, 10µg, 15µg, 20µg, and 25µg of BSA dissolved in 0.5M Tris-HCl (pH 6.8), which was made up to a volume of 800µL with distilled water. 10µL of sample was added to 790µL of distilled water, followed by 200µL of the Dye Reagent Concentrate to all standards and samples. Both standards and samples were mixed via vortexing and left to stand for 10 minutes at room temperature. The absorbance of each standard and sample was measured at 595nm (A<sub>595nm</sub>) using a Bio-Rad benchmark Plus™ microplate spectrometer. Graphs of each standard curve were constructed by plotting the measured absorbance of each standard (y-axis) against the amount of BSA protein evaluated (x-axis); the readings from each sample of interest was subsequently used to extrapolate the total protein concentration of each sample assessed.

### 2.8.3 Gelatin Zymography

Prior to performing SDS-PAGE, the sample were incubated (3-part sample:1-part buffer) in loading sample buffer (62.5Mm Tris-HCl, 10% v/v glycerol, 2% w/v SDS, 0.1% w/v bromophenol blue) for 1 hour at room temperature. For MMP2 (72kDa) and MMP9 (92kDa), 3µg of protein in 8% polyacrylamide gel containing 0.5% w/v gelatin at 100V for 1-1.5 hours. Once separation was complete, the gels were washed twice with 0.25% v/v Triton X-100 for 15 minutes to remove SDS. The gels were then incubated with incubation buffer (50mM Tris-HCl, 10mM CaCl<sub>2</sub>, 10% v/v Triton X-100, 1uM ZnCl<sub>2</sub>) at 37<sup>oC</sup> overnight to allow activation of MMP 2 and 9 to cleave gelatin. After digestion, the incubation

buffer was removed, and the gel was stained with Coomassie blue (1mg/mL Coomassie Brilliant Blue R-250, 40% v/v isopropanol) for one hour at room temperature with gentle shaking. The gels were de-stained (20% v/v methanol, 7% v/v acetic acid) at room temperature until the desired contrast was obtained. Clear bands on a dark background indicated gelatinolytic activity. The gels were scanned using BIO- RAD ChemiDoc™ MP Imaging System (Bio-Rad Laboratories, Gladesville, NSW, AU) and densitometry conducted on each band using Quantity-One software (Bio-Rad).

Images were analysed using ImageJ software (National Institute in Health, Bethesda, MD, USA). The background was removed, as per the manufacturer's instructions, to remove background fluorescence. A rectangular box of the same size was drawn around each band and the Bio-Rad software was able to determine the relative density of each band, which was then graphed.

## **2.9 HYDROXYPROLINE ASSAY**

Collagen constitutes a major portion of fibrotic scarring. As such, collagen levels within the lung were quantified to determine the severity of fibrosis. Collagen concentration measurements were determined by quantifying levels of the amino acid hydroxyproline (via colorimetric assay (Bergman & Loxley 1963)); as hydroxyproline is unique to collagen and has not been identified in any other mammalian proteins (Gallop & Paz 1975; Williams et al. 2002).

Equivalent portions of lung tissue (the second largest lobe) were collected, snap-frozen in liquid nitrogen prior to being lyophilisation in a freeze dryer (details) for dry weight measurement. Dried samples were rehydration with 0.5ml of hydrating buffer containing 150mM sodium chloride, 50mM Tris-hydrochloride and protease inhibitors (N-ethylmaleimide, phenylmethylsulfonylfluoride and benzamidine hydrochloride (Sigma-Aldrich, St. Louis, MO, USA)) for 4 hours at 4°C before being hydrolysed in 6M hydrochloric acid overnight (for 20 hours) at 110°C. The hydrolysed samples were freeze-dried overnight ahead of being re-suspended in 0.1M hydrochloric acid in preparation of hydroxyproline analysis using a scaled down version of the method described by Bergman and Loxley (1963).

To measure hydroxyproline content, 10µl of the hydrolysed tissue samples with 90µl distilled water, 200µl isopropranolol and 100µl oxidant buffer (7% w/v chloramines-T (Sigma-Aldrich) and acetate/citrate buffer in a volumetric ratio of 1:4). After being left at room temperature for 4 minutes, 1.3ml of Ehrlich's reagent (a mixture containing dimethylaminobenzaldehyde (Sigma-Aldrich) and isopropranolol) was added to each sample, giving then a bright yellow colour before being incubated for 25 minutes in a 60°C water bath with gentle shaking. At the end of the incubation period, the samples were observed to have developed a colour change; ranging from dark yellow to red; which dictated the level of hydroxyproline present in the sample.

Hydroxyproline makes up 14.4% of the amino acid composition of collagen in mammalian tissue (Gallop & Paz 1975). Therefore, collagen content was extrapolated from the level of hydroxyproline present in each sample; which was determined by constructing a standard curve; and multiplying this value by a factor of 6.94 (Gallop & Paz 1975). Resulting collagen content values were expressed as percentage collagen content the tissue dry weight (to correct for any differences in the size of the tissue sample acquired for this analysis).

## **2.10 LUNG HISTOPATHOLOGY**

The right lobe and trachea were fixed in 10% neutral buffered formalin for 12-18 hours and routinely processed before being embedded in paraffin wax. Serial 3µm sections were mounted onto Superfrost (Lomb Scientific Pty Ltd, Taren Point, NSW, Australia) slides, and incubated at 60<sup>o</sup>C for 30 minutes. Slides were dewaxed in xylene, absolute ethanol, and 70% ethanol, and rehydrated in running tap water before undergoing haematoxylin and eosin staining for peribronchial inflammation assessment, Masson trichrome for assessment of epithelial thickness and sub-epithelial collagen, and Alcian blue-periodic acid Schiff (AB-PAS) for goblet- cell quantification.

### **2.10.1 Haematoxylin and Eosin**

Slide-mounted sections were washed in distilled water for one minute after being dewaxed. Washed sections were incubated in Mayer's haematoxylin

(Amber Scientific, Midvale, WA, Australia) and then eosin (Amber Scientific, Midvale, WA, Australia) for five minutes, with one minute washes in running tap water for one minute before incubating in Scott's tap water for one minute. Following one final wash in tap water for one minute, sections were rinsed in 75% ethanol of 3 minutes, absolute ethanol (twice), and then xylene (twice) for 5 minutes each before mount with a resinous mounting medium.

### **2.10.2 Masson Trichrome**

Tissue was dewaxed and rehydrated as specified in section 2.10. Sections were stained in Weigert's iron hematoxylin working solution for 10 minutes. Subsequently, sections were rinsed in running warm tap water for 10 minutes, briefly incubated in Biebrich scarlet-acid fuchsin solution for 15 minutes, washed in distilled water and developed in phosphomolybdic-phosphotungstic acid solution for 15 minutes. Sections were then transferred directly (without rinse) to aniline blue solution and stained for 5-10 minutes, rinsed briefly in distilled water, differentiated in 1% acetic acid solution for 2-5 minutes and washed in distilled water. Finally, sections were rinsed in 75% ethanol of 3 minutes, absolute ethanol (twice), and then xylene (twice) for 5 minutes each before mount with a resinous mounting medium (DPX).

### **2.10.3 Alcian Blue-Periodic Acid Schiff**

Sections were incubated in Alcian blue pH 2.5 (1% Alcian blue in 3% acetic acid (w/v)) for 30 minutes at room temperature, before being rinsed in running

tap water till the water becomes clear and then washed in distilled water for one minute. Sections were then treated with 0.5% periodic acid (w/v) for 5 minutes, washed in distilled water for five minutes and then incubated in Schiff's reagent for 30 minutes at room temperature. After being washed in distilled water for five minutes, sections were stained in haematoxylin for 1-3 minutes and washed in running tap water for two minutes. Dip slides into 1% acid alcohol (v/v) and Scott's tap water (~10 dips), and wash in distilled water for five minutes before rinsing sections in 75% ethanol of 3 minutes, absolute ethanol (twice), and then xylene (twice) for 5 minutes each before mount with a resinous mounting medium (DPX).

#### 2.10.4 Immunohistochemistry

Following dewax, sections were incubated in 3% hydrogen peroxide (v/v) for 10 minutes, rinsed in distilled water for 1 minute before incubated and then heated in citrate buffer. Samples were then cooled to room temperature water, the tissue sections were circled using a pap pen (DAKO Denmark, Glostrup, Denmark) and incubated in 50 $\mu$ l of DAKO anti- body diluent. Once the diluent was blotted off, 50 $\mu$ l of primary antibody was added (which included biotin in tissue and primary antibody that were raised from the same species) and incubated overnight (**Table 2-1**). Slides were then wash-dipped and rinsed in 1M Tris buffer, before washing in two separate allocations of 1M Tris buffer. Slides were then incubated in HRP (from DAKO Kits) for 30-60 minutes (**Table 2-1**) before being rinsed/washed in 1M Tris buffer. DAB chromogen (DAKO Denmark,

**Table 2-1: List of various antibodies used for immunohistochemical staining**

<b>Aim</b>	<b>Target</b>	<b>Dilution</b>	<b>Secondary</b>
<b>1</b>	<b>Annexin V (S0961)</b>	<b>1:100</b>	<b>Rabbit</b>
<b>1</b>	<b>TGF-<math>\beta</math>1 (sc146)</b>	<b>1:800</b>	<b>Rabbit</b>
<b>2/3</b>	<b>TGF-<math>\beta</math>1 (sc146)</b>	<b>1:1000</b>	<b>Rabbit</b>
<b>2/3</b>	<b><math>\alpha</math>-SMA (M0851)</b>	<b>1:200</b>	<b>Mouse</b>
<b>2/3</b>	<b>TSLP (ABT330)</b>	<b>1:1000</b>	<b>Rabbit</b>
<b>2</b>	<b>Fibronectin (ab2413)</b>	<b>1:350</b>	<b>Rabbit</b>

**Table 2-1: List of various antibodies used for immunohistochemical staining.**

A summary of the various primary antibodies used for immunohistochemical staining, with their specific concentration used for each aim, and their corresponding secondary antibody

Glostrup, Denmark; 1:1000 dilution) was then added to sections for 5 minutes before slides were rinsed and washed in two separate water stations. Slides were then counter-stained with haematoxylin, rinsed in running water and incubated in Scott's tap water for one minute before they were subjected to one last wash in running tap water. Slides were finally rinsed in 75% ethanol, absolute ethanol, then xylene, before they were mounted with a resinous mounting medium (DPX).

## **2.11 MORPHOETRY**

Representative photomicrographs from haematoxylin and eosin, Masson trichrome, and AB-PAS, and all immunohistochemically-stained slides were captured from scanned images between x1 to x40 magnification using ScanScope AT Turbo (Aperio, CA, USA). Five to ten stained airways were randomly selected from across the tissue sample and analysed using Aperio ImageScope software.

### **2.11.1 Haematoxylin and eosin**

The haematoxylin and eosin stain was performed to observe the level of inflammatory cells that had amassed in the peribronchial region (outside the subepithelial layer) of the airway. This was scored based on severity (0 – no inflammatory aggregate present, 1 – mild inflammatory aggregate present, 2 – moderate inflammatory aggregate present, 3 – severe inflammatory aggregate

present), and results were expressed in arbitrary units, consistent with previous literature (Locke et al., 2007; Royce et al., 2014).

### **2.11.2 Masson trichrome**

Masson trichrome-stained slides were analysed by measuring the thickness of the epithelial and subepithelial layers and expressing the value as  $\mu\text{m}^2/\mu\text{m}$  basement membrane length, consistent with previous literature. Three regions of the airways selected were traced around using Aperio ImageScope: (i) between the airway lumen and the epithelial layer, (ii) between the epithelial layer and subepithelial layer (basement membrane), and (iii) on the outer edges of the subepithelial membrane. ImageScope provided the area and perimeter of each region traced. To determine epithelial thickness, area of region i was subtracted from region ii, and dividing it by the perimeter of region ii (basement membrane), to show the area on the epithelial layer per micrometer of basement membrane length. To determine subepithelial thickness, area of region ii was subtracted from region iii, and dividing it by the perimeter of region ii (basement membrane), to show the area on the epithelial layer per micrometer of basement membrane.

### **2.11.3 Alcian blue–periodic acid Schiff**

AB-PAS stain was used to determine the degree of goblet cell metaplasia that has developed in the airways of the samples. The AB-PAS stain dyes the mucin proteins found in the mucus secretory goblet cells purple, while the rest of the epithelium had a blue hue. Goblet cells were quantified and expressed as the number of goblet cells/100 $\mu\text{m}$  basement membrane length, consistent with

previous literature. Each of the selected airways from the slide had their basement membranes traced, and the number of purple stained goblet cells were quantified. By dividing the number of goblet cell to the length of the basement membrane, and multiplied by 100, to determine the number of goblet cells/100µm basement membrane length.

#### **2.11.4 Immunohistochemistry**

##### **2.11.4.1 Annexin V**

Annexin V is a marker of apoptosis in the airway epithelial layer and is used to measure determine the degree of epithelial damage that has development in the samples. Using immunohistochemistry, stained airways were scored based on staining intensity (0 – no staining present, 1 – mild staining present, 2 – moderate staining present, 3 – severe staining present), and results were expressed in arbitrary units, consistent with previous literature.

##### **2.11.4.2 Thymic stromal lymphopoietin**

Thymic stromal lymphopoietin (TSLP) is a marker of epithelial damage, and present in the nucleus and cytoplasm of airway epithelial cells, were immunohistochemically-stained and analysed. Similarly to the analysis of AB-PAS staining (2.11.3), cells in the epithelial layer that were immunohistochemically-stained for TSLP were quantified and expressed as the number of TSLP cells per 100µm of BM length. Each of the selected airways from the slide had their basement membranes traced, and the number of TSLP cells quantified. By dividing the number of TSLP cells to the length of the basement membrane, and

multiplied by 100, to determine the number of TSLP cells/100 $\mu$ m basement membrane length.

#### 2.11.4.3 Fibronectin

Fibronectin is a ECM protein, located in the subepithelial layer on the airway wall. Using immunohistochemistry, percentage of fibronectin in the subepithelial region was quantified using ImageScope. The epithelial layer was selected using ImageScope, and an in-built macro that was developed the accurately measure the levels of DAB chromagen in the immunohistochemically-stained sections. This categorised the stained pixels as either strong negative, weak negative, weak positive, or strong positive. The pixels marked at strong positive best represented to level of DAB-stained fibronectin in the subepithelial region, which was then expressed as a percentage to the total number of pixels detected in the subepithelial region selected.

#### 2.11.4.4 Transforming growth factor- $\beta$

Transforming growth factor (TGF)- $\beta$  is a potent profibrotic cytokine, was immunohistochemically-stained and analysed by scoring each airway based on staining intensity in Chapter 3 (0 – no staining present, 1 – mild staining present, 2 – moderate staining present, 3 – severe staining present), and results were expressed in arbitrary units.

In Chapter 4-6, a method with better accuracy was development to measure the level of TGF-  $\beta$  staining in the epithelial layer (like that used in 2.11.4.3). Using ImageScope, the epithelium was selected, and an in-built program was

used, allowing for the pixels found in the selected (epithelial) layer to be categorised, depending on the degree on staining measured in the pixel. Only the pixels that registered a strong positive stain were used and expressed as a percentage of the total number pixels.

#### 2.11.4.5 $\alpha$ -Smooth muscle actin

$\alpha$ -Smooth muscle actin ( $\alpha$ -SMA) is a marker found on myofibroblasts, which are the cells responsible for the release of ECM proteins into the subepithelial region of the airways. Using immunohistochemistry,  $\alpha$ -SMA-stained myofibroblasts were quantified in the subepithelial region, past the smooth muscle layer, which was also stained. Similarly, to AB-PAS (see 2.11.3) and TSLP (see 2.11.4.2),  $\alpha$ -SMA data was expressed at the number of  $\alpha$ -SMA-stained myofibroblasts per 100 $\mu$ m of basement membrane length. Each of the selected airways from the slide had their basement membranes traced, and the number of  $\alpha$ -SMA-stained myofibroblasts quantified. By dividing the number of  $\alpha$ -SMA-stained myofibroblasts to the length of the basement membrane, and multiplied by 100, to determine the number of TSLP cells/100 $\mu$ m basement membrane length.

## 2.12 STATISTICAL ANALYSIS

Except for data pertaining to lung function analysis, all comparative data were analysed using a one-way analysis of variance (ANOVA), with Newman-Keuls

*post-hoc* testing used to correct for multiple comparisons between groups (Prism 6; GraphPad Software Inc., San Diego, CA USA). Lung function data was analysed using a two-way ANOVA with Tukey *post-hoc* testing used to correct for multiple comparisons between groups (Prism 6). All data presented in graph or table format are expressed as mean  $\pm$  standard error of the mean (SEM), with  $p < 0.05$  considered as significantly significant.

## 2.13 REFERENCES

Bergman I, Loxley R (1963). Lung tissue hydrolysates: studies of the optimum conditions for the spectrophotometric determination of hydroxyproline. *Analyst*. **94**(120):575-584.

Essilfie AT, Simpson JL, Dunkley ML, Morgan LC, Oliver BG, Gibson PG, Foster PS, Hansbro PM (2012). Combined Haemophilus influenzae respiratory infection and allergic airways disease drives chronic infection and features of neutrophilic asthma. *Thorax*. **67**(7):588-599.

Gallop PM, Paz MA (1975). Posttranslational protein modifications, with special attention to collagen and elastin. *Physiol Rev*. **55**:418-487.

Hewitson TD, Ho WY, Samuel CS (2010). Antifibrotic properties of relaxin: in vivo mechanism of action in experimental renal tubulointerstitial fibrosis. *Endocrinology*. **151**(10):4938-4948.

Hossain MA, Rosengren KJ, Samuel CS, Shabanpoor F, Chan LJ, Bathgate RAD, WadeJD (2011). The minimal active structure of human relaxin-2. *J Biol Chem*. **286**(43):37555-37581.

Kumar RK, Herbert C, Foster PS (2008). The “classical” ovalbumin challenge model of asthma in mice. *Current drug targets*. **9**(6):485-494.

Jones ES, Black MJ, Widdop RE (2012). Influence of angiotensin II subtype 2 receptor (AT(2)R) antagonist, PD123319, on cardiovascular remodelling of aged spontaneously hypertensive rats during chronic angiotensin II subtype 1 receptor (AT(1)R) blockade. *Int J Hypertens.* **2012**(543062):1-11.

Mookerjee I, Hewitson TD, Halls ML, Summers RJ, Mathai ML, Bathgate RAD, Tregear GW, Samuel CS (2009). Relaxin inhibits renal myofibroblast differentiation via RXFP1, the nitric oxide pathway, and Smad2. *FASEBJ.* **23**(4):1219–1229.

Pini A, Shemesh R, Samuel CS, Bathgate RA, Zauberman A, Hermesh C, Wool A, Bani D, Rotman G (2010). Prevention of bleomycin-induced pulmonary fibrosis by a novel antifibrotic peptide with relaxin-like activity. *J Pharmacol Exp Ther.* **335**(3):589-599.

Royce SG, Li X, Tortorella S, Goodings LM, Chow BSM, Giraud AS, Tang MLK, Samuel CS (2014a). Mechanistic insights into the contribution of epithelial damage to airway remodelling. Novel therapeutic targets for asthma. *AJRCMB.* **50**(1)180-192.

Royce SG, Moodley Y, Samuel CS (2014). Novel therapeutic strategies for lung disorders associated with airway remodelling and fibrosis. *Pharmacol Ther.* **141**(3):250-260.

Samuel CS, Zhao C, Bathgate RAD, Bond CP, Burton MD, Parry LJ, Summers RJ, Tang MLK, Amento EP, Tregear GW (2003). Relaxin deficiency in mice is associated with an age-related progression of pulmonary fibrosis. *FACEBJ.* **17**(1):121–123.

Samuel CS, Royce SG, Burton MD, Zhao C, Tregear GW, Tang ML (2007). Relaxin plays an important role in the regulation of airway structure and function. *Endocrinology*. **148**(9):4259-4266.

Shefrin AE, Goldman RD (2009). Use of dexamethasone and prednisone in acute asthma exacerbations in pediatric patients. *Can Fam Physician*. **55**(7):704-706.

Tan JL, Lau SN, Leaw B, Nguyen HPT, Salamonsen LA, Saad MI, Chan ST, Zhu D, Krause M, Kim C, Sievert W, Wallace EM, Lim R (2018). Amnion Epithelial Cell-Derived Exosomes Restrict Lung Injury and Enhance Endogenous Lung Repair. *Stem Cell Transl Med*. **7**: 180-196.

Temelkovski J, Hogan SP, Shepherd DP, Foster PS, Kumar RK (1998). An improved murine model of asthma: selective Amnion Epithelial Cell-Derived Exosomes Restrict Lung Injury and Enhance Endogenous airway inflammation, epithelial lesions and increased methacholine responsiveness following chronic exposure to aerosolised allergen. *Thorax*. **53**(10):849-856.

Thim L, Norris K, Norris F, Nielsen PF, Bjørn SE, Christensen M, Petersen J (1993). Purification and characterization of the trefoil peptide human spasmolytic polypeptide (hSP) produced in yeast. *FEBS Lett*. **318**(3):345-352.

Williams JZ, Abumrad N, Barbul A (2002). Effect of a Specialised Amino Acid Mixture on Human Collagen Deposition. *Ann Surgery*. **236**(3):369-375.

---

**CHAPTER 3:**

**Characterizing a Refined  
Model of Allergic  
Airways Disease**

---

## Characterization of a novel model incorporating airway epithelial damage and related fibrosis to the pathogenesis of asthma

Simon G Royce<sup>1</sup>, Krupesh P Patel<sup>1</sup> and Chrisan S Samuel

Asthma develops from injury to the airways/lungs, stemming from airway inflammation (AI) and airway remodeling (AWR), both contributing to airway hyperresponsiveness (AHR). Airway epithelial damage has been identified as a new etiology of asthma but is not targeted by current treatments. Furthermore, it is poorly studied in currently used animal models of AI and AWR. Therefore, this study aimed to incorporate epithelial damage/repair with the well-established ovalbumin (OVA)-induced model of chronic allergic airway disease (AAD), which presents with AI, AWR, and AHR, mimicking several features of human asthma. A 3-day naphthalene (NA)-induced model of epithelial damage/repair was superimposed onto the 9-week OVA-induced model of chronic AAD, before 6 weeks of OVA nebulization (NA + OVA group), during the second last OVA nebulization period (OVA/NA group) or 1 day after the 6-week OVA nebulization period (OVA + NA group), using 6–8-week-old female Balb/c mice ( $n = 6–12/\text{group}$ ). Mice subjected to the 9-week OVA model, 3-day NA model or respective vehicle treatments (saline and corn oil) were used as appropriate controls. OVA alone significantly increased epithelial thickness and apoptosis, goblet cell metaplasia, TGF- $\beta$ 1, subepithelial collagen (assessed by morphometric analyses of various histological stains), total lung collagen (hydroxyproline analysis), and AHR (invasive plethysmography) compared with that in saline-treated mice (all  $P < 0.05$  vs saline treatment). NA alone caused a significant increase in epithelial denudation and apoptosis, TGF- $\beta$ 1, subepithelial, and total lung collagen compared with respective measurements from corn oil-treated controls (all  $P < 0.01$  vs corn oil treatment). All three combined models underwent varying degrees of epithelial damage and AWR, with the OVA + NA model demonstrating the greatest increase in subepithelial/total lung collagen and AHR (all  $P < 0.05$  vs OVA alone or NA alone). These combined models of airway epithelial damage/AAD demonstrated that epithelial damage is a key contributor to AWR, fibrosis and related AHR, and augments the effects of AI on these parameters.

*Laboratory Investigation* (2014) 94, 1326–1339; doi:10.1038/labinvest.2014.119; published online 29 September 2014

Asthma is a chronic inflammatory airway disease. According to the World Health Organization, ~300 million people worldwide suffer from this disease, equating to 1/250 deaths, and it is the most prevalent chronic disease affecting children.<sup>1</sup> There are three central components involved in the pathogenesis of asthma: airway inflammation (AI), airway remodeling (AWR), and airway hyperresponsiveness (AHR).<sup>1</sup> Repeated episodes of AI lead to AHR and may initiate irreversible structural changes in the airways (AWR).<sup>1</sup> However, studies have shown that AWR can also occur early in asthma pathogenesis and significantly contribute to AHR independently of AI.<sup>2</sup> Epithelial damage is a process that is emerging as a key cause of AWR, and has been shown

to expose the epithelial nerves to specific or nonspecific stimuli in patients with mild and severe AHR.<sup>3,4</sup> The epithelium is also an important physical barrier protecting the airway from pathogenic organisms and harmful substances that may be inhaled, while also having an important role in innate and adaptive immune function.<sup>3</sup> Genetic mutations can lead to the susceptibility of epithelial damage.<sup>5</sup> For example, a mutation or disruption to the E-cadherin gene, CDH1, leads to a reduction in E-cadherin levels.<sup>6</sup> This may be followed by denudation (shedding) of the epithelium, which leads to re-epithelialization, alterations in the cell types that make up the epithelium and aberrant wound healing.<sup>7,8</sup>

Fibrosis Laboratory, Department of Pharmacology, Monash University, Clayton, VIC, Australia  
Correspondence: Associate Professor CS Samuel or Dr SG Royce, Fibrosis Laboratory, Department of Pharmacology, Monash University, Clayton, VIC 3800, Australia.  
E-mail: chrisan.samuel@monash.edu or simon.royce@monash.edu

<sup>†</sup>These authors contributed equally to this work.

Received 16 December 2013; revised 5 August 2014; accepted 29 August 2014

1326

Laboratory Investigation | Volume 94 December 2014 | www.laboratoryinvestigation.org

Current asthma therapies work by either suppressing AHR<sup>9</sup> or inhibiting AI.<sup>10</sup> There are, however, several shortcomings of these currently used treatments for asthma. In the case of short- and long-acting  $\beta$ -agonists, even though they relieve AHR transiently, they do not suppress the processes that are involved in AI and AWR, which are the two main contributors to AHR.<sup>9</sup> Likewise, while corticosteroids inhibit AI and the contributions of AI to AHR, they only mildly affect AWR and, hence, AWR-induced AHR. Thus, to better develop novel treatments that can target all three central features of asthma, more research must be done in order to better understand the pathogenesis of asthma.

The limited availability of tissue and primary cells from the human airways has led many investigators to explore the potential of experimental models that can mimic the processes of human asthma. The experimental form of asthma that is induced in laboratory animals is allergic airways disease (AAD). Although all models of AAD exhibit several features of human asthma, none of these undergo the full spectrum of features seen in human disease. Currently there are several experimental models of ovalbumin (OVA)-induced AAD that have different time frames.<sup>11</sup> Acute and subacute models of AAD, which can be established over 3–4 and 7 days, respectively, undergo AI and some AWR, but do not present with airway fibrosis, which is a well-established hallmark of asthma.<sup>11,12</sup> On the other hand, chronic models of AAD exhibit AI, several features of AWR (epithelial thickening, goblet cell metaplasia) including fibrosis, an increase in the expression of pro-fibrotic factors and AHR,<sup>11</sup> but do not undergo severe epithelial damage.<sup>11</sup> There are currently several acute experimental animal models of epithelial damage, each using a different toxin to cause epithelial damage.<sup>13</sup> The best characterized is naphthalene (NA), a Clara cell-specific cytotoxicant.<sup>14</sup> Clara cells are located on the bronchial epithelium<sup>15,16</sup> and are responsible for the secretion of various products into the bronchial lining that are important for the protection of the epithelium (such as surfactant proteins)<sup>15,17</sup> as well as inhibiting inflammatory reactions mediated via the Th2 response.<sup>15,17</sup>

Our hypothesis was that superimposing the NA-induced model of epithelial damage onto the gold standard chronic OVA-induced model of AAD would exhibit a wider spectrum of features that were associated with asthma (ie, AI, airway epithelial damage, airway fibrosis, and AHR) and that may be used in the future as a better representative experimental model of human asthma. Therefore this study aimed to superimpose the NA-induced mouse model of epithelial damage onto the 9-week OVA-induced mouse model of AAD at three distinct time points to (1) determine how closely these combined models represented the features of human asthma and (2) use these models to determine the contributions of AI vs epithelial damage to fibrosis and AHR, which are the hallmarks of asthma.

## MATERIALS AND METHODS

### Animals

Six- to eight-week-old female Balb/c wild-type mice (provided by Monash University Animal Services) were allowed to acclimatize for at least 4 days prior to any experimentation and maintained on a 12-h light:dark cycle with free access to standard rodent chow (Barastoc Stockfeeds, Pakenham, VIC, Australia) and water. Female Balb/c wild-type mice have been shown to be more prone to a Th2 response and undergo higher airway reactivity (in response to allergens) compared with their male counterparts and other commonly used murine strains,<sup>18,19</sup> and as such have been used extensively in chronic AAD models.<sup>20,21</sup> All experimental procedures were performed according to the regulations approved by the Monash University Animal Ethics Committee, which adheres to the Australian Guidelines for the Care and Use of Laboratory Animal for Scientific Purposes.

### Establishing the Combined Models of AAD

Mice were subjected to three combined models of AAD: all mice were exposed to the 9-week OVA-induced model of chronic AI-induced AAD, as described previously.<sup>22</sup> Briefly, mice ( $n = 32$ ) were sensitized with two i.p. injections of 10  $\mu$ g Grade V OVA (Sigma-Aldrich, St Louis, MO, USA) and 1 mg aluminum potassium sulfate adjuvant (alum; AJAX Chemicals, Kotara, NSW, Australia) in 0.5 ml of saline on day 0 and day 14. They were then subjected to nebulization (inhalation of an aerosol) with 2.5% (w/v) OVA for 30 min, three times a week, between days 21 and 63, using an ultrasonic nebulizer (Omron NE-U07; Omron, Kyoto, Japan). Subgroups of mice received a single i.p. injection of the Clara cell-specific cytotoxicant, NA (200 mg/kg body weight; Sigma-Aldrich) (i) on day 20 (1 day before the first OVA nebulization period; NA + OVA group;  $n = 10$ ); (ii) on day 60 (during the second last OVA nebulization period; OVA/NA group;  $n = 10$ ); or (iii) on day 64 (1 day after the last OVA nebulization period; OVA + NA group;  $n = 12$ ; Figure 1).

Separate subgroups of mice subjected to the (iv) OVA-induced model of chronic AI-induced AAD alone ( $n = 10$ ) or injected with (v) 0.5 ml saline (vehicle control for OVA;  $n = 6$ ) and nebulized with saline instead of OVA (from days 21 to 63) were maintained until day 67 as controls of the combined model of AAD (Figure 1). Additionally, age-matched mice maintained under standard housing conditions until day 63 (to control for the period of time that OVA + NA-treated mice were being subjected to the 9-week OVA-induced model of AAD), and (vi) injected i.p. with NA ( $n = 10$ ) or (vii) corn oil (vehicle control for NA; Sigma-Aldrich;  $n = 6$ ) on day 64 and maintained until day 67 acted as separate controls of the combined model of AAD (Figure 1).

### Invasive Plethysmography

On day 67, all seven groups of mice ( $n = 64$  in total) had their airway resistance (AHR) measured by invasive

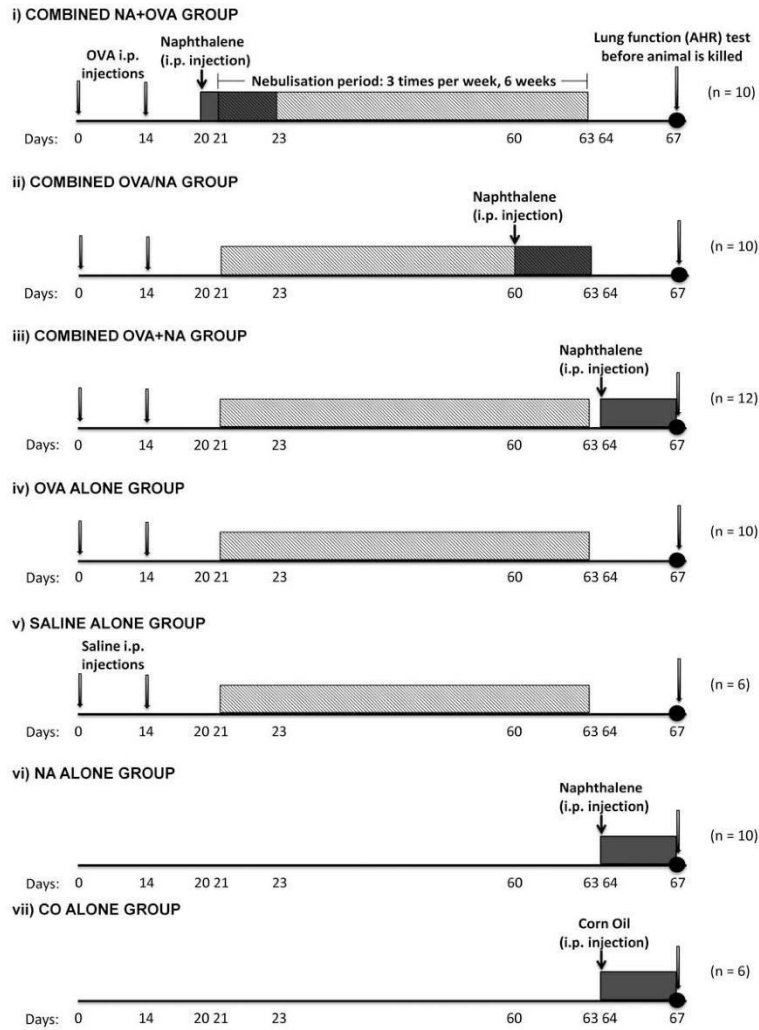


**Figure 1** A schematic illustration of how the combined (i) NA + OVA, (ii) OVA/NA, and (iii) OVA + NA-treated models were established, along with separate control groups subjected to (iv) OVA-induced AAD or (v) saline (vehicle for OVA), and (vi) NA-induced epithelial damage or (vii) CO (vehicle for NA). Note that the (vi) NA and (vii) CO alone groups were housed for 9 weeks prior to treatment, to control for the period of time that the combined groups (i–iii) were being subjected to the OVA-induced component of the model.

plethysmography, in response to increasing concentrations of methacholine-induced airway bronchoconstriction. Briefly, mice were anesthetized with an i.p. injection of ketamine (200 µg/g) and xylazine (10 µg/g), tracheostomized and the jugular vein cannulated. Mice were then ventilated with a small animal respirator (Harvard Apparatus, Holliston, MA, USA) delivering 0.01 ml/g body weight at a rate of 120 strokes per minute in a mouse plethysmograph chamber. Increasing doses of methacholine were delivered i.v. and AHR was measured (BioSystem XA version 2.7.9, Buxco Electronics, Troy, NY, USA) for 2 min after each dose. Results were then expressed as the maximal resistance after each dose of methacholine minus baseline resistance.

#### Bronchoalveolar Lavage (BAL)

Three 0.5 ml lavages were pooled in ice-cold 20% fetal calf serum (FCS)/phosphate-buffered saline (PBS) before red blood cells were lysed and cells washed twice in 5% FCS/PBS. Total viable cell counts were performed manually by trypan blue exclusion. Cytospin smears ( $2 \times 10^4$  cells) were prepared, fixed with methanol and stained with modified Wright's stain (Hema-Tek, Bayer Diagnostics, Leverkusen, Germany). Differential counts of eosinophils, neutrophils, lymphocytes and monocytes were determined using light microscopy ( $\times 40$  magnification, 100 cells counted) in a blinded manner.

#### Tissue Collection

Once airway reactivity measurements were completed, animals were killed with an overdose of anesthetic before their lung tissue isolated and rinsed in cold PBS. The lungs of each animal were then divided along the transverse plane, resulting in four separate lobes. The largest lobe was fixed in 10% neutral buffered formalin overnight, processed routinely and embedded in paraffin wax. The remaining three lobes were snap-frozen in liquid nitrogen and stored at  $-80^\circ\text{C}$  for further analyses, as detailed below.

#### Lung Histopathology

Formalin-fixed, paraffin-embedded tissues were sectioned (3 µm thickness) and placed on SuperFrost charged microscope slides (Gale Scientific, Melbourne, VIC, Australia). To assess peri-bronchial inflammation scores, one set of serial sections/mouse underwent Mayer's haematoxylin and eosin Y (H & E) staining. To assess epithelial thickness, epithelial denudation and subepithelial collagen deposition, another set of serial sections/mouse underwent Masson trichrome staining. To assess goblet cell metaplasia, a third set of serial sections/mouse underwent Alcian Blue Periodic Acid Schiff (AB-PAS) staining.

#### Histological Evaluation of Inflammation

Sections stained with H&E were observed under low power light microscopy ( $\times 40$  magnification). Histological

grading of inflammation severity from 0 to 4 was assigned to every slide (0 = no detectable inflammation; 1 = occasional inflammatory cell aggregates, pooled size  $< 0.1 \text{ mm}^2$ ; 2 = some inflammatory cell aggregates, pooled size  $\sim 0.2 \text{ mm}^2$ ; 3 = widespread inflammatory cell aggregates, pooled size  $\sim 0.3 \text{ mm}^2$ ; and 4 = widespread and massive inflammatory cell aggregates, pooled size  $\sim 0.6 \text{ mm}^2$ ), and was performed blinded by the same investigator. The area of inflammatory cell aggregates was measured using Image Pro Discovery software (Media Cybernetics, Silver Spring, MD, USA) in  $\mu\text{m}^2$  and converted to  $\text{mm}^2$ .

#### Immunohistochemistry

Paraffin-embedded lung sections were immunohistochemically stained for annexin V (a marker of apoptosis)<sup>23</sup> and TGF- $\beta$ <sup>23</sup> as described before utilizing polyclonal antibodies to annexin V (50961; 1:100 dilution; Eptomics, Burlingame, CA, USA) and TGF- $\beta$ 1 (sc146; 1:800 dilution; Santa Cruz Biotechnology, Santa Cruz, CA, USA), respectively. Detection of antibody staining was completed using the Dako EnVision anti-rabbit kit (Dako, Carpinteria, CA, USA) and 3,3'-diaminobenzidine (Sigma-Aldrich), where sections were counterstained with hematoxylin. Images of five bronchi (measuring 150–350 µm luminal diameter) per section were obtained and quantified by morphometry, as described below.

#### Morphometric Analysis

Representative photomicrographs from Masson trichrome- and AB-PAS-stained slides were captured from scanned images using ScanScope AT Turbo (Aperio, CA, USA), while immunohistochemically stained images were captured using an Olympus UC30 camera (Olympus Australia, Melbourne, VIC, Australia) attached to an Olympus BX51 microscope. Stained airways were randomly selected from across the tissue sample. Masson trichrome-stained slides were analyzed by measuring the thickness of the epithelial and subepithelial layers and expressing the value as  $\mu\text{m}^2/\mu\text{m}$  basement membrane length. AB-PAS slides were analyzed by counting the number of stained goblet cells, which were expressed as the number of goblet cells/100 µm basement membrane length. Annexin V- and TGF- $\beta$ 1-stained sections were analyzed by scoring the degree of staining around the membrane of the airway epithelial cells between 0 and 3 (where 0 represented no staining and 3 represented abundant staining).

#### Hydroxyproline Assay

The second largest lung lobe from each mouse was processed as described before<sup>11,23</sup> for the measurement of hydroxyproline content, which was determined from a standard curve of purified trans-4-hydroxy-L-proline (Sigma-Aldrich). Hydroxyproline values were multiplied by a factor of 6.94 (based on hydroxyproline representing  $\sim 14.4\%$  of the amino-acid composition of collagen in most mammalian

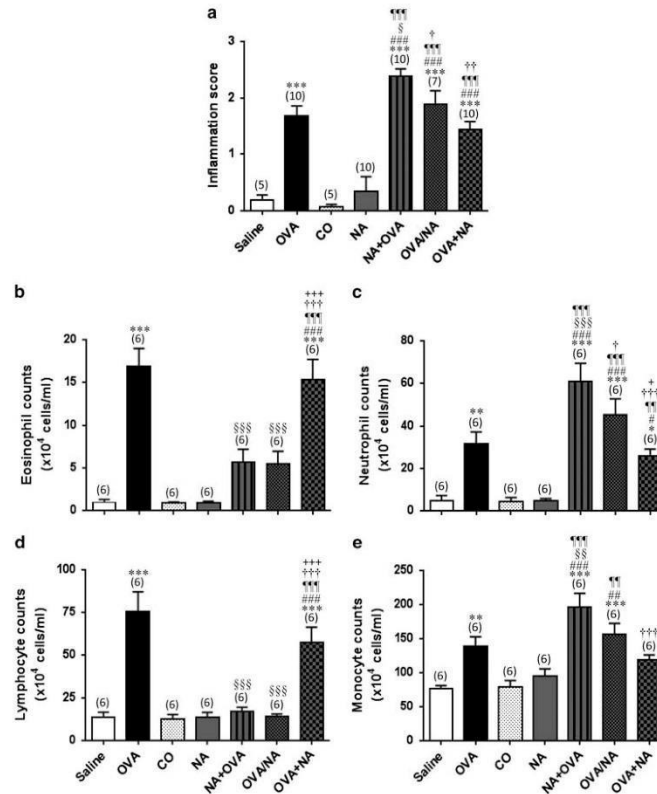


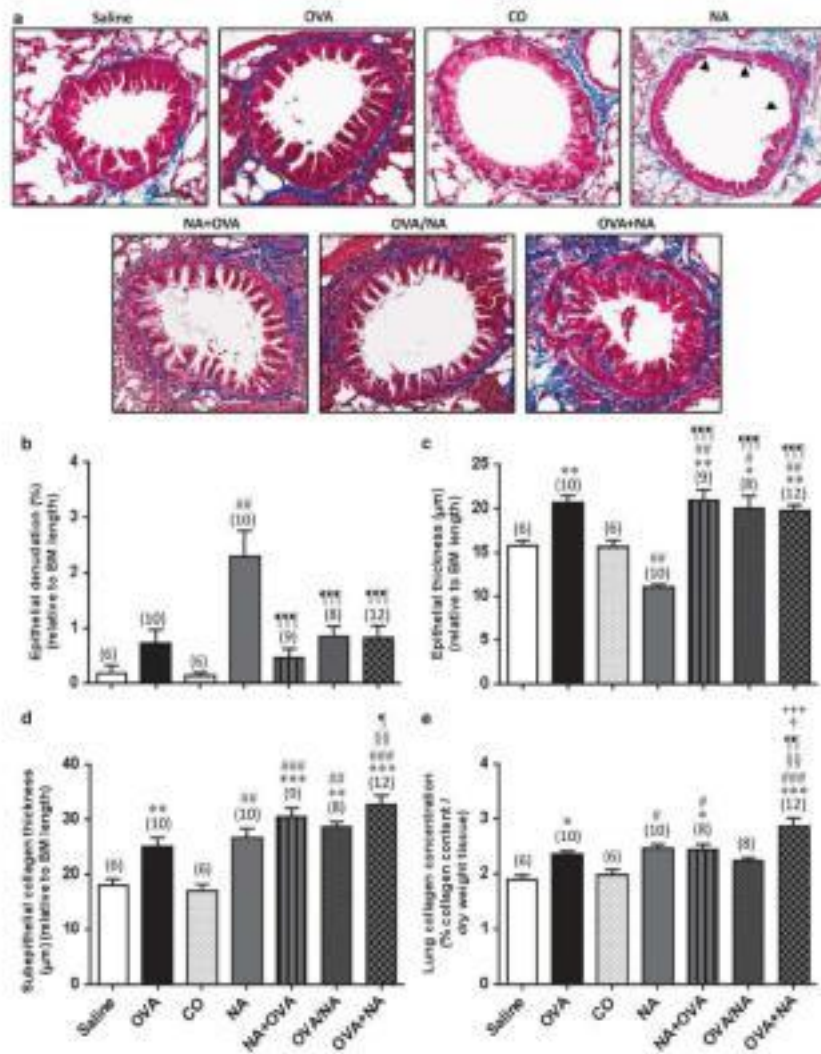
**Figure 2** Determination of airway inflammation score from H&E-stained airways and BAL differential cell counts. The mean  $\pm$  s.e.m. (a) inflammation score in H&E-stained lung sections, and number of (b) eosinophils, (c) neutrophils, (d) lymphocytes, and (e) monocytes in BAL fluid from saline-sensitized/challenged (saline), OVA-sensitized/challenged (OVA), CO-treated (CO), NA-treated (NA), and combined-treated mice. Numbers in parentheses represent the number of animals analyzed per group. \* $P < 0.05$ , \*\* $P < 0.01$ , \*\*\* $P < 0.001$  vs saline group; <sup>†</sup> $P < 0.05$ , <sup>††</sup> $P < 0.01$ , <sup>†††</sup> $P < 0.001$  vs CO group; <sup>§</sup> $P < 0.05$ , <sup>§§</sup> $P < 0.01$ , <sup>§§§</sup> $P < 0.001$  vs OVA group; <sup>¶</sup> $P < 0.01$ , <sup>¶¶</sup> $P < 0.001$  vs NA group; <sup>‡</sup> $P < 0.05$ , <sup>‡‡</sup> $P < 0.01$ , <sup>‡‡‡</sup> $P < 0.001$  vs NA + OVA group; <sup>+</sup> $P < 0.05$ , <sup>++</sup> $P < 0.01$ , <sup>+++</sup> $P < 0.001$  vs OVA/NA group.

**Figure 3** Determination of airway epithelial denudation, epithelial thickness and subepithelial collagen thickness from Masson trichrome-stained airways. (a) Representative photomicrographs of lung sections from saline-sensitized/challenged (saline), OVA-sensitized/challenged (OVA), CO-treated (CO), NA-treated (NA), and combined-treated mice, stained with Masson trichrome. The mean  $\pm$  s.e.m. (b) epithelial denudation (expressed as a % relative to BM length; indicated by arrows in the representative image of NA-treated mice), (c) epithelial thickness (in mm, relative to BM length), and (d) subepithelial collagen thickness (expressed in  $\mu$ m relative to BM length) were then morphometrically assessed from Masson trichrome-stained sections derived from each animal analyzed. Also shown is the mean  $\pm$  s.e.m. total collagen concentration (% collagen content per dry weight tissue), which was extrapolated from corresponding hydroxyproline values. Numbers in parentheses represent the number of animals analyzed per group. \* $P < 0.05$ , \*\* $P < 0.01$ , \*\*\* $P < 0.001$  vs saline group; <sup>†</sup> $P < 0.05$ , <sup>††</sup> $P < 0.01$ , <sup>†††</sup> $P < 0.001$  vs CO group; <sup>‡</sup> $P < 0.01$  vs OVA group; <sup>§</sup> $P < 0.05$ , <sup>§§</sup> $P < 0.01$ , <sup>§§§</sup> $P < 0.001$  vs NA group; <sup>||</sup> $P < 0.05$  vs NA + OVA group; <sup>|||</sup> $P < 0.001$  vs OVA/NA group.

tissues),<sup>24</sup> to extrapolate total collagen content, which in turn was divided by the dry weight of each corresponding tissue to yield percent collagen concentration.

**Statistical Analysis**

All data are expressed as the mean ± s.e.m. Lung function studies were analyzed by a two-way ANOVA with Bonferroni



*post hoc* test, whereas the remaining data were analyzed by a one-way ANOVA with Neuman–Keuls *post hoc* test for multiple comparisons between groups. In each case, significance was classified as being  $P < 0.05$ .

## RESULTS

### Individual vs Combined Effects of OVA-Induced AAD and NA-Induced Epithelial Damage on AI

Confirmation that OVA-treated mice were adequately sensitized/challenged was demonstrated by an increased inflammation score in these animals compared with that measured in saline-treated counterparts (OVA:  $1.68 \pm 0.18$  vs saline:  $0.20 \pm 0.08$ ;  $P < 0.001$  vs saline group; Figure 2a). Consistent with this, OVA-treated mice had significantly increased eosinophils (Figure 2b), neutrophils (Figure 2c), lymphocytes (Figure 2d), and monocytes (Figure 2e) in their BAL fluid compared with respective measurements obtained from saline-treated mice (all  $P < 0.01$  vs saline group). On the other hand, inflammation score and differential BAL counts were not significantly different between NA- vs CO-treated mice (Figure 2). Interestingly, NA+OVA-treated mice had a higher inflammation score than that measured in OVA-sensitized/challenged animals (NA+OVA:  $2.38 \pm 0.14$  vs OVA:  $1.68 \pm 0.18$ ;  $P < 0.05$  vs OVA group; Figure 2a). This was associated with significantly higher neutrophils (Figure 2c) and monocytes (Figure 2e; both  $P < 0.01$  vs respective measurements from the OVA group) in the BAL of these mice, while eosinophil (Figure 2b) and lymphocyte (Figure 2d) counts in NA+OVA-treated mice were significantly lower than the respective measurements obtained from their OVA alone-treated counterparts. OVA/NA-treated mice had a comparable inflammation score ( $1.89 \pm 0.23$ ; Figure 2a) as well as BAL neutrophil (Figure 2c) and monocyte (Figure 2e) counts, but significantly lower BAL eosinophils (Figure 2b) and lymphocytes than those measured in OVA alone-treated mice. Only OVA+NA-treated mice had a comparable inflammation score ( $1.44 \pm 0.14$ ; Figure 2a) and differential BAL counts (Figure 2b–e) to that measured in OVA-sensitized/challenged mice.

### Individual vs Combined Effects of OVA-Induced AAD and NA-Induced Epithelial Damage on Features of Epithelial Remodeling

#### Epithelial denudation

Epithelial denudation (extent of epithelial cell loss per  $100 \mu\text{m}$  of basement membrane) was assessed by morphometric analysis of Masson trichrome-stained lung tissue sections (Figure 3a). The mean denudation was not significantly different in OVA-sensitized/challenged mice compared with that from saline-sensitized/challenged animals (OVA:  $0.72 \pm 0.25$  vs saline:  $0.19 \pm 0.14$ ). Conversely, epithelial denudation in NA-treated mice was significantly increased compared with that measured from CO-treated mice (NA:  $2.31 \pm 0.45$  vs CO:  $0.13 \pm 0.06$ ;  $P < 0.001$  vs CO group). In comparison, epithelial denudation in NA+OVA

( $0.46 \pm 0.17$ ), OVA/NA ( $0.84 \pm 0.20$ ), and OVA+NA ( $0.83 \pm 0.22$ ) treated mice was comparable with that measured in OVA-sensitized/challenged mice ( $0.72 \pm 0.25$ ), but was significantly lower than that measured in NA-treated animals ( $2.31 \pm 0.45$ ; all  $P < 0.001$  vs the NA group; Figure 3b).

#### Epithelial thickness

Airway epithelial thickness was also assessed from Masson trichrome-stained lung tissue sections (Figure 3a) and was significantly increased in OVA-sensitized/challenged mice compared with that in saline-sensitized/challenged control animals (OVA:  $20.58 \pm 0.86$  vs saline:  $15.74 \pm 0.62$ ;  $P < 0.01$  vs saline group). Conversely, epithelial thickness in NA-treated mice was significantly decreased than that measured from CO-treated mice (NA:  $10.94 \pm 0.43$  vs CO:  $15.64 \pm 0.75$ ;  $P < 0.01$  vs CO group). In comparison, epithelial thickening in NA+OVA ( $20.90 \pm 1.25$ ), OVA/NA ( $19.99 \pm 1.41$ ) and OVA+NA ( $19.74 \pm 0.65$ ) treated mice was comparable to that measured in OVA-sensitized/challenged animals ( $20.58 \pm 0.86$ ), but was significantly higher than that measured in NA-treated mice ( $10.94 \pm 0.43$ ; all  $P < 0.001$  vs NA group; Figure 3c).

#### Goblet cell metaplasia

Goblet cell metaplasia (number of goblet cells/ $100 \mu\text{m}$  basement membrane length) was assessed by morphometric analysis of AB-PAS-stained lung tissue sections (Figure 4a). The mean number of goblet cells was significantly increased in OVA-sensitized/challenged mice compared with that from saline-sensitized/challenged animals (OVA:  $6.02 \pm 0.59$  vs saline:  $0.13 \pm 0.05$ ;  $P < 0.001$  vs saline group; Figure 4b). Conversely, there was no significant change in mean goblet cell numbers between NA-treated and CO-treated groups (NA:  $0.45 \pm 0.14$  vs CO:  $0.01 \pm 0.01$ ; Figure 4b). In comparison, goblet cell numbers in NA+OVA-treated mice ( $4.83 \pm 0.57$ ;  $P < 0.001$  vs saline, CO and NA alone groups) were not significantly different from that measured in OVA-sensitized/challenged mice ( $6.02 \pm 0.59$ ), but progressively decreased in OVA/NA ( $4.10 \pm 0.81$ ;  $P < 0.05$  vs OVA group;  $P < 0.01$  vs saline group;  $P < 0.001$  vs CO and NA alone groups), and OVA+NA ( $2.82 \pm 0.52$ ;  $P < 0.01$  vs OVA alone, CO and NA alone groups;  $P < 0.05$  vs saline and NA+OVA groups) treated animals (Figure 4b).

### Individual vs Combined Effects of OVA-Induced AAD and NA-Induced Epithelial Damage on Airway Fibrosis

#### Subepithelial lung collagen thickening

Subepithelial collagen thickness (relative to basement membrane length) was assessed from Masson trichrome-stained lung tissue sections (Figure 3a), was significantly increased in OVA-sensitized/challenged mice compared with that from saline-treated mice (OVA:  $24.95 \pm 1.70$  vs saline:  $17.99 \pm 1.19$ ;  $P < 0.01$  vs saline group), and separately in NA-treated mice compared with CO-treated control mice (NA:  $26.61 \pm 1.70$  vs CO:  $17.0 \pm 1.26$ ;  $P < 0.01$  vs CO group; Figure 3c). Sub-

epithelial collagen thickness in NA + OVA ( $30.46 \pm 1.60$ ) and OVA/NA ( $28.58 \pm 0.99$ ) treated mice were slightly higher but not statistically different from that in OVA alone ( $24.95 \pm 1.70$ ) and NA alone ( $26.61 \pm 1.70$ ) injured mice (both  $P < 0.01$  vs saline and CO groups; Figure 3c). Strikingly however, subepithelial collagen thickness in OVA + NA-treated mice ( $32.61 \pm 1.78$ ) was further increased such that it was significantly greater than that measured in OVA ( $P < 0.01$  vs OVA group) and NA ( $P < 0.05$  vs NA group) treated mice (Figure 3c).

#### Total lung collagen concentration

Total lung collagen concentration (percentage of collagen content/dry weight lung tissue) was extrapolated from hydroxyproline analysis (Figure 3d), significantly increased in OVA-sensitized/challenged mice compared with that measured from saline-sensitized/challenged control mice (OVA:  $2.35 \pm 0.07$  vs saline:  $1.90 \pm 0.07$ ;  $P < 0.05$  vs saline group), and separately in NA-treated mice compared with CO-treated mice (NA:  $2.47 \pm 0.07$  vs CO:  $1.98 \pm 0.10$ ;  $P < 0.05$  vs CO group; Figure 3d). In a similar trend to changes in subepithelial collagen thickness, total lung collagen concentration in NA + OVA ( $2.45 \pm 0.08$ ;  $P < 0.05$  vs saline and CO groups) and OVA/NA ( $2.25 \pm 0.05$ ) treated mice was not statistically different from that in OVA alone ( $2.35 \pm 0.07$ ) and NA alone ( $2.47 \pm 0.07$ ) injured mice, whereas collagen concentration in OVA + NA-treated animals ( $2.86 \pm 0.15$ ) was significantly greater than that measured in all other groups ( $P < 0.001$  vs saline, CO and OVA/NA groups;  $P < 0.01$  vs OVA alone and NA alone groups;  $P < 0.05$  vs NA + OVA group; Figure 3d).

#### Individual vs Combined Effects of OVA-Induced AAD and NA-Induced Epithelial Damage on AHR

Changes in AHR from baseline in response to increasing doses of nebulized methacholine were used to measure changes in AHR between treatment groups (Figure 5). There was a significant increase in AHR in OVA-sensitized/challenged mice compared with that measured from saline-sensitized/challenged controls ( $P < 0.05$  vs saline group). In contrast, there was no significant difference in airway reactivity between NA-treated and CO-treated mice, consistent with previous studies<sup>23</sup> and reflecting the fact that NA-treated mice undergo reparative healing by 3 days post injury, which is not associated with increased AHR. In comparison, only OVA + NA-treated mice exhibited significantly enhanced AHR compared with that measured from OVA-sensitized/challenged ( $P < 0.05$  vs OVA group) and NA-treated mice ( $P < 0.001$  vs NA group; Figure 5).

#### Individual vs Combined Effects of OVA-Induced AAD and NA-Induced Epithelial Damage on Other Parameters of Epithelial Damage and Fibrosis

Based on the findings detailed above, changes in airway epithelium apoptosis and the pro-fibrotic factor, transform-

ing growth factor (TGF)- $\beta$ 1, were additionally evaluated in OVA + NA-treated mice and compared with that in the four control groups:

#### Epithelium apoptosis

Epithelial cell apoptosis was assessed by morphometric analysis of annexin V-stained lung tissue sections (Figure 6a). Annexin V staining was significantly increased in OVA-sensitized/challenged mice compared with that from saline-sensitized/challenged animals (OVA:  $1.51 \pm 0.19$  vs saline:  $0.76 \pm 0.17$ ;  $P < 0.01$  vs saline group) and separately in NA-treated mice compared with that measured from CO-treated mice (NA:  $2.17 \pm 0.12$  vs CO:  $0.40 \pm 0.10$ ;  $P < 0.001$  vs CO group; Figure 6b). In comparison, OVA + NA-treated mice had significantly increased levels of annexin V staining compared with that from OVA-sensitized/challenged mice (OVA + NA:  $1.90 \pm 0.07$  vs OVA:  $1.51 \pm 0.19$ ;  $P < 0.05$  vs OVA group), but comparable levels of apoptosis to that measured from NA-treated animals (OVA + NA:  $1.90 \pm 0.07$  vs NA:  $2.17 \pm 0.12$  Figure 6b).

#### TGF- $\beta$ 1 expression

TGF- $\beta$ 1 expression/distribution was assessed by morphometric analysis of TGF- $\beta$ 1-stained lung tissue sections (Figure 6c). TGF- $\beta$ 1 staining was significantly increased in OVA-sensitized/challenged mice compared with that from saline-sensitized/challenged animals (OVA:  $2.36 \pm 0.26$  vs saline:  $1.00 \pm 0.15$ ;  $P < 0.001$  vs saline group) and separately in NA-treated mice compared with that measured from CO-treated animals (NA:  $2.07 \pm 0.73$  vs CO:  $1.07 \pm 0.35$ ;  $P < 0.01$  vs CO group; Figure 6d). Mean airway TGF- $\beta$ 1 staining levels trended to be higher in OVA + NA-treated mice ( $2.71 \pm 0.15$ ) compared with that in OVA alone ( $2.36 \pm 0.26$ ) and NA alone ( $2.07 \pm 0.73$ ) treated animals, although this did not reach statistical significance (Figure 6d).

#### DISCUSSION

Epithelial damage has emerged as a novel etiology of asthma, contributing to the development of AWR and subsequently AHR.<sup>23,25</sup> Despite its significance, epithelial damage has been poorly addressed in current experimental models used to study the pathogenesis of asthma, and also by currently available therapies for asthma. Thus, establishing experimental models of AAD that better reflect the pathogenesis of human asthma and incorporate the contribution of epithelial damage with other features of AWR and AHR is warranted. The current study, therefore, aimed to superimpose epithelial damage at varying time points onto the 'gold-standard' model of chronic AAD (that presents with AI, AWR, and AHR) in mice, and determined how closely these models presented with features of human asthma. The main findings obtained were that (1) airway fibrosis and AHR induced by superimposing epithelial damage after AI-induced AWR (in the OVA + NA-treated group) were further exacerbated and significantly increased

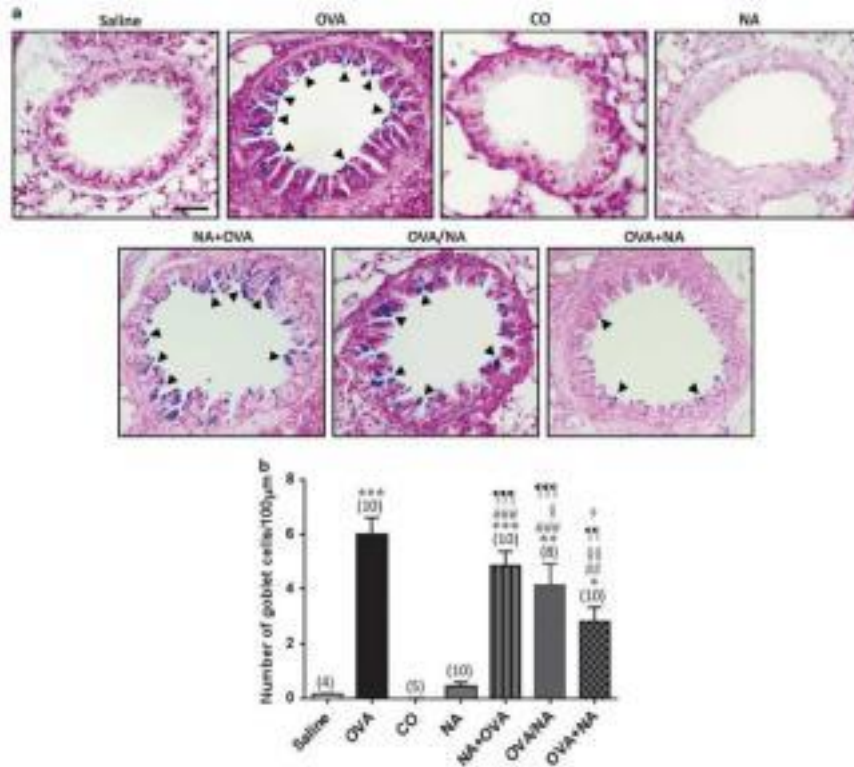


**Figure 4** Demonstration of goblet cell number from Alcian blue periodic acid Schiff (AB-PAS) stained airways. (a) Representative photomicrographs of lung sections from saline-sensitized/challenged (Saline), OVA-sensitized/challenged (OVA), CO-treated (CO), NA-treated (NA) and and combined-treated mice, stained with AB-PAS. The relative mass  $\pm$  SEM. (b) Goblet cell count (number of goblet cells/100  $\mu$ m) indicated by arrows in the representative image of OVA and combined-treated mice) was then morphometrically assessed from AB-PAS-stained sections derived from each animal analyzed. Numbers in parentheses represent the number of animals analyzed per group. \* $P < 0.05$ , \*\* $P < 0.01$ , \*\*\* $P < 0.001$  vs saline group; \*\* $P < 0.01$ , \*\*\* $P < 0.001$  vs CO group; \* $P < 0.05$ , \*\* $P < 0.01$  vs OVA group; \*\* $P < 0.01$ , \*\*\* $P < 0.001$  vs NA group; \* $P < 0.05$  vs NA + OVA group.

compared with that induced by AI alone (in the OVA-sensitized/challenged group) or epithelial damage alone (in the NA-treated group); and (2) AI and related AWR-induced bronchial epithelium apoptosis (in the OVA-sensitized/challenged group) was further exacerbated by epithelial damage (in the OVA + NA-treated group). However, (3) while epithelial damage in isolation (in the NA-treated group) led to a marked increase in epithelial denudation and significant reduction in epithelial thickness (compared with that measured in CO-treated control mice), it did not further affect these measures (in the NA + OVA, OVA/NA and

OVA + NA-treated groups) over and above that induced by AI-induced AWR (in the OVA-sensitized/challenged group). Additionally, (4) superimposing epithelial damage onto AI-induced AWR (in the combined models) resulted in a time-dependent progressive reduction in airway goblet cell metaplasia compared with that measured in OVA-sensitized/challenged mice, with the lowest levels of goblet cells observed when epithelial damage was induced after AI-induced AWR (in the OVA + NA group).

From studies performed on the NA-induced model of epithelial damage and in mice deficient of the epithelial

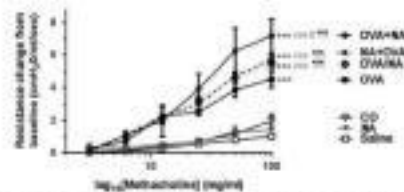


**Figure 5** Determination of airway resistance from dose-response to methacholine. The relative mean  $\pm$  s.e.m. of resistance change from baseline (0NF/OVA) was analyzed by conducting dose-responses to methacholine in bronchoconstrictor in saline-sensitized/challenged, OVA-sensitized/challenged, CO-treated, NA-treated, and combined-treated mice. \*\*\* $P < 0.001$  vs saline group; \*\* $P < 0.01$  vs CO group;  $^{\circ}P < 0.05$  vs OVA group; \*\*\* $P < 0.001$  in NA group.

repair peptide, trefoil factor 2,<sup>23,25</sup> it can be suggested that epithelial damage alone can lead to subepithelial airway fibrosis (as demonstrated by the increased NA-induced subepithelial collagen thickness and total lung collagen concentration), similar to processes occurring in human asthma where repeated episodes of epithelial injury lead to prolonged activation of the epithelial mesenchymal trophic unit.<sup>26,27</sup> Previous studies have shown that epithelial damage results in epithelial cells releasing pro-inflammatory factors such as IL-1 and tumor necrosis factor- $\alpha$ .<sup>28</sup> These factors in turn recruit and stimulate mast cells to release various factors including IL-10. IL-10 then actively recruits Th2 cells, which are stimulated to release IL-13, which in turn promotes the proliferation and differentiation of myofibroblasts from fibroblasts.<sup>3,28</sup> IL-13 also stimulates the release of the profibrotic factor TGF- $\beta$  from myofibroblasts,<sup>3,29</sup> which, when activated, stimulates the synthesis and deposition of increased matrix molecules in the subepithelial basement membrane region of the airway (resulting in increased subepithelial collagen thickness<sup>3,24,29</sup>) (Figure 7).

Additionally, the results of this study suggested that epithelial damage-induced fibrosis is further worsened when inflicted after the establishment of AI-induced AHR, leading to a concomitant worsening of AHR. Hence, both AI and epithelial damage can both independently cause inflammatory cell influx/activation and the release of various cytokines (IL-4, IL-10, IL-13, TGF- $\beta$ ) that result in myofibroblast differentiation and collagen secretion/deposition, and, when combined, result in an exacerbated level of fibrosis and related AHR (as demonstrated in the OVA + NA-treated group).

The findings from these studies also suggest that the degree of fibrosis is related to AHR, consistent with past studies<sup>30,31</sup> that have shown that in addition to collagen IV being increased in the subepithelial layer various interstitial collagens are also synthesized and deposited into areas surrounding the subepithelial and within interstitial regions of the airway in human asthma. This increase in aberrant

collagen deposition increases total wall thickness of the airway, resulting in a reduction in the diameter of the airway lumen.<sup>32,33</sup> This feature can lead to an increase in AHR, which has been extensively mathematically modeled.<sup>33,34</sup>

While this exaggerated fibrosis and AHR observed in the OVA + NA-treated model is more likely to mimic the sequence of events that take place during chronic asthma, the alterations in some aspects of the epithelial remodeling changes observed (in OVA + NA-treated mice; such as epithelial denudation and goblet cell metaplasia) were less prominent. As expected, epithelial denudation was significantly increased by NA treatment of mice (as demonstrated previously).<sup>13,35</sup> Comparatively though, epithelial denudation in OVA + NA-treated mice was similar to that measured OVA-sensitized/challenged animals, but significantly less than in NA alone-treated mice. OVA sensitization/challenge stimulates a cascade of effects that leads to the differentiation of Clara cells (the predominant cell type in the mouse airway epithelium) into goblet cells,<sup>36,37</sup> resulting in goblet cell metaplasia. Hence, by the time NA was administered to the combined model, few Clara cells may have been present (for the NA to target), correlating with the smaller amount of epithelial denudation that was observed in the OVA + NA-treated model. These findings potentially highlight the limitations of using isolated animal models of epithelial damage to mimic the pathology of human asthma, as the specific and exaggerated level of airway damage they undergo is likely to be higher than that associated with human disease. However, these findings also highlight that the etiology of epithelial damage is quite different in the combined murine model established from what occurs in humans, in which epithelial shedding is caused by an inherited predisposition to epithelial damage, which may include abnormal expression of cell-cell adhesion molecules.<sup>8</sup> Furthermore, the histology of the human airway is more complex than that of the mouse with different cell renewal lineages. Despite this, the OVA + NA-treated model still results in pathology and an end point that resembles the human epithelial lesion. Further work in this combined mouse model including time point studies and repeated epithelial injury may reveal more about the chronic asthma scenario representative of the lifelong asthma sufferer. Furthermore, this model may enable evaluation of the effect of drugs on wound healing, which has only been characterized in laboratory animals,<sup>38</sup> in the background of chronic inflammation and remodeling.

Expectedly, bronchial epithelium apoptosis was significantly higher in NA alone-treated mice (compared with that in CO-treated controls),<sup>31</sup> consistent with the epithelial denudation that these mice exhibited. Annexin V-associated apoptosis was also significantly higher in OVA-sensitized/challenged mice compared to that measured in saline controls,<sup>29</sup> and was further increased in OVA + NA-treated mice compared with OVA-sensitized/challenged animals, which was comparable to levels measured in NA alone-treated mice. As epithelial denudation was not observed in

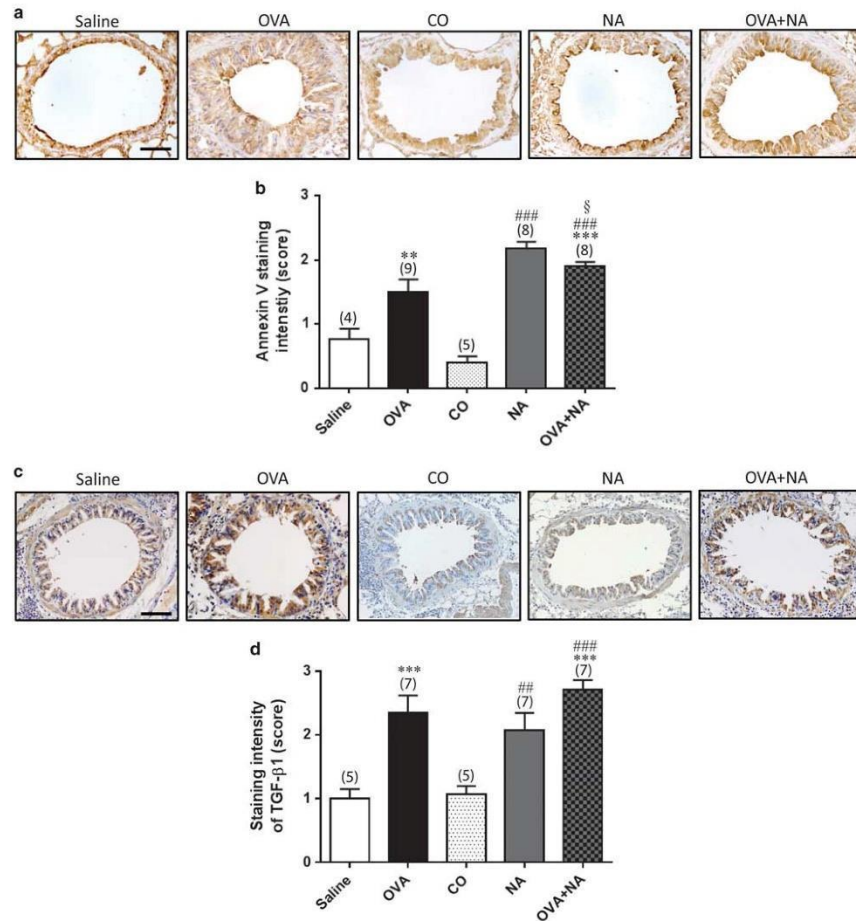
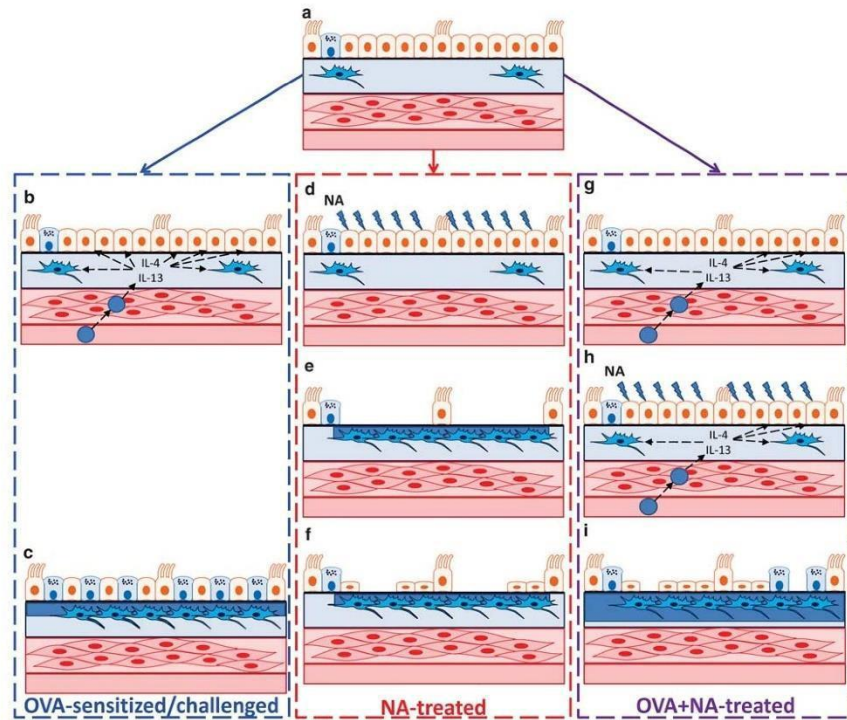


**Figure 6** Determination of epithelial cell apoptosis and TGF- $\beta$ 1 expression from immunohistochemically stained airways. Representative photomicrographs of lung sections from saline-sensitized/challenged (saline), OVA-sensitized/challenged (OVA), CO-treated (CO), NA-treated (NA), and combined-treated (OVA + NA) mice, stained for (a) annexin V (a marker of apoptosis), and (c) TGF- $\beta$ 1 expression (as a pro-fibrotic marker). The relative mean  $\pm$  s.e.m. (b) Annexin V (staining intensity scored between 0 and 3) and (d) TGF- $\beta$ 1 (staining intensity scored between 0 and 3) were then morphometrically assessed from immunohistochemically stained sections derived from each animal analyzed. Numbers in parentheses represent the number of animals analyzed per group. \*\* $P < 0.01$ , \*\*\* $P < 0.001$  vs saline group; ## $P < 0.01$ , ### $P < 0.001$  vs CO group; § $P < 0.05$  vs OVA group.

OVA-sensitized/challenged and OVA + NA-treated animals, it is likely that the cell apoptosis associated with OVA-sensitized/challenged and OVA + NA-treated mice was independent of epithelial denudation and was instead

associated with the corresponding levels of AWR and related fibrosis seen in these groups, respectively.

As demonstrated before,<sup>22</sup> goblet cell metaplasia was significantly increased in OVA-sensitized/challenged mice



**Legend:**

-  Smooth muscle cell
-  Fibroblast
-  Reticular basement membrane
-  Ciliated epithelial cell
-  Th2 cell
-  Collagen deposition
-  Clara cell
-  Induced damage
-  Subepithelial layer
-  Goblet Cell
-  Basement membrane
-  Blood vessel

**Figure 7** For caption please refer page 1338.

compared with saline controls. Interestingly, goblet cell metaplasia was less in OVA + NA-treated mice, compared with that measured in OVA mice. Airway epithelial

thickening leads to a reduction in airway lumen size, resulting in a greater degree of AHR and corresponding AHR.<sup>28</sup> Studies have shown that in nonfatal asthma epithelial

**Figure 7** The proposed sequence of events that occur in the OVA + NA-treated model. (a) The healthy lung contains airway epithelia that are primarily composed of Clara cells and, to a lesser extent, ciliated epithelial cells and goblet cells. (b) OVA sensitization/challenge-induced AI triggers an influx of inflammatory cells and Th2 cells that release a variety of cytokines, predominately IL-4 and IL-13 which stimulate (c) the (i) recruitment and differentiation of fibroblasts to myfibroblasts, resulting in increased collagen deposition and (ii) conversion of Clara cells into goblet cells. (d) On the other hand, administration of NA causes Clara cell death, resulting in (e) epithelial denudation. This in turn results in epithelium apoptosis/loss of cells from the epithelium, the recruitment and differentiation of fibroblasts into myfibroblasts, and increased collagen deposition. (f) By 72 h post NA administration, natural re-epithelialization and repair processes will be activated, resulting in the proliferation of basal cells on the exposed regions of the basement membrane. (g) In the combined model, OVA sensitization/challenge triggers the same sequences of events reported above and demonstrated in b. (h) The administration of NA on day 64 leads to limited Clara cell death (as a subset of Clara cells are already differentiated into goblet cells by OVA sensitization/challenge and epithelial denudation. (i) This in turn leads to epithelium apoptosis and exacerbated fibrosis and AHR (most likely due to OVA-induced AI and NA-induced epithelial-damage independently activating Th2 cells to secrete various factors that activate myfibroblast differentiation and myfibroblast-mediated collagen production (fibrosis). OVA-induced epithelial thickness was also maintained following NA administration.

thickness can increase by ~10–100%,<sup>11</sup> which is consistent with the findings of this study, which demonstrated that epithelial thickness was significantly and comparably increased in OVA-sensitized/challenged and OVA + NA-treated mice by ~20%, relative to that in saline animals. Based on the changes in AHR measurements between the groups, it was expected that epithelial thickness in OVA + NA-treated mice would have been greater than that measured in OVA-sensitized/challenged animals. However, the levels of epithelial thickness in the combined model may have been limited to a certain extent by NA-induced re-epithelialization. The relatively large surface area of the human respiratory tract allows for more heterogeneity with areas of normal epithelium, exposed basement membrane, goblet cell metaplasia, low re-epithelialization, and thickened epithelium, as well as squamous cell metaplasia (not seen in the mouse), corresponding to varying thicknesses and stages of the damage repair cycle related to focal lesions.<sup>39</sup>

In summary, a combined OVA + NA model was established, which developed several features of human asthma to a greater extent than the chronic AAD model. The potential advantage of this combined OVA + NA-treated model (over existing models) is that it incorporates AI, epithelial damage, AWR, and AHR as part of its pathology, and therefore is more likely to undergo structural and functional changes that are more reflective of human asthma. Additionally, given the striking increase in fibrosis and AHR that was observed in the combined model, perhaps this model can now be used to evaluate novel treatments that target epithelial damage (such as epithelial repair molecules and trefoil factors);<sup>25</sup> and related fibrosis (such as relaxin,<sup>40</sup> pirfenidone<sup>41</sup> and stem cells<sup>42</sup>). The characterization of this model has led us to demonstrate that epithelial damage is a key contributor to airway fibrosis and related AHR, and exacerbates AI-induced AWR.

#### ACKNOWLEDGMENTS

This study was supported in part by a Monash University MBio Postgraduate Discovery Scholarship (MPDS) to KPP, and Monash University Mid-Career and National Health & Medical Research Council (NHMRC) of Australia Senior Research Fellowships (APP1041766) to CSS.

#### DISCLOSURE/CONFLICT OF INTEREST

The authors declare no conflict of interest.

1. Tang ML, Wilson JW, Stewart AG, *et al*. Airway remodelling in asthma: current understanding and implications for future therapies. *Pharmacol Ther* 2006;112:474–488.
2. Malmstrom K, Pelkonen AS, Makela MJ. Remodeling, inflammation and airway responsiveness in early childhood asthma. *Curr Opin Allergy Clin Immunol* 2013;13:203–210.
3. Holgate ST. Epithelial damage and response. *Clin Exp Allergy* 2000;30(Suppl 1):37–41.
4. Laitinen LA, Heino M, Laitinen A, *et al*. Damage of the airway epithelium and bronchial reactivity in patients with asthma. *Am Rev Respir Dis* 1985;131:599–606.
5. Zhang Y, Moffatt MF, Cookson WO. Genetic and genomic approaches to asthma: new insights for the origins. *Curr Opin Pulm Med* 2012; 18:6–13.
6. Ierodiakonou D, Postma DS, Koppelman GH, *et al*. E-cadherin gene polymorphisms in asthma patients using inhaled corticosteroids. *Eur Respir J* 2011;38:1044–1052.
7. de Boer WI, Shama HS, Baelemans SM, *et al*. Altered expression of epithelial junctional proteins in atopic asthma: possible role in inflammation. *Can J Physiol Pharmacol* 2008;86:105–112.
8. Trautmann A, Kruger K, Akdis M, *et al*. Apoptosis and loss of adhesion of bronchial epithelial cells in asthma. *Int Arch Allergy Immunol* 2005; 138:142–150.
9. Sears MR, Taylor DR, Print CG, *et al*. Regular inhaled beta-agonist treatment in bronchial asthma. *Lancet* 1990;336:1391–1396.
10. Barnes PJ. New therapies for asthma: is there any progress? *Trends Pharmacol Sci* 2010;31:335–343.
11. Locke NR, Royce SG, Wainwright JS, *et al*. Comparison of airway remodeling in acute, subacute, and chronic models of allergic airways disease. *Am J Respir Cell Mol Biol* 2007;36:625–632.
12. Maes T, Provoost S, Lanckacker EA, *et al*. Mouse models to unravel the role of inhaled pollutants on allergic sensitization and airway inflammation. *Respir Res* 2010;11:7.
13. Hirota JA, Hackett TL, Inman MD, *et al*. Modeling asthma in mice: what have we learned about the airway epithelium? *Am J Respir Cell Mol Biol* 2011;44:431–438.
14. Van Winkle LS, Buckpitt AR, Nishio SJ, *et al*. Cellular response in naphthalene-induced Clara cell injury and bronchiolar epithelial repair in mice. *Am J Physiol* 1995;269:L800–L818.
15. Elizur A, Adair-Kirk TL, Kelley DG, *et al*. Clara cells impact the pulmonary innate immune response to LPS. *Am J Physiol Lung Cell Mol Physiol* 2007;293:L383–L392.
16. Gail DB, Lenfant CJ. Cells of the lung: biology and clinical implications. *Am Rev Respir Dis* 1983;127:366–387.
17. Singh G, Katyal SL. Clara cells and Clara cell 10 kD protein (CC10). *Am J Respir Cell Mol Biol* 1997;17:141–143.
18. Melgert BN, Postma DS, Kuipers I, *et al*. Female mice are more susceptible to the development of allergic airway inflammation than male mice. *Clin Exp Allergy* 2005;35:1496–1503.

19. Corteling R, Trifilieff A. Gender comparison in a murine model of allergen-driven airway inflammation and the response to budesonide treatment. *BMC Pharmacol* 2004;4:4.
20. Kumar RK, Herbert C, Foster PS. The 'classical' ovalbumin challenge model of asthma in mice. *Curr Drug Targets* 2008;9:485-494.
21. Zosky GR, Sly PD. Animal models of asthma. *Clin Exp Allergy* 2007;37:973-988.
22. Temelkovski J, Hogan SP, Shepherd DP, *et al*. An improved murine model of asthma: selective airway inflammation, epithelial lesions and increased methacholine responsiveness following chronic exposure to aerosolised allergen. *Thorax* 1998;53:849-856.
23. Royce SG, Li X, Tortorella S, *et al*. Mechanistic insights into the contribution of epithelial damage to airway remodeling: novel therapeutic targets for asthma. *Am J Respir Cell Mol Biol* 2014;50:180-192.
24. Gallop PM, Paz MA. Posttranslational protein modifications, with special attention to collagen and elastin. *Physiol Rev* 1975;55:418-487.
25. Royce SG, Lim C, Muljadi RC, *et al*. Trefoil factor-2 reverses airway remodeling changes in allergic airways disease. *Am J Respir Cell Mol Biol* 2013;48:135-144.
26. Phipps S, Benyahia F, Ou TT, *et al*. Acute allergen-induced airway remodeling in atopic asthma. *Am J Respir Cell Mol Biol* 2004;31:626-632.
27. Holgate ST, Lackie PM, Davies DE, *et al*. The bronchial epithelium as a key regulator of airway inflammation and remodelling in asthma. *Clin Exp Allergy* 1999;29(Suppl 2):90-95.
28. Elias JA, Zhu Z, Chupp G, *et al*. Airway remodeling in asthma. *J Clin Invest* 1999;104:1001-1006.
29. Tatler AL, Jenkins G. TGF-beta activation and lung fibrosis. *Proc Am Thorac Soc* 2012;9:130-136.
30. Boulet LP, Laviolette M, Turcotte H, *et al*. Bronchial subepithelial fibrosis correlates with airway responsiveness to methacholine. *Chest* 1997;112:45-52.
31. Chetta A, Foresi A, Del Donno M, *et al*. Airways remodeling is a distinctive feature of asthma and is related to severity of disease. *Chest* 1997;111:852-857.
32. Hoshino M, Nakamura Y, Sim JJ, *et al*. Inhaled corticosteroid reduced lamina reticularis of the basement membrane by modulation of insulin-like growth factor (IGF)-I expression in bronchial asthma. *Clin Exp Allergy* 1998;28:568-577.
33. Moreno RH, Hogg JC, Pare PD. Mechanics of airway narrowing. *Am Rev Respir Dis* 1986;133:1171-1180.
34. Wiggs BR, Bosken C, Pare PD, *et al*. A model of airway narrowing in asthma and in chronic obstructive pulmonary disease. *Am Rev Respir Dis* 1992;145:1251-1258.
35. Karagiannis TC, Li X, Tang MM, *et al*. Molecular model of naphthalene-induced DNA damage in the murine lung. *Hum Exp Toxicol* 2012;31:42-50.
36. Atherton HC, Jones G, Danahay H. IL-13-induced changes in the goblet cell density of human bronchial epithelial cell cultures: MAP kinase and phosphatidylinositol 3-kinase regulation. *Am J Physiol Lung Cell Mol Physiol* 2003;285:L730-L739.
37. Dabbagh K, Takeyama K, Lee HM, *et al*. IL-4 induces mucin gene expression and goblet cell metaplasia *in vitro* and *in vivo*. *J Immunol* 1999;162:6233-6237.
38. Erefalt JS, Korsgren M, Nilsson MC, *et al*. Prompt epithelial damage and restitution processes in allergen challenged guinea-pig trachea *in vivo*. *Clin Exp Allergy* 1997;27:1458-1470.
39. Crosby LM, Waters CM. Epithelial repair mechanisms in the lung. *Am J Physiol Lung Cell Mol Physiol* 2010;298:L715-L731.
40. Royce SG, Miao YR, Lee M, *et al*. Relaxin reverses airway remodeling and airway dysfunction in allergic airways disease. *Endocrinology* 2009;150:2692-2699.
41. Gomer RH. New approaches to modulating idiopathic pulmonary fibrosis. *Curr Allergy Asthma Rep* 2013;13:607-612.
42. Moodley Y, Atienza D, Manuepillai U, *et al*. Human umbilical cord mesenchymal stem cells reduce fibrosis of bleomycin-induced lung injury. *Am J Pathol* 2009;175:303-313.

---

**CHAPTER 4:**

**Treating a refined model of  
allergic airways disease  
with an epithelial repair  
factor, an antifibrotic, and  
a corticosteroid**

---

## RESEARCH PAPER

# Combining an epithelial repair factor and anti-fibrotic with a corticosteroid offers optimal treatment for allergic airways disease

Correspondence Associate Professor Christian S. Samuel and Dr Simon G. Royce, Department of Pharmacology, Monash University, Clayton, Vic. 3800, Australia. E-mail: christian.samuel@monash.edu

Received 3 February 2016; Revised 21 March 2016; Accepted 23 March 2016

K.P. Patel<sup>1</sup>, A.S. Giraud<sup>1,4</sup>, C.S. Samuel<sup>1</sup> and S.G. Royce<sup>1,2</sup>

<sup>1</sup>Fibrosis Laboratory, Cardiovascular Disease Program, Biomedical Discovery Institute and Department of Pharmacology, Monash University, Vic. Australia, <sup>2</sup>Respiratory Pharmacology Laboratory, Cardiovascular Disease Program, Biomedical Discovery Institute and Department of Pharmacology, Monash University, Vic. Australia, <sup>3</sup>Murdoch Children's Research Institute, University of Melbourne, Vic. Australia, and <sup>4</sup>Department of Paediatrics, University of Melbourne, Vic. Australia

### BACKGROUND AND PURPOSE

We evaluated the extent to which individual versus combination treatments that specifically target airway epithelial damage [trifol factor-2 (TFF2)], airway fibrosis [sarilixin (RLX)] or airway inflammation [desamethasone (DEX)] reversed the pathogenesis of chronic allergic airways disease (AAD).

### EXPERIMENTAL APPROACH

Following induction of ovalbumin (OVA)-induced chronic AAD in 6–8 week female Balb/c mice, animals were i.p. administered naphthalene (NA) on day 64 to induce epithelial damage, then received daily intranasal administration of RLX (0.8 mg mL<sup>-1</sup>), TFF2 (0.5 mg mL<sup>-1</sup>), DEX (0.5 mg mL<sup>-1</sup>), RLX + TFF2 or RLX + TFF2 + DEX from days 67–74. On day 75, lung function was assessed by invasive plethysmography, before lung tissue was isolated for analyses of various measures. The control group was treated with saline + corn oil (vehicle for NA).

### KEY RESULTS

OVA + NA-injured mice demonstrated significantly increased airway inflammation, airway remodelling (AWR) (epithelial damage/thickness; subepithelial myofibroblast differentiation, extracellular matrix accumulation and fibronectin deposition; total lung collagen concentration), and significantly reduced airway dynamic compliance (cDyn). RLX + TFF2 markedly reversed several measures of OVA + NA-induced AWR and normalized the reduction in cDyn. The combined effects of RLX + TFF2 + DEX significantly reversed peribronchial inflammation score, airway epithelial damage, subepithelial extracellular matrix accumulation/fibronectin deposition and total lung collagen concentration (by 50–90%) and also normalized the reduction of cDyn.

### CONCLUSIONS AND IMPLICATIONS

Combining an epithelial repair factor and anti-fibrotic provides an effective means of treating the AWR and dysfunction associated with AAD/asthma and may act as an effective adjunct therapy to anti-inflammatory corticosteroids.

### Abbreviations

AAD, allergic airways disease; AHR, airway hyperresponsiveness; AI, airway inflammation; AWR, airway remodelling; CO, corn oil; DEX, desamethasone; cDyn, dynamic compliance; ECM, extracellular matrix; GR, glucocorticoid receptor; H2, human gene-2; NA, naphthalene; OVA, ovalbumin; PDGF, platelet-derived growth factor; RLX, recombinant human relaxin drug/sarilixin; RXFP1 receptor, relaxin family peptide receptor 1; TFF2, trifol factor 2.

## Tables of Links

TARGETS	
<b>GPCRs<sup>a</sup></b>	<b>Enzymes<sup>b</sup></b>
$\beta_2$ -adrenoceptor	Caspase-3
EP2F1 receptor	MAP-2
<b>Nuclear hormone receptors<sup>a</sup></b>	MAP-9
Glucocorticoid receptor (GR)	

LIGANDS	
Decamethasone	TNF- $\alpha$
Fibronectin	Trans-4-hydroxy-proline
Methacholine	Thymic stromal lymphopoietin (TSLP)
TGF- $\beta$ 1	

These Tables list key protein targets and ligands in this article which are hyperlinked to corresponding entries in <http://www.guidetopharmacology.org>, the common portal for data from the IUPHAR/BPS Guide to PHARMACOLOGY (Pawson et al., 2014) and are permanently archived in the Concise Guide to PHARMACOLOGY 2015/16 (\*\*\*Alexander et al., 2015a,b,c).

## Introduction

Asthma is a chronic inflammatory airways disease and is the most prevalent chronic disease affecting children (Tang et al., 2006). According to the World Health Organization (WHO), ~300 million people worldwide suffer from the disease, attributing to 250 000 deaths annually. The WHO also estimated that a further 100 million people will suffer from asthma by the year 2025 (WHO – The Global Asthma Report 2014). The three central components of the pathogenesis of asthma are airway inflammation (AI), airway remodelling (AWR) and airway hyperresponsiveness (AHR) (Tang et al., 2006). AI is a heterogeneous T helper cell type 2 (Th2)-driven response, which has long been regarded as the central component of asthma, contributing to AHR. However, it is now known that irreversible structural changes in the airways (AWR) can occur early in the course of asthma pathogenesis and can also lead to AHR, independently of AI. AWR is a collective term used to describe many structural changes including epithelial damage and thickening, goblet cell metaplasia, subepithelial fibrosis, increased airway smooth muscle mass and neovascularization. Epithelial damage has emerged as an important aetiology of asthma, contributing to the development of AWR and subsequently, AHR (Holgate et al., 2003; Tang et al., 2006; Holgate, 2008a; Royce et al., 2014a). The airway epithelium provides physical and immunological protection against specific and non-specific inhaled stimuli (Holgate et al., 2003; Tang et al., 2006). Genetic susceptibility can impede the ability of the epithelium to protect the airway resulting in desmulation, followed by re-epithelialization, metaplasia and aberrant wound healing (leading to fibrosis) (Trautman et al., 2005; de Boer et al., 2008; Zhang et al., 2012). Despite this, it is not addressed in commonly used murine models of chronic allergic airways disease (AAD) that mimic several features observed in human asthma.

To address this limitation and the fact that currently used murine models in asthma therapy, including corticosteroids (which primarily act to suppress AI and/or short- and long-acting  $\beta_2$ -agonists (which suppress AHR independently of separating the pathogenesis of AI or AWR) do not target epithelial damage or the ensuing AWR, we recently superimposed naphthalene (NA)-induced epithelial damage onto the well-established ovalbumin (OVA)-induced murine model of chronic AAD, which presented with the three central components of asthma pathogenesis (Royce et al., 2014b). Although human asthma is not typically induced by injurious stimuli such as OVA or NA *per se*, which even in

combination would probably not cause the myriad of allergic, chemical and genetic factors associated with disease progression in humans, the strength of combining these agents in mice is that they create a model that allows investigation and therapeutic targeting of the contribution of epithelial damage to several morphological and functional processes that typify the human disease, without any confounding variables (Kumar et al., 2008). The induction of epithelial damage in the OVA + NA model was found to contribute to AWR, fibrosis and related AHR and exacerbate the effects of AI on these parameters (Royce et al., 2014b).

In the current study, we went on to use our newly established model of chronic allergic disease incorporating epithelial damage to assess how therapies targeting AI [with the anti-inflammatory corticosteroid, decamethasone (DEX)], epithelial damage [with the epithelial repair factor, trefoil factor 2 (TFE2)] and fibrosis [with the anti-fibrotic drug, serlesin (RLX)], in isolation and in combination, affected various endpoints associated with chronic asthma pathogenesis.

TFE2 is a protective molecule of the gut that is produced by intestinal epithelial cells and that promotes epithelial repair and senescence (migration) while inhibiting cell apoptosis (Amaro et al., 2014). TFE2 has also been shown to have a similar protective role in the airways/lungs (Hoffmann, 2007; Royce et al., 2014c). In the setting of chronic AAD, intranasal (i.n.) delivery of recombinant human TFE2 was able to reduce several features of AWR, subepithelial thickening and AHR (Royce et al., 2013a) by inhibiting the actions of TGF- $\beta$ 1 and PDGF, in the absence of any effects on AI. On the other hand, TFE2 knockout mice underwent exacerbated AWR when exposed to epithelial damage (Royce et al., 2014a).

RLX is a recombinantly produced peptide based on the human gene-2 (H2) relaxin sequence, which represents the major stored and circulating form of human relaxin) is a potent anti-fibrotic (Bennett, 2009; Royce et al., 2014c) that primarily acts to inhibit the actions of TGF- $\beta$ 1 on myofibroblast differentiation and myofibroblast-mediated aberrant collagen deposition. Additionally, RLX can also promote the expression and activity of various collagen-degrading MMPs (Umemoto et al., 1996) and/or inhibit tissue inhibitor of metalloproteinase activity to facilitate the breakdown of collagen, both systemic (Royce et al., 2009) and daily i.n. (Royce et al., 2014b) administration of serlesin significantly reversed several features of established AWR

(including epithelial thickening and subepithelial/total lung collagen deposition) and partially reversed AHR, in the absence of any marked effects on  $A_L$  when administered over a 2 week treatment period.

We had recently investigated the combined effects of RLX and the corticosteroid, methylprednisolone, in the chronic OVA-induced model of AAD-lacking epithelial damage as part of its pathophysiology, and found that the combined effects of both more effectively reduced subepithelial extracellular matrix (ECM) thickness compared with either therapy alone (Royce et al., 2013b). Hence, the current study was designed to further investigate the epithelial repair properties of TFF2, and whether it would potentiate the effects of RLX or RLX and DEX when added in combination, in the OVA + NA model associated with epithelial damage and the central features of human asthma. We hypothesized that combining therapies that target airway epithelial damage and fibrosis (with TFF2 and RLX, respectively) would effectively reverse AWR and AWR-induced AHR, offering a novel means to treat the structural changes associated with chronic asthma, particularly for patients that are resistant to corticosteroid exposure. We also hypothesized that combining an epithelial repair factor and anti-fibrotic could act as an adjunct therapy to the anti-inflammatory effects of DEX, which together would optimally reverse the central components of chronic asthma.

## Methods

### Animals

Six- to eight-week-old female Balb/c wild-type mice (provided by Monash University Animal Services, Clayton, Vic., Australia) were allowed to acclimatize for at least 4–5 days prior to experimentation and were maintained on a 12 h light:12 h dark cycle with free access to standard rodent chow (Barastoc Stockfeed, Pakenham, Vic., Australia) and water. Female Balb/c wild-type mice have been shown to be more prone to a Th2 response and undergo higher airway reactivity (in response to allergens) compared with their male counterparts and other commonly used murine strains (Kumar et al., 2008). All experimental procedures were performed according to the regulations approved by Monash University's Animal Ethics Committee, which adheres to the Australian Guidelines for the Care and Use of Laboratory Animals for Scientific Purposes. Animal studies are reported in compliance with the ARRIVE guidelines (Kilkenny et al., 2010; McGrath & Lilley, 2015).

### Induction and treatment of chronic AAD incorporating epithelial damage

Mice were subjected to the 9.5 week OVA-induced model of chronic AAD incorporating epithelial damage, as described previously (Royce et al., 2014b). Briefly, mice ( $n = 48$ ) were sensitized with two i.p. injections of 10  $\mu$ g grade V chicken egg OVA (Sigma-Aldrich, St Louis, MO, USA) and 1  $\mu$ g aluminium potassium sulfate adjuvant (alum; AJAX Chemicals, Kotara, NSW, Australia) in 0.5 mL of saline on days 0 and 14. They were then subjected to nebulization

(inhalation of an aerosol) with 2.5% ( $v/v$ ) OVA for 30 min, three times a week, between days 21 and 63, using an ultrasonic nebulizer (Omron NE-U07; Omron, Kyoto, Japan). The mice then received a single i.p. injection of the Clara cell-specific cytostatic, NA (200  $\text{mg}\cdot\text{kg}^{-1}$  body weight; Sigma-Aldrich) on day 64 (1 day after the last OVA nebulization period; OVA + NA group) and left for a further 3 days. From days 67 to 75, sub-groups of OVA + NA-injured mice were treated with daily i.p. administration of either (i) saline (the vehicle for OVA and all drug treatments; injury control group;  $n = 8$ ), (ii) RLX (0.8  $\text{mg}\cdot\text{mL}^{-1}$ ; kindly provided by Corthera Inc., San Carlos, CA, USA; a subsidiary of Novartis AG, Basel, Switzerland;  $n = 8$ ), (iii) recombinant human-glycosylated TFF2 (0.5  $\text{mg}\cdot\text{mL}^{-1}$ ;  $n = 8$ ), (iv) RLX and TFF2 ( $n = 8$ ), (v) DEX (0.5  $\text{mg}\cdot\text{mL}^{-1}$ ;  $n = 8$ ) or (vi) RLX, TFF2 and DEX ( $n = 8$ ). The doses of RLX (Royce et al., 2014b), TFF2 (Royce et al., 2013a) and DEX (Royce et al., 2014a) used had previously been demonstrated to mediate therapeutic and anti-fibrotic efficacy. A separate subgroup of mice subjected to (vii) i.p. injections of saline on days 0 and 14, nebulized saline instead of OVA between days 21 and 63, and an i.p. injection of corn oil (CO; the vehicle for NA;  $n = 8$ ) was included as a control group.

### Invasive plethysmography

On day 75, all seven groups of mice ( $n = 56$  in total) had their airway dynamic compliance (cDyn) measured by invasive plethysmography, in response to increasing concentrations of methacholine-induced airway bronchoconstriction. Mice were briefly anaesthetized with an i.p. injection of ketamine (100  $\text{mg}\cdot\text{kg}^{-1}$  body weight) and xylazine (20  $\text{mg}\cdot\text{kg}^{-1}$  body weight), tracheotomized and cannulated. Increasing doses of methacholine were nebulized, and AHR was measured (BioSystem EA version 2.7.5; Buxco Electronics, Troy, NY, USA) for 2 min after each dose. Differences in cDyn were analysed for statistical comparisons on the original data obtained. To then better illustrate changes in cDyn between the various treatment groups investigated, the respective baseline cDyn were subtracted from each original data point, and these data were converted to % change for each dose of methacholine used.

### Tissue collection

Once airway reactivity measurements were completed, mice were killed by an overdose of anaesthetic containing ketamine and xylazine, before their lung tissue was isolated. The lungs of each animal were then divided along the transverse plane, resulting in four separate lobes. The largest lobe was fixed in 10% neutral buffered formalin overnight, processed routinely and embedded in paraffin wax. The remaining three lobes were snap-frozen in liquid nitrogen and stored at  $-80^\circ\text{C}$  for further analyses, as detailed below.

### Lung histopathology

Formalin-fixed, paraffin-embedded tissues were sectioned (3  $\mu$ m thickness) and placed on SuperFrost charged microscope slides (Grate Scientific, Melbourne, Vic., Australia). To assess peribronchial inflammation score, one set of serial sections per mouse underwent Mayer's haematoxylin and eosin (H&E) staining. To assess epithelial and subepithelial

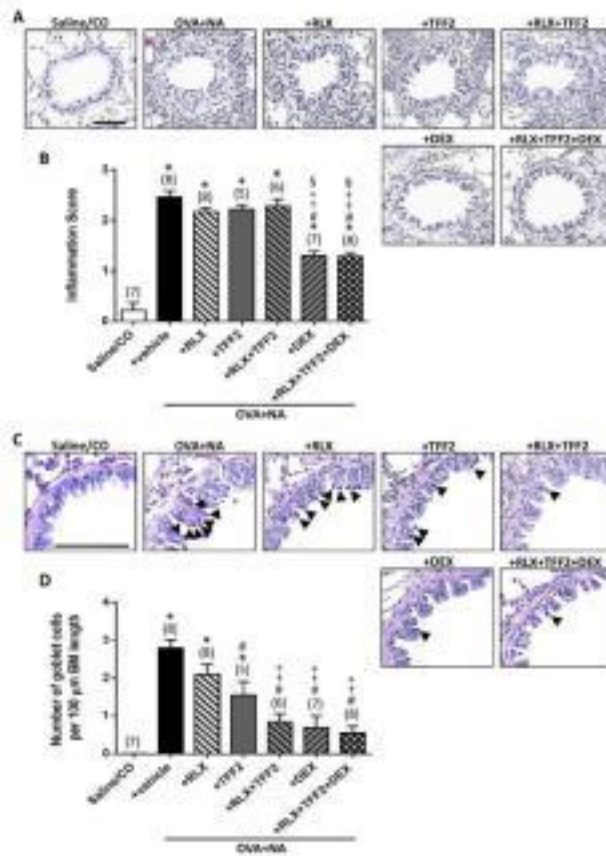


**Figure 1**

Individual versus combined effects of RLX, TFF2 and DEX on peribronchial inflammation and goblet cell metaplasia. Representative images of H&E- (A) and ABPAS-stained (C) lung sections from each of the groups studied show the extent of bronchial wall inflammatory cell infiltration (A) and goblet cells (indicated by arrows) present within the epithelial layer (C) respectively. Scale bar (A and C) = 100 μm. Also shown is the mean ± SEM inflammation score (B) and goblet cell count (per 100 μm of basement membrane length) (D) from five airways/mouse, where H&E-stained sections were scored for the number and distribution of inflammatory aggregates on a scale of 0 (no apparent inflammation) to 4 (severe inflammation). Numbers in parentheses represent the number of animals analysed per group. \**P* < 0.05 versus saline/CO-treated group; †*P* < 0.05 versus OVA + NA-treated group; ‡*P* < 0.05 versus OVA + NA + RLX-treated group; §*P* < 0.05 vs. OVA + NA + TFF2-treated group; ¶*P* < 0.05 versus OVA + NA + RLX + TFF2-treated group.

extracellular matrix thickness, another set of serial sections per mouse underwent Masson's trichrome staining. To assess goblet cell metaplasia, a third set of serial sections per mouse underwent Alcian blue periodic acid Schiff (ABPAS) staining. Stained sections were scanned using the whole-slide scanning platform Aperio Scanscope CS (Leica Biosystems,

Nussloch, Germany). All slides were then scanned at the maximum magnification available (40×) and stored as digital high-resolution images on a local server associated with the instrument. Digital slides were viewed and morphometrically analysed with the Aperio ImageScope v.12.1.0.5029 software (Leica Biosystems).

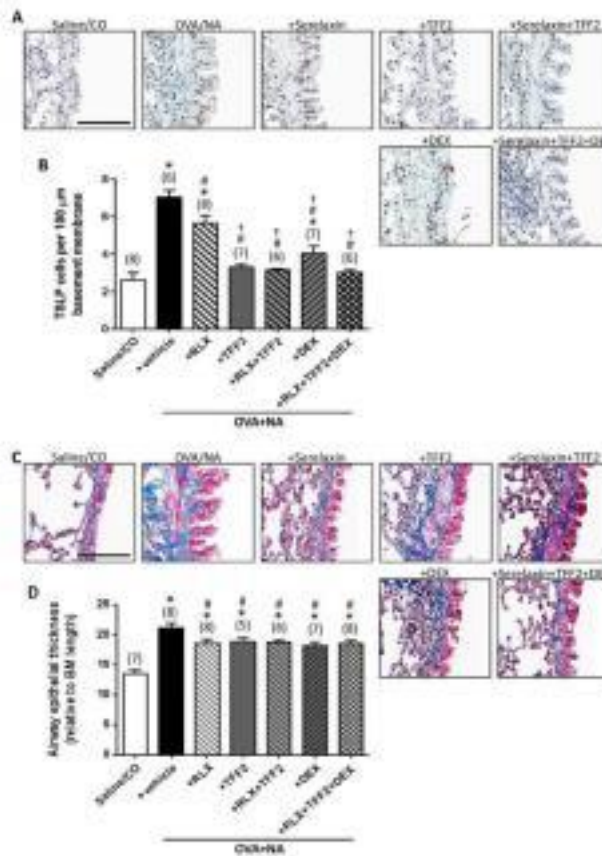


**Figure 2** Individual versus combined effects of Rlx, TFF2 and DEX on TSLP-associated epithelial damage and extent of airway epithelial thickness. Representative TSLP- (A) and Masson's trichrome-stained (C) lung sections from each of the groups studied show the extent of airway epithelial damage (A) and associated thickness (C) respectively. Scale bar (A and C) = 100 μm. Also shown is the mean ± SEM TSLP-stained cell counts (per 100 μm of basement membrane length) (B) and epithelial thickness (μm) relative to basement membrane length (D) from five airways/mouse. Numbers in parenthesis represent the number of animals analysed per group. \*P < 0.05 versus saline/CD-treated group; †P < 0.05 versus OVA + NA-treated group; ‡P < 0.05 versus OVA + NA + Rlx-treated group.

**Histological evaluation of airway inflammation**

Histological grading of inflammation severity from 0 to 4 was assigned to every slide, as described previously (Royce et al., 2014) (0 = no detectable inflammatory; 1 = occasional inflammatory cell aggregates, pooled size ~0.1 mm<sup>2</sup>; 2 = some inflammatory cell aggregates, pooled size ~0.2 mm<sup>2</sup>; 3 = widespread inflammatory cell aggregates, pooled size ~0.5 mm<sup>2</sup>; and

4 = widespread and massive inflammatory cell aggregates, pooled size ~0.6 mm<sup>2</sup>), and was performed blinded by the investigator.

**Immunohistochemistry**

Paraffin-embedded lung sections were immunohistochemically stained using either a monoclonal antibody to α-SMA (α-smooth

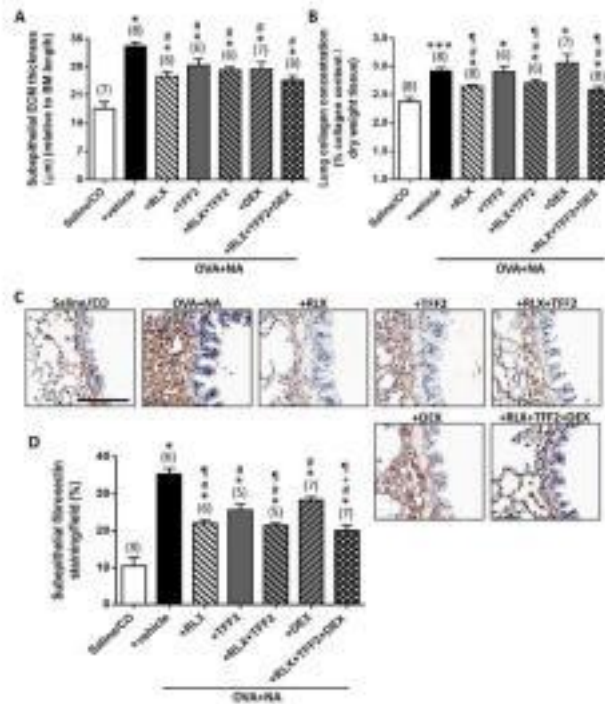


**Figure 3**

Individual versus combined effects of RLX, TF2 and DEX on subepithelial ECM thickness, lung collagen concentration and subepithelial fibronectin deposition, as measures of fibrosis. Representative fibronectin-stained (C) lung sections from each of the groups studied show the extent of subepithelial fibronectin deposition within the airways. Scale bar = 100 µm. Also shown is the mean ± SEM subepithelial ECM thickness (µm) relative to basement membrane length (which was morphometrically evaluated from Masson's trichrome-stained sections) (A), total lung collagen concentration (% collagen content per dry weight lung tissue) (B) and subepithelial fibronectin deposition (D) from five airways/mouse. Numbers in parenthesis represent the number of animals analysed per group. \**P* < 0.05 versus saline/CD-treated group; †*P* < 0.05 versus OVA + NA-treated group; ‡*P* < 0.05 versus OVA + NA + TF2-treated group; §*P* < 0.05 versus OVA + NA + DEX-treated group.

made actin; a marker of myofibroblast differentiation; M851; 1:200 dilution; DAKO, Carpinteria, CA, USA) or polyclonal antibodies to TGF-β1 (sc146; 1:1000 dilution; Santa Cruz Biotechnology, Santa Cruz, CA, USA), fibronectin (ab2413; 1:350 dilution; Cambridge, MA, USA) or thymic stromal lymphopoietin (TSLP; a marker of epithelial damage; 1:1000 dilution; EMD Millipore Corp., Temecula, CA, USA). Detection of antibody staining was completed using the DAKO EnVision anti-mouse or anti-rabbit kits, respectively, and 3,3'-diaminobenzidine (Sigma-Aldrich), where sections were counterstained with haematoxylin. Images of five bronchi (measuring 150–350 µm luminal diameter) per section were obtained and quantified by morphometry, as described below.

**Morphometric analysis**

Representative photomicrographs from H&E, Masson's trichrome- and ABPAS-stained slides, as well as immunohistochemically stained slides were captured from scanned images using ScanScope AT Turbo (Aperio, Vista, CA, USA). Matched airways were randomly selected from across the tissue sample. Masson's trichrome-stained slides were analysed by measuring the thickness of the epithelial and subepithelial layers and expressing values as µm<sup>2</sup>mm<sup>-1</sup> basement membrane length. ABPAS-stained slides were analysed by counting the number of stained goblet cells, which were expressed as the number of goblet cells 100 µm<sup>2</sup> basement membrane length. α-SMA and TSLP positively stained cells located within the subepithelial and epithelial spaces, respectively, of the airway were counted and expressed as

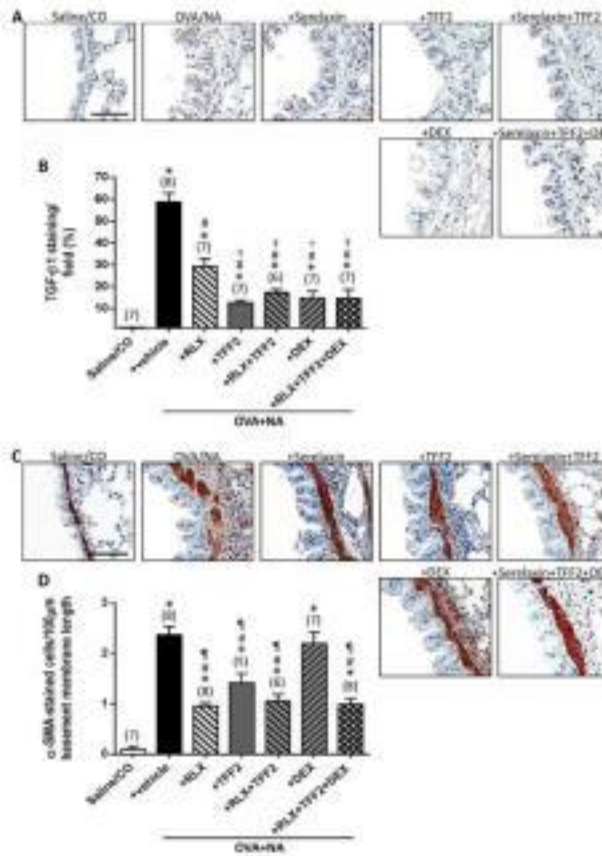


**Figure 4**

Individual versus combined effects of RLX, TFF2 and DEX on epithelial TGF-β1 expression and subepithelial myofibroblast accumulation. Representative images of immunohistochemically stained lung sections from each of the groups studied show the extent and distribution of epithelial TGF-β1 expression (A) and subepithelial myofibroblast accumulation (C) respectively. Scale bar (A and C) = 100 μm. Also shown is the mean ± SEM epithelial TGF-β1 staining (% per field) (B) and α-SMA-stained cells (per 100 μm of basement membrane length) within the subepithelial region (D) from 5 airways/mouse. Numbers in parenthesis represent the number of animals analysed per group. \*P < 0.05 versus saline/CO-treated group; †P < 0.05 versus OVA + NA-treated group; ‡P < 0.05 versus OVA + NA + RLX-treated group; §P < 0.05 versus OVA + NA + DEX-treated group.

number of positively stained cells 100 μm<sup>-2</sup> basement membrane length. Subepithelial fibronectin and epithelial TGF-β1 staining was quantified by measuring the levels of strong positively stained areas within the subepithelial and epithelial regions, respectively, and expressing the data as percentage staining per field.

**Hydroxyproline assay**

The second largest lung lobe from each mouse was processed as described previously (Bocan et al., 2009, 2014b,d) for the measurement of hydroxyproline content, which was determined from a standard curve of purified trans-4-hydroxy-L-proline (Sigma-Aldrich). Hydroxyproline values were multiplied by a

factor of 6.94 (based on hydroxyproline representing ~14.4% of the amino acid composition of collagen in most mammalian tissues) (Gallop and Fox, 1975) to extrapolate total collagen content, which in turn, was divided by the dry weight of each corresponding tissue to yield percent collagen concentration.

#### Gelatin zymography

The third largest lung lobe from each mouse was used for protein isolation and analysis of the gelatinases, MMP2 and MMP9, as described previously (Boyer et al., 2009, 2015). Equal amounts of protein extracts (4 µg) were analysed on zymogram gels consisting of 7.5% acrylamide and 1 mg·mL<sup>-1</sup> gelatin, and the gels were subsequently treated as described before (Wessner, 1995). Gelatinolytic activity was identified by clear bands at the appropriate molecular weight and quantified by densitometry using a BioRad 48710 Calibrated Imaging Densitometer (BioRad Laboratories, Richmond, CA, USA). The relative OD of the combined latent (L) and active (A) forms of MMP2 and MMP9 in each group was then expressed as the respective ratio to that of the saline/CO-treated mouse group, which was expressed as 1 in each case.

#### Statistical analysis

All data were analysed using GraphPad Prism v6.0 (La Jolla, CA, USA) and expressed as the mean ± SEM. Differences in the raw .Cdfm data were analysed by a two-way ANOVA with Bonferroni post hoc test, whereas the remaining data were analysed by a one-way ANOVA with Newman-Keuls post hoc test for multiple comparisons between groups. In each case, the significance was pre-determined as being  $P < 0.05$ . The data and statistical analysis comply with the recommendations on experimental design and analysis in pharmacology (Curtis et al., 2015).

## Results

#### Individual versus combined effects of RLX, TFF2 and DEX on airway inflammation

Confirmation that OVA + NA-treated mice were adequately sensitized/challenged to OVA was demonstrated by the elevated level of peribronchial inflammation score in these mice compared with that in their saline/CO-treated counterparts ( $P < 0.05$  vs. saline/CO group; Figure 1A and B). Treatment with RLX alone, TFF2 alone or a combination of both resulted in comparable inflammation scores with that in OVA + NA-treated mice (all  $P < 0.05$  vs. saline/CO group; Figure 1A and B). However, DEX administration, either alone or when added in combination with RLX and TFF2 resulted in a significant and equivalent reduction in inflammation score compared with that in OVA + NA-treated mice (both  $P < 0.05$  vs. OVA + NA group; Figure 1A and B), although not fully back to that measured in the saline/CO group (both  $P < 0.05$  vs. saline/CO group; Figure 1A and B). These combined findings suggested that the anti-inflammatory effects measured in the RLX + TFF2 + DEX group were probably the result of the effects of DEX alone.

#### Individual versus combined effects of RLX, TFF2 and DEX on airway remodelling

**Goblet cell metaplasia.** Goblet cell metaplasia (number of goblet cells 100 µm<sup>-2</sup> of basement length) was assessed by

morphometric analysis of ABPAS-stained lung tissue sections (Figure 1C) and was significantly increased in OVA + NA-treated mice compared with that in their saline/CO-treated counterparts ( $P < 0.05$  vs. saline/CO group; Figure 1C and D). Mean goblet cell numbers in RLX-treated mice were not significantly different from that measured in OVA + NA-treated animals ( $P < 0.05$  vs. saline/CO group; Figure 1C and D). However, goblet cell numbers were partially but significantly reduced by TFF2 treatment of mice ( $P < 0.05$  vs. OVA + NA group;  $P < 0.05$  vs. saline/CO group; Figure 1C and D) and further reduced to levels that were no longer different from that in saline/CO-treated mice by RLX + TFF2, DEX alone and the combined effects of RLX + TFF2 + DEX treatment (all  $P < 0.05$  vs. OVA + NA, OVA + NA + RLX and OVA + NA + TFF2 groups; Figure 1C and D). As a result, the combined effects of RLX + TFF2 were significantly greater than either treatment alone ( $P < 0.05$  vs. either RLX alone or TFF2 alone; Figure 1C and D).

**Epithelial damage.** Epithelial damage (measured as number of TSLP-positive cells 100 µm<sup>-2</sup> of basement membrane length) was assessed by morphometric analysis of TSLP-stained lung tissue sections (Figure 2A and B). Expectedly, OVA + NA-treated mice exhibited significantly exacerbated levels of epithelial damage compared with that measured in saline/CO-treated mice ( $P < 0.05$  vs. saline/CO group; Figure 2A and B). RLX-treated mice demonstrated a modest but significant reduction in TSLP-associated airway epithelial damage compared with that in OVA + NA-treated animals ( $P < 0.05$  vs. OVA + NA group), but which was still greater than that measured in saline/CO-treated mice ( $P < 0.05$  vs. saline/CO; Figure 2A and B). DEX treatment of mice also reduced epithelial damage ( $P < 0.05$  vs. OVA + NA group), but not fully back to that measured in saline/CO-treated controls ( $P < 0.05$  vs. saline/CO; Figure 2A and B). However, the epithelial repair factor TFF2 alone or in combination with RLX or RLX + DEX completely normalized the OVA + NA-induced increase in TSLP-associated epithelial damage after 7 days of treatment (all  $P < 0.05$  vs. OVA + NA and OVA + NA + RLX groups; no different to saline/CO-treated control group; Figure 2A and B).

**Epithelial thickness.** Epithelial thickness (relative to basement membrane length) was assessed by morphometric analysis of Masson's trichrome-stained lung tissue sections (Figure 2C and D) and was significantly increased in OVA + NA-treated mice compared with that in their saline/CO-treated counterparts ( $P < 0.05$  vs. saline/CO group). All treated groups partially but significantly reduced airway epithelial thickness to a similar extent compared with that measured in OVA + NA-treated animals (by ~30–40%; all  $P < 0.05$  vs. OVA + NA group), but not fully back to that measured in saline/CO-treated control mice (all  $P < 0.05$  vs. saline/CO group; Figure 2C and D).

#### Individual versus combined effects of RLX, TFF2 and DEX on airway fibrosis

**Subepithelial ECM thickness.** Subepithelial ECM thickness (relative to basement membrane length) was assessed by morphometric analysis of Masson's trichrome-stained lung tissue sections (Figure 3A) and was significantly increased in OVA + NA-treated mice compared with that measured from

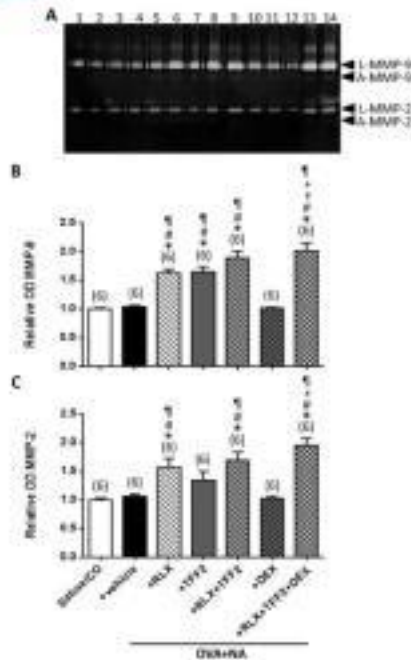


**Figure 5** Individual versus combined effects of RLX, TFF2 and DEX on lung MMP-9 and MMP-2 expression and activity. A representative gelatin zymograph (A) shows latent (L) MMP-9 (gelatinase B; 92 kDa) and MMP-2 (gelatinase A; 72 kDa) expression levels and their corresponding active (A) forms from each of the groups studied (2 samples per group). Two separate zymographs, each analyzing two additional samples per group, produced similar results. Also shown is the mean  $\pm$  SEM relative OD (of the combined L form and A forms of MMP-9 (B) and MMP-2 (C)) to that in the saline/CO-treated control group, which is expressed as 1 in each case; from  $n = 6$  mice per group. \* $P < 0.05$  versus saline/CO-treated group;  $^{\#}P < 0.05$  versus OVA + NA-treated group;  $^{\dagger}P < 0.05$  versus OVA + NA + RLX-treated group;  $^{\ddagger}P < 0.05$  versus OVA + NA + TFF2-treated group;  $^{\S}P < 0.05$  versus OVA + NA + DEX-treated group.

saline/CO-treated controls ( $P < 0.05$  vs. saline/CO group). All treated groups partially but significantly reduced subepithelial ECM thickness (by ~28–50%; all  $P < 0.05$  vs. OVA + NA groups). However, neither of the treatment groups investigated were able to fully restore the OVA + NA-induced increase in subepithelial collagen thickness back to that measured in saline/CO-treated mice after 7 days (all  $P < 0.05$  vs. saline/CO group) (Figure 3A).

**Total lung collagen concentration.** Total lung collagen concentration (% collagen content/dry weight lung tissue)

was extrapolated from hydroxyproline analysis of lung tissues (Figure 3B) and again was significantly elevated in OVA + NA-treated mice compared with that in their saline/CO-treated counterparts ( $P < 0.05$  vs. saline/CO). Interestingly, neither TFF2 nor DEX treatment alone significantly affected the OVA + NA-induced increase in lung collagen concentration. However, RLX alone and in combination with TFF2 or TFF2 + DEX significantly ameliorated the aberrant lung collagen concentration (by ~40–60%; all  $P < 0.05$  vs. OVA + NA and OVA + NA + DEX groups; Figure 3B). Again though, total lung collagen concentration in the RLX-treated groups was not fully reversed back to that measured in saline/CO-treated mice after 7 days (all  $P < 0.05$  vs. saline/CO group; Figure 3B).

**Subepithelial fibronectin expression.** As TFF2 and DEX were able to attenuate the OVA + NA-induced increase in subepithelial ECM thickness but not total lung collagen concentration, the effects of all treatments investigated on subepithelial fibronectin was then evaluated. Fibronectin expression in the subepithelial airway region (relative to basement membrane length) was assessed by morphometric analysis of fibronectin-stained lung tissue sections (Figure 3C and D) and was significantly greater in OVA + NA-treated mice compared with that in saline/CO-treated controls ( $P < 0.05$  vs. saline/CO group). TFF2 or DEX treatment alone significantly ameliorated the OVA + NA-induced increase in subepithelial fibronectin accumulation by ~30–40% (both  $P < 0.05$  vs. OVA + NA group; Figure 3C and D), suggesting that their ability to attenuate subepithelial ECM thickness was due to effects on fibronectin rather than collagen. RLX alone and in combination with TFF2 further ameliorated the OVA + NA-induced increase in aberrant subepithelial fibronectin deposition (by ~55–57%) to a greater extent than DEX alone (both  $P < 0.05$  vs. OVA + NA and OVA + NA + DEX groups), while the combined effects of RLX + TFF2 + DEX markedly reduced aberrant subepithelial fibronectin deposition (by ~60%) to a greater extent than either DEX alone or TFF2 alone ( $P < 0.05$  vs. OVA + NA, OVA + NA + DEX and OVA + NA + TFF2 groups; Figure 3D).

**TGF- $\beta$ 1 expression.** TGF- $\beta$ 1 expression and distribution in the airway epithelium (relative to basement membrane length) was assessed by morphometric analysis of TGF- $\beta$ 1-stained lung tissue sections (Figure 4A and B), and was markedly increased in OVA + NA-treated mice compared with that measured from saline/CO-treated animals ( $P < 0.05$  vs. saline/CO group). RLX alone partially but significantly reduced the aberrant epithelial TGF- $\beta$ 1 expression levels (by ~50%;  $P < 0.05$  vs. OVA + NA group). In comparison, epithelial TGF- $\beta$ 1 levels were further reduced to a greater extent (by ~70–80%) by all other treatment groups studied, compared with the effects of RLX alone (all  $P < 0.05$  vs. OVA + NA and OVA + NA + RLX groups; Figure 4A and B). Again though, neither treatment group was able to fully restore the OVA + NA-induced increase in epithelial TGF- $\beta$ 1 expression back to that measured in control mice (all  $P < 0.05$  vs. saline/CO-treated group).

**Myofibroblast differentiation.** The number of  $\alpha$ -SMA-stained positive cells (per 100  $\mu$ m of basement length) in the

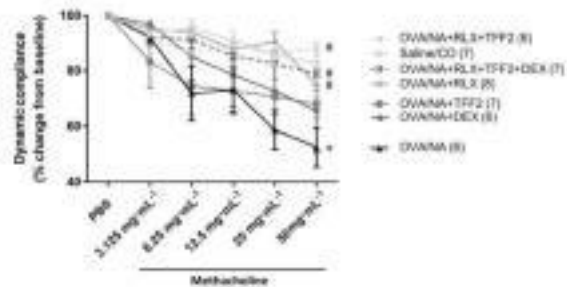


**Figure 6** Individual versus combined effects of RLX, TFF2 and DEX on cDyn. cDyn was measured in response to increasing concentrations of methacholine-induced airway bronchoconstriction, as an indicator of the lung's ability to stretch and expand. Shown is the mean  $\pm$  SEM loss of cDyn to each dose of methacholine tested. Numbers in parentheses represent the number of animals analysed per group. \* $P < 0.05$  versus saline/CO-treated group. † $P < 0.05$  versus OVA + NA-treated group.

**Table 1** Summary of the individual versus combined effects of RLX, TFF2 and DEX in the OVA + NA model

Key Features of human asthma		OVA + NA	OVA + NA + RLX	OVA + NA + TFF2	OVA + NA + RLX + TFF2	OVA + NA + DEX	OVA + NA + RLX + TFF2 + DEX
		AI	↑	–	–	–	–
AIR	Goblet cell count	↑	–	↓	↓	↓	↓
	Epithelial damage	↑	↓	↓	↓	↓	↓
	Epithelial thickness	↑	↓	↓	↓	↓	↓
Fibrosis	Subepithelial ECM	↑	↓	↓	↓	↓	↓
	Total collagen	↑	↓	–	↓	–	↓
	Fibronectin	↑	↓	↓	↓	↓	↓
	TGF- $\beta$ 1	↑	↓	↓	↓	↓	↓
	$\alpha$ -SMA	↑	↓	↓	↓	–	↓
	MMP-2	–	↑	–	↑	–	↑
	MMP-9	–	↑	↑	↑	–	↑
AHR	cDyn	↓	↑	–	↑	–	↑

A summary of the individual versus combined effects of RLX, TFF2 and DEX on chronic AAD-induced AI, AIR, fibrosis and cDyn. The arrows in the OVA + NA column are reflective of changes from that measured in saline/CO-treated mice, while the arrows in the various treatment groups are reflective of changes to that in the OVA + NA group. – denotes no changes compared to the effects of OVA + NA alone. AAD, allergic airways disease; AI, airway inflammation; AHR, airway hyperresponsiveness; AIR, airway remodeling; cDyn, dynamic compliance; CO, corn oil; DEX, dexamethasone; NA, naphthalene; OVA, ovalbumin; RLX, relaxin; TFF2, trefoil factor 2.

subepithelial layer of various airways was assessed by morphometric analysis of  $\alpha$ -SMA-stained lung tissue sections (Figure 4C and D) and was significantly increased in OVA + NA-treated mice compared with that measured in their saline/CO-treated counterparts ( $P < 0.05$  vs. saline/CO group). With the exception of DEX alone, all other treatment groups were able to significantly reduce the OVA + NA-induced increase in subepithelial myofibroblast accumulation (by  $\sim$ 43–62% all  $P < 0.05$  vs. OVA + NA and OVA + NA + DEX groups; Figure 4C and D), however, not

fully back to that measured in saline/CO-treated mice (all  $P < 0.05$  vs. saline/CO-treated group; Figure 4C and D).

**Gelatinase expression and activity.** Changes in gelatinase expression and activity were assessed by zymography to determine if the treatment-induced changes in fibrosis observed were associated with their ability to regulate enzymes involved in collagen degradation. Both MMP2 (Figure 5A and C) and MMP9 (Figure 5A and B) levels were comparable between saline/CO-treated, OVA + NA-treated and OVA + NA + DEX-

treated mice. However, MMP9 expression and activity was significantly increased by RLX alone (by +63%), TFF2 alone (by +65%), RLX + TFF2 (by +89%) and RLX + TFF2 + DEX (by +101%) after 7 days of administration (all  $P < 0.05$  vs. saline/CO), OVA + NA and OVA + NA + DEX groups (Figure 5A and B). Similarly, MMP-2 expression and activity was significantly increased by RLX alone (by +57%), RLX + TFF2 (by +68%) and RLX + TFF2 + DEX (by +95%) (all  $P < 0.05$  vs. saline/CO, OVA + NA and OVA + NA + DEX groups (Figure 5A and C), but not by TFF2 alone over the same time period. The combined effects of all three drugs also promoted both MMP9 levels to a greater extent than either RLX alone or TFF2 alone ( $P < 0.05$  vs. OVA + NA + RLX and OVA + NA + TFF2 groups (Figure 5A and B) and MMP-2 levels to a greater extent than TFF2 alone ( $P < 0.05$  vs. OVA + NA + TFF2 group (Figure 5A and C).

**Individual versus combined effects of RLX, TFF2 and DEX on dynamic airway compliance.** Changes in cDyn between treatment groups were measured by invasive plethysmography in response to increasing doses of nebulized methacholine (Figure 6). Consistent with the increased AI, AWR and fibrosis associated with OVA + NA-treated mice, these mice with chronic AAD demonstrated significantly reduced cDyn (by almost 50%;  $P < 0.05$  vs. saline/CO-treated group (Figure 6). RLX alone, but not TFF2 alone or DEX alone, was able to normalize the OVA + NA-induced reduction in cDyn back to that measured in saline/CO-treated mice ( $P < 0.05$  vs. OVA + NA-treated group; no different to saline/CO group (Figure 6). The combined effects of RLX + TFF2 or RLX + TFF2 + DEX also completely normalized the OVA + NA-induced reduction in cDyn after 7 days of treatment (both  $P < 0.05$  vs. OVA + NA-treated group (Figure 6).

## Discussion and conclusions

In this study, we evaluated how inhaled therapies targeting AI (with the anti-inflammatory corticosteroid, DEX), epithelial damage (with the epithelial repair factor, TFF2) or airway/lung fibrosis (with the anti-fibrotic drug, RLX) in isolation and in combination, affected various endpoints associated with the pathogenesis of asthma (see Table 1 for summary). Given that either RLX (Royce et al., 2009; Royce et al., 2014b) or TFF2 (Royce et al., 2013a) alone demonstrated significant anti-fibrotic efficacy after 14 days of administration in the OVA-induced model of chronic AAD, a 7 day treatment period was intentionally chosen so that the potential additive effects of these drugs could be examined in the current investigation.

DEX alone significantly reversed the AI, goblet cell metaplasia, epithelial damage and thickness as well as the aberrant epithelial TGF- $\beta$ 1 and subepithelial fibronectin expression induced by chronic AAD, but did not affect the AAD-induced myofibroblast differentiation, total lung collagen concentration, gelatinase activity nor cDyn over the 7 day treatment period. These findings are consistent with those of others demonstrating that corticosteroids primarily target the AI and, to a lesser extent, epithelial damage, but not AWR and related fibrosis associated with asthma (Knight and Holgate, 2003; Girodet et al., 2011; Royce et al., 2014c), which contributes to their progressive ineffectiveness in treating the airway/lung dysfunction in chronic/severe disease settings. However, while they may seem at odds with the DEX-induced reduction of MMP-2 and

MMP-9 that have been reported in mice subjected to OVA-induced AAD alone (Xu et al., 2012; Gurusamy et al., 2016), this may be explained by the fact that NA administration is likely to change the cellular composition of the airway epithelium, from mainly differentiated secretory cell types (which are the main source of MMPs (Tang et al., 2006)) to cuboidal cells that have a reduced secretory phenotype, which would produce significantly less MMPs. This is consistent with there being no marked changes in MMP-2 or MMP-9 level in the OVA + NA model, in which the lack of an up-regulation of these MMPs may not have provided an aberrant target for DEX to mediate its gelatinase-inhibitory actions.

On the other hand, TFF2 alone partially reversed the goblet cell metaplasia, epithelial damage and thickness, aberrant TGF- $\beta$ 1 expression, myofibroblast differentiation and fibronectin deposition associated with chronic AAD and promoted MMP9 but not MMP-2 expression and activity. However, it did not affect the AAD-induced AI, aberrant lung collagen deposition or loss of cDyn, suggesting that its direct epithelial-repairing properties were able to indirectly alleviate AWR to some extent, but not to that which affected airway/lung fibrosis and related dysfunction. In comparison, RLX alone significantly reduced the chronic AAD-induced epithelial damage and thickness, aberrant TGF- $\beta$ 1 expression, subepithelial myofibroblast differentiation and fibronectin expression as well as total lung collagen concentration in the absence of any direct effects on AI. RLX also significantly increased both MMP-2 and MMP-9 expression and activity and normalized the OVA + NA-induced reduction in cDyn after just 7 days of treatment. These findings are consistent with the anti-remodelling and anti-fibrotic effects of both systemic (Royce et al., 2009, 2013b) and i.n. (Royce et al., 2014b) RLX administration that partially restored the chronic AAD-induced increase in AHR.

Combining RLX and TFF2 was able to markedly reduce the chronic AAD-induced goblet cell metaplasia to a greater extent than either therapy alone, significantly lower epithelial damage and thickness as well as aberrant epithelial TGF- $\beta$ 1 expression levels to an equivalent extent as TFF2 alone, reverse the chronic AAD-induced increase in myofibroblast accumulation, subepithelial ECM/fibronectin deposition and total lung collagen concentration and promote collagen-degrading MMP-2 and MMP-9 levels to an equivalent extent as RLX alone, in the absence of any direct effects on AI, which remarkably resulted in the complete normalization of the AAD-induced loss of cDyn after as little as 7 days of treatment. Further combining DEX with RLX and TFF2 offered even greater protection against the AI, epithelial damage, AWR and lung dysfunction associated with chronic AAD/asthma, resulting in the complete normalization of chronic AAD-induced epithelial damage and loss of cDyn, suggesting that these combination therapies may serve as the basis of future personalized therapies for particular asthma endotypes.

This study confirmed a number of important findings: firstly that airway epithelial damage and the ensuing fibrosis it causes are key contributors to lung dysfunction and exacerbate the effects of AI on AWR and AHR (Royce et al., 2014d) as well as cDyn. Epithelial damage has been shown to result in epithelial cells releasing pro-inflammatory factors such as IL-1 and TNF- $\alpha$  (Elias et al., 1999; Holgate, 2000), which in turn, recruit and stimulate mast cells to release various factors including IL-10. IL-10 then actively recruits Th2 cells, which are stimulated to release IL-13, which in turn, can both promote fibroblast proliferation and differentiation into activated

myofibroblasts, while also stimulating the release of pro-fibrotic TGF- $\beta$ 1 activity (Elias *et al.*, 1999; Holgate, 2000). TGF- $\beta$ 1 potently stimulates myofibroblast-mediated ECM and collagen deposition in the subepithelial basement membrane and eventually the interstitial space, resulting in the aberrant increase of subepithelial and interstitial ECM/collagen accumulation. Consistent with this, superimposing epithelial damage onto the pathogenesis of chronic AAD exacerbated airway epithelial TGF- $\beta$ 1 expression levels, subepithelial myofibroblast differentiation and ECM/fibronectin accumulation, total lung collagen concentration and related AHR (Royce *et al.*, 2014d), while all treatments that targeted both airway epithelial damage and fibrosis were able to somewhat restore, if not fully reverse, the OVA + NA-induced loss of cDyn.

Secondly with respect to fibrosis, this study confirmed that ameliorating the aberrant collagen deposition (rather than other extracellular matrix proteins such as fibronectin) associated with chronic AAD-induced AWR is key to improving the lung dysfunction that results from persistent AWR, as only RLX alone or its combined effects with TFF2 or TFF2 and DEX that significantly ameliorated lung collagen concentration were able to normalize the OVA + NA-induced loss of cDyn. On the other hand, TFF2 or DEX administration, which only partially ameliorated the aberrant subepithelial fibronectin accumulation, but not total lung collagen concentration, did not effectively protect against the OVA + NA induced loss of lung function. These findings are somewhat consistent with those of others that utilized experimental models of other organ disease (Liao *et al.*, 2010; Qu *et al.*, 2014), suggesting that the amelioration of disease-induced aberrant collagen deposition is required for protection against organ damage and related dysfunction. Furthermore, they demonstrate the necessity to be cautious when interpreting data from Masson's trichrome-stained sections, which although stain all ECM proteins (i.e. most of that staining is thought to represent collagen deposition). The separate analysis of collagen by other means is clearly required to supplement Masson's trichrome staining of ECM deposition.

Thirdly, this study demonstrated that combining an epithelial repair factor with an anti-fibrotic may provide a novel means to effectively treat several aspects of AWR associated with asthma, including epithelial damage and thickening, goblet cell metaplasia, smooth muscle hyperplasia, epithelial TGF- $\beta$ 1 expression/activity, subepithelial myofibroblast differentiation and ECM/fibronectin deposition as well as total lung collagen concentration, all of which are associated with human disease pathogenesis (Tang *et al.*, 2006; Holgate, 2008); Royce *et al.*, 2014c). This combination therapy may therefore offer greater protection against the AWR-induced AHR and lung dysfunction that is associated with chronic/severe asthma, compared with current standard of care and protection for the 5–10% of asthmatics that are resistant to corticosteroid therapy (Fleming *et al.*, 2007; Hetherington and Heaney, 2015). Furthermore, this combination therapy (of RLX + TFF2) may serve as an effective adjunct therapy to the anti-inflammatory effects of corticosteroids to treat the three central components of asthma: AI, AWR and AHR. Of further note, corticosteroids can be slow-acting and cause several side-effects when chronically administered, particularly at high doses. Various inhaled corticosteroids (administered at 0.5–4.4 mg day<sup>-1</sup>) (Dahl, 2006) have been shown to induce both local side-effects such as pharyngitis, dysphonia, cough and bronchospasm, as well as systemic side-effects primarily

involving suppressed hypothalamic-pituitary-adrenal (HPA)-axis function and growth retardation. Animal mortality or body weight, however, were not affected in this study by DEX alone (0.5 mg ml<sup>-1</sup> day<sup>-1</sup>, i.n.) or in combination with RLX and TFF2 and in our previous study (Royce *et al.*, 2013b) using methylprednisolone (0.3 mg kg<sup>-1</sup> day<sup>-1</sup>; i.p.) alone or in combination with RLX (0.5 mg kg<sup>-1</sup> day<sup>-1</sup>, s.c.; equivalent to the 0.8 mg ml<sup>-1</sup> day<sup>-1</sup>, i.n. used in this study). There is no reason to suggest that RLX or TFF2 treatment would exacerbate the side-effects of DEX. On the contrary, the muscle-relaxant properties of RLX (Bacani *et al.*, 2004) may be helpful in protecting from broncho-spasm, while the marked epithelial-repairing and TGF- $\beta$ 1-inhibitory properties of TFF2 may aid to a certain extent in protecting from epithelial damage-induced AWR. Hence, the wide-ranging positive effects of RLX and TFF2 might enable optimal dosing of corticosteroids used to be titrated to safer levels when used in combination, and the feasibility of combining these therapies was provided by the current study albeit at the experimental level.

Even the pleiotropic organ-protective effects of RLX alone would likely be effective enough to complement and augment the therapeutic effects of corticosteroid-based therapies against the pathogenesis of asthma, as demonstrated previously in the chronic AAD model (Royce *et al.*, 2013b). Not only has RLX been shown to activate glucocorticoid receptors (GRs) (Dschietzig *et al.*, 2004) and inhibit TNF- $\alpha$ -induced endothelial dysfunction via GRs (Dschietzig *et al.*, 2012), but also its ability to reverse AAD-induced epithelial damage and thickening, TGF- $\beta$ 1-mediated myofibroblast contractility (Huang *et al.*, 2011), differentiation and aberrant ECM deposition (Umemori *et al.*, 1996; Royce *et al.*, 2014b), and AWR-induced AHR (Royce *et al.*, 2009; Royce *et al.*, 2014b) and loss of cDyn are consistent with its reported ability to enhance the therapeutic effects of methylprednisolone against chronic AAD-induced subepithelial ECM deposition and related AHR (Royce *et al.*, 2013b). In this study, the combined effects of RLX and DEX also markedly enhanced collagen-degrading gelatinase expression and activity over the effects of DEX alone, suggesting that this combination therapy may be more effective in mediating the gelatinase-induced breakdown of the mature collagen fibers that contribute to subepithelial fibrosis. Furthermore, RLX's added anti-inflammatory actions via suppression of mast cell degranulation and leukocyte infiltration (Barré *et al.*, 1997), anti-apoptotic actions through its ability to increase the Bcl2/Bax ratio (Moore *et al.*, 2007) and inhibit caspase-3 activity (Montel *et al.*, 2006), vasodilatory actions in blood vessels of several organs including the lung (Bani, 1997), pro-angiogenic actions via the stimulation of vascular endothelial growth factor expression and new blood vessel growth (Umemori *et al.*, 2000) and muscle-healing properties (Mu *et al.*, 2010) may also indirectly contribute to its ability to inhibit the AWR associated with chronic AAD and synergistically complement the anti-inflammatory effects of corticosteroids.

In conclusion, we have evaluated the individual versus combined effects of a clinically used corticosteroid (DEX), an epithelial repair factor (TFF2) and anti-fibrotic (RLX) in an experimental model of chronic AAD, which incorporates epithelial damage as part of its pathology and demonstrated that (i) RLX alone or in combination with TFF2 offers significant protection against the chronic AAD-induced AWR, fibrosis and loss of lung function (for which there is currently no effective cure). Both



drugs have been shown to be safe, and BIX at least has been well documented to specifically ameliorate pro-fibrotic cytokine-induced fibrosis progression without affecting normal fibrinolytic function and ECM production (Limenton et al., 1996). Furthermore, (ii) combining BIX and TRF2 with the anti-inflammatory effects of DEX offered even greater protection against the AL AWR and lung dysfunction associated with chronic AAD, suggesting that this combination therapy may offer a better alternative to current mainstay therapy for asthma sufferers. Not only do our findings demonstrate the feasibility of combining these therapies, but also they represent progress in the field of asthma pharmacology that has been static since the development of corticosteroids and  $\beta_2$ -adrenoceptor agonists some decades ago.

### Acknowledgements

This study was supported in part by a Monash University MBio Postgraduate Discovery Scholarship (MFDIS) to K.P.P. and National Health & Medical Research Council (NHMRC) of Australia Senior Research Fellowships to A.S.G. (UNT1002288) and C.S.S. (GNT1041766).

### Author contributions

A.S.G., C.S.S. and S.G.R. participated in research design. K.P.P., C.S.S. and S.G.R. conducted experiments. A.S.G., C.S.S. and S.G.R. contributed reagents or tools. K.P.P., C.S.S. and S.G.R. performed data analysis. K.P.P., C.S.S. and S.G.R. wrote or contributed to writing of manuscript.

### Conflict of interest

The authors declare no conflicts of interest.

### Declaration of transparency and scientific rigour

This Declaration acknowledges that this paper adheres to the principles for transparent reporting and scientific rigour of pre-clinical research recommended by funding agencies, publishers and other organizations engaged with supporting research.

### References

Alexander SPH, Callaway JA, Kelly E, Morrison N, Peters JA, Benson HE et al. (2015b). The Concise Guide to PHARMACOLOGY 2015/16: Nuclear hormone receptors. *Br J Pharmacol* 172: 5956–5978.

Alexander SPH, Davenport AP, Kelly E, Morrison N, Peters JA, Benson HE et al. (2015a). The Concise Guide to PHARMACOLOGY 2015/16: G protein-coupled receptors. *Br J Pharmacol* 172: 5744–5869.

Alexander SPH, Hahnel D, Kelly E, Morrison N, Peters JA, Benson HE et al. (2015c). The Concise Guide to PHARMACOLOGY 2015/16: Erythropoiesis. *Br J Pharmacol* 172: 6024–6109.

Amann L, Veithgard EM, Greenback B (2014). TGF $\beta$  factors in inflammatory bowel disease. *World J Gastroenterol* 20: 3223–3230.

Baccan MC, Rao D, Rigau M, Calamita F (2009). Influence of relaxin on the neurally induced relaxant response of the mouse gastric fundus. *Biol Reprod* 71: 1525–1529.

Rao D (1997). Relaxin: a pleiotropic hormone. *Gen Pharmacol* 28: 13–22.

Rao D, Bellati L, Mastri E, Rigau M, Sacchi TB (1997). Relaxin counteracts asthma-like reaction induced by inhaled antigen in sensitized guinea pigs. *Endocrinology* 138: 1909–1913.

Brenner JG (2009). Relaxin and its role in the development and maturation of fibrosis. *Transl Res* 154: 1–4.

Curtis MJ, Bond RA, Spina D, Akhondola A, Alexander SP, Glenzys MA et al. (2013). Experimental design and analysis and their reporting: new guidance for publication in *Br J Pharmacol* 172: 3461–3471.

Dahl R (2006). Systemic side effects of inhaled corticosteroids in patients with asthma. *Respir Med* 100: 1307–1317.

de Boer WJ, Sharma HS, Ruckenstein SM, Hoogstraaten HC, Lambrecht BN, Baumann GJ (2008). Altered expression of epithelial junctional proteins in streptococcal possible role in inflammation. *Can J Physiol Pharmacol* 86: 105–112.

Dichering T, Bartsch C, Saugl V, Baumann G, Saugl K (2009). Identification of the pregnancy hormone relaxin as glucocorticoid receptor agonist. *FASEB J* 23: 1530–1538.

Dichering T, Becht A, Bartsch C, Baumann G, Saugl K, Alexiou K (2012). Relaxin improves TNF- $\alpha$ -induced endothelial dysfunction: the role of glucocorticoid receptor and phosphatidylinositol 3-kinase signaling. *Circulation Res* 90: 97–107.

Ellis JA, Zhu Z, Chappo G, Homer R (1995). Airway remodeling in asthma. *J Clin Invest* 104: 1001–1006.

Herning L, Wilson N, Bush A (2007). Difficult to control asthma in children. *Curr Opin Allergy Clin Immunol* 7: 190–195.

Gallop PM, Par MA (1975). Posttranslational protein modifications, with special attention to collagen and elastin. *Physiol Rev* 55: 419–487.

Girardet PO, Orler A, Rana I, Taroni de Lana JM, Marthan R, Berger P (2011). Airway remodeling in asthma: new mechanisms and potential for pharmacological intervention. *Pharmacol Therapeut* 130: 325–337.

Gazvani M, Namer S, Lee H, Jung R, Lee D, Khang G et al. (2016). Eosinophil receptor antagonist B1013823 reduces allergen-induced airway inflammation and mucus secretion in mice. *Pharm Res* 334: 132–139.

Hetherington KJ, Heaney JG (2015). Drug therapies in severe asthma – the era of stratified medicine. *Clin Med (Lond)* 15: 452–456.

Hoffmann W (2007). TGF $\beta$  (transforming growth factor) peptides and their potential roles for differentiation processes during airway remodeling. *Can Med Chem* 14: 2756–2779.

Holgate ST (2000). Epithelial damage and response. *Clin Exp Allergy* 30 (Suppl 1): 37–41.

Holgate ST (2008a). The airway epithelium is central to the pathogenesis of asthma. *Allergy Int* 57: 1–10.

Holgate ST (2008b). Pathogenesis of asthma. *Clin Exp Allergy* 38: 872–897.

Holgate ST, Davies DE, Puddicombe S, Holford A, Ladhani P, Loutch J et al. (2003). Mechanisms of airway epithelial damage: epithelial-

- mesenchymal interactions in the pathogenesis of asthma. *Eur Respir J Suppl* 44: 246–256.
- Huang X, Gu Y, Tang N, Lu B, Samuel CS, Thammichai VJ *et al.* (2013). Relacin regulates myofibroblast contractility and protects against lung fibrosis. *Am J Pathol* 179: 2751–2765.
- Kilbenny C, Browne W, Cahill JC, Lawson M, Altman DG (2016). Animal research: reporting *in vivo* experiments: the ARRIVE guidelines. *Br J Pharmacol* 180: 1577–1579.
- Knight DA, Holgate ST (2003). The airway epithelium: structural and functional properties in health and disease. *Respiology* 8: 432–446.
- Kumar BK, Herbert C, Foster PS (2008). The “classical” ovalbumin challenge model of asthma in mice. *Curr Drug Targets* 9: 483–494.
- Liu TD, Yang XP, D’Ambrosio M, Zhang Y, Hsieh SL, Carretero OA (2009). N-acetyl-seryl-aspartyl-lyso-proline attenuates renal injury and dysfunction in hypertensive rats with reduced renal mass: control for high blood pressure research. *Hypertension* 53: 459–467.
- Mason E, Cavasotto S, Mason E, Motta C, Vannacci A, Fabiani F *et al.* (2006). Protective effects of relacin in ischemia/reperfusion-induced intestinal injury due to splenic artery occlusion. *Br J Pharmacol* 148: 1124–1132.
- McGuath JC, Lilley E (2015). Implementing guidelines on reporting research using animals (ARRIVE etc.): new requirements for publication in *BJP*. *Br J Pharmacol* 172: 1389–1393.
- Moser M, Dai SL, Lu CY, Fang L, Su YD, Gao XM *et al.* (2007). Relacin antagonizes hypertrophy and apoptosis in neonatal rat cardiomyocytes. *Endocrinology* 148: 1582–1589.
- Mu X, Uno M, Marny K, Fu F, Li Y (2010). Relacin regulates MMP expression and promotes satellite cell mobilization during muscle healing in both young and aged mice. *Am J Pathol* 177: 2399–2410.
- Prison A, Sharma J, Benson HE, Faccenda L, Altstuler MF, Berman CP *et al.* (2014). The IUPHAR/STP guide to PHARMACOLOGY: an expert-driven knowledge base of drug targets and their ligands. *Nucleic Acids Res* 42: D1159–D1166.
- Qin W, Huang H, Li K, Qiu C (2014). Dacryma-mediated protective effect against hepatic fibrosis induced by carbon tetrachloride in rat. *Pathol Res* 62: 348–353.
- Royce SG, Li X, Tortorella S, Goodings L, Chow BK, Girard AS *et al.* (2014a). Mechanistic insights into the contribution of epithelial damage to airway remodeling. Novel therapeutic targets for asthma. *Am J Respir Cell Mol Biol* 50: 180–192.
- Royce SG, Liu C, Maljuck BC, Samuel CS, Vorverfsk, Karagiannis TC *et al.* (2013a). TGF- $\beta$ 2 reverses airway remodeling changes in allergic airways disease. *Am J Respir Cell Mol Biol* 48: 135–144.
- Royce SG, Liu CX, Patel KP, Wang B, Samuel CS, Tang ML (2014b). Intranasally administered relacin abrogates airway remodeling and attenuates airway hyperresponsiveness in allergic airways disease. *Clin Exp Allergy* 44: 1393–1408.
- Royce SG, Miao VL, Lee M, Samuel CS, Truong GW, Tang ML (2009). Relacin reverses airway remodeling and airway dysfunction in allergic airways disease. *Endocrinology* 150: 2692–2699.
- Royce SG, Moodley Y, Samuel CS (2014c). Novel therapeutic strategies for lung diseases associated with airway remodeling and fibrosis. *Pharm Therap* 141: 250–260.
- Royce SG, Patel KP, Samuel CS (2014d). Characterization of a novel model incorporating airway epithelial damage and related fibrosis to the pathogenesis of asthma. *Lab Invest* 94: 1325–1339.
- Royce SG, Sekhriwala A, Samuel CS, Tang ML (2013b). Combination therapy with relacin and methylprednisolone augments the effects of efflux ligament alone in inhibiting subepithelial fibrosis in an experimental model of allergic airways disease. *Clin Sci (Lond)* 124: 41–51.
- Royce SG, Shen M, Patel KP, Haskett BM, Riccardi M, Samuel CS (2012). Mesenchymal stem cells and relacin synergistically abrogate established airway fibrosis in an experimental model of chronic allergic airways disease. *Stem Cell Res* 15: 495–505.
- Tang ML, Wilson JW, Stewart AG, Royce SG (2004). Airway remodeling in asthma: current understanding and implications for future therapies. *Pharm Therap* 112: 474–486.
- Tantraman A, Ergun S, Akhri M, Miller-Wyting D, Akkaya A, Buckler EB *et al.* (2005). Apoptosis and loss of adhesion of bronchial epithelial cells in asthma. *Int Arch Allergy Immunol* 138: 142–150.
- Uemura EN, Lewis M, Constant J, Arnold G, Giese RH, Normand J *et al.* (2008). Relacin induces vascular endothelial growth factor expression and angiogenesis selectively at wound sites. *Wound Rep Regen* 16: 361–370.
- Uemura EN, Pickford LB, Selles AI, Percy CE, Grove RL, Erikson ME *et al.* (1996). Relacin induces an extracellular matrix-degrading phenotype in human lung fibroblasts *in vitro* and inhibits lung fibrosis in a murine model *in vivo*. *J Clin Invest* 98: 2749–2755.
- Wassenaar J Jr (1995). Quantification of matrix metalloproteinases in tissue samples. *Methods Enzymol* 248: 310–320.
- Xu ZP, Hao JM, Song YL, Kang J, Li X (2012). Effects of acetic trioxide (AT2630) on airway remodeling in a murine model of bronchial asthma. *Canad J Physiol Pharmacol* 90: 1576–1584.
- Zhang Y, Moffat MF, Cookson WO (2012). Genetic and genomic approaches to asthma: new insights for the origins. *Curr Opin Pulm Med* 18: 6–15.

---

**CHAPTER 5:**

**Treating a refined model of  
allergic airways disease  
with an antifibrotic, and  
human amnion epithelial  
cell-derived exosomes**

---

## **Combining human amnion epithelial cell-derived exosomes with an anti-fibrotic offers optimal protection against allergic airways disease**

### **5.0 ABSTRACT**

There has been growing interest in stem cell-derived exosomes for their therapeutic and regenerative benefits given their manufacturing and regulatory advantages over cell-based therapies. As the presence of excessive collagen (fibrosis) significantly impedes the viability and efficacy of stem cell-based strategies for treating chronic diseases, we recently showed that the anti-fibrotic hormone-based drug, serelaxin, can improve the environment into which stem cells can be administered into and improve their ability to migrate and reduce tissue damage. In this study, we determined if the antifibrotic effects of serelaxin would further benefit the therapeutic efficacy of human amnion epithelial cell (AEC)-derived exosomes in the refined model of chronic allergic airways disease (AAD). Female Balb/c mice (n=8/group) were subjected to the 9.5-week model of ovalbumin and naphthalene (OVA/NA)-induced chronic AAD; then administered increasing concentrations of AEC-exosomes (5 g or 25 g), in the absence or presence of serelaxin (0.5mg/kg/day) in each case for 7-days. A sub-group of mice (n=8) were also treated with  $1 \times 10^6$  AECs co-administered with serelaxin over the corresponding time-period, for comparison. The control group (n=8) received saline/corn oil, respectively. Mice with OVA/NA-induced chronic AAD presented with significant tissue inflammation, remodelling, fibrosis and airway dysfunction at the time-point studied (all  $p < 0.01$  vs saline/corn oil-

treated controls). While therapeutic AEC-exosome (5µg or 25µg)- administration alone demonstrated some benefits in the model, the presence of serelaxin was required for AEC-exosomes (25µg) to rapidly normalise chronic AAD-induced airway fibrosis and airway reactivity (all  $p < 0.01$  vs chronic AAD alone;  $p < 0.05$  vs 25µg AEC-exosomes alone). The combined effects of serelaxin and AEC-exosomes (25µg) also demonstrated greater anti-inflammatory and airway remodelling effects compared to the combined effects of serelaxin and  $1 \times 10^6$  AECs (all  $p < 0.05$  vs AECs + serelaxin). Hence, serelaxin can enhance the therapeutic efficacy of AEC-exosomes, particularly in treating basement membrane-related fibrosis and related airway dysfunction.

## 5.1 INTRODUCTION

Asthma is commonly characterised as an inflammatory respiratory disease and is the most prevalent chronic disease affecting children (Chung, 2014). It affects over 300 million people around the world, leading to 1/250 deaths annually. In Australia, 1 in 10 adults suffer from this debilitating disease, with the rate of incidence being slightly higher in children under the age of 14. There are three central components to the pathogenesis of asthma: airway inflammation (AI), airway remodelling (AWR), and airway hyperresponsiveness (AHR) (Chung, 2014). Continual T-helper cell type 2-driven AI, along with irreversible changes to the structure of the airways (AWR) contribute to the development of AHR. It has emerged that epithelial damage is an important contributor to early-stage

AWR and ultimately AHR in mild and chronic asthma sufferers (Chung, 2014). The airway epithelial layer plays an important immunological and physical barrier to various specific and non-specific stimuli that are inhaled on a daily basis. The epithelium is also prone to the genetic mutation, making it more susceptible to damage, while also impairing the epitheliums ability to repair itself, causing epithelial denudation, metaplasia, and aberrant wound healing (leading to fibrosis) (Chung, 2014). However, despite all this, epithelial damage is not addressed in commonly used murine models of chronic allergic airway disease (AAD) that mimics several features associated with human asthma.

To address these limitations, our Lab recently utilised the well-established chronic ovalbumin (OVA)-induced murine model of AAD, which presents with AI, AWR, and AHR; and superimposed a single acute dose of naphthalene (NA) in order to introduce epithelial damage into this refined model (Royce et al., 2014). The strength of combining these agents in mice is that they create a model that allows investigation and therapeutic targeting of the contribution of epithelial damage to several morphological and functional processes that typify the human disease. **Importantly, the induction of epithelial damage in the OVA + NA model was found to contribute to AWR, fibrosis and related AHR and exacerbate the effects of AI on these parameters (Royce et al.,2014).** It should be noted, however, that this combination (of OVA + NA) would probably not cause the entire number of allergic, chemical and genetic factors associated with disease progression in humans, as neither OVA and/or NA are typically used to induce asthma in humans.

In the previous Chapter, the therapeutic effects of an epithelial repair factor (TFF-2), anti-fibrotic drug (RLX) and clinically-used corticosteroid (DEX) were assessed in isolation and in combination, for their ability to treat the three central components of asthma and in particular various measures of AWR. Concurrent studies in the Lab (by others) also determined if the anti-fibrotic effects of RLX could be combined with stem cell-based therapies, including human bone marrow-derived mesenchymal stem cells (Royce et al., 2015; Royce et al., 2016) and human amnion epithelial cells (AECs) (Royce et al., 2016) to reverse the AI, AWR and AHR associated with chronic allergic airways disease/asthma. The anti-fibrotic effects of RLX were added to create an improved environment into which cell-based therapies could be administered to, as the fibrosis associated with chronic disease settings has been shown to hamper exogenously administered stem cell survival, homing to sites of damage, integration with resident cells and/or differentiation (Knight et al., 2010) AECs are non-immunogenic and can be easily and ethically harvested via non-invasive procedures from the amniotic sac of the mature placenta (Koike et al., 2014). They were shown to partially reduce AI, AWR and AHR in the setting of OVA-induced chronic AAD (lacking incorporation of NA-induced epithelial damage) when administered alone; while their therapeutic effects were enhanced in the presence of RLX (Royce et al., 2016). As a result, combining AECs ( $1 \times 10^6$  cells per mouse) with RLX resulted in the normalisation of the OVA-induced airway fibrosis and AHR when administered over a 2-week treatment period (Royce et al., 2016). However, it is thought that these cells, like human bone marrow-

derived mesenchymal stem cells (Royce et al., 2015), are cleared from the injured lung by 3-4 days post-administration. While this limitation was addressed by administering AECs once weekly to OVA-injured mice over the 2-week treatment period (Royce et al., 2016), it has been proposed that the vesicles or exosomes secreted by AECs (and other stem cells) may contain the factors that facilitate the long-lasting protective effects of these cells even after they have been cleared from the damaged organ. Stem cell-derived exosomes have been described as a novel mechanism by which cell-to-cell communication occurs (Schorey & Bhatnagar, 2008). Exosomes are 30-150nm extracellular vesicles and can be derived from a number of cell sources (Squadrito et al., 2014; Vlassov et al., 2012). It has also been suggested that exosomes possess stable chemical properties, high biosecurity and could exert similar functional properties to recipient cells from which they are derived (Lai et al., 2010), as they contain bioactive substances such as proteins and microRNAs that are secreted by stem cells. It is also believed that exosomes can avoid recognition by the immune system and maintain the integrity of cell membrane to avoid degradation (Vader et al., 2016). Encapsulation of the active biological ingredients and regeneration within non-living exosome carriers may offer process, manufacturing and regulatory advantages over stem cell-based therapies; allowing for the transfer of proteins and nucleic acids across cellular boundaries.

Hence, in the current Chapter, the OVA + NA-induced mouse model of chronic AAD incorporating epithelial damage was used to assess the therapeutic effects of AECs-derived exosomes against the three central components of

asthma, both in isolation and in combination with RLX. The combined effects of AECs + RLX (which were previously shown to demonstrate optimal therapeutic efficacy in the OVA model (Royce et al., 2016)) were used as a positive control.

## 5.2 METHODS

### 5.2.1 Animals

Six- to eight-week-old female Balb/c wild-type mice (provided by Monash University Animal Services; as per what was used in Chapters 3 and 4) were allowed to acclimatise for at least 4 days prior to any experimentation and maintained on a 12h light:dark cycle with free access to standard rodent chow (Barastoc Stockfeeds, Pakenham, VIC, Australia) and water. All experimental procedures were performed according to the regulations approved by the Monash University Animal Ethics Committee (MARF/2016/107), which adheres to the Australian Guidelines for the Care and Use of Laboratory Animal for Scientific Purposes.

### 5.2.2 Isolation and characterisation of AEC-derived EXO

AECs were isolated from placentae of women undergoing elective caesarean section (at 38-42 weeks of gestation) in accordance with guidelines and approval from the Monash Health Human Research Ethics Committee. AECs were isolated from several pooled amnions and reconstituted overnight once thawed from being stored in liquid nitrogen, as described before (Murphy *et al.*, 2010;

Murphy *et al.*, 2014).  $1 \times 10^6$  AECs were then resuspended in saline for therapeutic administration as detailed below. EXO were isolated from several pooled amnions and characterised as described previously (Tan *et al.*, 2018). EXO were then dissolved in saline for therapeutic administration as detailed below. Characterisation of EXO, proteomic pathway clustering analysis including proteins significantly enriched by EXO and RNA sequencing analysis of EXO were recently reported (Tan *et al.*, 2018).

### 5.2.3 Establishing the refined models of AAD

On day 0 and day 14, mice (n=48) were sensitised with an i.p. injections of 10mg Grade V OVA (Sigma-Aldrich, St Louis, MO, USA) and 1mg aluminium potassium sulfate adjuvant (alum; AJAX Chemicals, Kotara, NSW, Australia) in 0.5 ml of saline. Between days 21 and 63, mice were then subjected to nebulization (inhalation of an aerosol) with 2.5% (w/v) OVA for 30 min, three times a week, using an ultrasonic nebuliser (Omron NE-U07; Omron, Kyoto, Japan). On day 64, 24hr after the last OVA nebulisation period, mice received a single i.p. injection of NA (200 mg/kg body weight; Sigma-Aldrich) and left for a further 3 days. From days 67 to 75, sub-groups of OVA + NA-injured mice were treated with daily i.n. administration of either (i) saline (the vehicle for AECs and AEC-derived exosomes; injury control group; n = 8), (ii) 5µg exosomes (EXO) (kindly provided by Dr Rebecca Lim, Hudson Institute of Medical Research, Clayton, Victoria, Australia; n 8), (iii) 25µg EXO (n = 8), (iv) 5µg EXO + RLX ( $0.8 \text{ mg} \cdot \text{mL}^{-1}$ , kindly provided by Corthera Inc., San Carlos, CA, USA; a subsidiary of Novartis AG, Basel, Switzerland; n = 8), (v) 25µg EXO + RLX (n = 8) or (vi)  $1 \times 10^6$  AEC + RLX (n =

8). AEC or AEC-derived EXO were administered once (on day 67), while saline or RLX were administered once daily over the 7-day treatment period; and all treatments were administered in 50  $\mu$ l of saline (25  $\mu$ l per nare). A separate subgroup of mice subjected to (vii) 0.5 ml saline (vehicle controls for OVA; n = 8), nebulised with saline instead of OVA (from days 21 to 63), injected with 200mg/kg CO (vehicle control for NA), and treated with daily i.n. administrations of saline between day 67 to 75 were used as an uninjured control group (Figure 5-1).

#### 5.2.4 Invasive plethysmography

On day 75, all seven groups of mice (n = 56 in total) had their airway resistance measured by invasive plethysmography, in response to increasing concentrations of methacholine-induced airway bronchoconstriction. Mice were briefly anaesthetised with an i.p. injection of ketamine (100 mg·kg<sup>-1</sup> body

Figure 5-1:

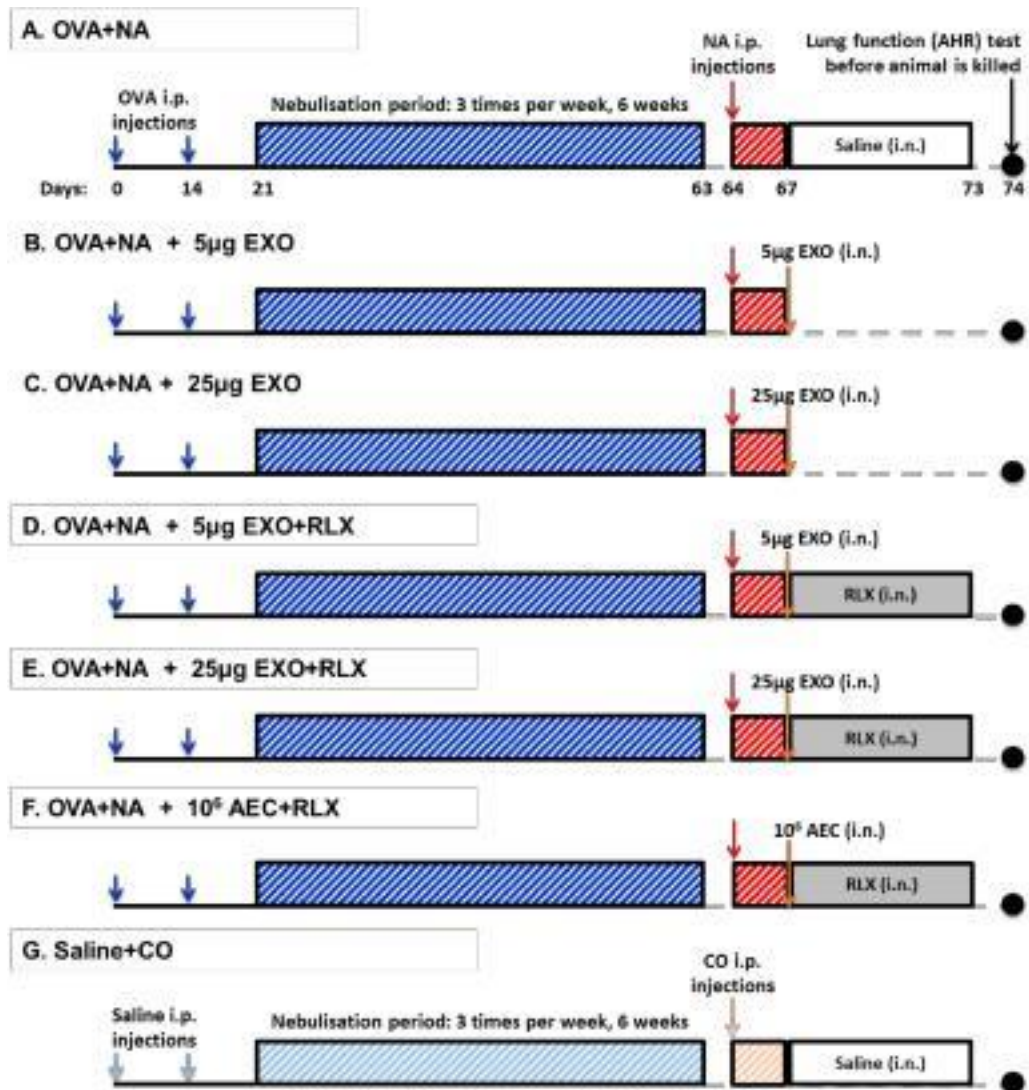


**Figure 5-1: Schematic illustration of experimental model models and treatments.**

A schematic illustration of how the A) OVA+NA, H) Saline+CO, injured and uninjured control groups respectively. There various treatment combinations investigated were B) 5µg EXO alone, C) 25µg EXO alone, D) 5µg EXO + RLX, E) 25µg EXO + RLX, F) AEC + RLX.

weight) and xylazine (20 mg·kg<sup>-1</sup> body weight), tracheostomised and cannulated. Increasing doses of methacholine were nebulised, and AHR was measured (Biosystem XA version 2.7.9, Buxco Electronics, Troy, NY, USA) for 2 min after each dose. Results were then expressed as the maximal resistance after each dose of methacholine minus baseline resistance.

### **5.2.5 Tissue collection**

Once airway reactivity measurements were completed, mice were killed by an overdose of anaesthetic containing ketamine and xylazine, before their lung tissue was isolated. The lungs of each animal were then divided along the transverse plane, resulting in **five separate lobes**. The largest lobe was fixed in 10% neutral buffered formalin overnight, processed routinely and embedded in paraffin wax. The remaining **four lobes** were snap-frozen in liquid nitrogen and stored at 80°C for further analyses, as detailed below.

### **5.2.6 Lung histopathology**

Formalin-fixed, paraffin-embedded tissues were sectioned (3µm thickness) and placed on SuperFrost charged microscope slides (Grale Scientific, Melbourne, Vic., Australia). To assess peribronchial inflammation score, one set of serial sections per mouse underwent Mayer's haematoxylin and eosin (H&E) staining. To assess epithelial and subepithelial extracellular matrix thickness, another set of serial sections per mouse underwent Masson's trichrome staining. To assess goblet cell metaplasia, a third set of serial sections per mouse underwent Alcian blue periodic acid Schiff (ABPAS) staining. Stained sections

were scanned using the whole-slide scanning platform Aperio Scanscope CS (Leica Biosystems, Nussloch, Germany). All slides were then scanned at the maximum magnification available (40×) and stored as digital high-resolution images on a local server associated with the instrument. Digital slides were viewed and morphometrically analysed with the Aperio Imagescope v.12.1.0.5029 software (Leica Biosystems).

### **5.2.7 Histological evaluation of airway inflammation**

Histological grading of inflammation severity from 0 to 4 was assigned to every slide, as described previously (Royce et al., 2014d) (0 = no detectable inflammation; 1 = occasional inflammatory cell aggregates, pooled size <0.1 mm<sup>2</sup>; 2 = some inflammatory cell aggregates, pooled size ~0.2 mm<sup>2</sup>; 3 = widespread inflammatory cell aggregates, pooled size ~0.3 mm<sup>2</sup>; and 4 = widespread and massive inflammatory cell aggregates, pooled size ~0.6 mm<sup>2</sup>), and was performed blinded by the investigator.

### **5.2.8 Immunohistochemistry**

Paraffin-embedded lung sections were immunohistochemically stained using either a monoclonal antibody to  $\alpha$ -SMA( $\alpha$ -smooth muscle actin; a marker of myofibroblast differentiation; M0851; 1:200 dilution; DAKO, Carpinteria, CA, USA) or polyclonal antibodies to TGF- $\beta$ 1 (sc146; 1:1000 dilution; Santa Cruz Biotechnology, Santa Cruz, CA, USA), fibronectin (ab2413; 1:350 dilution; Cambridge, MA, USA) or thymic stromal lymphopoietin (TSLP; a marker of epithelial damage; 1:1000 dilution; EMD Millipore Corp., Temecula, CA, USA).

Detection of antibody staining was completed using the DAKO EnVision anti-mouse or anti-rabbit kits, respectively, and 3,3-diaminobenzidine (Sigma-Aldrich), where sections were counterstained with haematoxylin. Images of five bronchi (measuring 150–350  $\mu\text{m}$  luminal diameter) per section were obtained and quantified by morphometry, as described below.

### **5.2.9 Morphometric analysis**

Representative photomicrographs from H&E-, Masson's trichrome- and ABPAS-stained slides, as well as immunohistochemically stained slides were captured from scanned images using ScanScope AT Turbo (Aperio, Vista, CA, USA). Stained airways were randomly selected from across the tissue sample. Masson's trichrome-stained slides were analysed by measuring the thickness of the epithelial and subepithelial layers and expressing values as  $\mu\text{m}^2\cdot\text{mm}^{-1}$  basement membrane length. ABPAS-stained slides were analysed by counting the number of stained goblet cells, which were expressed as the number of goblet cells 100  $\mu\text{m}^{-1}$  basement membrane length.  $\alpha$ -SMA and TSLP positively stained cells located within the subepithelial and epithelial regions, respectively, of the airway were counted and expressed as number of positively stained cells 100  $\mu\text{m}^{-1}$  basement membrane length. Epithelial TGF- $\beta$ 1 staining was quantified by measuring the level of strong positively stained areas within the epithelial regions, respectively, and expressing the data as percentage staining per field.

### **5.2.10 Hydroxyproline assay**

The second largest lung lobe from each mouse was processed as described previously (Royce et al., 2009, 2014) for the measurement of hydroxyproline content, which was determined from a standard curve of purified trans-4-hydroxy-L-proline (Sigma-Aldrich). Hydroxyproline values were multiplied by a factor of 6.94 (based on hydroxyproline representing ~14.4% of the amino acid composition of collagen in most mammalian tissues) (Gallop and Paz, 1975) to extrapolate total collagen content, which in turn, was divided by the dry weight of each corresponding tissue to yield percent collagen concentration.

### **5.2.11 Statistical analysis**

All data were analysed using GraphPad PRISM v6.0 (La Jolla, CA, USA) and expressed as the mean  $\pm$  SEM. Differences in the raw airway resistance data were analysed by a two-way ANOVA with Bonferroni post hoc test, whereas the remaining data were analysed by a one-way ANOVA with Newman–Keuls post hoc test for multiple comparisons between groups. In each case, the significance was pre-determined as being  $P < 0.05$ . The data and statistical analysis comply with the recommendations on experimental design and analysis in pharmacology (Curtis et al., 2015).

## 5.3 RESULTS

### 5.3.1 Individual versus combined effects of EXO and RLX on airway

#### inflammation

Peribronchial inflammation was scored from H&E-stained lung tissue (**Figure 5-2A**), as described in previous chapters. OVA/NA-treated mice were sufficiently sensitised/challenged to OVA as demonstrated by the elevated level of peribronchial inflammation score in these mice compared to that measured in their saline/CO-treated counterparts (OVA/NA:  $2.16 \pm 0.09$  vs Saline/CO:  $0.15 \pm 0.09$ ;  $P < 0.001$  vs. saline/CO group; **Figures 5-2A and B**). Exosomes (EXO) alone partially and dose-dependently reduced the OVA + NA-induced increase in peribronchial inflammation score (+5 $\mu$ g EXO:  $1.45 \pm 0.07$  vs. +25 $\mu$ g EXO:  $1.13 \pm 0.08$ ;  $P < 0.05$  vs +5 $\mu$ g EXO group; both  $P < 0.01$  vs. OVA/NA group; **Figures 5-2A and B**). Co-administration of RLX with exosomes further reduced the OVA + NA-induced increase in airway inflammation (+5 $\mu$ g EXO + RLX:  $1.16 \pm 0.08$ ;  $P < 0.05$  vs. +5 $\mu$ g EXO group / +25 $\mu$ g EXO + RLX:  $0.91 \pm 0.11$ ;  $P < 0.01$  vs. +5 $\mu$ g EXO group; both  $P < 0.001$  vs. OVA/NA group); although not fully back to that measured from saline/CO-treated mice ( $P < 0.01$  vs. saline/CO group). 25 $\mu$ g EXO + RLX also reduced the OVA + NA-induced increase in peribronchial inflammation score to a greater extent than AECs + RLX did ( $1.29 \pm 0.05$ ;  $P < 0.05$  vs. +25 $\mu$ g EXO + RLX group;  $P < 0.001$  vs. OVA/NA group;  $P < 0.001$  vs. saline/CO group; **Figures 5-2A and B**). The effects of RLX alone was retrospectively included (as determined in Chapter 4) to comparatively show that RLX alone did not exert any marked anti-inflammatory effects against the OVA + NA-induced peribronchial inflammation (**Figures 5-2A and B**).

Figure 5-2:

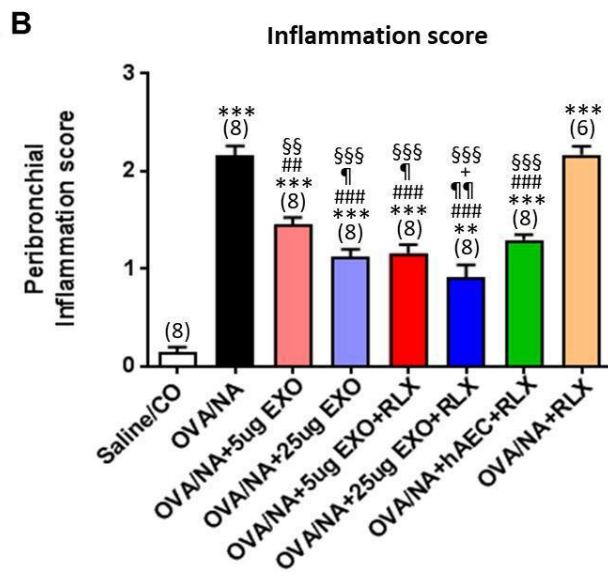
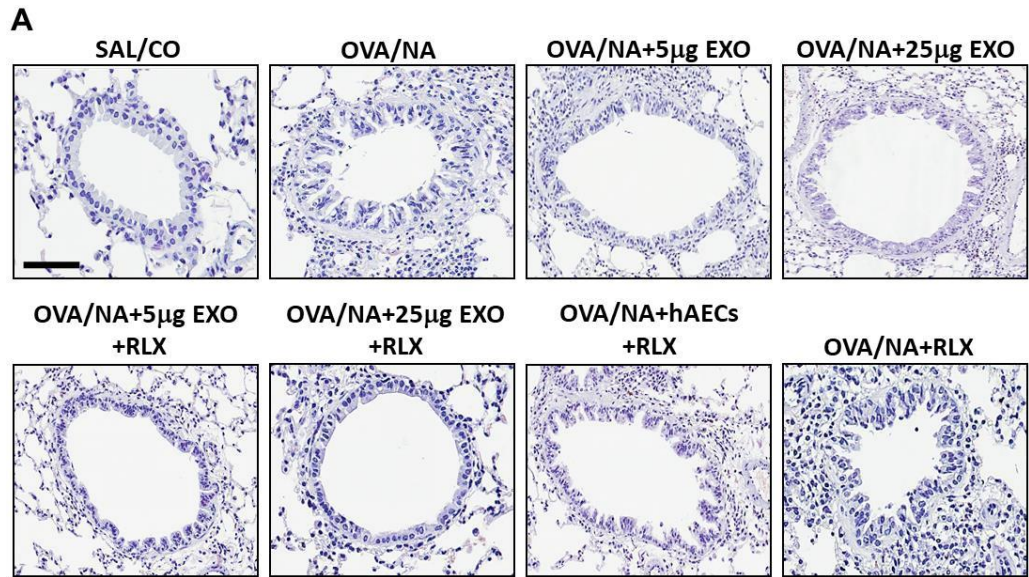


**Figure 5-2: Individual vs. combined effects of EXO + RLX vs. AECs + RLX on peribronchial inflammation.**

**A)** Representative images of hematoxylin and eosin-stained lung sections from each group studied - demonstrating the extent of inflammatory cell infiltration within the bronchial wall. Scale bar = 50 $\mu$ m. The effects of hAECs + recombinant human relaxin (RLX) or RLX alone (extrapolated from Chapter 4) are included for comparison. **B)** Also shown is the mean + S.E.M peribronchial inflammation score from 5 airways/mouse (where sections were scored based on the number and distribution of inflammatory cell aggregates on a scale of 0 (no visible inflammation) to 4 (severe inflammation)); from n=6-8 animals per group. \*\*P<0.01, \*\*\*P<0.001 vs Saline/corn oil-treated uninjured control group; ##P<0.01, ###P<0.001 vs OVA/NA-treated chronic allergic airways disease (AAD) group; ¶P<0.05, ¶¶P<0.01 vs OVA/NA+5mg hAEC-derived exosome (EXO)-treated group; +p<0.05 vs OVA/NA+hAEC+RLX-treated group; §§P<0.01, §§§P<0.001 vs OVA/NA+RLX-treated group.

### 5.3.2 Individual versus combined effects of EXO and RLX on airway remodelling

#### 5.3.2.1 Goblet cell metaplasia

Goblet cell metaplasia (number of goblet cells per 100µm of basement length) was assessed by morphometric analysis of ABPAS-stained lung tissue sections (**Figures 5-3A**), and was significantly increased in OVA + NA-treated mice compared to that measured from their saline/CO-treated counterparts (OVA/NA:  $2.61 \pm 0.19$ ; Saline/CO:  $0.12 \pm 0.04$ ;  $P < 0.001$  vs. saline/CO group; **Figures 5-3A and B**). Interestingly, exosomes alone did not have any obvious effect on the OVA + NA- induced increase in goblet cell metaplasia (+5µg EXO:  $2.89 \pm 0.22$ ; +25µg EXO:  $2.48 \pm 0.08$ ; both no different vs. OVA/NA group; both  $P < 0.001$  vs. saline/CO group; **Figures 5-3A and B**). However, the combined effects of exosomes + RLX were able to partially but significantly reduce goblet cell metaplasia (+5µg EXO + RLX:  $1.83 \pm 0.12$ ; +25µg EXO + RLX:  $1.31 \pm 0.13$ ; both  $P < 0.01$  vs. OVA/NA group; both  $P < 0.01$  vs. saline/CO group). Of note, 25µg EXO + RLX ( $1.31 \pm 0.13$ ) was able to reduce goblet cell metaplasia to a greater extent than 5µg EXO + RLX ( $1.83 \pm 0.12$ ;  $P < 0.05$  vs. +5µg EXO + RLX group) or AECs + RLX ( $1.82 \pm 0.19$ ;  $P < 0.05$  vs AECs + RLX group; **Figures 5-3A and B**). Once again, the effect of RLX alone was retrospectively included (as determined in Chapter 4) to comparatively show that RLX alone did not exert any marked effects against the OVA + NA-induced increase in goblet cell metaplasia (**Figures 5-3A and B**).

Figure 5-3:

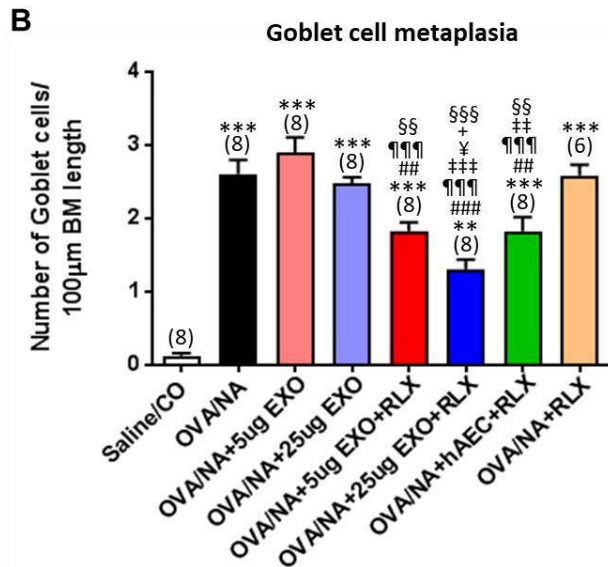
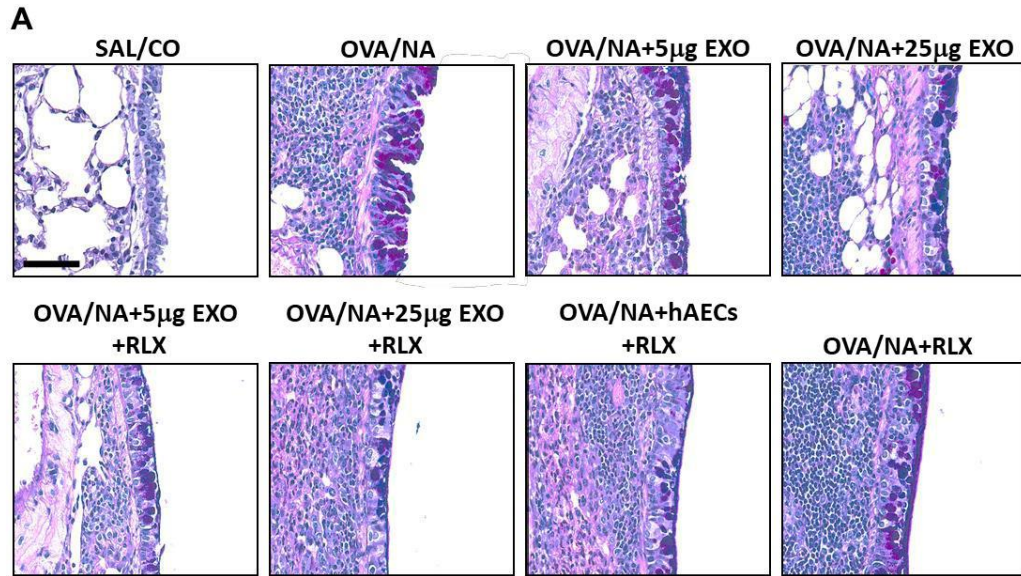


**Figure 5-3: Individual vs. combined effects of EXO + RLX vs. AECs + RLX on goblet cell metaplasia.**

**A)** Representative images of Alcian blue periodic acid Schiff-stained lung sections from each group studied - demonstrating the extent of goblet cell metaplasia. Scale bar = 50 $\mu$ m. The effects of hAECs + recombinant human relaxin (RLX) or RLX alone (extrapolated from Chapter 4) are included for comparison. **B)** Also shown is the mean + S.E.M goblet cell count (represented as the number of goblet cells per 100mm basement membrane (BM) length) from 5 airways/mouse; n=6-8 animals per group. \*\*P<0.01, \*\*\*P<0.001 vs Saline/corn oil-treated uninjured control group; ##P<0.01, ###P<0.001 vs OVA/NA-treated chronic allergic airways disease (AAD) group; ¶¶¶P<0.001 vs OVA/NA+5mg hAEC-derived exosome (EXO)-treated group; ‡‡‡p<0.001 vs OVA/NA+25mg hAEC-derived EXO-treated group; ¥p<0.05 vs OVA/NA+5mg hAEC-derived EXO+RLX-treated group; +p<0.05 vs OVA/NA+hAEC+RLX-treated group; §§P<0.01, §§§P<0.001 vs OVA/NA+RLX-treated group.

### 5.3.2.2 Epithelial damage

TSLP was used as a measure of epithelial damage and was assessed by morphometric analysis of TSLP-stained lung tissue sections (measured as number of TSLP-positive cells  $100 \mu\text{m}^{-1}$  of basement membrane length; **Figures 5-4A and B**). Expectedly, OVA + NA-treated mice exhibited significantly exacerbated levels of TSLP-associated epithelial damage compared with that measured from saline/CO-treated mice (OVA/NA:  $6.98 \pm 0.34$ ; Saline/CO:  $2.35 \pm 0.15$ ;  $P < 0.001$  vs. saline/CO group; **Figures 5-4A and B**). All treatments demonstrated a marked ability to reduce the OVA + NA-induced increase in TSLP-associated epithelial damage (+5 $\mu\text{g}$  EXO:  $3.64 \pm 0.12$ ; +25 $\mu\text{g}$  EXO:  $3.09 \pm 0.09$ ; +5 $\mu\text{g}$  EXO + RLX:  $3.22 \pm 0.10$ ; +25 $\mu\text{g}$  EXO + RLX:  $2.82 \pm 0.11$ ; +AEC + RLX:  $2.92 \pm 0.07$ ; all  $P < 0.001$  vs. OVA/NA group); with the combined effects of 25 $\mu\text{g}$  EXO  $\pm$  RLX or AECs + RLX normalising TSLP-associated epithelial damage back to that which was no longer different to the number of TSLP-positive cells detected from saline/CO-treated mice (**Figures 5-4A and B**). The effects of RLX alone ( $5.66 \pm 0.40$ ;  $P < 0.01$  vs OVA/NA group;  $P < 0.001$  vs. saline/CO group) was retrospectively included (as determined in Chapter 4) to comparatively show that it only had a partial but significant effect alone in reducing the OVA + NA-induced increase in TSLP-associated epithelial damage (**Figures 2A and B**).

Figure 5-4:

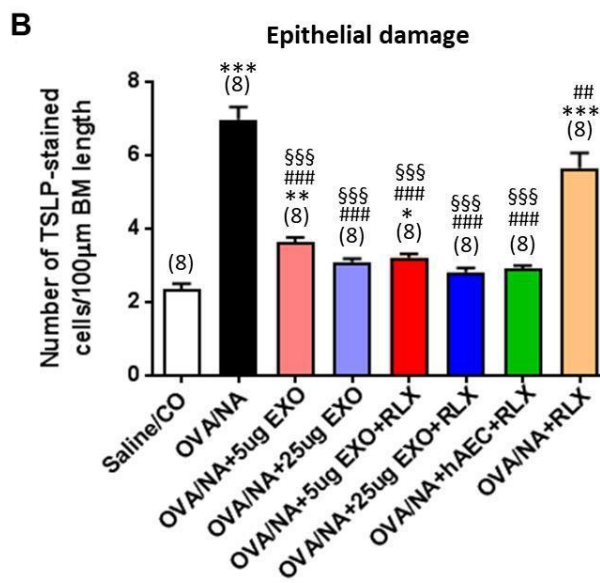
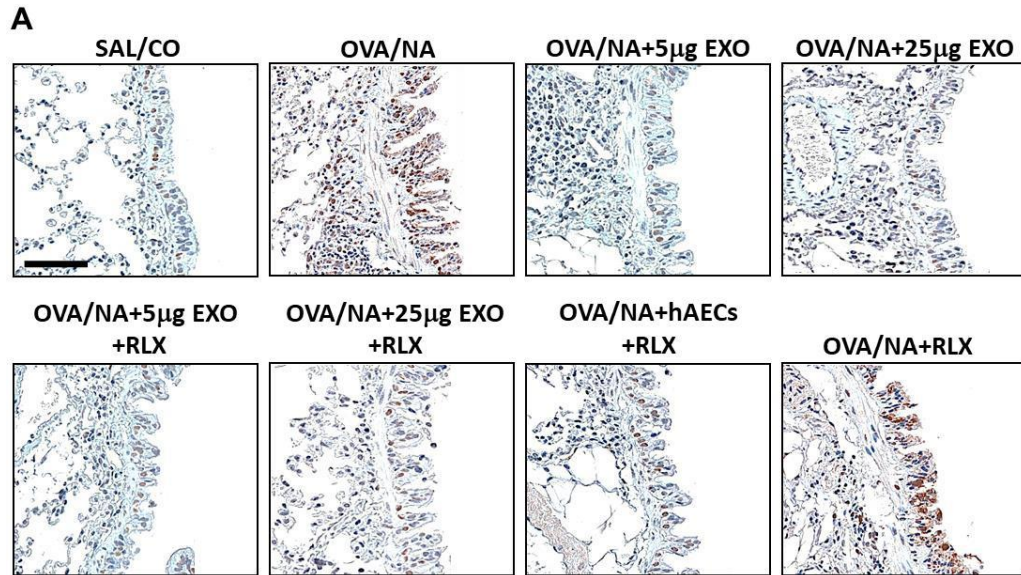


**Figure 5-4: Individual vs. combined effects of EXO + RLX vs. AECs + RLX on TSLP-associated epithelial damage.**

**A)** Representative images of immunohistochemically-stained lung sections for thymic stromal lymphopoietin (TSLP; a marker of epithelial damage) from each group studied. Scale bar = 50 $\mu$ m. The effects of hAECs + recombinant human relaxin (RLX) or RLX alone (extrapolated from Chapter 4) are included for comparison. **B)** Also shown is the mean + S.E.M TSLP-stained cell counts (per 100mm basement membrane (BM) length) from 5 airways/mouse; n=8 animals per group. \*p<0.05, \*\*P<0.01, \*\*\*P<0.001 vs Saline/corn oil-treated uninjured control group; ##P<0.01, ###P<0.001 vs OVA/NA-treated chronic allergic airways disease (AAD) group; §§§P<0.001 vs OVA/NA+RLX-treated group.

### 5.3.2.3 Epithelial thickness

Epithelial thickness (relative to basement membrane length) was assessed by morphometric analysis of Masson's trichrome-stained lung tissue sections (**Figures 5-5A and B**) and was significantly increased in OVA + NA-treated mice compared that in their saline/CO-treated counterparts (OVA/NA:  $20.68 \pm 0.16$ ; Saline/CO:  $16.11 \pm 0.19$ ;  $P < 0.001$  vs. saline/CO group). All treated groups significantly reduced airway epithelial thickness back to levels which were no longer different to that measured from saline/CO-treated mice (+5 $\mu$ g EXO:  $17.45 \pm 0.29$ ; +25 $\mu$ g EXO:  $17.35 \pm 0.26$ ; +5 $\mu$ g EXO + RLX:  $17.57 \pm 0.24$ ; +25 $\mu$ g EXO + RLX:  $17.22 \pm 0.27$ ; +AEC + RLX:  $17.45 \pm 0.24$ ; +RLX:  $18.53 \pm 0.74$ ; all  $P < 0.001$  vs. OVA/NA group); whereas the effects of RLX alone was retrospectively included (as determined in Chapter 4) to show that it only had a partial but significant effect in reversing the OVA + NA-induced increase in epithelial thickness treatment (all  $P < 0.01$  vs. OVA/NA group;  $P < 0.01$  vs. saline/CO group; **Figures 5-5A and B**).

### 5.3.3 Individual versus combined effects of EXO and RLX on airway fibrosis

#### 5.3.3.1 Subepithelial ECM thickness

Subepithelial ECM thickness (relative to basement membrane length) was assessed by morphometric analysis of Masson's trichrome-stained lung tissue sections (**Figures 5-5A**) and was significantly increased in OVA + NA-treated mice compared with that measured from saline/CO-treated controls (OVA + NA:  $32.22 \pm 0.95$ ; Saline/CO:  $17.17 \pm 0.52$ ;  $P < 0.001$  vs. saline/CO group). EXO alone-treated groups induced a dose-dependent reduction of aberrant subepithelial

Figure 5-5:

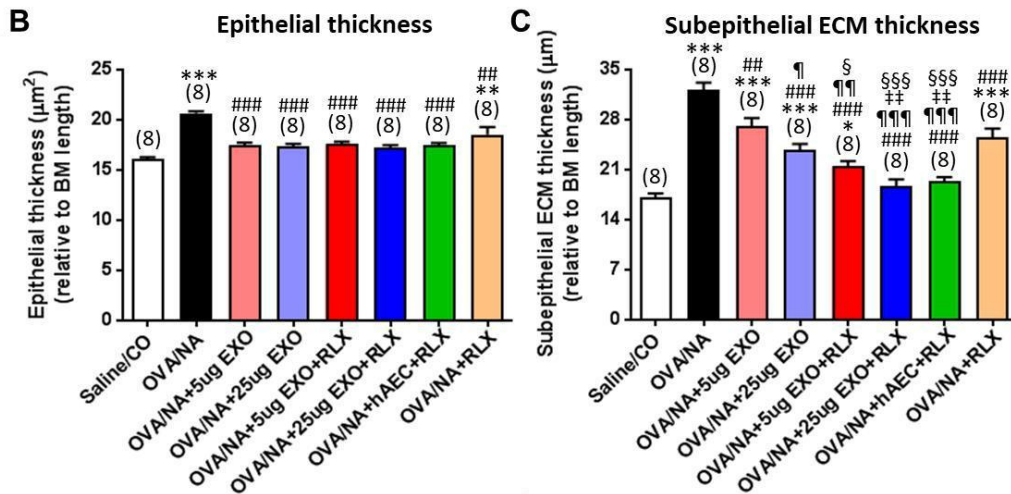
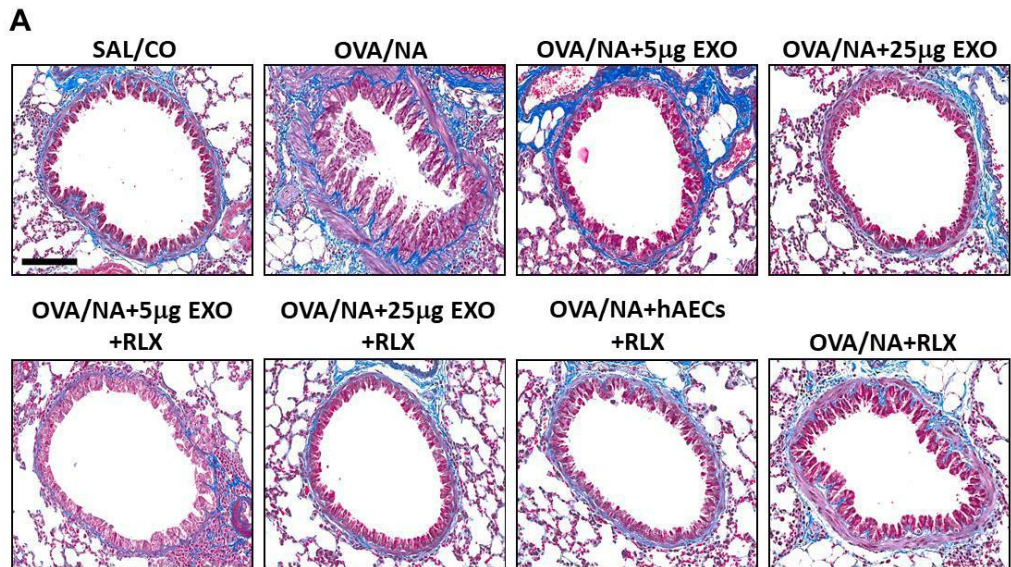


**Figure 5-5: Individual vs. combined effects of EXO + RLX vs. AECs + RLX on the extent of airway epithelial and subepithelial thickness.**

**A)** Representative Masson's trichrome-stained lung sections – demonstrating the extent of epithelial thickness and subepithelial extracellular matrix (ECM/blue staining) thickness from each group studied. Scale bar = 50 $\mu$ m. The effects of hAECs + recombinant human relaxin (RLX) or RLX alone (extrapolated from Chapter 4) are included for comparison. Also shown is the mean + S.E.M

**B)** epithelial thickness (mm<sup>2</sup>; relative to basement membrane (BM) length) and **C)** subepithelial ECM thickness (mm; relative to BM length – a measure of fibrosis) from 5 airways/mouse; n=8 animals per group. \*p<0.05, \*\*P<0.01, \*\*\*P<0.001 vs Saline/corn oil-treated uninjured control group; ##P<0.01, ###P<0.001 vs OVA/NA-treated chronic allergic airways disease (AAD) group; ¶p<0.05; ¶¶p<0.01, ¶¶¶P<0.001 vs OVA/NA+5mg hAEC-derived exosome (EXO)-treated group; ‡p<0.01 vs OVA/NA+25mg hAEC-derived EXO-treated group; §P<0.05, §§§P<0.001 vs OVA/NA+RLX-treated group.

ECM thickness (+5 $\mu$ g EXO:  $27.09 \pm 1.14$ ; +25 $\mu$ g EXO:  $23.81 \pm 0.80$ ;  $P < 0.05$  vs +5 $\mu$ g EXO group; both  $P < 0.01$  vs OVA/NA group; **Figures 5-5A and C**). Co-administration of RLX with EXO further the anti-fibrotic efficacy of EXO alone (+5 $\mu$ g EXO + RLX:  $21.45 \pm 0.76$ ;  $P < 0.05$  vs. +5 $\mu$ g EXO group / +25 $\mu$ g EXO + RLX:  $18.58 \pm 1.01$ ;  $P < 0.01$  vs. +25 $\mu$ g EXO group; both  $P < 0.001$  vs. OVA/NA group); such that 25 $\mu$ g EXO + RLX was able to normalise subepithelial collagen deposition to levels measured from saline/CO-treated mice (no different vs. saline/CO group). Likewise, AECs + RLX ( $19.40 \pm 0.57$ ;  $P < 0.001$  vs. OVA/NA group) was able to normalise subepithelial collagen deposition to that measured from saline/CO-treated mice (no different vs. saline/CO group; **Figures 5-5A and C**). The effects of RLX alone ( $25.58 \pm 1.17$ ;  $P < 0.001$  vs OVA/NA group;  $P < 0.001$  vs saline/CO group) was retrospectively included (as determined in Chapter 4) to comparatively show that it only had a partial but significant effect alone in reducing the OVA + NA-induced increase in subepithelial collagen deposition (**Figures 5-5A and C**).

#### 5.3.3.2 Total lung collagen concentration

Total lung collagen concentration (% collagen content/dry weight lung tissue) was extrapolated from hydroxyproline analysis of lung tissues (**Figures 5-6**) and was also significantly elevated in OVA + NA-treated mice compared to that measured from their saline-CO-treated counterparts (OVA/NA:  $2.94 \pm 0.08\%$ ; Saline/CO:  $2.09 \pm 0.09\%$ ;  $P < 0.001$  vs. saline/CO). 25 $\mu$ g EXO ( $2.62 \pm 0.14\%$ ;  $P < 0.05$  vs. OVA/NA group;  $P < 0.01$  vs. saline/CO group), but not 5 $\mu$ g EXO ( $2.73 \pm 0.12\%$ ; no different vs. OVA/NA group;  $P < 0.001$  vs. saline/CO group) alone

Figure 5-6:

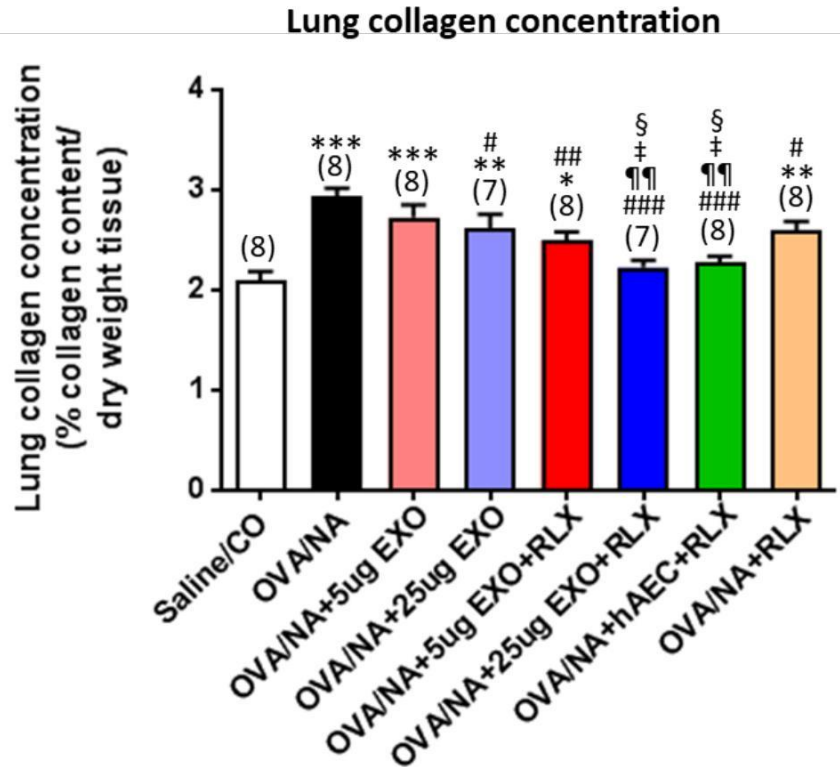


**Figure 5-6: Individual vs. combined effects of EXO + RLX vs. AECs + RLX on lung collagen concentration, as a measure of fibrosis.**

Shown is the mean + S.E.M total lung collagen concentration (% lung collagen content/dry weight tissue – a measure of fibrosis); from n=7-8 animals per group. \*p<0.05, \*\*P<0.01, \*\*\*P<0.001 vs Saline/corn oil-treated uninjured control group; #P<0.05, ##P<0.01, ###P<0.001 vs OVA/NA-treated chronic allergic airways disease (AAD) group; ¶¶ p<0.01 vs OVA/NA+5mg hAEC-derived exosome (EXO)-treated group; ‡p<0.05 vs OVA/NA+25mg hAEC-derived EXO-treated group; §P<0.05 vs OVA/NA+RLX-treated group (extrapolated from Chapter 4).

partially but significantly reduced the OVA + NA-induced aberrant total lung collagen concentration (**Figures 5-6**). The collagen-inhibitory effects of EXO appeared to be again enhanced by the presence of RLX (+5 $\mu$ g EXO + RLX:  $2.50 \pm 0.09\%$ ;  $P < 0.01$  vs. ONA/NA group;  $P < 0.05$  vs. saline/CO group / +25 $\mu$ g EXO + RLX:  $2.23 \pm 0.07\%$ ;  $P < 0.001$  vs. OVA + NA group;  $P < 0.05$  vs +25 $\mu$ g EXO group; no different vs. saline/CO group). Similarly, AECs + RLX also normalised the OVA + NA-induced increase in total lung collagen concentration ( $2.28 \pm 0.06\%$ ;  $P < 0.001$  vs. OVA + NA group; no different vs. saline/CO group; **Figures 5-6**). The effects of RLX alone ( $2.59 \pm 0.03\%$ ;  $P < 0.05$  vs. OVA + NA group;  $P < 0.01$  vs. saline/CO group) was retrospectively included (as determined in Chapter 4) to show that it only partially but significantly reduced the OVA + NA-induced increase in total lung collagen concentration (**Figures 5-6**).

#### 5.3.3.3 TGF- $\beta$ 1 expression

TGF- $\beta$ 1 expression and distribution in the airway epithelium (relative to basement membrane length) was assessed by morphometric analysis of TGF- $\beta$ 1-stained lung tissue sections (**Figures 5-7A and B**), and was markedly increased in OVA + NA-treated mice compared with that measured from saline/CO-treated animals (OVA + NA:  $69.44 \pm 1.67\%$ ; Saline/CO:  $1.22 \pm 0.07\%$ ;  $P < 0.001$  vs. saline/CO group; **Figures 5-7A and B**). 5 $\mu$ g EXO was able to partially, but significantly reduce TGF-  $\beta$ 1 levels (+5 $\mu$ g EXO:  $46.35 \pm 2.04\%$ ;  $P < 0.01$  vs. OVA/NA group;  $P < 0.001$  vs. saline/CO group). RLX alone (retrospectively added from being determined in Chapter 4;  $29.27 \pm 3.64\%$ ;  $P < 0.001$  vs. OVA/NA group;  $P < 0.01$  vs. saline/CO group) further reduced the aberrant TGF- 1

Figure 5-7:

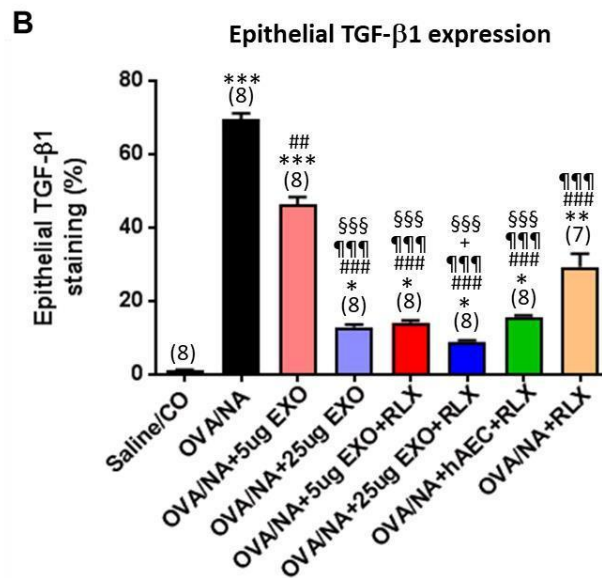
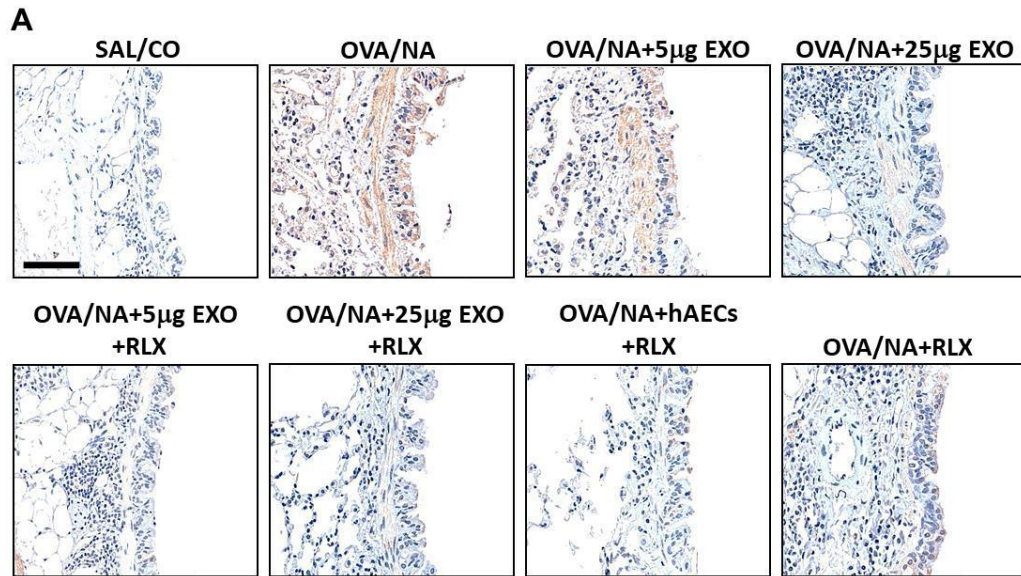


**Figure 5-7: Individual vs. combined effects of EXO + RLX vs. AECs + RLX on epithelial TGF- $\beta$ 1 expression.**

**A)** Representative images of immunohistochemically-stained lung sections for epithelial TGF- $\beta$ 1 expression levels from each group studied. Scale bar = 50 $\mu$ m. The effects of hAECs + recombinant human relaxin (RLX) or RLX alone (extrapolated from Chapter 4) are included for comparison. **B)** Also shown is the mean + S.E.M TGF- $\beta$ 1-staining (expressed as % staining per area analysed) from 5 airways/mouse; n=7-8 animals per group. \*p<0.05, \*\*P<0.01, \*\*\*P<0.001 vs Saline/corn oil-treated uninjured control group; ##P<0.01, ###P<0.001 vs OVA/NA-treated chronic allergic airways disease (AAD) group; ¶¶¶P<0.001 vs OVA/NA+5mg hAEC-derived exosome (EXO)-treated group; +p<0.05 vs OVA/NA+hAEC+RLX-treated group; §§§P<0.001 vs OVA/NA+RLX-treated group.

expression levels; while all other treatments reduced aberrant TGF- 1 expression levels to an even greater extent (+25 $\mu$ g EXO:  $12.95 \pm 0.68$ ; +5 $\mu$ g EXO + RLX:  $14.13 \pm 0.57$ ; +25 $\mu$ g EXO + RLX:  $8.98 \pm 0.33$ ; +AECs + RLX:  $15.67 \pm 0.52$ ; all  $P < 0.001$  vs. OVA/ NA-treated group; all  $P < 0.001$  vs. RLX alone group), although not full back to that measured from saline/CO-treated mice (all  $P < 0.05$  vs. saline/CO group; **Figures 5-7A and B**). Of note, 25 $\mu$ g EXO + RLX reduced TGF- 1 staining to a greater extent than AECs + RLX ( $P < 0.05$  vs. AECs + RLX group; **Figures 5-7A and B**).

#### 5.3.3.4 Myofibroblast differentiation

The number of  $\alpha$ -SMA-stained positive cells (per 100 $\mu$ m of basement length) in the subepithelial layer of various airways was assessed by morphometric analysis of  $\alpha$ -SMA-stained lung tissue sections (**Figures 5-8A and B**) and was significantly increased in OVA + NA-treated mice compared with that measured in their saline/CO-treated counterparts (OVA/ NA:  $2.49 \pm 0.08$ ; Saline/CO:  $0.13 \pm 0.03$ ;  $P < 0.001$  vs. saline/CO group). EXO alone-treatment dose-dependently reduced myofibroblast differentiation (+5 $\mu$ g EXO:  $1.11 \pm 0.19$ ;  $P < 0.001$  vs OVA/NA group;  $P < 0.001$  vs saline/CO group / +25 $\mu$ g EXO:  $0.31 \pm 0.05$ ;  $P < 0.001$  vs. OVA/NA group;  $P < 0.001$  vs 5 $\mu$ g EXO group; no different vs. saline/CO group). Co-administration of RLX enhanced the effects of 5 $\mu$ g EXO alone (+5 $\mu$ g EXO + RLX:  $0.66 \pm 0.05$ ;  $P < 0.05$  vs. 5 $\mu$ g EXO group); and normalised myofibroblast differentiation in combination with 25 $\mu$ g EXO (+25 $\mu$ g EXO + RLX:  $0.20 \pm 0.04$ ;  $P < 0.001$  vs OVA/NA group; no different vs. saline/CO group; **Figures 5-8A and B**). 25 $\mu$ g  $\pm$  RLX also reduced myofibroblast differentiation to a

Figure 5-8:

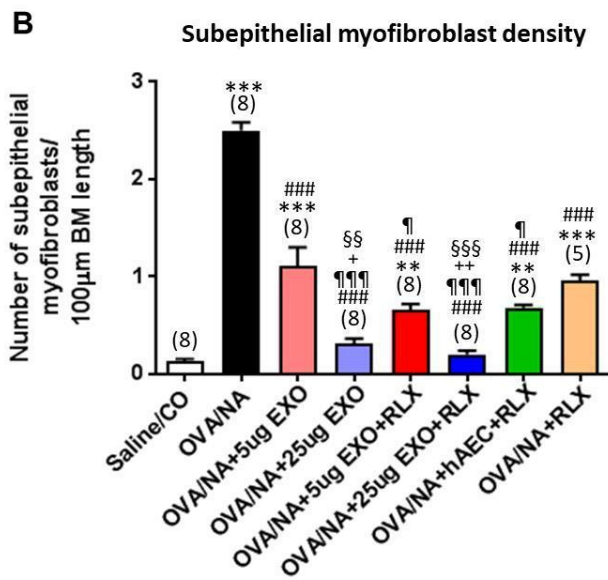
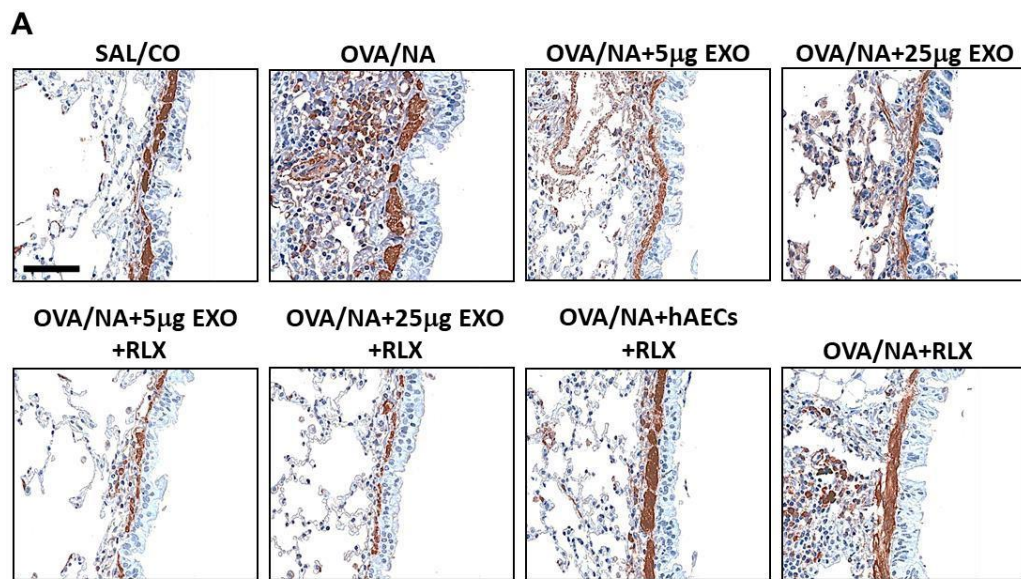


**Figure 5-8: Individual vs. combined effects of EXO + RLX vs. AECs + RLX on subepithelial myofibroblast accumulation.**

**A)** Representative images of immunohistochemically-stained lung sections for subepithelial myofibroblast density. Scale bar = 50 $\mu$ m. The effects of hAECs + recombinant human relaxin (RLX) or RLX alone (extrapolated from Chapter 4) are included for comparison. **B)** Also shown is the mean + S.E.M number of  $\alpha$ -smooth muscle actin-stained myofibroblasts in the subepithelial region (per 100mm basement membrane (BM) length) from 5 airways/mouse; n=5-8 animals per group. \*p<0.05, \*\*P<0.01, \*\*\*P<0.001 vs Saline/corn oil-treated uninjured control group; ##P<0.01, ###P<0.001 vs OVA/NA-treated chronic allergic airways disease (AAD) group; ¶P<0.05, ¶¶¶P<0.001 vs OVA/NA+5mg hAEC-derived exosome (EXO)-treated group; +p<0.05, ++p<0.01 vs OVA/NA+hAEC+RLX-treated group; ; §§P<0.01, §§§P<0.001 vs OVA/NA+RLX-treated group.

greater extent than AECs + RLX ( $0.68 \pm 0.03$ ;  $P < 0.01$  vs.  $25\mu\text{g}$  EXO + RLX group;  $P < 0.001$  vs OVA/NO group;  $P < 0.01$  vs saline/CO group) or RLX alone ( $0.96 \pm 0.07$ ;  $P < 0.001$  vs.  $25\mu\text{g}$  EXO + RLX group;  $P < 0.001$  vs OVA/NO group;  $P < 0.001$  vs saline/CO group; **Figures 5-8A and B**).

#### **5.3.4 Individual versus combined effects of EXO and RLX on airway resistance.**

Changes in airway resistance between treatment groups were measured by invasive plethysmography in response to increasing doses of nebulised methacholine (**Figures 5-9**). Consistent with the increased AI, AWR and fibrosis associated with OVA + NA-treated mice, these mice with chronic AAD demonstrated significantly increase in airway resistance compared to that measured from saline/CO-treated mice ( $P < 0.001$  vs. saline/CO-treated group; **Figures 5-9**).  $5\mu\text{g}$  EXO alone, did not significantly affect the OVA + NA-induced increase in airway resistance ( $P < 0.001$  vs. saline/CO-treated group; **Figures 5-9**), whereas  $25\mu\text{g}$  EXO alone partially but significantly reduced airway resistance by ~50% ( $P < 0.01$  vs. OVA/NA group;  $P < 0.05$  vs.  $5\mu\text{g}$  EXO group;  $P < 0.01$  vs. saline/CO-treated group; **Figures 5-9**). RLX alone (retrospectively added from being determined in Chapter 4) and AECs + RLX also partially but significantly reduced airway resistance by ~50% (both  $P < 0.05$  vs. OVA/NA group;  $P < 0.05$  vs.  $5\mu\text{g}$  EXO group;  $P < 0.01$  vs. saline/CO-treated group; **Figures 5-9**). Interestingly, the combined effects of RLX and  $5\mu\text{g}$  EXO reduced the OVA + NA-induced airway resistance by ~70% ( $P < 0.001$  vs. OVA/NA group;  $P < 0.001$  vs.  $5\mu\text{g}$  EXO group;  $P < 0.05$  vs. saline/CO group); while the combined effects of RLX and  $25\mu\text{g}$  EXO further reduced the aberrant airway resistance to that which was no longer

**Figure 5-9:**

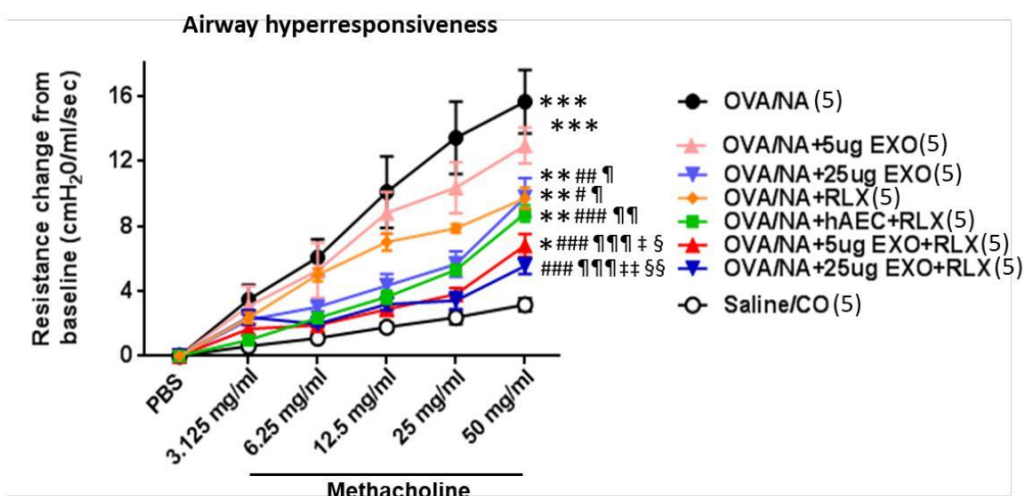


**Figure 5-9: Individual vs. combined effects of EXO + RLX vs. AECs + RLX on airway resistance (AHR).**

Effects of the various groups evaluated on airway hyperresponsiveness (AHR). Airway resistance (reflecting changes in AHR) was assessed via invasive plethysmography in response to increasing doses of nebulised methacholine (a bronchoconstrictor). Results are expressed as resistance change from baseline. Shown is the mean  $\pm$  S.E.M. airway resistance to each dose of methacholine testes (n=5 animals per group). The effects of hAECs + recombinant human relaxin (RLX) or RLX alone are included for comparison. \*p<0.05, \*\*P<0.01, \*\*\*P<0.001 vs Saline/corn oil-treated uninjured control group; ##P<0.01, ###P<0.001 vs OVA/NA-treated chronic allergic airways disease (AAD) group; ¶P<0.05, ¶¶ P<0.01, ¶¶¶P<0.001 vs OVA/NA+5mg hAEC-derived exosome (EXO)-treated group; †p<0.05, ‡p<0.01 vs OVA/NA+25mg hAEC-derived exosome (EXO)-treated group; §P<0.05, §§P<0.01 vs OVA/NA+RLX-treated group (extrapolated from Chapter 4).

different to that measured from saline/CO-treated mice ( $P < 0.001$  vs. OVA/NA group;  $P < 0.01$  vs. 25 $\mu$ g EXO group;  $P < 0.01$  vs. RLX alone group; no different vs. saline/CO group; **Figures 5-9**).

#### **5.4 DISCUSSION**

Exosomes (EXO) were first described in 1983, over 30 years ago, but were considered to only be important for discarding unwanted molecular components (Rasposo & Stoorvogel, 2013; Kruh-Garcia et al., 2015). Interest in EXO began in the mid 1990's when it was discovered that they were vital for intercellular communication and were secreted by many cell types including epithelial, muscle, neuronal and stem cells (Johnstone, 1992). While there is very little literature on AEC-derived EXO, bone marrow-derived mesenchymal stem cell (MSC)-derived EXO have been shown to have anti-apoptotic and anti-inflammatory actions (Huang et al., 2015). In a previous study, we were able to show that AECs were able to match or outperform the effect of MSCs on AI, AWR and AHR associated with the classical OVA-induced model of chronic AAD. Therefore AEC-derived EXO were used as it was believed that these EXO would possess the therapeutic and reparative proteins, lipids, mRNA and miRNA that would be more beneficial against the AI, AWR, and AHR associated with the refined OVA/NA-model of chronic AAD.

In this study, we demonstrated that AEC-derived EXO alone dose-dependently offered some level of protection against the AI, AWR and AHR associated with chronic AAD (**Table 5-1**), when intranasally administered to mice. As previously shown (in Chapter 4 and published in Patel et al., 2016), intranasal administration of RLX alone also partially reduced measures of AWR, airway fibrosis and AHR in the model studied, in the absence of having any effects on AI. Strikingly, combining EXO with RLX demonstrated greater therapeutic efficacy compared to either treatment alone and further reduced the chronic AAD-induced AI, AWR, airway fibrosis and AHR. Of particular note, combining 25 g EXO (which would be extracted from  $\sim 50 \times 10^6$  AECs) with RLX was able to normalise the chronic AAD-induced epithelial damage and thickness, subepithelial and total lung collagen deposition (fibrosis), subepithelial myofibroblast density and AHR to equivalent levels measured from saline/CO<sub>2</sub>-treated uninjured mice over a one-week treatment period, and also significantly decreased AI (**Table 5-1**). Comparatively, combining 25 g EXO and RLX also offered greater protection against the chronic AAD-induced AI, goblet cell metaplasia, aberrant airway epithelial TGF- $\beta$ 1 expression and subepithelial myofibroblast accumulation compared to the combined effects of AECs and RLX (**Table 5-1**).

These findings confirm that the anti-fibrotic and organ-protective effects of RLX can enhance the therapeutic efficacy of RFXP1-expressing AECs (Royce et al., 2016) or the EXO they secrete in chronic disease settings. There are several advantages though to using EXO over AECs, including 1) the fact that mice can

**Table 5-1: Summary of the individual vs combined effects of EXO ± RLX vs. AECs**

**+ RLX in the OVA+NA model**

	Key features of human asthma	OVA/NA	OVA/NA +5µg EXO	OVA/NA +25µg EXO	OVA/NA +5µg EXO +RLX	OVA/NA +25µg EXO +RLX	OVA/NA +AECs +RLX
<b>AI</b>	Inflammation score	↑↑↑	↓	↓	↓	↓↓ <sup>+</sup>	↓
	Goblet cell count	↑↑↑	–	–	↓	↓↓ <sup>+</sup>	↓
<b>AWR</b>	Epithelial damage	↑↑↑	↓↓	↓↓↓	↓↓	↓↓↓	↓↓↓
	Epithelial thickness	↑↑↑	↓↓↓	↓↓↓	↓↓↓	↓↓↓	↓↓↓
<b>FIBROSIS</b>	Subepithelial ECM	↑↑↑	–	↓	↓↓	↓↓↓	↓↓↓
	Total Collagen	↑↑↑	–	↓	↓↓	↓↓↓	↓↓↓
	TGF-β1	↑↑↑	↓	↓↓	↓↓	↓↓ <sup>+</sup>	↓↓
	α-SMA	↑↑↑	↓	↓↓↓ <sup>+</sup>	↓↓	↓↓↓ <sup>++</sup>	↓↓
<b>AHR</b>	Airway resistance	↑↑↑	–	↓	↓↓	↓↓↓	↓↓

**Table 5-1. Summary of the individual vs combined effects of EXO ± RLX vs. AECs + RLX in the OVA+NA model.**

A summary of the individual vs combined effects of EXO ± RLX vs. AECs + RLX on chronic AAD-induced AI, AWR, fibrosis and AHR. The arrows in the OVA/NA column are reflective of changes to that measured in saline/CO-treated mice, while the arrows in the various treatment groups are reflective of changes to that in the OVA/NA group. – denotes no changes compared to the effects of OVA+NA alone; + P < 0.05, ++P < 0.01 vs. AEC + RLX-treated group.

physically only be treated with  $1-2 \times 10^6$  AECs (Moodley et al., 2010) whereas they can be subjected to the therapeutic equivalent of a much greater number of stem cells via the administration of EXO (i.e the 5 g and 25 g EXO administered to mice in this study would be equivalent to administering  $10 \times 10^6$  and  $50 \times 10^6$  AECs, respectively); 2) the direct administration of EXO would allow for the transfer of proteins and nucleic acids across cellular boundaries; 3) the use of EXO may avoid other stem cell-based limitations such as donor-dependent variability, culture-induced loss of function and genetic instability; and 4) the use of EXO offers manufacturing and regulatory advantages over stem cell-based therapies (Burke et al., 2016). Although the delivery of EXO was not tracked, a previous study showing that intranasal-administration of AECs was delivered directly to the lungs of OVA-injured mice (Royce et al., 2016) suggests that AEC-derived EXO were also delivered directly to the damaged lungs of OVA/NA-injured animals.

Several important findings were confirmed by the studies conducted: firstly, AECs of chronic airways/lung disease. The use of  $5 \mu\text{g}$  EXO alone was able to reduce the OVA/NA-induced AI (by  $\sim 35\%$ ), subepithelial ECM deposition (by  $\sim 35\%$ ), epithelial TGF- $\beta 1$  (by  $\sim 33\%$ ) and myofibroblast differentiation (by  $\sim 60\%$ ) but failed to affect total lung collagen concentration and consequently, AHR. Comparatively, the use of  $25 \mu\text{g}$  EXO alone further reduced AI (by  $\sim 50\%$ ), subepithelial ECM deposition (by  $\sim 55\%$ ), total lung collagen concentration (by 35-40%) and epithelial TGF- 1 expression levels as well as subepithelial myofibroblast density (by 80-90%), resulting in their ability to partially suppress

chronic AAD-induced AHR (by ~50%). Of note though, EXO alone were able to significantly reduce TSLP-associated epithelial damage, suggesting that they could mediate a significant level of tissue repair, even in the setting of chronic AAD.

Secondly, the finding that the combined effects of AEC-derived EXO (particularly 25 g EXO) with the anti-fibrotic drug RLX normalised several measures of chronic AAD-induced AWR, most notably the aberrant subepithelial and total lung collagen concentration (fibrosis), resulting in the combined effects of 25 g EXO and RLX normalising AHR – confirms our previous observations demonstrated in Chapter 4 (Patel et al., 2016) that treating aberrant lung collagen deposition/concentration (over other measures of AWR or AI) is the key to reversing the AHR associated with chronic AAD. This study showed that the treatments that were most effective in reversing airway/lung collagen deposition and more specifically total lung collagen concentration: 25 g EXO + RLX = AECs + RLX > 5 g EXO + RLX > 25 g EXO = RLX > 5 g EXO most notably reduced AHR in the same order. On the other hand, therapies that targeted other ECM proteins such as fibronectin and other measures of AWR (such as TFF2 or DEX alone) but were less effective in reducing aberrant total lung collagen accumulation were also less effective in treating AHR (Patel et al., 2016). Likewise, AECs alone reduced the chronic AAD-induced AHR (by around 35-40%) to a greater extent than bone marrow-derived MSCs (which did not significantly affect AHR) because AECs unlike bone marrow-derived MSCs were

able to reduce the chronic AAD-induced total lung collagen concentration by 40% (Royce et al., 2016).

Thirdly, however, as the combined effects of 25 g EXO + RLX normalised the chronic OVA/NA-induced AHR, whereas the combined effects of AECs + RLX did not, despite both combination therapies reducing subepithelial and total lung collagen deposition as well as airway epithelial damage and thickening to a similar extent – these findings suggest that treating other measures of AWR is then a secondary means of reducing the AHR associated with chronic AAD. In this regard, the optimal ability of 25 g EXO + RLX to reverse AHR in the model studied (compared to the effects of AECs + RLX) may have likely been attributed to the greater ability of 25 g EXO + RLX to reverse goblet cell metaplasia, aberrant epithelial TGF- 1 expression levels and/or subepithelial myofibroblast density compared to the effects of AECs + RLX (in addition to their ability to effectively lower aberrant lung collagen concentration/ accumulation). Similar findings were observed when RLX was co-administered with TFF2 or TFF2 and DEX, which optimally restored the chronic AAD-induced loss of dynamic compliance, as both sets of combination therapies markedly and equivalently reduced goblet cell metaplasia, aberrant epithelial TGF- 1 expression levels, subepithelial myofibroblast and collagen density as well as total lung collagen concentration (Patel et al., 2016). The fact that the combined effects of RLX and TFF2 could restore the chronic AAD-induced loss of dynamic compliance without affecting AI (Patel et al., 2016), further suggests that AWR makes a greater contribution to AHR compared to AI in a chronic disease setting; and

hence, targeting AWR over AI is more likely to impact on treating chronic AAD-induced AHR.

As the findings observed in the current study suggest that combining 25µg EXO + RLX offered significant protection against the AI and optimal protection against the AWR and related AHR associated with chronic AAD (equivalent to severe asthma), this combination therapy may represent a stand-alone means of treating the 5–10% of asthmatics that are resistant to corticosteroid therapy (Hetherington & Heaney, 2015). Furthermore, this combination therapy (of 25µg EXO + RLX) may serve as an effective adjunct therapy to the anti-inflammatory effects of clinically-used corticosteroids to treat the three central components of asthma: AI, AWR and AHR. As outlined previously, corticosteroids can be slow acting and cause several side-effects when chronically administered, particularly at high doses. Various inhaled corticosteroids (administered at 0.5–6.4mg·day<sup>-1</sup>) (Dahl, 2006) have been shown to induce both local side-effects such as pharyngitis, dysphonia, cough and bronchospasm, as well as systemic side-effects primarily involving suppressed hypothalamic–pituitary–adrenal (HPA)-axis function and growth retardation. In our previous study (Royce et al., 2013) methylprednisolone (0.3 mg kg<sup>-1</sup>·day<sup>-1</sup>; i.p.) was combined with RLX (0.5mg·kg<sup>-1</sup>·day<sup>-1</sup>; s.c.; equivalent to the 0.8mg·mL<sup>-1</sup>·day<sup>-1</sup>; i.n. used in this study) to reduce airway fibrosis to a greater extent than methylprednisolone in the absence of any side-effects on animal body weight or behaviour. Similarly, lower doses of corticosteroids may be combined with EXO + RLX to treat the three central components of asthma without causing any of the side-effects associated with higher concentrations of corticosteroid use alone. The muscle-relaxant

(Baccari et al., 2004) and bronchodilatory (Lam et al., 2016) properties of RLX may be also be helpful in protecting from bronchospasm, while the marked tissue-repairing properties of AEC-derived EXO may limit the overuse of corticosteroid treatment. Hence, the wide-ranging positive effects of 25µg EXO and RLX might enable optimal dosing of corticosteroids to be titrated to safer levels when used in combination.

In conclusion, we have evaluated and compared the combined effects of AECs or AEC-derived EXO with the anti-fibrotic effects of RLX in an experimental model of chronic AAD, which incorporates epithelial damage as part of its pathology and further confirmed that (i) epithelial damage and the ensuing AWR and fibrosis it causes are key contributors to AHR; (ii) AEC-derived EXO alone dose-dependently and partially reduce the AI, AWR and AHR associated with chronic AAD (as per AECs alone); while (iii) the presence of RLX appears to enhance the effects of AEC- derived EXOs such that the combination therapy (particularly 25 g EXO + RLX) offered optimal protection against the AWR and AWR-induced AHR compared to either therapy alone or AECs + RLX. This combination therapy may represent a novel replacement strategy for treating asthmatics that are resistant to corticosteroid therapy or may be used in conjunction with clinically-used corticosteroid to better treat severe asthma. The additional organ-protective effects of RLX, which protects from aberrant TGF- 1-stimulated pathology without affecting normal fibroblast function and ECM production (Unemori et al., 1996), and tissue-repairing effects of AEC-derived EXO offers additional advantages over current asthma medications. While our findings demonstrate

the feasibility of combining these therapies, additional studies aimed at maximally combining them (i.e. engineering EXO to express and deliver RLX to the damaged lung) and further understanding their mode of action are key to their translation as a therapy of the future.

## 5.5 REFERENCES

Baccari MC, Nistri S, Quattrone S, Bigazzi M, Bani Sacchi T, Calamai F, Bani D (2004). Depression by relaxin of neurally induced contractile responses in the mouse gastric fundus. *Biol Reprod.* **70**(1):222-228.

Burke J, Kolhe R, Hunter M, Isales C, Hamrick M4, Fulzele S (2016). Stem Cell-Derived Exosomes: A Potential Alternative Therapeutic Agent in Orthopaedics. *Stem Cells Int.* **2016**:5802529.

Dahl R (2006). Systemic side effects of inhaled corticosteroids in patients with asthma. *Respir Med.* **100**(8):1307-1317.

Chung KF, Wenzel SE, Brozek JL, Bush A, Castro M, Sterk PJ, Adcock IM, Bateman ED, Bel EH, Bleecker ER, Boulet LP, Brightling C, Chanaz P, Dahlen SE, Djukanovic R, Frey U, Gaga M, Gibson P, Hamid Q, Jajour NN, Mauad T, Sorkness RL, Teague WG (2014). International ERS/ATS guidelines on definition, evaluation and treatment of severe asthma. *Eur Respir J.* **43**(2):343-373.

Hetherington KJ, Heaney LG (2015). Drug therapies in severe asthma - the era of stratified medicine. *Clin Med (Lond).* **15**(5):452-456.

Huang L, Ma W, Ma Y, Feng D, Chen H, Cai B (2015). Exosomes in mesenchymal stem cells, a new therapeutic strategy for cardiovascular diseases? *Int J Biol Sci.* **11**(2):238-245.

Johnstone RM (1992). The Jeanne Manery-Fisher Memorial Lecture 1991. Maturation of reticulocytes: formation of exosomes as a mechanism for shedding membrane proteins. *Biochem Cell Biol.* **70**(3-4):179-190.

Knight DA, Rossi FM, Hackett TL (2010). Mesenchymal stem cells for repair of the airway epithelium in asthma. *Expert Rev Respir Med.* **4**(6):747-758.

Koike C, Zhou K, Takeda Y, Fathy M, Okabe M, Yoshida T, Nakamura Y, Kato Y, Nikaido T (2014). Characterization of amniotic stem cells. *Cell Reprogram.* **16**(4):298-305.

Kruh-Garcia NA, Wolfe LM, Dobos KM (2015). Deciphering the role of exosomes in tuberculosis. *Tuberculosis (Edinb).* **95**(1):26-30.

Lai RC, Arslan F, Lee MM, Sze NS, Choo A, Chen TS, Salto-Tellez M, Timmers L, Lee CN, El Oakley RM, Pasterkamp G, de Kleijn DP, Lim SK (2010). Exosome secreted by MSC reduces myocardial ischemia/reperfusion injury. *Stem Cell Res.* **4**(3):214-222.

Lam M, Royce SG, Donovan C, Jelinic M, Parry LJ, Samuel CS, Bourke JE (2016). Serelaxin Elicits Bronchodilation and Enhances  $\beta$ -Adrenoceptor-Mediated Airway Relaxation. *Front Pharmacol.* **7**:406.

Moodley Y, Ilancheran S, Samuel C, Vaghjiani V, Atienza D, Williams ED, Jenkin G, Wallace E, Trounson A, Manuelpillai U (2010). Human amnion epithelial cell transplantation abrogates lung fibrosis and augments repair. *Am J Respir Crit Care Med.* ;**182**(5):643-651.

Murphy S, Rosli S, Acharya R, Mathias L, Lim R, Wallace E, *et al.* (2010). Amnion epithelial cell isolation and characterization for clinical use. *Curr Prot Stem Cell Biol* Chapter 1: Unit 1E 6.

Murphy SV, Kidyoor A, Reid T, Atala A, Wallace EM, Lim R (2014). Isolation, cryopreservation and culture of human amnion epithelial cells for clinical applications. *J Vis Exp* 2014: 94.

Patel KP, Giraud AS, Samuel CS, Royce SG (2016). Combining an epithelial repair factor and anti-fibrotic with a corticosteroid offers optimal treatment for allergic airways disease. *Br J Pharmacol.* **173**(12):2016-2029.

Raposo G1, Stoorvogel W (2013). Extracellular vesicles: exosomes, microvesicles, and friends. *J Cell Biol.* **200**(4):373-383.

Royce SG, Patel KP, Samuel CS (2014). Characterization of a novel model incorporating airway epithelial damage and related fibrosis to the pathogenesis of asthma. *Lab Invest.* **94**:1326–1339.

Royce SG, Sedjahtera A, Samuel CS, Tang ML (2013b). Combination therapy with relaxin and methylprednisolone augments the effects of either treatment alone in inhibiting subepithelial fibrosis in an experimental model of allergic airways disease. *Clin Sci (Lond)* **124**:41–51.

Royce SG, Shen M, Patel KP, Huuskes BM, Ricardo SD, Samuel CS (2015). Mesenchymal stem cells and serelaxin synergistically abrogate established airway fibrosis in an experimental model of chronic allergic airways disease. *Stem Cell Res.* **15**: 495–505.

Royce SG, Tominaga AM, Shen M, Patel KP, Huuskes BM, Lim R, Ricardo SD, Samuel CS (2016). Serelaxin improves the therapeutic efficacy of RFXP1-expressing human amnion epithelial cells in experimental allergic airway disease. *Clin Sci (Lond)*. **130**(23):2151-2165.

Schorey JS1, Bhatnagar S (2008). Exosome function: from tumor immunology to pathogen biology. *Traffic*. **9**(6):871-881.

Squadrito ML, Baer C, Burdet F, Maderna C, Gilfillan GD, Lyle R, Ibberson M, De Palma M (2014). Endogenous RNAs modulate microRNA sorting to exosomes and transfer to acceptor cells. *Cell Rep*. **8**(5):1432-1446.

Tan JL, Lau SN, Leaw B, Nguyen HPT, Salamonsen LA, Saad MI, *et al.* (2018). Amnion Epithelial Cell-Derived Exosomes Restrict Lung Injury and Enhance Endogenous Lung Repair. *Stem Cell Transl Med* **7**: 180-196.

Unemori EN, Pickford LB, Salles AL, Piercy CE, Grove BH, Erikson ME, Amento EP (1996). Relaxin induces an extracellular matrix-degrading phenotype in human lung fibroblasts in vitro and inhibits lung fibrosis in a murine model in vivo. *J Clin Invest*. **98**(12):2739-2745.

Vader P, Mol EA, Pasterkamp G, Schiffelers RM (2016). Extracellular vesicles for drug delivery. *Adv Drug Deliv Rev.* **106**(Pt A):148-156.

Vlassov AV, Magdaleno S, Setterquist R, Conrad R (2012). Exosomes: current knowledge of their composition, biological functions, and diagnostic and therapeutic potentials. *Biochim Biophys Acta.* **1820**(7):940-948.

---

**CHAPTER 6:**

**Discussion and Conclusion**

---

## 5.0 DISCUSSION AND CONCLUSION

Currently-available therapies for human asthma either manage or subdue episodes of AHR (e.g. with 2-adrenergic receptor agonists), or target and treat AI and subsequent AI-induced AHR (e.g. with corticosteroids). Unfortunately, these therapies do not specifically target epithelial damage or other features of AWR (such as pro-fibrotic cytokine release and pro-fibrotic cytokine-induced myofibroblast differentiation), which can lead to the development of AHR independently of AI. Therefore, the studies reported in this thesis were conducted to i) establish a refined experimental model of chronic allergic airways disease that would better mimic key features of human asthma (associated with epithelial damage); and ii) investigate potential therapies that may be able to target and reverse epithelial damage and related AWR and AWR-induced AHR. Additionally, the combined effects of several therapies were evaluated in comparison to, and in combination with, a clinically-used corticosteroid to determine the optimal approach for treating the three central components of asthma: AI, AWR and AHR.

### 5.1 MAIN FINDINGS

Aim-1 (Royce et al., 2014) demonstrated that superimposing epithelial damage (with naphthalene) onto established ovalbumin-induced chronic AAD (rather than prior to or during the progression of AAD) led to a significant increase in

eosinophil-induced AI, and substantial increases in epithelial damage and thickening, TGF- $\beta$ 1-induced subepithelial and total collagen deposition/concentration (fibrosis), cell apoptosis and AHR; mimicking several features of human asthma.

Aim-2 utilised the OVA+NA-induced model of chronic AAD incorporating epithelial damage (established in Aim-1) to demonstrate that the anti-remodelling and anti-fibrotic effects of RLX were able to effectively reduce AHR, compared to the epithelial repair properties of TFF2 and anti-inflammatory properties of the corticosteroid, DEX (Patel et al., 2016). Furthermore, this Aim demonstrated that combining RLX, TFF2 and DEX offered maximal protection against the AI, AWR and AHR/dynamic compliance associated with chronic AAD.

Aim-3 utilised the OVA+NA-induced model of chronic AAD incorporating epithelial damage (established in Aim-1) to demonstrate that the anti-inflammatory, anti-remodelling and anti-fibrotic effects of AEC-EXO (25 g) in combination with RLX were also able to effectively reduce AHR, compared to the combined effects of  $1 \times 10^6$  AECs + RLX (which did not suppress AI or some features of AWR to the same extent as the combined effects of AEC-EXO+RLX). This Aim also demonstrated that combining RLX with EXO (25 g) offered optimal protection against AWR and AHR, with some protection against AI. Several implications could be extrapolated from these combined findings:

i) DEX administration alone was able to significantly reverse AI, AI-induced goblet cell metaplasia, epithelial damage and thickness as well as aberrant airway epithelial TGF- $\beta$ 1 levels; but modestly reduced subepithelial fibronectin levels in the absence of having any effects on subepithelial myofibroblast differentiation or total collagen concentration; which resulted in no significant changes to chronic AAD-induced AHR (**Table 5-1**). Our lab has also investigated the effects of another corticosteroid, methylprednisolone, in the setting of the traditional 9-week mouse model of OVA-induced chronic AAD, where methylprednisolone was shown to effectively reduce AI, but only modestly reduced AI-induced AWR and AHR (Royce et al., 2013).

These combined findings demonstrate the limited extent AI contributes to AHR in the setting of chronic AAD/asthma, and hence, the limited benefits asthma sufferers receive with corticosteroid therapy. In other words, primarily suppressing AI, with modest to no effects on AWR or airway fibrosis led to modest effects of the suppression of chronic AAD-induced AHR.

ii) In comparison, TFF2 administration led to marked reductions in airway epithelial damage and thickening as well as airway epithelial TGF- $\beta$ 1 expression, partial effects on subepithelial myofibroblast differentiation and fibronectin deposition in the absence of any effects on total lung collagen concentration, and stimulation of collagen-degrading MMP-9, but not MMP-2 levels (**Table 5-1**). These combined findings also led to no significant changes to chronic AAD-induced AHR; suggesting that epithelial damage and related thickness/cytokine

release also contributed to AHR to a minor extent. Hence, these findings demonstrated that therapies mainly targeting epithelial damage and related thickness/cytokine release alone, would also modestly impact on chronic AAD-induced AHR. Consistent with this, a low dose of AEC-EXO (5 g) alone that effectively reduced epithelial damage and thickening, but only modestly reduced airway TGF- 1 expression as well as subepithelial myofibroblast differentiation and ECM deposition without affecting total lung collagen concentration, did not significantly affect chronic AAD-induced AHR.

iii) Administration of the anti-fibrotic hormone, RLX, led to marked reductions in chronic AAD-induced epithelial thickening and TGF- $\beta$ 1 expression, subepithelial myofibroblast differentiation and fibronectin deposition, and total lung collagen concentration while increasing levels of collagen-degrading MMP-2 and MMP-9; which in turn led to a 50-70% reduction in AHR (Royce et al., 2009; Royce et al., 2013; Patel et al, 2016) (**Table 5-1**). These combined findings suggest that aberrant collagen concentration/airway fibrosis (resulting from AWR) is the most prominent contributor to AHR compared to the effects of AI or other features of AWR remodelling such as epithelial damage and thickening. As such, the extent to which airway fibrosis is therapeutically diminished appears to correlate with how effectively AHR can be reduced. To this extent, whereas a lower dose of AEC- EXO (5 g) that did not affect chronic AAD-induced collagen concentration (fibrosis), failed to significantly lower AHR, a higher dose of AEC- EXO (25 g) alone, that partially but significantly lowered chronic AAD-induced

total collagen concentration and subepithelial ECM deposition was able to lower AHR by ~50%.

iv) However, reducing airway fibrosis alone was found to not necessarily normalise AHR. Despite the combined effects of RLX and  $1 \times 10^6$  AECs normalising chronic AAD-induced subepithelial ECM deposition and total lung collagen concentration, the limited ability of this combination therapy to reduce other features of AWR including goblet cell metaplasia and myofibroblast differentiation, resulted in its ability to only reduce AHR by ~50-80% (Royce et al., 2016) (**Table 5-1**). This suggests that therapies that can more broadly target several features of chronic AAD-induced AWR are more likely to normalise AHR.

v) Consistent with this, combining the use of RLX (to treat airway fibrosis) with TFF2 (to treat epithelial damage and related thickness), demonstrated maximal protection against chronic AAD-induced AHR; indicating that the reduction of aberrant collagen concentration and epithelial damage/thickness at the same time could lead to the normalisation of AHR (**Table 5-1**). Importantly, as these effects occurred in the absence of a reduction in AI, these findings indicate that targeting epithelial damage/thickness and the ensuing fibrosis that results from AWR, can lead to the normalisation of AHR without the need to lower AI; confirming that AWR can contribute to AHR independently of AI. **To this extent, although treatment strategies that do not affect AI would not be used to treat mainstream asthma, they may offer relief of steroid-resistant asthma sufferers that do not respond to corticosteroid treatment.**

While 300 million people around the world suffer from asthma, approximately 5% of asthma sufferers are associated with steroid-resistant asthma, which means that they are unable to respond to the anti-inflammatory effects of corticosteroids (WHO, 2007). One theory for the development of steroid-resistant asthma is that it occurs due to a bacterial or fungal infection during the development of asthma (Wang et al., 2010). This results in (i) a reduction in T-cells that possess receptors for the corticosteroids to act upon, and (ii) an alteration in the binding site of the remaining corticosteroid receptors which prevents the binding of therapeutic corticosteroids (Ito et al., 2006; Adcock & Barnes, 2008). As people whom suffer from steroid-resistant asthma still present with epithelial damage and related AWR, fibrosis and AHR, strategies that target airway fibrosis and epithelial damage/thickening (such as RLX and TFF2) may be a potential therapeutic option for these patients.

vi) Finally, combining the anti-fibrotic effects of RLX with the epithelial-repair properties of TFF2 and anti-inflammatory effects of the corticosteroid, DEX, offered maximal protection against the three central components of chronic AAD/asthma (Patel et al., 2016) (Table 5-1). Not only was this combination therapy shown to be feasible without impacting/diminishing the individual effects of either treatment alone, it demonstrated that the combined effects of RLX and TFF2 could serve as a suitable adjunct therapy to clinical available corticosteroids, to offer more comprehensive protection of asthma disease pathology over the effects of corticosteroid treatment alone. Likewise,

**Table 6-1: Summary of the various individual and combined therapies investigated**

Characteristics of Human Asthma		OVA/NA	+DEX	+TFF2	+RLX	+TFF2+RLX	+TFF2+RLX+DEX	+25mg EXO	+5mg EXO+RLX	+25mg EXO+RLX	+AEC+RLX
AI	Inflammation score	↑↑↑	↓↓	-	-	-	↓↓	↓	↓	↓↓	↓
	Goblet cell count	↑↑↑	↓↓↓	↓↓	-	↓↓↓	↓↓↓	-	↓	↓↓	↓
AWR	Epithelial damage	↑↑↑	↓↓	↓↓↓	↓	↓↓↓	↓↓↓	↓↓↓	↓↓	↓↓↓	↓↓↓
	Epithelial thickness	↑↑↑	↓↓	↓↓	↓↓	↓↓	↓↓	↓↓↓	↓↓↓	↓↓↓	↓↓↓
Fibrosis	Subepithelial ECM	↑↑↑	↓↓	↓	↓↓	↓↓	↓↓↓	↓	↓↓	↓↓↓	↓↓↓
	Total collagen	↑↑↑	-	-	↓↓	↓↓	↓↓↓	↓	↓↓	↓↓↓	↓↓↓
	Fibronectin	↑↑↑	↓	↓	↓↓	↓↓	↓↓	ND	ND	ND	ND
	TGF-β1	↑↑↑	↓↓	↓↓	↓	↓↓	↓↓	↓↓	↓↓	↓↓	↓↓
	α-SMA	↑↑↑	-	↓	↓↓	↓↓	↓↓	↓↓↓	↓↓	↓↓↓	↓↓
	MMP-2	-	-	-	↑↑	↑↑	↑↑↑	ND	ND	ND	ND
	MMP-9	-	-	↑↑↑	↑↑↑	↑↑↑	↑↑↑	ND	ND	ND	ND
AHR		↑↑↑	-	-	↓↓	↓↓↓	↓↓↓	↓	↓↓	↓↓↓	↓↓

**Table 6-1: Summary of the various individual and combined therapies investigated.**

A summary of the individual vs combined effects of DEX, TFF2, RLX, TFF2+RLX, TFF2+RLX+DEX, 25mg EXO, 5mg EXO+RLX, 25mg EXO+RLX vs. 1x10<sup>6</sup> AECs+RLX on chronic AAD-induced AI, AWR, fibrosis and AHR. The arrows in the OVA/NA column are reflective of changes to that measured in saline/CO-treated mice, while the arrows in the various treatment groups are reflective of changes to that in the OVA/NA group. – denotes no changes compared to the effects of OVA+NA alone; ND denotes not determined.

combining AEC-EXO (25 g) with RLX offered the complete normalisation of AHR by not only abrogating airway fibrosis, but also significantly reducing AI and several features of AWR (such as goblet cell metaplasia, epithelial damage/thickness, epithelial TGF- $\beta$ 1 expression and subepithelial myofibroblast differentiation) (**Table 5-1**). The studies presented in this thesis also demonstrated the feasibility of combining RLX with stem cells or stem cell-derived EXO, the latter which could represent a stand-alone therapy for mainstream asthma sufferers as well as those that are resistant to corticosteroid therapy.

## 5.2 LIMITATIONS

The major limitation with any animal-based study is the model used to replicate human disease. It is very hard to completely replicate a human disease in an animal, and this is a commonly-found issue with animal models of human asthma.

While the commonly used 9-week mouse model of OVA-induced AAD does undergo AI and, AI-induced AWR (goblet cell metaplasia, epithelial thickness, up-regulation of airway TGF- $\beta$ 1 expression and myofibroblast density and smooth muscle thickening) and AHR, it lacks epithelial damage as a component of its pathology, which is now believed to be a major component of the pathogenesis of asthma.

Therefore, although OVA is not a typical instigator of human asthma, due to its ability to induce several features of human asthma in mice, a refined mouse model of OVA-induced AAD was developed that not only incorporated epithelial damage onto the pathogenesis of OVA-induced chronic AAD, but also did not compromise the other features that this model presented with, as all the above-mentioned processes play a role in contributing to the development of fibrosis and deterioration of lung function in asthma sufferers.

It was discovered that by superimposing a 3-day model of NA-induced epithelial damage **after** the 9-week mouse model of OVA-induced AAD, the features of the chronic AAD model were maintained, with the inclusion of epithelial damage, resulting in exacerbated airway fibrosis levels and worsening of lung function. However, while this model now presents with an additional feature commonly associated with asthma (epithelial damage), it is still not perfect. Epithelial damage is a process that occurs repeatedly throughout the pathogenesis of human asthma. Hence, a more accurate animal model of human asthma would need to replicate this. Angiogenesis is also a feature of human asthma that needs to be investigated and incorporated (Chetta et al., 2007) to fully replicate human asthma pathology.

Moreover, these therapies were only tested in an animal model that is used to mimic the key features associated with chronic eosinophilic allergic asthma. Further studies could evaluate the treatment strategies investigated in the more clinically-relevant house dust mite model. Furthermore, as there are a number

of other factors that can drive the development of asthma (such as neutrophilia, viral and/or bacterial infections, and exercise, to name a few), further studies should also evaluate the individual and combination therapies investigated in models that specifically replicate the features of human asthma, that are induced by these other factors.

Furthermore, as many of the therapies evaluated in this thesis were intranasally-administered to mice, which is a feasible mode of drug/cell administration to mice but not humans, finding suitable modes of administering these drugs/cells into asthma patients (i.e. by endotracheal or intravenous means) would need to be completed. The data presented in this thesis warrant this, as the therapies evaluated demonstrated feasible anti-remodelling and anti-fibrotic effects in experimental chronic AAD.

Finally, the time-frame of the treatment strategies employed would need to be extended to effectively treat human asthma. While a 7-day treatment strategy was sufficient enough to reduce and even normalise several measures of AWR and AHR in the murine model investigated, several weeks to months of treatment is likely going to be required to treat the AWR associated with human asthma (Bergeron et al., 2010; Elias et al., 1999; Fehrenbach et al., 2017). To this extent, it would also be interesting to see if these results presented in this thesis can be repeated in larger animal models such as sheep or primates; to enhance their translational potential. Sheep are recognised for having anatomically similar lungs to humans. Also, due to the size similarities between human and

sheep lungs, it means diagnostic measurements can be made in the same way that they are made in a human patient suffering from asthma, or any other respiratory disease (Zosky & Sly, 2007; Meeusen et al., 2009).

## **5.5 CONCLUSION**

In conclusion, the findings presented in this thesis demonstrated 1) the relative contributions of AI, epithelial damage and airway fibrosis to the pathogenesis of chronic AAD/asthma-induced AHR; and 2) the feasibility of targeting and treating several aspects of AWR associated with chronic AAD/asthma, with various individual vs. combination treatment strategies. These studies revealed that targeting aberrant collagen concentration, over other aspects of AWR and AI, is key to normalising chronic AAD/asthma-induced AHR; and offered greater protection to what was offered by an anti-inflammatory corticosteroid. As many of these therapies such as RLX (Teerlink J et al., 2013), AECs (Lim R et al., 2017) and AEC-EXO (ClinicalTrials.gov Identifier NCT02138331; NCT03384433) are already being evaluated in various clinical trials, novel strategies incorporating these therapies can hopefully fast-tracked as treatments for asthma in the not too distant future.

## 5.6 REFERENCES

Adcock IM, Barnes PJ (2008). Molecular mechanisms of corticosteroid resistance. *Chest*. **134**(2):394-401.

Bergeron C, Tulic MK, Hamid Q (2010). Airway remodelling in asthma: from benchside to clinical practice. *Can Respir J*. **17**(4):e85-e93.

Chetta A, Zanini A , Torre O , Olivieri D (2007). Vascular remodelling and angiogenesis in asthma: morphological aspects and pharmacological modulation. *Inflamm Allergy Drug Targets*. **6**(1):41-45.

Elias JA, Zhu Z, Chupp G, Homer RJ (1999). Airway remodelling in asthma. *J Clin Invest*. **104**(8):1001-1006.

Fehrenbach H, Wagner C, Wegmann M (2017). Airway remodelling in asthma: what really matters. *Cell Tissue Res*. **367**(3):551-569.

Ito K, Chung KF, Adcock IM (2006). Update on glucocorticoid action and resistance. *J Allergy Clin Immunol*. **117**:522–543

Lim R, Hodge A, Moore G, Wallace EM, Sievert W (2017). A Pilot Study Evaluating the Safety of Intravenously Administered Human Amnion Epithelial Cells for the Treatment of Hepatic Fibrosis. *Front Pharmacol*. **8**:549.

Meeusen EN, Snibson KJ, Hirst SJ, Bischof RJ (2009). Sheep as a model species for the study and treatment of human asthma and other respiratory diseases. *Drug Discovery Today: Disease Models* **6**(4):101-106.

Moodley Y, Ilancheran S, Samuel C, Vaghjiani V, Atienza D, Williams ED, Jenkin G, Wallace E, Trounson A, Manuelpillai U (2010). Human amnion epithelial cell transplantation abrogates lung fibrosis and augments repair. *Am J Respir Crit Care Med.* **182**(5):643-651.

Patel KP, Giraud AS, Samuel CS, Royce SG (2016). Combining an epithelial repair factor and anti-fibrotic with a corticosteroid offers optimal treatment for allergic airways disease. *Br J Pharmacol.* **173**(12):2016-2029.

Royce SG, Miao YR, Lee M, Samuel CS, Tregear GW, Tang ML (2009). Relaxin reverses airway remodelling and airway dysfunction in allergic airways disease. *Endocrinology.* **150**(6):2692-2699.

Royce SG, Patel KP, Samuel CS (2014). Characterization of a novel model incorporating airway epithelial damage and related fibrosis to the pathogenesis of asthma. *Lab Invest.* **94**(12):1326-1339.

Royce SG, Sedjahtera A, Samuel CS, Tang MLK (2013). Combination therapy with relaxin and methylprednisolone augments the effects either treatment alone in

inhibiting subepithelial fibrosis in an experimental model of allergic airways disease. *Clin Sci*. **124**:41-51.

Royce SG, Tominaga AM, Shen M, Patel KP, Huuskens BM, Lim R, Ricardo SD, Samuel CS (2016). Serelaxin improves the therapeutic efficacy of RFXFP1-expressing human amnion epithelial cells in experimental allergic airway disease. *Clin Sci (Lond)*. **130**(23):2151-2165.

Teerlink JR<sup>1</sup>, Cotter G, Davison BA, Felker GM, Filippatos G, Greenberg BH, Ponikowski P, Unemori E, Voors AA, Adams KF Jr, Dorobantu MI, Grinfeld LR, Jondeau G, Marmor A, Masip J, Pang PS, Werdan K, Teichman SL, Trapani A, Bush CA, Saini R, Schumacher C, Severin TM, Metra M; RELAXin in Acute Heart Failure (RELAX-AHF) Investigators (2013). Serelaxin, recombinant human relaxin-2, for treatment of acute heart failure (RELAX-AHF): a randomised, placebo-controlled trial. *Lancet*. **381**(9860):29-39.

Wang W<sup>1</sup>, Li JJ, Foster PS, Hansbro PM, Yang M (2010). Potential therapeutic targets for steroid-resistant asthma. *Curr Drug Targets*. **11**(8):957-970.

WHO (2007). Global surveillance, prevention and control of chronic respiratory diseases: a comprehensive approach. WHO Press. **2007**:1-155.

Zosky GR, Sly PD (2007). Animal models of asthma. *Clin Exp Allergy*. **37**(7):973-988.

---

# **Appendix 1**

---

## Intranasally administered serelaxin abrogates airway remodelling and attenuates airway hyperresponsiveness in allergic airways disease

S. G. Royce<sup>1,2</sup>, C. X. F. Lim<sup>1</sup>, K. P. Patel<sup>2</sup>, B. Wang<sup>3</sup>, C. S. Samuel<sup>2,4,5</sup> and M. L. K. Tang<sup>1,6,7</sup>

<sup>1</sup>Allergy and Immune Disorders, Murdoch Children's Research Institute, Melbourne, Vic., Australia, <sup>2</sup>Department of Pharmacology, Monash University, Melbourne, Vic., Australia, <sup>3</sup>Department of Anatomy and Developmental Biology, Monash University, Melbourne, Vic., Australia, <sup>4</sup>The Florey Institute of Neuroscience and Mental Health, The University of Melbourne, Melbourne, Vic., Australia, <sup>5</sup>Department of Biochemistry and Molecular Biology, The University of Melbourne, Melbourne, Vic., Australia, <sup>6</sup>Department of Paediatrics, The University of Melbourne, Melbourne, Vic., Australia and <sup>7</sup>Department of Allergy and Immunology, Royal Children's Hospital, Melbourne, Vic., Australia

### Clinical & Experimental Allergy

#### Summary

**Background** The peptide hormone relaxin plays a key role in the systemic hemodynamic and renovascular adaptive changes that occur during pregnancy, which is linked to its anti-remodelling effects. Serelaxin (a recombinant form of human gene-2 relaxin) has been shown to inhibit lung fibrosis in various disease models and reverse airway remodelling and airway hyperresponsiveness (AHR) in allergic airways disease (AAD).

**Objective** Although continuous systemic delivery of exogenous serelaxin alleviates allergic fibrosis and AHR, more direct routes for administration into the lung have not been investigated. Thus, intranasal administration of serelaxin was evaluated for its ability to reverse airway remodelling and AHR associated with AAD.

**Methods** Female Balb/c mice were subjected to a 9-week model of chronic AAD. Subgroups of animals ( $n = 12/\text{group}$ ) were then treated intranasally with serelaxin (0.8 mg/mL) or vehicle once daily for 14 days (from weeks 9–11). Saline-sensitized/challenged mice treated with intranasal saline served as additional controls. Differential bronchoalveolar lavage (BAL) cell counts, ovalbumin (OVA)-specific IgE levels, tissue inflammation, parameters of airway remodelling and AHR were then assessed.

**Results** Chronic AAD was associated with significant increases in differential BAL cell counts, OVA-specific IgE levels, inflammation, epithelial thickening, goblet cell metaplasia, TGF- $\beta$ 1 expression, epithelial Smad2 phosphorylation (pSmad2), subepithelial collagen thickness, total lung collagen concentration and AHR (all  $P < 0.05$  vs. respective measurements from saline-treated mice). Daily intranasal delivery of serelaxin significantly diminished AAD-induced epithelial thickening, epithelial pSmad2, subepithelial and total lung collagen content (fibrosis) and AHR (all  $P < 0.05$  vs. vehicle-treated AAD mice).

**Conclusions and Clinical Relevance** Intranasal delivery of serelaxin can effectively reduce airway remodelling and AHR, when administered once daily. Respirable preparations of serelaxin may have therapeutic potential for the prevention and/or reversal of established airway remodelling and AHR in asthma.

**Keywords** airway hyperresponsiveness, airway remodelling, allergic airways disease, asthma, intranasal, serelaxin

Submitted 15 February 2014; revised 3 March 2014; accepted 8 May 2014

Correspondence: Professor Mimi L. K. Tang, Department of Allergy and Immunology, Level 3, West Building, Royal Children's Hospital, Flemington Road, Melbourne, Vic. 3052, Australia. E-mail: mimi.tang@rch.org.au and Associate Professor Chrishan S. Samuel, Department of Pharmacology, Building 13E, Ring Road South, Monash University, Melbourne, Vic. 3800, Australia. E-mail: chrishan.samuel@monash.edu  
Cite this as: S. G. Royce, C. X. F. Lim, K. P. Patel, B. Wang, C. S. Samuel and M. L. K. Tang, *Clinical & Experimental Allergy*, 2014 (44) 1399–1408.

#### Introduction

Asthma is a chronic inflammatory disease of the airways that affects both adults and children [1, 2]. Certain symptoms and airway inflammation can be effectively controlled using inhaled aerosols of beta agonists and/or corticosteroids or other anti-inflammatory

agents. However, in many cases, these therapies are not sufficient to eliminate progression of long-term structural remodelling of the airways [3, 4]. Airway remodelling consists of epithelial thickening and goblet cell metaplasia, subepithelial fibrosis, smooth muscle thickening and angiogenesis; which can occur early in asthma pathogenesis. Finding a therapy that reverses or

even prevents airway remodelling is critical, as remodelling contributes to airway hyperresponsiveness (AHR) and fixed airway obstruction independently of inflammation [5, 6], and is likely associated with disease severity and steroid resistance.

In this regard, we and others have shown that the naturally occurring hormone relaxin has pleiotropic effects that effectively attenuate remodelling and related dysfunction in several organs [7–9]. Mainly produced in reproductive organs of women and men, relaxin expression has also been identified in the mammalian lung, particularly in epithelial cells, fibroblasts and airway smooth muscle cells [10]. In addition to softening the pelvic ligaments and relaxing the uterus in preparation for parturition [11], relaxin augments the hemodynamic and renovascular adaptive changes that occur during pregnancy [12] through its vasorelaxant and matrix remodelling properties [7, 9]. Consistent with this, other preclinical studies have shown the antifibrotic actions of relaxin in several organs including the lung [7–11].

Of further relevance to its actions in the allergic lung, relaxin has been found to inhibit the infiltration of pro-inflammatory cells [13, 14], promote dilation of alveolar blood capillaries, reduce the thickness of the air-blood barrier [14] and inhibit airway fibrosis and AHR [10, 15] in models of allergic airways disease (AAD) that undergo several features of human asthma. Furthermore, serelaxin (a recombinant form of human gene-2 relaxin) markedly attenuated the fibrosis associated with interstitial and parenchymal lung disease [16, 17] and hypoxic pulmonary hypertension [18] in experimental models, suggesting that its antiremodelling actions are independent of aetiology. The proposed mechanisms involved in serelaxin's actions include its ability to inhibit the profibrotic influence of transforming growth factor (TGF)- $\beta$ 1 [16] and myofibroblast contractility [17], which in turn limits myofibroblast-mediated extracellular matrix (ECM)/collagen deposition. Additionally, serelaxin promotes the activity of various matrix metalloproteinases (MMPs) that facilitate collagen degradation [10, 16].

The beneficial effects of serelaxin have previously been demonstrated by systemic administration via microinfusion pumps [10, 15–19]. In the setting of systemic sclerosis (scleroderma), systemic delivery was critical for serelaxin effects [20]. However, the use of systemically delivered relaxin for the treatment of asthma in the patient setting poses significant barriers, and a more feasible means for drug delivery to the target organ (such as intranasal delivery) is required [21]. The purpose of this study was to evaluate the efficacy of intranasally administered serelaxin once daily in a murine model of chronic AAD [22, 23] that presents with the three central features of asthma: airway inflammation, airway remodelling and AHR.

## Materials and methods

### Animals

Six to eight-week-old female Balb/c mice were obtained from the Walter and Eliza Hall Institute (Melbourne, Victoria, Australia), housed in the Murdoch Children's Research Institute (MCRI) Animal Facility under specific pathogen-free conditions and maintained on a 12 h light–12 h dark cycle. All procedures were approved by the MCRI Animal Ethics Committee, which adheres to the Australian Code of Conduct for care and use of laboratory animals for scientific purposes.

### Induction of chronic AAD

A chronic model of ovalbumin (OVA)-induced AAD [22] was established in mice ( $n = 24$ ). Mice were sensitized i.p. on day 0 and 14 with 10  $\mu$ g Grade V chicken egg ovalbumin (Sigma–Aldrich Corp., St. Louis, MO, USA) and 0.4 mg aluminium potassium sulphate (alum) in 0.5 mL saline, then challenged by whole body inhalation exposure to aerosolized 2.5% OVA (weight/volume of saline) three times a week from days 21–63 (30 min per session) using an ultrasonic nebulizer [23]. Control mice ( $n = 12$ ) were sensitised with 0.4 mg alum in 0.5 mL saline and challenged with nebulised saline.

### Intranasal treatment

Ovalbumin (OVA)-sensitized/challenged mice (with established AAD) were treated once daily with vehicle (20 mM sodium acetate buffer, pH 5.0;  $n = 12$ ) or 0.8 mg/mL serelaxin (equivalent to the 0.5 mg/kg/day dose that was previously shown to be effective for the treatment of AAD [10]; kindly provided by Corthera Inc, San Carlos, CA, USA; a subsidiary of Novartis Pharma AG, Basel, Switzerland;  $n = 12$ ) from days 64–77 via intranasal administration. Briefly, mice were lightly anesthetized with isoflurane inhalation, held in a supine position and administered 50  $\mu$ L of vehicle or serelaxin peptide solution into both nostrils (25  $\mu$ L per nostril) using an automatic pipette. A fourteen-day treatment period was chosen to replicate the time frame used to evaluate the effects of systemic serelaxin treatment [10]. Saline-sensitized/challenged control mice received 50  $\mu$ L of saline intranasally, once daily over the 14-day treatment period.

### Measurement of AHR

Twenty-four hours after the last vehicle/drug administration, methacholine-induced airway reactivity was assessed by invasive plethysmography as described before [10, 23]. Mice were anaesthetized intraperitoneally

with 200 µg/g ketamine and 10 µg/g xylazine. Tracheotomy was performed using an 18-gauge tracheotomy tube and jugular vein cannulated with a 0.61 × 0.28 mm polyethylene tube (Microtube Extrusions, North Rocks, NSW, Australia). Mice were then placed in a plethysmograph chamber (Buxco Research Systems, Wilmington, NC, USA) where increasing concentrations of acetyl-β-methacholine (from 31.25 µg/kg to 500 µg/kg) were delivered intravenously in five doses. After every dose, airway resistance and compliance were measured (Biosystem XA version 2.7.9; Buxco Electronics Inc, Wilmington, NC, USA). The change in airway resistance calculated by the maximal resistance after each dose minus baseline resistance (PBS alone) was plotted against each dose of methacholine evaluated.

#### *Bronchoalveolar lavage (BAL)*

Three 0.5 mL lavages were pooled in ice-cold 20% FCS/PBS before red blood cells were lysed, and cells were washed twice in 5% FCS/PBS. Total viable cell counts were performed manually by trypan blue exclusion. Cytospin smears ( $2 \times 10^4$  cells) were prepared, fixed with methanol and stained with modified Wright's stain (Hema-Tek®; Bayer Diagnostics, Leverkusen, Germany). Differential counts of eosinophils, neutrophils, lymphocytes and macrophages were determined using light microscopy ( $\times 40$  magnification, 100 cells counted) in a blinded manner.

#### *Determination of OVA-specific IgE and serelaxin levels by ELISA*

Serum was obtained by cardiac puncture 24 h after the last vehicle/drug administration and stored at  $-80^\circ\text{C}$ . Serum OVA-specific IgE titres were determined from the three groups of animals studied by ELISA, as previously described [24]. Additionally, serum and BAL serelaxin levels were determined from serelaxin-treated mice (24 h after the last drug administration;  $n = 5$ ), using the human relaxin-2 Quantikine ELISA kit (R&D Systems, Minneapolis, MN, USA); as per the manufacturer's instructions.

#### *Lung histopathology*

The right lung was fixed in 10% neutral buffered formalin for 24–48 h before it was transversely cut into three pieces, processed and embedded routinely in paraffin wax. Representative sections of tissue, 3 µm each, were taken and stained with haematoxylin and eosin (for assessment of lung inflammation), alcian blue-periodic acid-Schiff (for assessment of goblet cell metaplasia) and Masson trichrome (for assessment of epithelial thickness and subepithelial collagen deposition). All

analyses of histological sections were performed in a randomized and blinded fashion.

#### *Histological evaluation of inflammation*

Sections were stained with Mayer's haematoxylin and eosin Y (Grale Scientific, Melbourne, Vic., Australia) and observed under low-power light microscopy ( $\times 50$  magnification). Histological grading of inflammation severity from 0 to 4 was assigned to every slide (0 = no detectable inflammation; 1 = occasional inflammatory cell aggregates, pooled size  $< 0.1 \text{ mm}^2$ ; 2 = some inflammatory cell aggregates, pooled size  $\sim 0.2 \text{ mm}^2$ ; 3 = widespread inflammatory cell aggregates, pooled size  $\sim 0.3 \text{ mm}^2$ ; 4 = widespread and massive inflammatory cell aggregates, pooled size  $\sim 0.6 \text{ mm}^2$ ); and was performed blinded by the same investigator. The area of inflammatory cell aggregates was measured using Image Pro Discovery software (Media Cybernetics, Silver Spring, MD, USA) in  $\mu\text{m}^2$  and converted to  $\text{mm}^2$ .

#### *Assessment of goblet cell metaplasia*

Sections were stained with alcian blue-periodic acid-Schiff (ABPAS) to enumerate goblet cells. Mucin-positive cells observed at high power ( $\times 400$  magnification) were manually counted from four to five different airways per section and expressed as the mean number of goblet cells per 100 µm of basement membrane (Image Pro Discovery).

#### *Masson trichrome staining*

Masson trichrome staining was performed to detect subepithelial collagen deposition in the airways. Briefly, dewaxed sections (passed through xylene, absolute ethanol, 70% ethanol and tap water) were post-fixed in Bouin's fixative (Grale Scientific) for 1 h; stained with Weigert's haematoxylin for 10 min, incubated with Masson's Red for 45 min; followed by 7 min treatment with phosphotungstic acid and 15 min incubation with aniline blue. Slides were then rinsed briefly, dehydrated, cleared and mounted.

#### *Immunohistochemistry*

Paraffin-embedded lung sections were immunohistochemically stained for TGF-β1 [23, 25] and phosphorylation of Smad2 (pSmad2; an intracellular protein that promotes TGF-β1 signal transduction/activity) [25], using primary antibodies to TGF-β1 (sc146; 1 : 200 dilution; Santa Cruz Biotechnology Inc, Santa Cruz, CA, USA) and pSmad2 (#3108; 1 : 250 dilution; Cell Signaling Technology, Danvers, MA, USA) as described before. Detection of antibody staining was completed

using the DAKO EnVision anti-rabbit kit (DAKO Corp., Carpinteria, CA, USA) and 3,3'-diaminobenzidine (DAKO Corp.); where sections were counterstained with haematoxylin.

#### Morphometric analysis of structural changes

Changes in airway TGF- $\beta$ 1 expression and epithelial pSmad2 levels were assessed by image analysis of corresponding immunohistochemical-stained sections, while changes in epithelial thickness and subepithelial collagen (fibrosis) around the airway lumen were assessed from Masson trichrome-stained sections; which were all captured (at  $\times 100$  magnification) using a SPOT digital camera (Q Imaging, Burnaby, BC, Canada) and analysed with Image Pro Discovery (Media Cybernetics). Four to five airways (150–350  $\mu$ m in diameter) per mouse were assessed. Epithelial thickness and subepithelial collagen regions were traced with a digital pen and the thickness of each region calculated by the imaging software. Results were expressed as mean thickness ( $\mu$ m) of the 4–5 airways sampled. Airway TGF- $\beta$ 1 staining was calculated as a percentage of the total area within each field analysed, while the number of pSmad2 positively stained nuclei per epithelial layer was determined and expressed per 100  $\mu$ m basement membrane length.

#### Hydroxyproline analysis

The second largest lung lobe from each mouse was treated as described previously [10, 19] for the determination of hydroxyproline content. Hydroxyproline values were estimated based on a standard curve constructed with serial dilutions of a 0.1 mg/mL stock of trans-4-hydroxyproline-L-proline (Sigma-Aldrich) and expressed per 2nd largest lung lobe ( $\mu$ g).

#### Statistical analysis

All data were expressed as the mean  $\pm$  SEM and analysed using GraphPad Prism (GraphPad Software Inc., San Diego, CA, USA). A Mann-Whitney *U*-test was used to compare differences between non-parametric groups in all experiments performed except for the analysis of the lung function (AHR) data, which was assessed by a two-way ANOVA with Bonferroni's *post hoc* test.  $P < 0.05$  was considered to be statistically significant.

## Results

#### Validation of the mouse model of chronic AAD

Mice subjected to the chronic model of AAD were confirmed to be adequately sensitized to OVA, by demon-

strating increased BAL cell counts and OVA-specific IgE levels compared to saline-treated controls (both  $P < 0.05$  vs. saline group; Table 1). Of the BAL cell counts determined, eosinophil cell numbers ( $P < 0.01$  vs. saline group) and monocytes ( $P < 0.05$  vs. saline group) in particular, were significantly higher in lung washouts of OVA-vehicle mice compared with that measured in saline-treated animals (Table 1), indicative of OVA-induced allergic disease.

As expected, vehicle-treated OVA mice (OVA-vehicle) were also associated with markedly increased inflammation (Fig. 1), epithelial thickening (Fig. 2), goblet cell metaplasia (Fig. 3b,d), subepithelial collagen deposition (Fig. 4b,d), lung hydroxyproline content (Fig. 4c), TGF- $\beta$ 1 expression (Fig. 5b,g), epithelial pSmad2 levels (Fig. 5e,h) and AHR (Fig. 6) compared with respective measurements obtained from saline-treated controls (all  $P < 0.05$  vs. saline group), validating the murine model of chronic AAD [10, 22, 23].

#### Effects of intranasal serelaxin treatment on inflammation, airway remodelling and AHR in chronic AAD Airway inflammation

Confirmation that serelaxin (0.8 mg/mL) treatment (OVA-serelaxin) was delivered to mice was established by the ELISA measurements of serelaxin in the BAL ( $39.81 \pm 5.89$  ng/mL) and serum ( $9.02 \pm 0.93$  ng/mL) of OVA-serelaxin animals. BAL differential cell counts (Table 1) and inflammation score of H&E-stained lung sections (Fig. 1) from OVA-serelaxin mice were not significantly different to corresponding measurements obtained from OVA-vehicle animals.

#### Epithelium morphology

Epithelial thickness in Masson trichrome-stained sections from OVA-serelaxin mice was significantly reduced compared with that measured in OVA-vehicle

Table 1. Evaluation of allergic responses by bronchoalveolar lavage (BAL) differential cell counts ( $\times 10^4$  cell/mL) and OVA-specific IgE by ELISA

Groups	Saline	OVA-vehicle	OVA-serelaxin
Total cells*	12.33 $\pm$ 1.89	25.50 $\pm$ 4.10 <sup>†</sup>	25.38 $\pm$ 2.85 <sup>†</sup>
Eosinophils*	0.08 $\pm$ 0.31	1.05 $\pm$ 0.64 <sup>‡</sup>	0.85 $\pm$ 0.27 <sup>‡</sup>
Neutrophils*	0.28 $\pm$ 0.56	0.56 $\pm$ 0.13	0.69 $\pm$ 0.27
Lymphocytes*	2.38 $\pm$ 2.04	5.58 $\pm$ 1.66	5.73 $\pm$ 1.44
Monocytes*	9.56 $\pm$ 2.61	18.31 $\pm$ 1.40 <sup>†</sup>	18.09 $\pm$ 1.33 <sup>†</sup>
OVA-specific IgE (AU)*	0 $\pm$ 0.01	0.37 $\pm$ 0.08 <sup>‡</sup>	0.4 $\pm$ 0.04 <sup>‡</sup>

\*Values are the mean  $\pm$  SEM cells or OVA-specific IgE analysed from 9 to 12 mice/group.

<sup>†</sup> $P < 0.05$  and <sup>‡</sup> $P < 0.01$  vs. corresponding value from saline group.

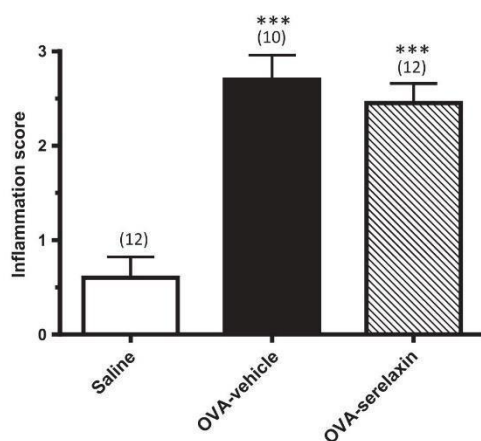


Fig. 1. Effect of intranasal serelaxin treatment on overall lung inflammation in chronic allergic airways disease. Shown in the mean  $\pm$  SEM inflammation score in H&E-stained lung tissue sections obtained from saline, OVA-vehicle and OVA-serelaxin mice. Sections were scored for the number and distribution of inflammatory aggregates on a scale of 0 (no apparent inflammation) to 4 (severe inflammation). Numbers in parentheses represent number of mice analysed per group. \*\*\* $P < 0.001$  vs. saline group.

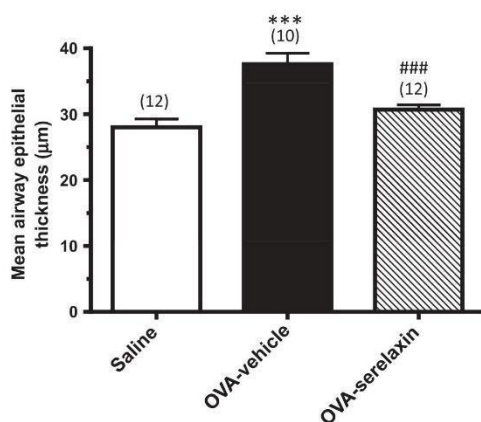


Fig. 2. Effect of intranasal serelaxin treatment on airway epithelial thickness in chronic allergic airways disease. Shown is the mean  $\pm$  SEM airway epithelial thickness ( $\mu\text{m}$ ) in Masson trichrome-stained lung sections from saline, OVA-vehicle and OVA-serelaxin mice; as measured by morphometric analysis. Numbers in parentheses represent number of mice analysed per group. \*\*\* $P < 0.001$  vs. saline group, ### $P < 0.001$  vs. OVA-vehicle group.

animals ( $P < 0.001$  vs. OVA-vehicle group; and approached that of saline-sensitized/challenged mice (no significant difference to saline group; Fig. 2).

However, no differences in goblet cell metaplasia (ABPAS-positive cells) were observed between OVA-serelaxin (Fig. 3c,d) and OVA-vehicle (Fig. 3b,d) mice (both  $P < 0.001$  vs. saline group; Fig. 3a,d).

#### Airway remodelling and fibrosis

Subepithelial collagen deposition and lung hydroxyproline levels (Fig. 4) were used as measures of airway remodelling and fibrosis in the chronic model of AAD. Subepithelial collagen deposition was significantly lower in OVA-serelaxin mice (Fig. 4c,d) as compared to OVA-vehicle mice (Fig. 4b,d;  $P < 0.001$  vs. OVA-vehicle group), but remained significantly greater than that measured in saline-treated (Fig. 4a,d) animals ( $P < 0.05$  vs. saline group). Remarkably, lung hydroxyproline content in OVA-serelaxin mice was normalized back to levels measured in saline-treated controls ( $P < 0.01$  vs. OVA-vehicle group; no significant difference to saline group; Fig. 4e).

TGF- $\beta$ 1 and pSmad2 levels were additionally assessed to determine the mechanisms by which collagen deposition (fibrosis) was significantly diminished in OVA-serelaxin mice. While airway TGF- $\beta$ 1 staining was unchanged between OVA-vehicle (Fig. 5b,g) and OVA-serelaxin (Fig. 5c,g) mice, epithelial pSmad2 nuclear staining was significantly lower in OVA-serelaxin mice (Fig. 5f,h) compared with that measured in OVA-vehicle mice (Fig. 5e,h), but remained significantly greater than that measured in saline-treated mice (Fig. 5d,h;  $P < 0.01$  vs. OVA-vehicle group;  $P < 0.01$  vs. saline group).

#### AHR

Airway reactivity was significantly lower in OVA-serelaxin mice compared with OVA-vehicle animals (three highest doses of methacholine were all  $P < 0.05$  vs. OVA-vehicle group; Fig. 6). However, airway reactivity in OVA-serelaxin mice remained significantly higher than that measured in saline-treated control animals (4 highest doses of methacholine were all  $P < 0.01$  vs. saline group; Fig. 6).

#### Discussion

The OVA-induced model of chronic AAD used in the present study resembles clinical asthma and is highly suitable for studying the pathophysiology of airway remodelling and its contribution to AHR [10, 23]. We observed significantly increased inflammation, epithelial thickness, goblet cell metaplasia, subepithelial collagen deposition, lung hydroxyproline content, TGF- $\beta$ 1 and pSmad2 staining as well as AHR in mice sensitized and challenged with OVA, as previously characterized

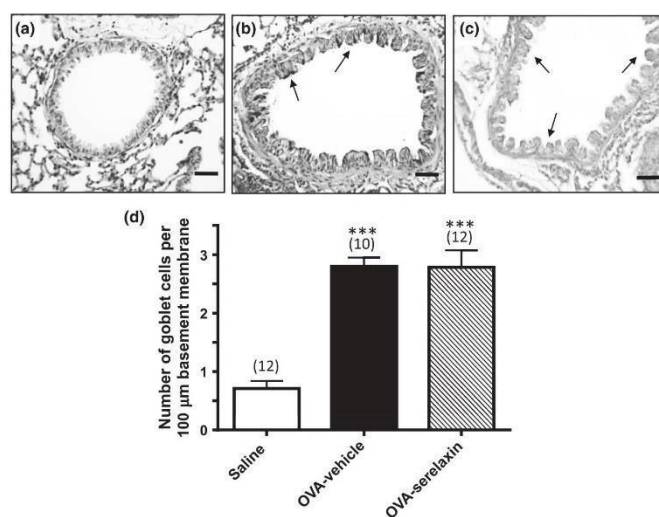


Fig. 3. Effect of intranasal serelaxin treatment on goblet cell metaplasia in chronic allergic airways disease. Representative photomicrographs of ABPAS-stained airways taken from (a) saline, (b) OVA-vehicle and (c) OVA-serelaxin mice. Scale bar = 100 μm. Also shown is mean ± SEM goblet cell numbers/100 μm basement membrane length (d) from each of the groups studied. Numbers in parentheses represent number of mice analysed per group. \*\*\* $P < 0.001$  vs. saline group.

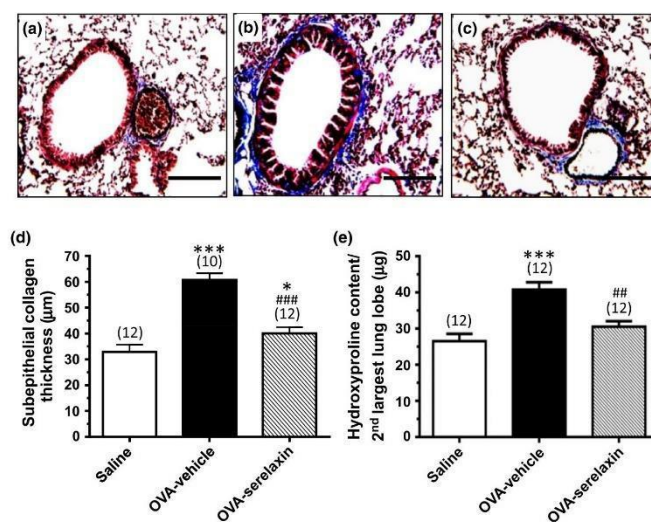


Fig. 4. Effect of intranasal serelaxin treatment on measures of fibrosis in chronic allergic airways disease. Representative photomicrographs of Masson trichrome-stained lung airway sections of (a) saline, (b) OVA-vehicle and (c) OVA-serelaxin mice. Scale bar = 300 μm. Also shown is the mean ± SEM subepithelial collagen thickness (μm) in the lamina reticularis (d) and lung hydroxyproline content (e) from each of the groups studied. Numbers in parentheses represent number of mice analysed per group. \* $P < 0.05$ , \*\*\* $P < 0.001$  vs. saline group, ## $P < 0.01$ , ### $P < 0.001$  vs. OVA-vehicle group.

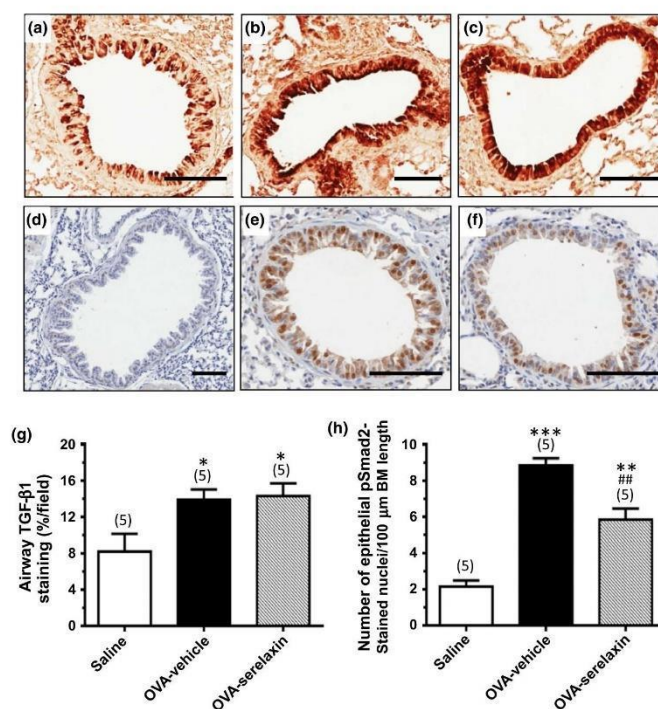


Fig. 5. Effect of intranasal serelaxin treatment on airway TGF- $\beta$ 1 and pSmad2 staining: promoters of collagen deposition in chronic allergic airways disease. Representative photomicrographs of TGF- $\beta$ 1 and pSmad2-stained lung airway sections of (a and d, respectively) saline, (b and e, respectively) OVA-vehicle and (c and f, respectively) OVA-serelaxin mice. Scale bar = 100  $\mu$ m. Also shown are the mean  $\pm$  SEM TGF- $\beta$ 1 staining levels expressed as a percentage per field analysed (g) and number of epithelial pSmad2-stained nuclei per 100  $\mu$ m BM length (h) from each of the groups studied. Numbers in parentheses represent number of mice analysed per group. \* $P$  < 0.05, \*\*\* $P$  < 0.001 vs. saline group, \*\* $P$  < 0.01 vs. OVA-vehicle group.

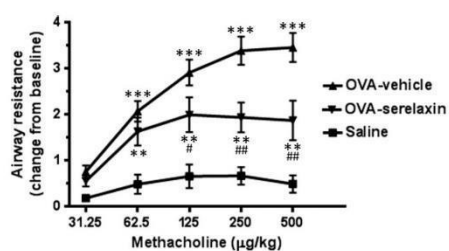


Fig. 6. Effect of intranasal serelaxin treatment on airway hyperresponsiveness (AHR). Shown is the mean  $\pm$  SEM airway resistance (AHR; change from baseline) in saline, OVA-vehicle and OVA-serelaxin mice ( $n$  = 11–12 mice/group), in response to increasing concentrations of the bronchoconstrictor, methacholine, by invasive plethysmography. \*\* $P$  < 0.01, \*\*\* $P$  < 0.001 vs. saline group, # $P$  < 0.05, ## $P$  < 0.01 vs. OVA-vehicle group.

[23]. The key finding of the current study was that intranasal delivery of serelaxin produced detectable levels of the drug in the BAL fluid ( $\sim$  40 ng/mL) that were comparable to circulating levels resulting from its systemic administration [19]; and this intranasal treatment could reverse several structural components of established airway remodelling and improve related lung dysfunction in a mouse model of chronic AAD, when administered once daily over a 14-day treatment period. Serelaxin significantly diminished AAD-induced epithelial thickening, epithelial pSmad2, subepithelial collagen, lung hydroxyproline content (fibrosis) and AHR in the absence of any direct effects on airway inflammation, highlighting a novel and feasible approach to the treatment of airway remodelling in human asthma. Of further note, the ability of intranasal serelaxin delivery to completely reverse AAD-induced lung hydroxyproline content (to that measured in saline-treated control

mice) and reduce AAD-induced AHR by ~50% was comparable to that achieved by its systemic administration [10].

The intranasal route of delivery is particularly attractive as it can deliver a drug directly to the airways, allowing efficient onset of action. Given that epithelial dysfunction is a fundamental pathology leading to asthma [26], administration of a drug directly to this site would be highly advantageous. Furthermore, an intranasally administered drug offers ease of use and promotes patient adherence to treatment, thereby offering greater feasibility than systemic delivery.

In addition to the current widespread use of inhaled  $\beta$ -agonists and corticosteroids [27] as treatments for asthma, there has been intensive development of inhaled protein therapeutics for other disease conditions. The most prominent example of this technology is inhaled insulin for the treatment of diabetes, which was an important milestone in the development of inhaled therapeutics [28]. Inhaled DNase to breakdown mucus has become the mainstay of therapy for cystic fibrosis, while inhaled interferon- $\gamma$  is being developed for idiopathic pulmonary fibrosis and there is interest in inhaled  $\alpha$ 1-antitrypsin for emphysema [28]. Serelaxin has a two-chain structure [7, 8, 11] and activates a distinct leucine-rich repeat-containing G-protein coupled receptor, Relaxin Family Peptide Receptor 1 (RXFP1). The findings of our current study, along with the identification of strong RXFP1 expression in the airway epithelium [10] confirms that serelaxin can have local effects in the lung, adding to its potential viability as an inhaled treatment.

In this study, intranasal administration of serelaxin abrogated the aberrant airway remodelling changes associated with AAD, which in turn significantly attenuated AHR. Several preclinical studies have shown that serelaxin has potent antifibrotic effects which are mediated by its ability to disrupt the pro-fibrotic actions of TGF- $\beta$ 1 [16, 18], while augmenting the activity of various collagen-degrading MMPs [10, 16]. Although its effects on MMP activity were not investigated in the current study, it is likely that serelaxin, regardless of whether it is administered intranasally or systemically [10, 15] inhibits both TGF- $\beta$ 1-induced collagen deposition and promotes MMP-induced collagen degradation to reverse AAD-induced airway fibrosis and related AHR. Consistent with its reported actions in other organs [29, 30], our present findings in the lung demonstrated that serelaxin disrupted the pro-fibrotic actions of TGF- $\beta$ 1 on ECM/collagen production by inhibiting the phosphorylation of the intracellular protein, Smad2 (in the absence of any effects on airway TGF- $\beta$ 1 expression itself). Serelaxin can also inhibit lung myofibroblast contractility [17]. It is plausible that these antifibrotic actions of serelaxin, in addition to its

ability to normalise epithelial damage (which is emerging as a novel aetiology in asthma pathogenesis [26]) and inhibit the vasoconstricting effects of endothelin-1 [31] to promote dilation [14] all contribute to its ability to significantly attenuate AHR.

The finding that serelaxin administration could not fully reverse AHR may be explained by our current data demonstrating that it did not significantly influence AAD-induced inflammation (as determined by BAL differential counts and inflammation score) and hence, the AHR that is separately caused by airway inflammation. This is consistent with our previous data in this model [10], and its inability to regulate inflammation derived from other aetiologies [32], but differs from separate studies demonstrating that serelaxin significantly attenuated the levels of cardiac and circulating mast cells and histamine release in rat [13], guinea pig [13] and swine [33] models of acute myocardial infarction. This may suggest that the anti-inflammatory properties of serelaxin are species-dependent or dependent on the cell type involved in the pathogenesis of inflammation, as it does not appear to have any effects on eosinophil [10] or macrophage [32] infiltration.

In this regard, it is possible that combining the antiremodelling properties of serelaxin with the anti-inflammatory actions of corticosteroids may yield improved efficacy in reversing AHR in the setting of AAD/asthma. In our recent studies attempting to evaluate such combination therapy [34], we found that serelaxin could modulate a broader range of airway remodelling changes compared with methylprednisolone, but that the combined effects of both treatments offered enhanced control of airway fibrosis and to an extent, AHR. These findings suggest that serelaxin has the potential to supplement corticosteroid treatments, which have powerful anti-inflammatory effects but only modest airway remodelling effects. Thus, intranasal delivery of serelaxin in combination with inhaled corticosteroids would have great potential to help treat the three major components of asthma. Further dose titration and duration studies are warranted though to optimise the therapeutic efficacy of intranasal serelaxin administration.

In conclusion, the data provided in this study demonstrated that serelaxin can be effective in reversing established airway remodelling and AHR when administered intranasally once daily, for as little as a 2-week treatment period. This data further supports the therapeutic potential of serelaxin as a future treatment for asthma and suggests that a once daily intranasal mode of delivery is efficacious enough to target the airway remodelling that contributes to AHR. Future studies combining intranasal serelaxin and corticosteroids may yield further protection from asthma pathogenesis.

### Acknowledgements

This study was supported by a Project Grant from the National Health and Medical Research Council (NHMRC) of Australia (546428); a CASS Foundation Grant (SM/09/2490) and NHMRC Senior Research Fellowship (APP1041766) to Chrisan S. Samuel; and by the

Victorian Government's Operational Infrastructure Support Programme.

### Conflict of interest

The authors declare no conflict of interest.

### References

- Hargreave FE, Nair P. The definition and diagnosis of asthma. *Clin Exp Allergy* 2009; 39:1652–8.
- Bush A, Zar HJ. WHO universal definition of severe asthma. *Curr Opin Allergy Clin Immunol* 2011; 11:115–21.
- Tang ML, Wilson JW, Stewart AG, Royce SG. Airway remodelling in asthma: current understanding and implications for future therapies. *Pharmacol Ther* 2006; 112:474–88.
- Royce SG, Tang ML. The effects of current therapies on airway remodeling in asthma and new possibilities for treatment and prevention. *Curr Mol Pharmacol* 2009; 2:169–81.
- James AL, Wenzel S. Clinical relevance of airway remodelling in airway diseases. *Eur Respir J* 2007; 30:134–55.
- Baldwin L, Roche WR. Does remodeling of the airway wall precede asthma? *Paediatr Respir Rev* 2002; 3:315–20.
- Samuel CS, Hewitson TD, Unemori EN, Tang ML. Drugs of the future: the hormone relaxin. *Cell Mol Life Sci* 2007; 64:1539–57.
- Bennett RG. Relaxin and its role in the development and treatment of fibrosis. *Transl Res* 2009; 154:1–6.
- Bathgate RA, Halls ML, van der Westhuizen ET, Callander GE, Kocan M, Summers RJ. Relaxin family peptides and their receptors. *Physiol Rev* 2013; 93:405–80.
- Royce SG, Miao YR, Lee M, Samuel CS, Tregear GW, Tang ML. Relaxin reverses airway remodeling and airway dysfunction in allergic airways disease. *Endocrinology* 2009; 150:2692–9.
- Sherwood OD. Relaxin's physiological roles and other diverse actions. *Endocr Rev* 2004; 25:205–34.
- Conrad KP. Emerging role of relaxin in the maternal adaptations to normal pregnancy: implications for preeclampsia. *Semin Nephrol* 2011; 31:15–32.
- Masini E, Bani D, Bigazzi M, Mannai-oni PF, Bani-Sacchi T. Effects of relaxin on mast cells. In vitro and in vivo studies in rats and guinea pigs. *J Clin Invest* 1994; 94:1974–80.
- Bani D, Ballati L, Masini E, Bigazzi M, Sacchi TB. Relaxin counteracts asthma-like reaction induced by inhaled antigen in sensitized guinea pigs. *Endocrinology* 1997; 138:1909–15.
- Kenyon NJ, Ward RW, Last JA. Airway fibrosis in a mouse model of airway inflammation. *Toxicol Appl Pharmacol* 2003; 186:90–100.
- Unemori EN, Pickford LB, Salles AL *et al*. Relaxin induces an extracellular matrix-degrading phenotype in human lung fibroblasts in vitro and inhibits lung fibrosis in a murine model in vivo. *J Clin Invest* 1996; 98:2739–45.
- Huang X, Gai Y, Yang N *et al*. Relaxin regulates myofibroblast contractility and protects against lung fibrosis. *Am J Pathol* 2011; 179:2751–65.
- Tozzi CA, Poiani GJ, McHugh NA *et al*. Recombinant human relaxin reduces hypoxic pulmonary hypertension in the rat. *Pulm Pharmacol Ther* 2005; 18:346–53.
- Samuel CS, Zhao C, Bathgate RA *et al*. Relaxin deficiency in mice is associated with an age-related progression of pulmonary fibrosis. *FASEB J* 2003; 17:121–3.
- Erikson MS, Unemori EN. Relaxin clinical trials in systemic sclerosis. In: Tregear GW, Ivell R, Bathgate RA, Wade JD, eds. *Relaxin 2000: proceedings of the third international conference on relaxin and related peptides*. Amsterdam: Kluwer, 2001:373–82.
- Rottier BL, Rubin BK. Asthma medication delivery: mists and myths. *Paediatr Respir Rev* 2013; 14:112–8.
- Temelkovski J, Hogan SP, Shepherd DP, Foster PS, Kumar RK. An improved murine model of asthma: selective airway inflammation, epithelial lesions and increased methacholine responsiveness following chronic exposure to aerosolised allergen. *Thorax* 1998; 53:849–56.
- Locke NR, Royce SG, Wainwright JS, Samuel CS, Tang ML. Comparison of airway remodeling in acute, subacute, and chronic models of allergic airways disease. *Am J Respir Cell Mol Biol* 2007; 36:625–32.
- Fiscus LC, Van Herpen J, Steeber DA, Tedder TF, Tang ML. L-Selectin is required for the development of airway hyperresponsiveness but not airway inflammation in a murine model of asthma. *J Allergy Clin Immunol* 2001; 107:1019–24.
- Gallop PM, Paz MA. Posttranslational protein modifications, with special attention to collagen and elastin. *Physiol Rev* 1975; 55:418–87.
- Royce SG, Li X, Tortorella S *et al*. Mechanistic insights into the contribution of epithelial damage to airway remodeling: novel therapeutic targets for asthma. *Am J Respir Cell Mol Biol* 2014; 50:180–92.
- Cates CJ, Jaeschke R, Schmidt S, Ferrer M. Regular treatment with salmeterol and inhaled steroids for chronic asthma: serious adverse events. *Cochrane Database Syst Rev* 2013; (3): CD006922.
- Hickey AJ. Back to the future: inhaled drug products. *J Pharm Sci* 2013; 102:1165–72.
- Mookerjee I, Hewitson TD, Halls ML *et al*. Relaxin inhibits renal myofibroblast differentiation via RXFP1, the nitric oxide pathway, and Smad2. *FASEB J* 2009; 23:1219–29.
- Bennett RG, Heimann DG, Singh S, Simpson RL, Tuma DJ. Relaxin decreases the severity of established hepatic fibrosis in mice. *Liver Int*.
- Dschietzig T, Bartsch C, Richter C, Laule M, Baumann G, Stangl K. Relaxin, a pregnancy hormone, is a functional endothelin-1 antagonist: attenuation of endothelin-1-mediated vasoconstriction

- by stimulation of endothelin type-B receptor expression via ERK-1/2 and nuclear factor-kappaB. *Circ Res* 2003; **92**:32–40.
- 32 Samuel CS, Cendrawan S, Gao XM *et al*. Relaxin remodels fibrotic healing following myocardial infarction. *Lab Invest* 2011; **91**:675–90.
- 33 Nistri S, Cinci L, Perna AM, Masini E, Mastroianni R, Bani D. Relaxin induces mast cell inhibition and reduces ventricular arrhythmias in a swine model of acute myocardial infarction. *Pharm Res* 2008; **57**:43–8.
- 34 Royce SG, Sedjahtera A, Samuel CS, Tang ML. Combination therapy with relaxin and methylprednisolone augments the effects of either treatment alone in inhibiting subepithelial fibrosis in an experimental model of allergic airways disease. *Clin Sci (Lond)* 2013; **124**:41–51.

---

## **Appendix 2**

---



## Mesenchymal stem cells and serelaxin synergistically abrogate established airway fibrosis in an experimental model of chronic allergic airways disease



Simon G. Royce<sup>a,1</sup>, Matthew Shen<sup>a,1</sup>, Krupesh P. Patel<sup>a</sup>, Brooke M. Huuskens<sup>b</sup>, Sharon D. Ricardo<sup>b,\*</sup>, Chrishan S. Samuel<sup>a,\*\*</sup>

<sup>a</sup> Fibrosis Laboratory, Department of Pharmacology, Monash University, Clayton, Victoria 3800, Australia

<sup>b</sup> Kidney Regeneration and Stem Cell Laboratory, Department of Anatomy and Developmental Biology, Monash University, Clayton, Victoria 3800, Australia

### ARTICLE INFO

#### Article history:

Received 20 May 2015

Received in revised form 3 August 2015

Accepted 20 September 2015

Available online 25 September 2015

#### Keywords:

Asthma

Airway remodeling

Fibrosis

Mesenchymal stem cells

Serelaxin

### ABSTRACT

This study determined if the anti-fibrotic drug, serelaxin (RLN), could augment human bone marrow-derived mesenchymal stem cell (MSC)-mediated reversal of airway remodeling and airway hyperresponsiveness (AHR) associated with chronic allergic airways disease (AAD/asthma). Female Balb/c mice subjected to the 9-week model of ovalbumin (OVA)-induced chronic AAD were either untreated or treated with MSCs alone, RLN alone or both combined from weeks 9–11. Changes in airway inflammation (AI), epithelial thickness, goblet cell metaplasia, transforming growth factor (TGF)- $\beta$ 1 expression, myofibroblast differentiation, subepithelial and total lung collagen deposition, matrix metalloproteinase (MMP) expression, and AHR were then assessed. MSCs alone modestly reversed OVA-induced subepithelial and total collagen deposition, and increased MMP-9 levels above that induced by OVA alone (all  $p < 0.05$  vs OVA group). RLN alone more broadly reversed OVA-induced epithelial thickening, TGF- $\beta$ 1 expression, myofibroblast differentiation, airway fibrosis and AHR (all  $p < 0.05$  vs OVA group). Combination treatment further reversed OVA-induced AI and airway/lung fibrosis compared to either treatment alone (all  $p < 0.05$  vs either treatment alone), and further increased MMP-9 levels. RLN appeared to enhance the therapeutic effects of MSCs in a chronic disease setting; most likely a consequence of the ability of RLN to limit TGF- $\beta$ 1-induced matrix synthesis complemented by the MMP-promoting effects of MSCs.

© 2015 Published by Elsevier B.V. This is an open access article under the CC BY-NC-ND license (<http://creativecommons.org/licenses/by-nc-nd/4.0/>).

### 1. Introduction

Approximately 300 million people worldwide suffer from asthma, leading to one in every 250 deaths each year (Bousquet et al., 2010). Asthma has three main components to its pathogenesis: airway inflammation (AI); airway remodeling (AWR), structural changes in the lung leading to fibrosis and airway obstruction; and lastly, airway hyperresponsiveness (AHR), the major clinical endpoint seen in asthma (Holgate, 2008). Th2 cell infiltration and IgE-mediated responses in AI can lead to lung injury resulting in AWR (Holgate, 2012). However, AWR can also occur independently of AI. AWR often results in epithelial damage, goblet cell metaplasia, fibrosis, smooth muscle hypertrophy and angiogenesis around the airways (Royce, Cheng, Samuel, and Tang, 2012).

The two major therapies in the treatment of asthma include corticosteroids (that primarily target AI) and  $\beta$ 2-adrenoreceptor agonists (that suppress episodes of AHR) (Jadad et al., 2000); which can be used in conjunction depending on the severity of asthma (Crompton, 2006). However, as these therapies do not effectively treat AWR and approximately 5–10% of asthmatics are resistant to corticosteroid therapy (Durham, Adcock, and Tliba, 2011), alternative treatments that can suppress AWR and the resulting AWR-associated AHR are urgently required.

The use of human (Bonfield et al., 2010; Weiss et al., 2006) or mouse (Ge et al., 2013; Srour and Thebaud, 2014) stem cells (such as mesenchymal, induced pluripotent and embryonic stem cells) in acute to moderate lung disease settings has been shown to provide effective reparative functions. While exogenous stem cells can also mediate some repair following severe/chronic AAD associated with their clonal expansion, ultimately their proliferative, reparative and differentiation capacity is not maintained (Dolgachev, Ullenbruch, Lukacs, and Phan, 2009; Giangreco et al., 2009). It has been postulated that the fibrosis which results from injury-induced aberrant healing and subsequent AWR results from increased extracellular matrix ECM and in particular, collagen deposition, which hinders stem cell survival as well as their homing to

\* Correspondence to: S. D. Ricardo, Department of Anatomy and Developmental Biology, Monash University, Clayton, Victoria 3800, Australia.

\*\* Corresponding author.

E-mail addresses: [simon.royce@monash.edu](mailto:simon.royce@monash.edu) (S.G. Royce), [sharon.ricardo@monash.edu](mailto:sharon.ricardo@monash.edu) (S.D. Ricardo), [chrishan.samuel@monash.edu](mailto:chrishan.samuel@monash.edu) (C.S. Samuel).

<sup>1</sup> These two authors contributed equally to this manuscript.

damaged tissue, proliferation and integration with resident tissue cells (Knight, Rossi, and Hackett, 2010). In this regard, it would appear logical that combining stem cells with an anti-fibrotic agent may aid their viability and reparative capacity.

In pathological settings, human bone marrow-derived mesenchymal stem cells (MSCs) injected intravenously (i.v) home to the site of injury through facilitated processes from chemokine receptors present in the blood stream (Ponte et al., 2007). During their migration and engraftment, MSCs are able to evade recognition from T- and NK- cells, and thereby can inhibit proliferation of immune cells and recruitment of inflammatory cells (Jiang et al., 2005; Krampner et al., 2003). Human MSCs are therefore immunoprivileged (suitable for allogeneic applications), a property beneficial for cell-based therapy as it allows for human MSCs to be transplanted into animal models without eliciting strong immune responses and rejection. Although the exact mechanisms of tissue repair are unknown, studies in acute models of asthma have shown early transplantation of MSCs inhibited the development of AI. These studies suggested that MSCs can modulate cytokines towards an altered Th1–Th2 profile and up-regulate T-regulatory cells (Aggarwal and Pittenger, 2005). Studies have also shown that exogenous introduction of MSCs are capable of decreasing the expression of transforming growth factor (TGF)- $\beta$ 1 thereby preventing myofibroblast differentiation in acute models of lung disease. However, this effect was significantly diminished in chronic lung injury models (Wang et al., 2011; Weiss et al., 2006), suggesting that the presence of an anti-fibrotic agent may be required to improve the viability and facilitate MSC-induced tissue repair in chronic disease settings.

Serelaxin (RLN; a recombinantly-produced peptide based on the human gene-2 (H2) relaxin sequence; which represents the major stored and circulating form of human relaxin) exerts potent anti-fibrotic actions in the airways/lung (Bennett, 2009; Huang et al., 2011; Kenyon, Ward, and Last, 2003; Royce et al., 2014; Royce et al., 2009; Unemori et al., 1996). These actions are mediated through its cognate G protein-coupled receptor, Relaxin Family Peptide Receptor 1 (RXFP1), which has been identified in several tissues (Bathgate, Ivell, Sanborn, Sherwood, and Summers, 2006; Hsu et al., 2002) including the lung (Royce, Sedjajhera, Samuel, and Tang, 2013). Serelaxin can inhibit TGF- $\beta$ 1-mediated collagen deposition (Unemori et al., 1996) by disrupting the phosphorylation of Smad2 (pSmad2), an intracellular protein that promotes TGF- $\beta$ 1 signal transduction (Royce et al., 2014). Additionally, serelaxin mediates its anti-fibrotic actions by promoting various matrix metalloproteinases (MMPs) that play a role in collagen degradation (Royce et al., 2012; Royce et al., 2009; Unemori et al., 1996).

We recently used human MSCs in combination with serelaxin in a unilateral ureteric obstruction-induced model of chronic kidney disease, and demonstrated that this combination therapy significantly prevented renal fibrosis to a greater extent than either therapy alone, while augmenting MSC viability and tissue repair. This was primarily achieved through a serelaxin-induced promotion of MSC proliferation and migration and up-regulation of MMP-2 activity in combination therapy-treated mice (Huuskens et al., 2015). However, the functional relevance of those findings could not be measured in the experimental model studied. Furthermore, as it remains unknown if this combination therapy can be applied to other disease models characterized by fibrosis, this study aimed to evaluate the therapeutic (structural and functional) potential of this combination therapy in an experimental model of chronic AAD, which presents with AI, AWR and AHR.

## 2. Materials and methods

### 2.1. Animals

Six-to-eight week-old female BALB/c mice were obtained from Monash Animal Services (Clayton, Victoria, Australia) and housed under a controlled environment: on a 12-h light/12-h dark lighting schedule and free access to water and lab chow (Barastock Stockfeeds,

Pakenham, Victoria, Australia). All mice were provided an acclimatization period of 4–5 days before any experimentation and all procedures outlined were approved by a Monash University Animal Ethics Committee (Ethics number: MARP/2012/085), which adheres to the Australian Guidelines for the Care and Use of Laboratory Animal for Scientific Purposes.

### 2.2. Induction of chronic allergic airways disease (AAD)

To assess the individual vs combined effects of MSCs and serelaxin in chronic AAD, a chronic model of ovalbumin (OVA)-induced AAD was established in mice ( $n = 24$ ), as described before (Royce et al., 2014; Royce et al., 2009; Royce et al., 2013). Mice were sensitized with two intraperitoneal (i.p) injections of 10  $\mu$ g of Grade V chicken egg OVA (Sigma-Aldrich, MO, USA) and 400  $\mu$ g of aluminum potassium sulfate adjuvant (alum; AJAX Chemicals, NSW, Australia) in 500  $\mu$ l of 0.9% normal saline solution (Baxter Health Care, NSW, Australia) on days 0 and 14. They were then challenged by whole body inhalation exposure (nebulization) to aerosolized OVA (2.5% w/v in 0.9% normal saline) for thirty minutes, three times a week, between days 21 and 63, using an ultrasonic nebulizer (Omron NE-U07; Omron, Kyoto, Japan). Control mice ( $n = 6$ ) were given i.p injections of 500  $\mu$ l 0.9% saline and nebulized with 0.9% saline instead of OVA.

### 2.3. Intranasal delivery of MSCs and/or serelaxin

Twenty-four hours after the establishment of chronic AAD (on day 64), sub-groups of mice were lightly anesthetized with isoflurane inhalation (Baxter Health Care, NSW, Australia), held in a supine position and intranasally (i.n)-administered with the treatments described below. In all cases, a fourteen day treatment period (from days 64–77) was chosen to replicate the time-frame used to evaluate the effects of systemic (Royce et al., 2009) and intranasal (Royce et al., 2014) serelaxin administration in the OVA-induced chronic model of AAD; before all animals were killed on day 78.

MSCs alone: Human MSCs, purchased from the Tulane Centre for Stem Cell Research and Regenerative Medicine (Tulane University, New Orleans, LA, USA) and transduced to express enhanced green fluorescent protein (eGFP) and firefly luciferase (fluc) (Payne et al., 2013), were characterized and cultured as previously described (Wise et al., 2014). Prior to administration,  $1 \times 10^6$  MSCs (per mouse) were resuspended in 50  $\mu$ l of phosphate buffered saline (PBS) and i.n- administered into mice. Sub-groups of mice received either 50  $\mu$ l of MSCs in PBS ( $n = 6$ ) or 50  $\mu$ l of PBS alone (vehicle;  $n = 6$ ) into both nostrils (25  $\mu$ l per nostril) using an automatic pipette, on days 64 and 71.

Serelaxin alone: A separate sub-group of mice ( $n = 6$ ) i.n. received 50  $\mu$ l (25  $\mu$ l per nostril) of 0.8 mg/ml (equivalent to 0.5 mg/kg/day) serelaxin (kindly provided by Corthera Inc., San Carlos, CA, USA; a subsidiary of Novartis Pharma AG, Basel, Switzerland) daily, over the 2 week treatment period (from days 64–77). This dose of i.n-administered serelaxin had previously been shown to successfully reverse features of AWR, airway fibrosis and AHR in the OVA-induced chronic AAD model over this treatment period (Royce et al., 2014).

MSCs and serelaxin: A separate sub-group of mice ( $n = 6$ ) were treated with MSCs and serelaxin, as described above over the 2-week treatment period. On days 64 and 71, serelaxin was first administered to anesthetized mice before they were allowed to recover for thirty minutes, then briefly anesthetized again for MSC administration.

Saline: Saline sensitized and challenged control mice i.n-received 50  $\mu$ l (25  $\mu$ l per nostril) of PBS daily over the 2 week treatment period.

### 2.4. Bioluminescence imaging of MSCs

To confirm that i.n-administered MSCs homed to the inflamed lung, a separate sub-group of mice were subjected to an acute model of ovalbumin (OVA)-induced AAD ( $n = 3$ ), as described before (Locke, Royce,

Wainwright, Samuel, and Tang, 2007). These mice were sensitized with an i.p injection of OVA on day 0, then nebulized with OVA (2.5% w/v in 0.9% normal saline) for 30 min per day from days 14–17. As per the chronic AAD model, control mice (n = 3) received a saline injection and were nebulized with 0.9% saline instead of OVA. On day 18, OVA and saline-treated mice were i.n-administered with  $1 \times 10^6$  MSCs expressing eGFP and fluc. To image these cells in vivo, anesthetized animals were i.p-injected with 200  $\mu$ l of D-luciferin (15 mg/ml in PBS; VivoGlo Luciferin; Promega, San Luis Obispo, CA, USA) at 24 and 48 h post-cell injection. Mice and isolated lung tissue were imaged with the IVIS 200 System (Xenogen, Alameda, CA, USA), as described previously (Huskes et al., 2015).

#### 2.5. Invasive plethysmography (chronic AAD)

On day 78 (24 h after the final i.n-administration of PBS or serelaxin treatment), mice were anesthetized with an i.p injection of ketamine (10 mg/kg body weight) and xylazine (2 mg/kg body weight) in 0.9% saline. Tracheostomy was then performed and anesthetized mice were then positioned in the chamber of the Buxco Fine Pointe plethysmograph (Buxco, Research Systems, Wilmington, NC, USA). The airway resistance of each mouse was then measured (reflecting changes in AHR) in response to increasing doses of nebulized acetyl- $\beta$ -methylcholine chloride (methacholine; Sigma Aldrich, MO, USA), delivered intratracheally, from 3.125–50 mg/ml over 5 doses, to elicit bronchoconstriction. The change in airway resistance calculated by the maximal resistance after each dose minus baseline resistance (PBS alone) was plotted against each dose of methacholine evaluated.

#### 2.6. Tissue collection

Following invasive plethysmography, blood was collected from each mouse for serum isolation and storage at  $-80^\circ\text{C}$ . Lung tissues were then isolated and rinsed in cold PBS before divided into four separate lobes. The largest lobe was fixed in 10% neutral buffered formaldehyde overnight and processed to be cut and embedded in paraffin wax. The remaining three lobes were snap-frozen in liquid nitrogen for hydroxyproline assay, and extraction of proteins and MMPs.

#### 2.7. Lung histopathology

Once the largest lobe from each mouse had been processed and paraffin-embedded, each tissue block was serially sectioned (3  $\mu$ m thickness) and placed on charged Mikro Glass slides (Grale Scientific, Ringwood, Victoria, Australia) and subjected to various histological stains or immunohistochemistry. To assess inflammation score, one slide from each mouse (n = 30 in total) was sent to Monash Histology Services and underwent Mayer's hematoxylin and eosin (H&E) (Amber Scientific, Midvale, WA) staining. Similarly, to assess epithelial thickness and sub-epithelial collagen deposition, another set of slides underwent Masson's trichrome staining. To assess goblet cell metaplasia, a third set of slides underwent Alcian blue periodic acid Schiff (ABPAS) staining. The H&E, Masson's trichrome and ABPAS-stained sections were morphometrically analyzed as detailed below.

#### 2.8. Immunohistochemistry (IHC)

Immunohistochemistry was used to detect markers of fibrosis, inclusive of TGF- $\beta$ 1 and  $\alpha$ -smooth muscle actin ( $\alpha$ -SMA; a marker of myofibroblast differentiation). In each case, representative slides from each mouse were subjected to either a polyclonal anti-TGF- $\beta$ 1 (1:1000 dilution; Santa Cruz Biotechnology; Santa Cruz, CA, USA) or biotinylated monoclonal anti-human SMA (1:200 dilution; DAKO Corp., Carpinteria, CA, USA) primary antibody overnight. For negative controls, primary antibody was omitted. Detection of antibody staining was completed with the DAKO envision anti-rabbit (for TGF- $\beta$ 1) or anti-mouse (for

$\alpha$ -SMA) kit and 3,3'-diaminobenzidine (DAKO Corp.); where sections were counterstained with hematoxylin.

#### 2.9. Morphometric analysis

H&E-, Masson's trichrome-, ABPAS- and IHC-stained slides were scanned with ScanScope AT Turbo (Aperio, CA, USA) for morphometric analysis. Five stained airways per animal (of  $\sim$ 150–350  $\mu$ m in diameter) were randomly selected and analyzed using Aperio ImageScope software (Aperio, CA, USA). H&E-stained slides were semi-quantitated with a peri-bronchial inflammation score as described previously (Royce et al., 2014), where the experimenter was blinded and scored individual airways from 0 to 4 for inflammation severity; where 0 = no detectable inflammation; 1 = occasional inflammatory cell aggregates, pooled size  $<0.1$  mm $^2$ ; 2 = some inflammatory cell aggregates, pooled size  $\sim$ 0.2 mm $^2$ ; 3 = widespread inflammatory cell aggregates, pooled size  $\sim$ 0.3 mm $^2$ ; and 4 = widespread and massive inflammatory cell aggregates, pooled size  $\sim$ 0.6 mm $^2$ ). Masson's trichrome- stained slides were analyzed by measuring the thickness of the epithelial and sub-epithelial layers and expressing the values as  $\mu\text{m}^2/\mu\text{m}$  basement membrane (BM) length; where BM length was traced (and expressed in  $\mu\text{m}$ ) in calibrated scanned images using the drawing tool provided in Imagescope Aperio. ABPAS-stained slides were analyzed by counting the number of stained goblet cells expressed as the number of goblet cells/100  $\mu\text{m}$  BM length relative to saline controls.

#### 2.10. Hydroxyproline assay

The second largest lung lobe from each mouse was processed as described before (Royce et al., 2014; Royce et al., 2009; Royce et al., 2013) for the measurement of hydroxyproline content, which was determined from a standard curve of purified trans-4-hydroxy-L-proline (Sigma-Aldrich). Hydroxyproline values were multiplied by a factor of 6.94 (based on hydroxyproline representing  $\sim$ 14.4% of the amino acid composition of collagen in most mammalian tissues (Gallop and Paz, 1975); to extrapolate total collagen content), which in turn was divided by the dry weight of each corresponding tissue to yield collagen concentration (expressed as a percentage).

#### 2.11. Gelatin zymography

To determine if the treatment-induced effects on subepithelial collagen were mediated via the regulation of gelatinases, gelatin zymography of lung tissue protein extracts, which were isolated using the method of Woessner (Woessner, 1995); was performed to assess changes in MMP-2 (gelatinase-A) and MMP-9 (gelatinase-B). Equal aliquots of the protein extracts (2  $\mu\text{g}$ ) were analyzed on zymogram gels consisting of 7.5% acrylamide and 1 mg/ml gelatin, and the gels were subsequently treated as previously detailed. (Woessner, 1995) Gelatinolytic activity was identified by clear bands at the appropriate molecular weight, quantitated by densitometry and the relative optical density (OD) of MMP-9 in each group expressed as the respective ratio of that in the saline-treated mouse group, which was expressed as 1.

#### 2.12. Statistical analysis

All statistical analysis was performed using GraphPad Prism v6.0 (GraphPad Software Inc., CA, USA) and expressed as the mean  $\pm$  SEM. AHR results were analyzed by a two-way ANOVA with Bonferroni post-hoc test. The remaining data was analyzed via one-way ANOVA with Neuman-Keuls post-hoc test for multiple comparisons between groups. In each case, data was considered significant with a p-value less than 0.05.

### 3. Results

#### 3.1. MSCs home to the AAD-inflamed lung

Whole body bioluminescence imaging was used to confirm that i.n-administered MSCs homed to both the normal and inflamed lung following AAD (Fig. 1), but were retained in higher numbers in the inflamed lung 24 and 48 h post-administration (as the bioluminescence intensity observed is directly proportional to the number of labeled MSCs present (Togel, Yang, Zhang, Hu, and Westenfelder, 2008)). MSCs were clearly detected on the ventral surface of mice over the area of the lungs, at 24 and 48 h post-administration; and specifically in lung tissues isolated from OVA-inflamed mice 48 h post-administration (insert; Fig. 1).

#### 3.2. Effects of MSCs, serelaxin and combination treatment on airway inflammation

Airway inflammation was semi-quantitated from H&E-stained lung sections, using an inflammation scoring system as described (Fig. 2). The peri-bronchial inflammation score of OVA-treated mice ( $1.35 \pm 0.11$ ) were significantly increased compared to that measured in saline-treated controls ( $0.03 \pm 0.02$ ;  $p < 0.001$  vs saline group), confirming that these mice had been successfully sensitized and challenged with OVA. While the administration of MSCs ( $1.07 \pm 0.11$ ) or RLN ( $1.17 \pm 0.10$ ) alone only induced a trends towards reduced OVA-induced inflammation score, when added in combination, these treatments significantly lowered inflammation score ( $0.85 \pm 0.05$ ;  $p < 0.01$  vs OVA alone group;  $p < 0.05$  vs OVA + RLN group), although not fully back to that measured in saline-treated mice ( $p < 0.01$  vs saline group) (Fig. 2A, B).

#### 3.3. Effects of MSCs, serelaxin and combination treatment on airway remodeling

##### 3.3.1. Goblet cell metaplasia

Goblet cell metaplasia was morphometrically assessed from ABPAS-stained lung sections and expressed as the number of goblet cells/100  $\mu\text{m}$  basement membrane length (Fig. 2C, D). OVA-treated mice had significantly increased goblet cell numbers ( $7.79 \pm 1.02$ ) compared to their saline-treated counterparts ( $1.00 \pm 0.12$ ;  $p < 0.001$  vs saline group). Neither the administration of MSCs alone ( $6.56 \pm 1.33$ ), serelaxin alone ( $6.22 \pm 0.88$ ) or the combined effects of both

treatments ( $5.95 \pm 1.01$ ) significantly affected the OVA-induced increase in goblet cell metaplasia (all  $p < 0.01$  vs saline group) (Fig. 2C, D).

##### 3.3.2. Epithelial thickness

Epithelial thickness was morphometrically assessed from Masson's trichrome-stained lung sections and expressed as  $\mu\text{m}^2/\mu\text{m}$  basement membrane length (Fig. 3A, B). The epithelial thickness of OVA-treated mice ( $21.60 \pm 0.31$ ) was significantly increased compared to that measured in saline-treated controls ( $16.82 \pm 0.27$ ;  $p < 0.001$  vs saline group). While the administration of MSCs alone ( $20.11 \pm 0.40$ ) only induced a trend towards reduced OVA-mediated epithelial thickness, serelaxin alone ( $17.65 \pm 1.11$ ) significantly reduced epithelial thickness when compared with measurements obtained from OVA alone and OVA + MSC treated mice ( $p < 0.01$  vs OVA alone group;  $p < 0.05$  vs OVA + MSC group), which was not significantly different to that measured in saline-treated controls (Fig. 3A, B). Similarly, combination-treated mice had significantly reduced OVA-mediated epithelial thickness ( $18.69 \pm 0.57$ ;  $p < 0.05$  vs OVA alone group), which was not significantly different to that measured in saline-treated control mice (Fig. 3A, B).

##### 3.3.3. Subepithelial collagen deposition (fibrosis)

Changes in airway fibrosis were evaluated by two methods: i) morphometric analysis of sub-epithelial collagen deposition from Masson's trichrome-stained lung sections (Fig. 3A, C) and ii) hydroxyproline analysis of total lung collagen concentration (Fig. 3D). Sub-epithelial collagen staining relative to BM length, was significantly increased in OVA-treated mice ( $32.03 \pm 1.87$ ) compared to that measured in saline-treated controls ( $17.70 \pm 0.67$ ;  $p < 0.001$  vs saline group; Fig. 3C). MSCs alone ( $27.19 \pm 1.04$ ) modestly but significantly reduced the OVA-mediated sub-epithelial collagen deposition ( $p < 0.01$  vs OVA alone group), while serelaxin alone ( $22.79 \pm 0.52$ ) further reversed the OVA-induced build-up of sub-epithelial collagen deposition ( $p < 0.001$  vs OVA alone group;  $p < 0.01$  vs OVA + MSC group; Fig. 3C). In combination-treated mice, sub-epithelial collagen deposition ( $19.74 \pm 0.65$ ) was significantly reversed to a greater extent compared to either treatment alone ( $p < 0.001$  vs OVA alone and OVA + MSC groups;  $p < 0.05$  vs OVA + RLN group), and was no longer different to that measured in saline-treated control mice (Fig. 3C).

##### 3.3.4. Total lung collagen concentration (fibrosis)

Total lung collagen concentration (% collagen content/dry weight lung tissue) was also used to measure airway fibrosis (Fig. 3D), and

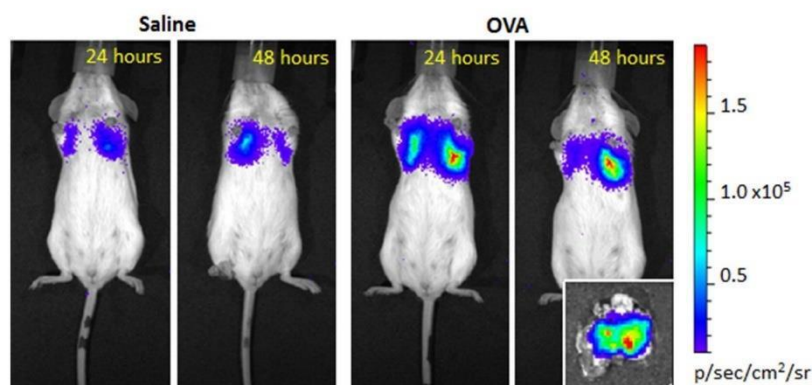


**Fig. 1.** Representative bioluminescence visualization of MSCs in saline-treated (normal) and OVA-treated (AAD/inflamed) mice. MSCs expressing eGFP and luc were i.n-administered into saline ( $n = 3$ ) or OVA-treated ( $n = 3$ ) mice and clearly detected on the ventral surface of mice over the area of the lungs, at 24 and 48 h post-administration; but were retained in higher numbers in OVA-treated mice. MSCs were also specifically detected in lung tissues isolated from OVA-inflamed mice 48 h after they were i.n-delivered to these animals (insert).

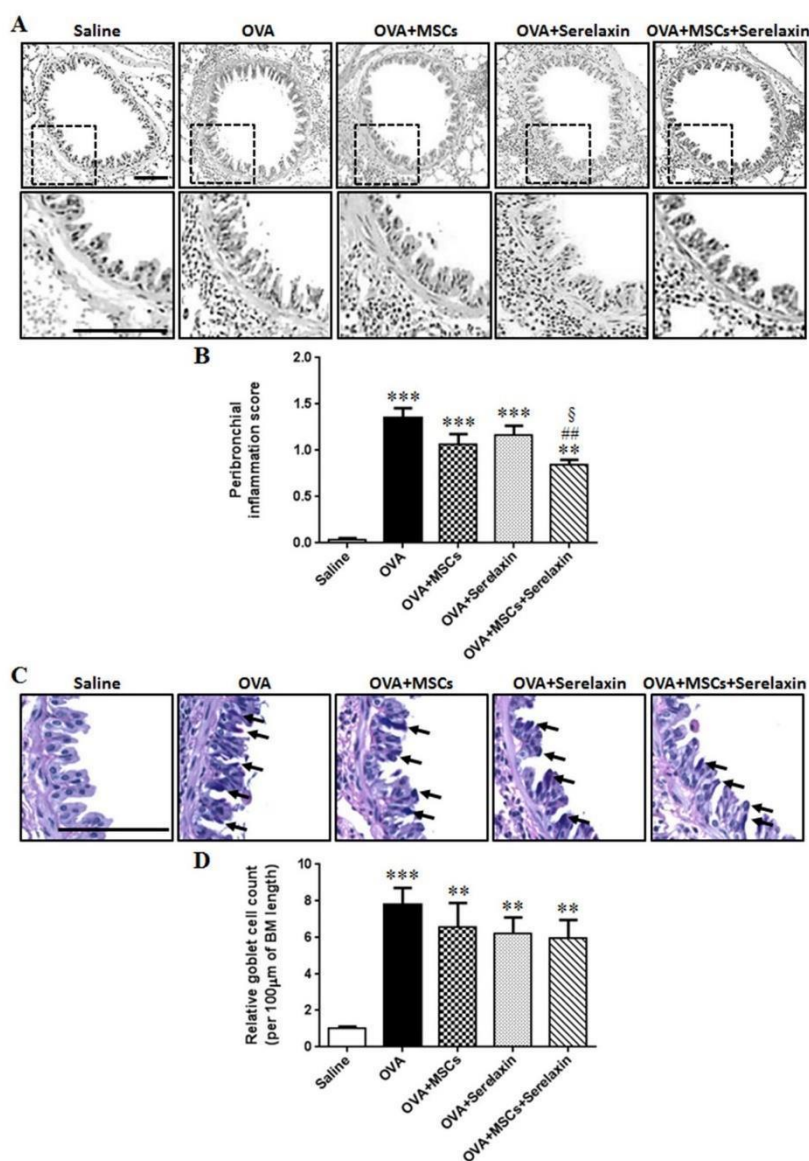


**Fig. 2.** Effects of MSCs, serelaxin and combination treatment on peri-bronchial inflammation and goblet cell metaplasia. Representative photomicrographs of (A) H&E- and (C) ABPAS-stained lung sections from each of the groups studied, showing the extent of (A) bronchial wall inflammatory cell infiltration and (C) goblet cells (indicated by arrows) present within the epithelial layer. Magnified inserts (of the boxed areas shown in the lower-powered images) of inflammatory cell infiltration (A) are also included. Scale bar = 100 μm. Also shown is the mean ± SEM (B) inflammation score and (D) goblet cell count (number of goblet cells/100 μm BM length, relative to saline goblet cell count) from 5 airways/mouse, n = 6 mice/group; where (B) sections were scored for the number and distribution of inflammatory aggregates on a scale of 0 (no apparent inflammation) to 4 (severe inflammation). \*\*p < 0.01, \*\*\*p < 0.001 vs saline group; \*p < 0.01 vs OVA alone group; <sup>§</sup>p < 0.05 vs. OVA + serelaxin group.

extrapolated from the quantity of hydroxyproline present within the second largest lung lobe of each mouse analyzed. Total lung collagen concentration was significantly increased in OVA-treated mice ( $4.58 \pm 0.29\%$ ) compared to that in saline-treated controls ( $2.85 \pm$

$0.21\%$ , p < 0.001 vs saline group). MSCs ( $3.37 \pm 0.23\%$ ) and serelaxin ( $3.25 \pm 0.22\%$ ) alone significantly reversed the OVA-induced increase in total lung collagen deposition by ~70% and ~77%, respectively (both p < 0.01 vs OVA alone group; Fig. 3D). Similarly to what occurred with

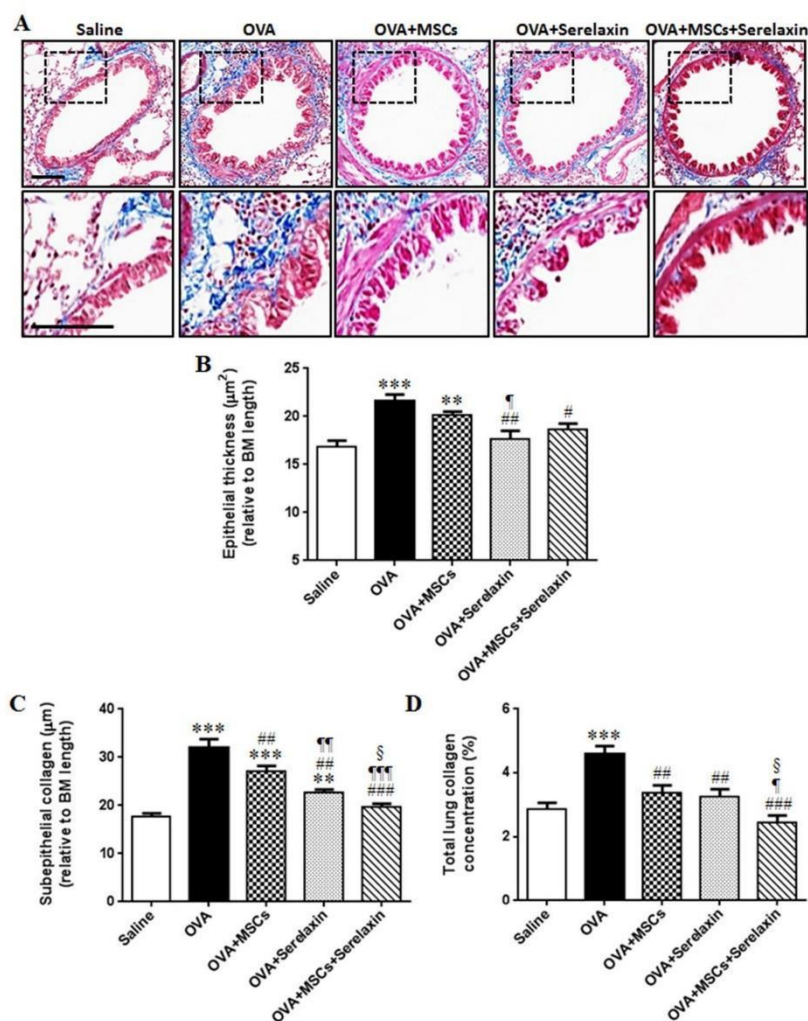


**Fig. 3.** Effects of MSCs, serelaxin and combination treatment on epithelial thickness and airway/lung collagen deposition (fibrosis). (A) Representative photomicrographs of Masson trichrome-stained lung sections from each group studied, showing the extent of epithelial thickness. Magnified inserts (of the boxed areas shown in the lower-powered images) of extracellular matrix/collagen deposition (A) are also included. Scale bar = 100 μm. Also shown is the mean ± SEM (B) epithelial thickness (μm<sup>2</sup>) and (C) subepithelial collagen thickness (μm) (relative to BM length) from 5 airways/mouse, n = 6 mice/group; and (D) mean ± SEM total lung collagen concentration (% collagen content/dry weight tissue) from n = 6 mice/group. \*\*p < 0.01, \*\*\*p < 0.001 vs saline group; #p < 0.05, ##p < 0.01, ###p < 0.001 vs OVA alone group; §p < 0.05, §§p < 0.01, §§§p < 0.001 vs OVA + MSCs group; §p < 0.05 vs OVA + serelaxin group.

sub-epithelial collagen deposition (Fig. 3C), the combined effects of both treatments significantly reversed total lung collagen concentration to a greater extent than either treatment alone, and back to baseline measurements in saline -treated control mice (Fig. 3D).

### 3.3.5. TGF-β1 expression

To determine the mechanisms by which the combined effects of MSCs and RLN were able to fully reverse OVA-induced sub-epithelial (Fig. 3C) and total lung collagen (Fig. 3D) deposition, changes in TGF-β1 expression (Fig. 4A, B), α-SMA expression (Fig. 4C, D) and gelatinase levels (Fig. 5) were then measured in each of the experimental groups.

TGF-β1 expression was morphometrically assessed from IHC-stained lung sections (Fig. 4A) and expressed as % staining per airway analyzed (which was averaged from 5 airways per mouse; Fig. 4B). TGF-β1 was evident in saline controls ( $6.30 \pm 0.77\%$ ) and was significantly increased in OVA-treated mice ( $12.88 \pm 0.45\%$ ,  $p < 0.001$  vs saline group; Fig. 4B). MSCs alone induced a trend towards reduced OVA-mediated TGF-β1 staining ( $10.69 \pm 1.47\%$ ), while both serelaxin alone ( $8.28 \pm 1.17\%$ ) and the combination therapy ( $9.04 \pm 0.72\%$ ) significantly reduced TGF-β1 expression (both  $p < 0.05$  vs OVA alone group) to levels that were not significantly different to that measured in saline-treated controls (Fig. 4B).

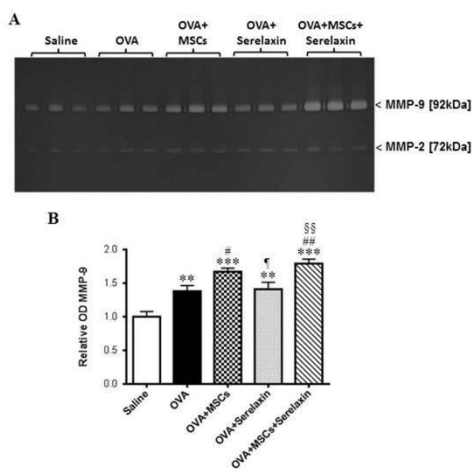


**Fig. 5.** Effects of MSCs, serelaxin and combination treatment on gelatinase expression. (A) A representative gelatin zymograph showing MMP-9 (gelatinase B; 92 kDa) and MMP-2 (gelatinase A; 72 kDa) expression in the each of the groups studied. A separate zymograph analyzing three additional samples per group produced similar results. (B) Also shown is relative mean  $\pm$  SEM optical density (OD) MMP-9 (which was most abundantly expressed in the lung of female Balb/c mice) from  $n = 6$  mice/group. \*\* $p < 0.01$ , \*\*\* $p < 0.001$  vs saline group; \* $p < 0.05$ , \*\* $p < 0.01$  vs OVA alone group; † $p < 0.05$  vs OVA + MSCs group; ‡ $p < 0.01$  vs OVA + serelaxin group.

reduced OVA-mediated myofibroblast numbers, however serelaxin alone ( $1.5 \pm 0.2$ ) and the combination treatment ( $1.4 \pm 0.1$ ) significantly reduced  $\alpha$ -SMA protein expression localized around the airways compared to that measured in OVA-treated mice (both  $p < 0.01$  vs OVA alone group; Fig. 4D), but not completely back to corresponding measurements in saline-treated mice (both  $p < 0.05$  vs saline group). These results suggested that the greater ability of the combination therapy to reverse airway fibrosis compared to either treatment alone was not explained by the changes in TGF- $\beta$ 1 expression and myofibroblast density measured (which both contribute to matrix synthesis).

### 3.3.7. Gelatinase expression

Based on the findings obtained above, changes in gelatinase A (MMP-2) and gelatinase B (MMP-9) levels, which can both degrade basement membrane collagen IV and collagenase-digested interstitial collagen fragments into gelatin were measured (Fig. 5). Interestingly, high expression of MMP-9 was observed in the lungs of female Balb/c mice, while comparatively lower levels of MMP-2 were detectable (Fig. 5A); and hence, changes in the optical density (OD) of MMP-9 were semi-quantitated by densitometry between the groups studied (Fig. 5B). OVA-treated mice (relative OD:  $1.38 \pm 0.09$ ) had a modest but significant increase in lung MMP-9 expression compared to relative levels measured from their saline-treated counterparts ( $p < 0.01$  vs saline group; Fig. 5B). MSCs alone (relative OD:  $1.67 \pm 0.05$ ), but not serelaxin alone (relative OD:  $1.41 \pm 0.11$ ) further increased lung MMP-9 expression beyond that measured in OVA-treated mice ( $p < 0.001$  vs saline group;  $p < 0.05$  vs OVA alone group). In comparison, combination-treated mice (relative OD:  $1.79 \pm 0.07$ ) had the highest lung MMP-9 levels compared to that measured in the other OVA-treated groups ( $p < 0.01$  vs OVA alone group,  $p < 0.01$  vs OVA + serelaxin group,  $p = 0.08$  vs OVA + MSC group; Fig. 5B). A similar trend was also observed for MMP-2 expression between the various groups studied. These results suggested that the greater ability of the combination therapy to reverse airway fibrosis compared to either treatment alone, was most likely explained by the enhanced MMP-

promoting effects of MSCs (which would likely result in MSC-induced collagen degradation), complemented by the ability of serelaxin to block aberrant matrix synthesis from occurring.

### 3.4. Effects of MSCs, serelaxin and combination treatment on AHR

Airway reactivity (reflecting changes in AHR) was assessed via invasive plethysmography in response to increasing doses of nebulized methacholine, a bronchoconstrictor. As expected, OVA-treated mice had significantly increased airway reactivity, particularly in response to the three highest doses of methacholine tested (12.5–50 mg/ml), compared to that measured in saline-treated control mice (Fig. 6). OVA + serelaxin-treated mice but not OVA + MSC-treated mice demonstrated significantly reduced AHR compared to their OVA alone-treated counterparts, particularly at the two highest doses of methacholine tested (25–50 mg/ml) ( $p < 0.01$  vs OVA group; Fig. 6). Likewise, OVA + MSC + serelaxin-treated mice demonstrated significantly reduced AHR compared to their OVA alone-treated counterparts, particularly at the three highest doses of methacholine tested (12.5–50 mg/ml) ( $p < 0.01$  vs OVA group), which was not significantly different to AHR measurements obtained from OVA + serelaxin-treated mice at each of the methacholine doses tested. Importantly, AHR in OVA + serelaxin and OVA + MSC + serelaxin-treated mice was not significantly different to that measured in saline-treated controls (Fig. 6).

## 4. Discussion

This study aimed to determine if the presence of an anti-fibrotic (serelaxin) would create a more favorable environment and/or aid human bone marrow-derived MSCs in being able to reverse the pathological features of AWR and related AHR associated with chronic AAD – and a summary of the main findings of the study is provided in Table 1. As such, it provided the first report establishing an effective outcome of the combined effects of MSCs and RLN in reversing the development of fibrosis associated with AWR, and to a lesser extent AI, in an experimental murine model of chronic AAD, which mimics several features of human asthma. As indicated by the morphometric analysis of sub-epithelial collagen and hydroxyproline analysis of total lung collagen concentration, the OVA-induced aberrant accumulation of collagen (fibrosis) was totally ablated in combined-treated mice when compared with untreated OVA-injured mice and those receiving either therapy alone. The striking anti-fibrotic effects of the combined treatment may be explained by the greater ability of RLN to limit TGF- $\beta$ 1 and myofibroblast differentiation-induced matrix synthesis, whereas MSCs appeared to play more of a role in stimulating MMP-9 levels, which can degrade collagen in the lung (Curley et al., 2003; Zhu et al., 2001). Additionally, the combined anti-fibrotic and anti-inflammatory effects of both therapies contributed to their ability of effectively reversing AHR by ~50–60%, in line with previous findings demonstrating that mouse skeletal myoblasts engineered to over-express serelaxin

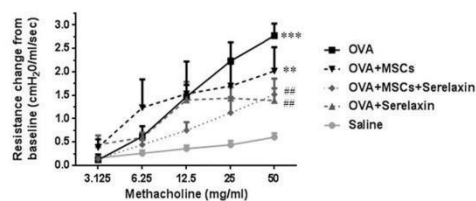


**Fig. 6.** Effects of MSCs, serelaxin and combination treatment on airway resistance (AHR). Airway resistance (reflecting changes in AHR) was assessed via invasive plethysmography in response to increasing doses of nebulized methacholine (and expressed as resistance change from baseline). Shown is the mean  $\pm$  upper SEM (for improved clarity of the data presented) airway resistance to each dose of methacholine tested. \*\* $p < 0.01$ , \*\*\* $p < 0.001$  vs saline group; † $p < 0.01$  vs OVA alone group.

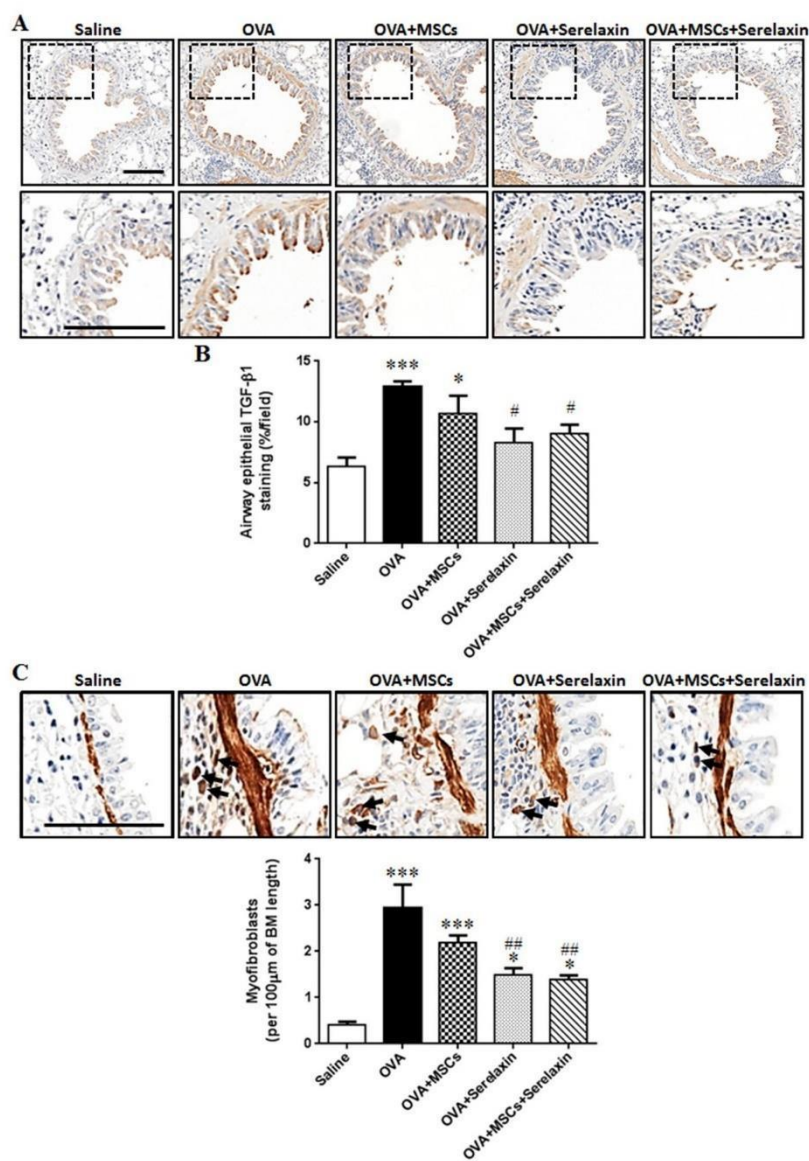


**Fig. 4.** Effects of MSCs, serelaxin and combination treatment on TGF- $\beta$ 1 expression and  $\alpha$ -SMA-stained myofibroblast density. Representative photomicrographs of IHC-stained lung sections from each group studied, showing the amount of (A) TGF- $\beta$ 1 expression within the airway epithelial layer and (B)  $\alpha$ -SMA expression (representative of myofibroblast density; as indicated by the arrows). Magnified inserts (of the boxed areas shown in the lower-powered images) of TGF- $\beta$ 1 staining (A) are also included. Scale bar = 100  $\mu$ m. Also shown is mean  $\pm$  SEM (C) TGF- $\beta$ 1 staining (expressed as %/field) and (D) number of myofibroblasts (per 100  $\mu$ m BM length) from 5 airways/mouse, n = 6 mice/group. \*p < 0.05, \*\*\*p < 0.001 vs saline group; #p < 0.05, ##p < 0.01 vs OVA alone group.

### 3.3.6. Myofibroblast differentiation

Changes in alpha-smooth muscle actin ( $\alpha$ -SMA; a marker of myofibroblast differentiation) were also morphometrically assessed from IHC-stained lung sections (Fig. 4C) and expressed as the number of myofibroblasts per 100  $\mu$ m BM length (which was averaged from 5

airways per mouse; Fig. 4D). Trace numbers of  $\alpha$ -SMA-positive myofibroblasts were detected in the airways of saline control mice ( $0.4 \pm 0.2$ ), while OVA-treated mice had significantly increased myofibroblast numbers ( $2.9 \pm 0.5$ ) in comparison ( $p < 0.001$  vs saline group; Fig. 4D). MSCs alone ( $2.2 \pm 0.2$ ) induced a trend towards

**Table 1**  
Summary of the effects of MSCs, serelaxin and combination treatment in reversing the pathologies of chronic AAD.

		OVA	OVA + MSCs	OVA + serelaxin	OVA + MSCs + serelaxin
AI	Inflammation score	↑↑↑	–	–	↓*
	Epithelial thickness	↑↑↑	–	↓↓	↓↓
	Goblet cell metaplasia	↑↑↑	–	–	–
Fibrosis	Subepithelial collagen	↑↑↑	↓	↓↓	↓↓↓*
	Total lung collagen	↑↑↑	↓↓	↓↓	↓↓↓*
	TGF- $\beta$ 1 expression	↑↑↑	–	↓	↓
	$\alpha$ -SMA expression	↑↑↑	–	↓↓	↓↓
AHR	MMP-9 levels	↑↑	↑	–	↑↑
	Airway reactivity	↑↑↑	–	↓↓	↓↓

A summary of the effects of MSCs, serelaxin and combination treatment on chronic AAD-induced AI, AWR, fibrosis and AHR. The arrows in the OVA column are reflective of changes to that measured in saline-treated control mice, while the arrows in the treatment groups are reflective of changes to that in the OVA alone group. (–) implies no change compared to OVA alone.

\* Denotes  $p < 0.05$  vs either treatment alone.

improved various measures of cardiac function when administered to the infarcted/ischemic pig (Formigli et al., 2007) and rat (Bonacchi et al., 2009) heart. Taken together, not only did the reported findings demonstrate the feasibility and viability of combining MSCs and serelaxin in chronic AAD, they demonstrated that this combination therapy had some synergistic effects in reducing airway fibrosis associated with AWR, AI and AHR in a model of chronic AAD.

While i.n-administered MSCs were clearly detected in the lungs of normal mice, and to a greater extent, the inflamed lungs of mice with chronic AAD 48 h later, previous studies in murine models of kidney disease (Huuskies et al., 2015; Togel et al., 2008) had shown that these cells could not be detected by bioluminescence imaging 7 days after administration. These studies suggested that most of the exogenously administered MSCs had vanished after a week, regardless of the route of administration applied; but that these cells were able to induce longer-term paracrine effects that persisted long after they had been cleared. Consistent with the latter, and previous studies showing that repeated (once weekly) administration of MSCs markedly improved their protective effects against kidney injury and related fibrosis (Lee et al., 2010), our findings demonstrated that once weekly administration of human MSCs were able to ameliorate the airway/lung fibrosis associated with chronic AAD by increasing collagen-degrading MMP-9 levels in the murine model studied; confirming that they were still capable of protecting the allergic lung from adverse AWR despite progressively diminishing in numbers post-administration.

Airway inflammation occurs in response to respiratory damage, as the lung attempts to eliminate the original insult by recruiting inflammatory cells to remove cellular debris to restore lost tissue and function (Holgate, 2008). In this study, AI was morphometrically assessed by peri-bronchial inflammation score and was significantly up-regulated in response to OVA-mediated chronic AAD in mice, as reported previously (Royce et al., 2014; Royce et al., 2009). Although both intranasal administration of MSCs alone, which homed to and were retained in the inflamed lung (for at least 48 h), or serelaxin alone induced a trend towards reduced inflammation score, the combination of the two treatments was able to significantly reduce AI, however, not fully back to levels measured in saline-treated controls. A possible explanation for these findings may be that either treatment alone only affected the infiltration of a sub-set of OVA-induced inflammatory cells into the lung, whereas the combined effects of both treatments were able to target a broader subset of inflammatory cells. For example, studies performed with intravenous (i.v) tail vein injection or intratracheal administration of bone marrow-derived MSCs in OVA-treated mice with chronic AAD demonstrated through BAL extraction and inflammatory cell counts, that MSCs were able to significantly reduce eosinophil and lymphocyte counts (Bonfield et al., 2010). On the other hand, studies have shown that RLN primarily targets neutrophil (Masini et al., 2004), mast cell

and leukocyte infiltration (Bani, Ballati, Masini, Bigazzi, and Sacchi, 1997), but not eosinophil (Royce et al., 2014; Royce et al., 2009) or macrophage (Samuel et al., 2011) infiltration. However, it appeared that the combination treatment was not able to fully reverse OVA-induced AI, perhaps due to the fact that both treatments were not able to prevent the infiltration of all inflammatory cells including monocytes, which represented a large proportion of the inflammatory cells identified in the lungs of OVA-injured mice (Royce et al., 2014; Royce et al., 2009); although RLN has been found to prevent monocyte-endothelium contact (Brecht, Bartsch, Baumann, Stangl, and Dschietzig, 2011).

Along with AI, AWR can occur as injury to the lungs is the culmination of a number of factors, including allergens or mechanical insult and possible genetic disorders destroying the architecture and function of the airways. In normal lungs, lung tissue turnover and airway restructuring is a homeostatic process which may aid in preserving optimal functions of the airway (Laurent, 1986). In asthma however, the lungs have the capacity to undergo endogenous remodeling of the airways in attempt to self-repair respiratory structure and function damaged by allergens or genetic causes; with aberrant healing leading to the progressive deposition of collagen, that eventually leads to airway fibrosis, airway obstruction and a positive feedback loop resulting in AHR (Cohn, Elias, and Chupp, 2004; Holgate, 2008). In this study, AWR was assessed via epithelial thickness and goblet cell metaplasia (measures of airway epithelial damage) and airway fibrosis. As observed, MSCs alone did not affect epithelial thickness, goblet cell metaplasia and had only modest effects in reducing aberrant sub-epithelial and total collagen deposition. This is somewhat consistent with the modest effects of adipose tissue-derived MSCs in suppressing the airway contractile tissue mass that was up-regulated in a house dust mite-induced model of AAD (Marinas-Pardo et al., 2014), where the effects of those cells were found to decline under sustained allergen challenge. Conversely, RLN alone had broader anti-remodeling effects and was able to significantly reduce epithelial thickness and aberrant sub-epithelial/total collagen deposition (Table 1). The combined effects of both treatments did not further reverse epithelial thickness (compared to the effects of serelaxin alone), but fully reversed the OVA-induced increase in sub-epithelial and total collagen deposition, to a greater extent than either therapy alone.

The occurrence of airway epithelial thickening in asthma leads to a decrease in airway lumen size, consequently resulting in increased airway resistance corresponding to AHR (Elias, Zhu, Chupp, and Homer, 1999). Data from pediatric and non-fatal asthma studies have shown epithelial thickness of the airways can increase 2-fold (James, Maxwell, Pearce-Pinto, Elliot, and Carroll, 2002; Kim et al., 2007), which is consistent with current findings in the study that demonstrated OVA-challenged mice had a clear significant increase in epithelial thickness as compared to saline-treated controls. The finding that MSCs were unable to reduce epithelial thickness is consistent with past studies using i.v tail vein injections of MSCs in OVA-injured mice with chronic AAD (Bonfield et al., 2010), whereas the ability of RLN to reverse epithelial thickness is consistent with its previously reported effects in the AAD model (Royce et al., 2014; Royce et al., 2009). These findings may explain 1) why RLN, but not MSCs, was able to reduce AHR (as only RLN decreased both epithelial thickness and airway/lung fibrosis, which both contribute to AHR); and 2) perhaps why the combined effects of MSCs and RLN did not further reduce AHR beyond that reversed by RLN alone (as the combination treatment was not able to reverse epithelial thickness beyond that induced by RLN alone). This would suggest that reducing both the originating epithelial damage, activation and thickening on top of the subsequent airway/lung fibrosis may better protect from AAD-induced AWR and the contributions of.

#### 4.1. AWR to AHR

The key finding of this study was that the combination treatment not only successfully reduced aberrant sub-epithelial and total collagen

levels comparable to uninjured saline-treated mice, but also reversed airway fibrosis more effectively than either therapy alone. These results coincide with our recent study using a similar combination therapy in treating renal fibrosis induced by obstructive nephropathy (Huuskens et al., 2015). To identify the possible mechanisms involved with the reversal of aberrant collagen levels found in the lungs of combination-treated mice, expression of markers of collagen synthesis: TGF- $\beta$ 1, myofibroblast differentiation, and collagen degradation: MMP-2 and MMP-9 were assessed. Morphometric analysis of IHC-stained sections revealed that MSCs did not significantly affect these markers of matrix synthesis in the chronic AAD model studied. This is somewhat consistent with previous studies which demonstrated that while exogenous administration of MSCs were capable of decreasing markers of fibrosis, their effects were significantly diminished in experimental models of chronic lung damage (Wang et al., 2011; Weiss et al., 2006). On the other hand, RLN, a well-established anti-fibrotic was able to reduce TGF- $\beta$ 1 and  $\alpha$ -SMA expression in the lung, consistent with its ability to reduce these markers when applied to other models of heart (Samuel et al., 2011), lung (Unemori et al., 1996) and kidney (Hewitson, Ho, and Samuel, 2010) disease. As the combined effects of both treatments were not able to reverse matrix synthesis to a greater extent that RLN alone, these findings suggested that the greater ability of the combination treatment to reverse airway fibrosis in the chronic AAD model studied, was not fully explained by the changes in matrix synthesis markers measured.

Gelatin zymography was then used to assess MMP-2 and MMP-9 levels, to determine whether the greater ability of the combination therapy to reverse airway fibrosis (over either treatment alone) was attributed to both treatments being able to increase expression of MMPs that play roles in collagen degradation. Following lung injury, MMPs appear to be increased regardless of whether the injury was induced by OVA or bleomycin treatment (Locke et al., 2007; Moodley et al., 2010), thus explaining the up-regulation of MMP-9 expression observed in OVA-injured mice. The higher expression of MMP-9 (compared to MMP-2) present within the lungs of female Balb/c mice was similar to previous findings from the chronic AAD model (Locke et al., 2007). Consistent with previous findings of other stem cells being able to promote MMP-9 expression and activity when administered to mouse models of lung injury (Moodley et al., 2009; Moodley et al., 2010), MSCs were able to significantly promote MMP-9 expression over and above that induced by OVA alone. On the other hand, RLN alone could not further promote MMP-9 levels beyond that induced by OVA, as demonstrated previously (Royce et al., 2009); as was the case in the setting of obstructive nephropathy-induced renal injury (Hewitson et al., 2010). In line with recent findings demonstrating that the combined effects of MSCs and RLN increased MMP-2 levels over and above that induced by either treatment alone post-obstructive nephropathy (Huuskens et al., 2015), the combined effects of both treatments significantly increased MMP-9 levels over and above that induced by OVA and OVA + serelaxin treatment, which trended to be higher than that induced by MSC treatment alone; and most likely explains why the combined effects of both treatments could effectively reverse airway fibrosis in the chronic AAD model studied.

Functional analysis of airway resistance was measured by invasive plethysmography. OVA-challenged mice demonstrated significantly increased AHR, which was unaffected by MSC treatment. This is consistent with the modest anti-remodeling effects of these cells (Table 1). However, AHR was significantly abrogated by RLN and the combination treatment (consistent with the broader therapeutic effects of these treatments, as demonstrated in this and previous studies (Kenyon et al., 2003; Royce et al., 2014; Royce et al., 2009; Royce et al., 2013); confirming that both AI and AWR contribute to AHR and treatment strategies that target AI and AWR can more effectively reduce the functional impact of AHR.

In conclusion, the current study combined two therapies in treating AAD, more specifically AWR, which may provide a possible clinical

option for patients that may not respond to existing therapeutic treatments for asthma. As seen in the current study, the combination treatment effectively reduced AI and AWR via the synergistic effects of RLN in inhibiting matrix synthesis and MSCs in possibly promoting MMP-mediated collagen degradation, thereby reducing AWR and subsequently AHR. Thus, the results from this study demonstrate that MSC therapy combined with an agent that has anti-fibrotic properties may provide future therapeutic options for patients with chronic asthma, particularly those that are resistant to corticosteroid therapy.

#### Acknowledgments

We sincerely thank Mr. Junli (Vingo) Zhuang for maintaining the MSCs required for the outlined studies. This work was supported in part by a Monash University MBio Postgraduate Discovery Scholarship (MPDS) to Krupesh P. Patel; a Kidney Health Australia Medical and Science Research Scholarship to Brooke M. Huuskens; and a National Health & Medical Research Council (NHMRC) of Australia Senior Research Fellowship (GNT1041766) to Chrishan S. Samuel.

#### References

- Aggarwal, S., Pittenger, M.F., 2005. Human mesenchymal stem cells modulate allogeneic immune cell responses. *Blood* 105 (4), 1815–1822.
- Bani, D., Ballati, L., Masini, E., Bigazzi, M., Sacchi, T.B., 1997. Relaxin counteracts asthma-like reaction induced by inhaled antigen in sensitized guinea pigs. *Endocrinology* 138 (5), 1909–1915.
- Bathgate, R.A., Ivell, R., Sanborn, B.M., Sherwood, O.D., Summers, R.J., 2006. International union of pharmacology: recommendations for the nomenclature of receptors for relaxin family peptides. *Pharmacol. Rev.* 58 (1), 7–31.
- Bennett, R.G., 2009. Relaxin and its role in the development and treatment of fibrosis. *Transl. Res.* 154 (1), 1–6.
- Bonacchi, M., Nistri, S., Nanni, C., Gelsomino, S., Pini, A., Cinci, L., Maiani, M., Zecchi-Orlandini, S., Lorusso, R., Fanti, S., Silvertown, J., Bani, D., 2009. Functional and histopathological improvement of the post-infarcted rat heart upon myoblast cell grafting and relaxin therapy. *J. Cell. Mol. Med.* 13 (9B), 3437–3448.
- Bonfield, T.L., Kolozs, M., Lennon, D.P., Zuchowski, B., Yang, S.E., Caplan, A.L., 2010. Human mesenchymal stem cells suppress chronic airway inflammation in the murine ovalbumin asthma model. *Am. J. Physiol. Lung Cell. Mol. Physiol.* 299 (6), L760–L770.
- Bousquet, J., Mantzouranis, E., Cruz, A.A., Ait-Khaled, N., Baena-Cagnani, C.E., Bleeker, E.R., Brightling, C.E., Burney, P., Bush, A., Busse, W.W., Casale, T.B., Chan-Yeung, M., Chen, R., Chowdhury, B., Chung, K.F., Dahl, R., Drazen, J.M., Fabbri, L.M., Holgate, S.T., Kauffmann, F., Haahela, T., Khaltaev, N., Kiley, J.P., Masjedi, M.R., Mohammad, Y., O'Byrne, P., Partridge, M.R., Rabe, K.F., Togias, A., van Weel, C., Wenzel, S., Zhong, N., Zuberbier, T., 2010. Uniform definition of asthma severity, control, and exacerbations: document presented for the World Health Organization Consultation on Severe Asthma. *J. Allergy Clin. Immunol.* 126 (5), 926–938.
- Brecht, A., Bartsch, C., Baumann, G., Stangl, K., Dschietzig, T., 2011. Relaxin inhibits early steps in vascular inflammation. *Regul. Pept.* 166 (1–3), 76–82.
- Cohn, L., Elias, J.A., Chupp, G.L., 2004. Asthma: mechanisms of disease persistence and progression. *Annu. Rev. Immunol.* 22, 789–815.
- Crompton, G., 2006. A brief history of inhaled asthma therapy over the last fifty years. *Prim. Care Respir. J.* 15 (6), 326–331.
- Curley, A.E., Sweet, D.G., Thornton, C.M., O'Hara, M.D., Chesshyre, E., Pizzotti, J., Wilbourn, M.S., Halliday, H.L., Warner, J.A., 2003. Chorioamnionitis and increased neonatal lung lavage fluid matrix metalloproteinase-9 levels: implications for antenatal origins of chronic lung disease. *Am. J. Obstet. Gynecol.* 188 (4), 871–875.
- Dolgachev, V.A., Ullenbruch, M.R., Lukacs, N.W., Phan, S.H., 2009. Role of stem cell factor and bone marrow-derived fibroblasts in airway remodeling. *Am. J. Pathol.* 174 (2), 390–400.
- Durham, A., Adcock, I.M., Tliba, O., 2011. Steroid resistance in severe asthma: current mechanisms and future treatment. *Curr. Pharm. Des.* 17 (7), 674–684.
- Elias, J.A., Zhu, Z., Chupp, G., Homer, R.J., 1999. Airway remodeling in asthma. *J. Clin. Invest.* 104 (8), 1001–1006.
- Forrnigli, L., Perna, A.M., Meacci, E., Cinci, L., Margheri, M., Nistri, S., Tani, A., Silvertown, J., Orlandini, G., Porciani, C., Zecchi-Orlandini, S., Medin, J., Bani, D., 2007. Paracrine effects of transplanted myoblasts and relaxin on post-infarction heart remodelling. *J. Cell. Mol. Med.* 11 (5), 1087–1100.
- Gallop, P.M., Paz, M.A., 1975. Posttranslational protein modifications, with special attention to collagen and elastin. *Physiol. Rev.* 55 (3), 418–487.
- Ge, X., Bai, C., Yang, J., Lou, G., Li, Q., Chen, R., 2013. Effect of mesenchymal stem cells on inhibiting airway remodeling and airway inflammation in chronic asthma. *J. Cell. Biochem.* 114 (7), 1595–1605.
- Giangreco, A., Arwert, E.N., Rosewell, I.R., Snyder, J., Watt, F.M., Stripp, B.R., 2009. Stem cells are dispensable for lung homeostasis but restore airways after injury. *Proc. Natl. Acad. Sci. U. S. A.* 106 (23), 9286–9291.
- Hewitson, T.D., Ho, W.Y., Samuel, C.S., 2010. Antifibrotic properties of relaxin: in vivo mechanism of action in experimental renal tubulointerstitial fibrosis. *Endocrinology* 151 (10), 4938–4948.
- Holgate, S.T., 2008. Pathogenesis of asthma. *Clin. Exp. Allergy* 38 (6), 872–897.

- Holgate, S.T., 2012. Innate and adaptive immune responses in asthma. *Nat. Med.* 18 (5), 673–683.
- Hsu, S.Y., Nakabayashi, K., Nishi, S., Kumagai, J., Kudo, M., Sherwood, O.D., Hsueh, A.J., 2002. Activation of orphan receptors by the hormone relaxin. *Science* 295 (5555), 671–674.
- Huang, X., Gai, Y., Yang, N., Lu, B., Samuel, C.S., Thannickal, V.J., Zhou, Y., 2011. Relaxin regulates myfibroblast contractility and protects against lung fibrosis. *Am. J. Pathol.* 179 (6), 2751–2765.
- Huuskies, B.M., Wise, A.F., Cox, A.J., Lim, E.X., Payne, N.L., Kelly, D.J., Samuel, C.S., Ricardo, S.D., 2015. Combination therapy of mesenchymal stem cells and serelaxin effectively attenuates renal fibrosis in obstructive nephropathy. *FASEB J.* 29 (2), 540–553.
- Jadad, A.R., Moher, M., Browman, G.P., Booker, L., Sigouin, C., Fuentes, M., Stevens, R., 2000. Systematic reviews and meta-analyses on treatment of asthma: critical evaluation. *BMJ* 320 (7234), 537–540.
- James, A.L., Maxwell, P.S., Pearce-Pinto, G., Elliot, J.G., Carroll, N.G., 2002. The relationship of reticular basement membrane thickness to airway wall remodeling in asthma. *Am. J. Respir. Crit. Care Med.* 166 (12 Pt 1), 1590–1595.
- Jiang, X.X., Zhang, Y., Liu, B., Zhang, S.X., Wu, Y., Yu, X.D., Mao, N., 2005. Human mesenchymal stem cells inhibit differentiation and function of monocyte-derived dendritic cells. *Blood* 105 (10), 4120–4126.
- Kenyon, N.J., Ward, R.W., Last, J.A., 2003. Airway fibrosis in a mouse model of airway inflammation. *Toxicol. Appl. Pharmacol.* 186 (2), 90–100.
- Kim, E.S., Kim, S.H., Kim, K.W., Park, J.W., Kim, Y.S., Sohn, M.H., Kim, K.E., 2007. Basement membrane thickening and clinical features of children with asthma. *Allergy* 62 (6), 635–640.
- Knight, D.A., Rossi, F.M., Hackett, T.L., 2010. Mesenchymal stem cells for repair of the airway epithelium in asthma. *Expert Rev. Respir. Med.* 4 (6), 747–758.
- Krampera, M., Glennie, S., Dyson, J., Scott, D., Laylor, R., Simpson, E., Dazzi, F., 2003. Bone marrow mesenchymal stem cells inhibit the response of naive and memory antigen-specific T cells to their cognate peptide. *Blood* 101 (9), 3722–3729.
- Laurent, G.J., 1986. Lung collagen: more than scaffolding. *Thorax* 41 (6), 418–428.
- Lee, S.R., Lee, S.H., Moon, J.Y., Park, J.Y., Lee, D., Lim, S.J., Jeong, K.H., Park, J.K., Lee, T.W., Ihm, C.G., 2010. Repeated administration of bone marrow-derived mesenchymal stem cells improved the protective effects on a remnant kidney model. *Ren. Fail.* 32 (7), 840–848.
- Locke, N.R., Royce, S.G., Wainwright, J.S., Samuel, C.S., Tang, M.L., 2007. Comparison of airway remodeling in acute, subacute, and chronic models of allergic airways disease. *Am. J. Respir. Cell Mol. Biol.* 36 (5), 625–632.
- Marinas-Pardo, L., Mirones, I., Amor-Carro, O., Fraga-Iriso, R., Lema-Costa, B., Cubillo, I., Rodriguez Milla, M.A., Garcia-Castro, J., Ramos-Barbon, D., 2014. Mesenchymal stem cells regulate airway contractile tissue remodeling in murine experimental asthma. *Allergy* 69 (6), 730–740.
- Masini, E., Nistri, S., Vannacci, A., Bani Sacchi, T., Novelli, A., Bani, D., 2004. Relaxin inhibits the activation of human neutrophils: involvement of the nitric oxide pathway. *Endocrinology* 145 (3), 1106–1112.
- Moodley, Y., Atienza, D., Manuelpillai, U., Samuel, C.S., Tchongue, J., Ilancheran, S., Boyd, R., Trounson, A., 2009. Human umbilical cord mesenchymal stem cells reduce fibrosis of bleomycin-induced lung injury. *Am. J. Pathol.* 175 (1), 303–313.
- Moodley, Y., Ilancheran, S., Samuel, C., Vaghjiani, V., Atienza, D., Williams, E.D., Jenkin, G., Wallace, E., Trounson, A., Manuelpillai, U., 2010. Human amnion epithelial cell transplantation abrogates lung fibrosis and augments repair. *Am. J. Respir. Crit. Care Med.* 182 (5), 643–651.
- Payne, N.L., Sun, G., McDonald, C., Layton, D., Moussa, L., Emerson-Webber, A., Veron, N., Siatskas, C., Herszfeld, D., Price, J., Bernard, C.C., 2013. Distinct immunomodulatory and migratory mechanisms underpin the therapeutic potential of human mesenchymal stem cells in autoimmune demyelination. *Cell Transplant.* 22 (8), 1409–1425.
- Ponte, A.L., Marais, E., Gally, N., Langonne, A., Delorme, B., Herault, O., Charbord, P., Domenech, J., 2007. The in vitro migration capacity of human bone marrow mesenchymal stem cells: comparison of chemokine and growth factor chemotactic activities. *Stem Cells* 25 (7), 1737–1745.
- Royce, S.G., Miao, Y.R., Lee, M., Samuel, C.S., Tregear, G.W., Tang, M.L., 2009. Relaxin reverses airway remodeling and airway dysfunction in allergic airways disease. *Endocrinology* 150 (6), 2692–2699.
- Royce, S.G., Cheng, V., Samuel, C.S., Tang, M.L., 2012. The regulation of fibrosis in airway remodeling in asthma. *Mol. Cell. Endocrinol.* 351 (2), 167–175.
- Royce, S.G., Sedjajthera, A., Samuel, C.S., Tang, M.L., 2013. Combination therapy with relaxin and methylprednisolone augments the effects of either treatment alone in inhibiting subepithelial fibrosis in an experimental model of allergic airways disease. *Clin. Sci.* 124 (1), 41–51.
- Royce, S.G., Lim, C.X., Patel, K.P., Wang, B., Samuel, C.S., Tang, M.L., 2014. Intranasally administered serelaxin abrogates airway remodeling and attenuates airway hyperresponsiveness in allergic airways disease. *Clin. Exp. Allergy* 44 (11), 1399–1408.
- Samuel, C.S., Cendrawan, S., Gao, X.M., Ming, Z., Zhao, C., Kiriazis, H., Xu, Q., Tregear, G.W., Bathgate, R.A., Du, X.J., 2011. Relaxin remodels fibrotic healing following myocardial infarction. *Lab. Investig.* 91 (5), 675–690.
- Srouf, N., Thebaud, B., 2014. Stem cells in animal asthma models: a systematic review. *Cytotherapy* 16 (12), 1629–1642.
- Togel, F., Yang, Y., Zhang, P., Hu, Z., Westenfelder, C., 2008. Bioluminescence imaging to monitor the in vivo distribution of administered mesenchymal stem cells in acute kidney injury. *Am. J. Physiol. Ren. Physiol.* 295 (1), F315–F321.
- Unemori, E.N., Pickford, L.B., Salles, A.L., Piercy, C.E., Grove, B.H., Erikson, M.E., Amento, E.P., 1996. Relaxin induces an extracellular matrix-degrading phenotype in human lung fibroblasts in vitro and inhibits lung fibrosis in a murine model in vivo. *J. Clin. Invest.* 98 (12), 2739–2745.
- Wang, D., Zhang, F., Shen, W., Chen, M., Yang, B., Zhang, Y., Cao, K., 2011. Mesenchymal stem cell injection ameliorates the inducibility of ventricular arrhythmias after myocardial infarction in rats. *Int. J. Cardiol.* 152 (3), 314–320.
- Weiss, D.J., Berberich, M.A., Borok, Z., Gail, D.B., Kolls, J.K., Penland, C., Prockop, D.J., 2006. Adult stem cells, lung biology, and lung disease. NHLBI/Cystic Fibrosis Foundation Workshop. *Proc. Am. Thorac. Soc.* 3 (3), 193–207.
- Wise, A.F., Williams, T.M., Kiewiet, M.B., Payne, N.L., Siatskas, C., Samuel, C.S., Ricardo, S.D., 2014. Human mesenchymal stem cells alter macrophage phenotype and promote regeneration via homing to the kidney following ischemia-reperfusion injury. *Am. J. Physiol. Ren. Physiol.* 306 (10), F1222–F1235.
- Woessner Jr., J.F., 1995. Quantification of matrix metalloproteinases in tissue samples. *Methods Enzymol.* 248, 510–528.
- Zhu, Y.K., Liu, X.D., Skold, C.M., Umino, T., Wang, H.J., Spurzem, J.R., Kohyama, T., Ertl, R.F., Rennard, S.I., 2001. Synergistic neutrophil elastase-cytokine interaction degrades collagen in three-dimensional culture. *Am. J. Physiol. Lung Cell. Mol. Physiol.* 281 (4), L868–L878.

---

## **Appendix 3**

---

## Serelaxin improves the therapeutic efficacy of RXFP1-expressing human amnion epithelial cells in experimental allergic airway disease

Simon G. Royce\*<sup>1</sup>, Anna M. Tominaga\*<sup>1</sup>, Matthew Shen\*, Krupesh P. Patel\*, Brooke M. Huuskens†, Rebecca Lim‡, Sharon D. Ricardo† and Chrislan S. Samuel\*

\*Fibrosis Laboratory, Cardiovascular Disease Program, Department of Pharmacology, Biomedicine Discovery Institute, Monash University, Clayton, Victoria 3800, Australia

†Kidney Regeneration and Stem Cell Laboratory, Development & Stem Cells Program, Department of Anatomy and Developmental Biology, Biomedicine Discovery Institute, Monash University, Clayton, Victoria 3800, Australia

‡The Ritchie Centre, Hudson Institute of Medical Research and Department of Obstetrics and Gynaecology, Monash University, Clayton, Victoria 3800, Australia

### Abstract

Current asthma therapies primarily target airway inflammation (AI) and suppress episodes of airway hyperresponsiveness (AHR) but fail to treat airway remodelling (AWR), which can develop independently of AI and contribute to irreversible airway obstruction. The present study compared the anti-remodelling and therapeutic efficacy of human bone marrow-derived mesenchymal stem cells (MSCs) to that of human amnion epithelial stem cells (AECs) in the setting of chronic allergic airways disease (AAD), in the absence or presence of an anti-fibrotic (serelaxin; RLX). Female Balb/c mice subjected to the 9-week model of ovalbumin (OVA)-induced chronic AAD, were either vehicle-treated (OVA alone) or treated with MSCs or AECs alone [intranasally (i.n.)-administered with  $1 \times 10^6$  cells once weekly], RLX alone (i.n.-administered with 0.8 mg/ml daily) or a combination of MSCs or AECs and RLX from weeks 9–11 ( $n = 6$ /group). Measures of AI, AWR and AHR were then assessed. OVA alone exacerbated AI, epithelial damage/thickness, sub-epithelial extracellular matrix (ECM) and total collagen deposition, markers of collagen turnover and AHR compared with that in saline-treated counterparts (all  $P < 0.01$  compared with saline-treated controls). RLX or AECs (but not MSCs) alone normalized epithelial thickness and partially diminished the OVA-induced fibrosis and AHR by ~40–50% (all  $P < 0.05$  compared with OVA alone). Furthermore, the combination treatments normalized epithelial thickness, measures of fibrosis and AHR to that in normal mice, and significantly decreased AI. Although AECs alone demonstrated greater protection against the AAD-induced AI, AWR and AHR, compared with that of MSCs alone, combining RLX with MSCs or AECs reversed airway fibrosis and AHR to an even greater extent.

**Key words:** asthma, airway remodelling, fibrosis, serelaxin, stem cells.

### INTRODUCTION

Asthma is a chronic respiratory disease involving obstruction of the airways and bronchospasm [1], and has three main components to its pathogenesis: airway inflammation (AI), airway remodelling (AWR; representing the structural changes in the lung that lead to fibrosis and airway obstruction) and airway hyperresponsiveness (AHR). The prevalence of asthma in developed countries has increased dramatically in recent decades [2], and has been

estimated to affect 300 million people worldwide [3]. Asthma is responsible for one in every 250 deaths worldwide each year, as well as the loss of an estimated 15 million disability-adjusted life years (DALYs) and costs the health care system \$21.65 billion in Europe per year [4].

Corticosteroids and  $\beta_2$ -adrenoreceptor agonists are the most widely-used treatments for asthma [5]. These therapies can suppress AHR; the constrictive response of the airways to a bronchoconstrictor [6] by targeting AI or AHR directly respectively.

**Abbreviations:** AAD, allergic airways disease; ABPAS, Alcian blue periodic acid Schiff; AEC, human amnion epithelial cell; AHR, airway hyperresponsiveness; AI, airway inflammation; AWR, airway remodelling; BAL, bronchoalveolar lavage; BM, basement membrane; ECM, extracellular matrix; hRF, human renal fibroblast; IF, immunofluorescence; IHC, immunohistochemistry; MSC, human bone marrow-derived mesenchymal stem cell; OVA, ovalbumin; RLX, serelaxin; RXFP1, relaxin family peptide receptor 1;  $\alpha$ -SMA,  $\alpha$ -smooth muscle actin; TGF- $\beta$ 2, transforming growth factor- $\beta$ 2; Th2, T helper cell-type 2; TSLP, thymic stromal lymphopoietin

**Correspondence:** Associate Professor Chrislan S. Samuel (email chrislan.samuel@monash.edu) or Dr Simon G. Royce (simon.royce@monash.edu).

<sup>1</sup> These authors contributed equally to this work.

However, they are limited in that they do not target the AWR associated with asthma, which can lead to AHR independently of AI [7].

Stem cells possess attractive reparative properties [8], act via paracrine signalling [9], as well as increasing regulatory T-cell (Treg) activity [10] and therefore may be applicable to the treatment of AWR. Stem cells have been successfully used in acute animal models of allergic airways disease (AAD) to reduce inflammation and associated fibrosis, predominantly via immunomodulation [11–13]. However, the use of stem cells has been less promising in chronic AAD models due to reductions in their proliferative, differentiation and reparative capabilities [14]. This is potentially attributed to the presence of extensive fibrosis in chronic AAD which impairs stem cell survival, migration to the target damaged tissue, proliferation and integration with resident tissue cells [15]. It has been postulated that treatment with stem cells in combination with an anti-fibrotic may enhance the viability and regenerative capacity of these cells, as the anti-fibrotic drug, serelaxin (RLX) has been shown to create a more favourable environment in disease tissue, in which introduced stem cells could more likely survive [16].

RLX is the drug-based version of the major stored and circulating form of the human relaxin hormone, termed human gene-2 (H2) relaxin. In addition to having rapid-occurring anti-fibrotic actions [11] which are mediated through its cognate G protein coupled receptor, relaxin family peptide receptor-1 (RXFP1), RLX is currently being clinically assessed for its vasodilatory benefits in patients with acute heart failure [17] and is also biologically active in mice [18]. RLX alone demonstrates therapeutic efficacy in various models of lung injury [19–22]. In the setting of chronic AAD, systemic [23] and intranasal [24] treatment with RLX has been demonstrated to reduce excessive collagen deposition and airway epithelial thickening as well as prevent the development of AHR.

In recently completed studies, combining RLX with human bone marrow-derived mesenchymal stem cells (MSCs) was found to improve the viability and proliferative capacity of these cells, and more effectively prevent obstructive nephropathy-induced renal fibrosis [25], while being able to reverse subepithelial and total lung collagen deposition to a greater extent than either treatment alone [26]. The reduction in airway/lung fibrosis translated to a reduction in AHR which was no longer different to that measured from saline-treated control mice [26]. These data provide compelling evidence that combining MSCs with an anti-fibrotic like RLX can improve the therapeutic efficacy of these stem cells. However, it remains unclear if MSCs are the only kind of stem cells whose therapeutic efficacy can be improved through combination treatment with an anti-fibrotic. Hence, it is of interest to investigate other types of stem cells which have demonstrated therapeutic efficacy in lung disease.

Human amnion epithelial stem cells (AECs) possess several properties which make them an ideal candidate for assessing their therapeutic efficacy in combination with an anti-fibrotic. Firstly, they are non-immunogenic [27] and can be easily and ethically harvested via non-invasive procedures from the amnion sac of the mature placenta [28]. AECs were shown to reduce both inflammation and fibrosis in a chronic mouse model of bleomycin-induced

interstitial lung injury [13], unlike MSCs which displayed only limited therapeutic efficacy when used in isolation in chronic disease settings [25]. Given the promising results of AEC therapy in models of lung injury [13,29,30], the therapeutic efficacy of these cells in the setting of chronic AAD was investigated and compared with that of MSCs, in the absence or presence of RLX.

## MATERIALS AND METHODS

### Animals

Six-to-eight week-old female Balb/c mice were obtained from Monash Animal Services (Monash University, Clayton, Victoria, Australia) and housed under a controlled environment, on a 12 h light/12 h dark lighting cycle with free access to water and lab chow (Barastock Stockfeeds). All mice were provided an acclimatization period of 4–5 days before any experimentation and all procedures performed were approved by a Monash University Animal Ethics Committee (Ethics number: MARP/2012/085), which complies with the Australian Guidelines for the Care and Use of Laboratory Animals for Scientific Purposes.

### Induction of chronic AAD

To assess the individual compared with combined effects of MSCs, AECs and RLX in chronic AAD, a chronic model of ovalbumin (OVA)-induced AAD was established in mice ( $n = 36$ ), as described previously [24,26,31]. Mice were sensitized with two i.p. injections of 10  $\mu\text{g}$  of Grade V chicken egg OVA (Sigma–Aldrich) and 400  $\mu\text{g}$  of aluminium potassium sulfate adjuvant (alum; AJAX Chemicals) in 500  $\mu\text{l}$  of 0.9% normal saline solution (Baxter Health Care) on day 0 and day 14. They were then challenged by whole body inhalation exposure (nebulization) to aerosolized OVA (2.5% w/v in 0.9% normal saline) for 30 min, three times a week, between days 21 and 63, using an ultrasonic nebulizer (Omron NE-U07; Omron). Control mice ( $n = 6$ ) were given i.p. injections of 500  $\mu\text{l}$  0.9% saline and nebulized with 0.9% saline instead of OVA.

### Intranasal treatment with stem cells and/or RLX

On day 64 (1 day following completion of induction of the chronic AAD model), mice were lightly anaesthetized with isoflurane (Baxter Health Care) and held in a semi-supine position while intranasal administration of the appropriate treatment took place. The following treatments were administered to mice from days 64 to 77, over a 2-week period.

OVA alone: mice ( $n = 6$ ) received 50  $\mu\text{l}$  of PBS (the vehicle for MSCs and AECs) (25  $\mu\text{l}$  per nare), using an automatic pipette on days 64 and 71 over the 2-week treatment period; and used as the injury control group.

RLX alone: mice ( $n = 6$ ) daily received 50  $\mu\text{l}$  (25  $\mu\text{l}$  per nare) of a 0.8 mg/ml (equivalent to 0.5 mg/kg per day) RLX solution (kindly provided by Corthera Inc, San Carlos, CA, USA; a subsidiary of Novartis Pharma AG, Basel, Switzerland), via intranasal delivery [24,26], over the 2-week treatment period (from days 64 to 77).

MSCs alone: MSCs (from the Tulane Center for Stem Cell Research and Regenerative Medicine; New Orleans, LA, USA;

pooled from  $n = 3-4$  healthy donors) were characterized and cultured as previously described [32]; and used between passages 3 and 6 for the outlined studies. Prior to administration,  $1 \times 10^6$  MSCs were resuspended in 50  $\mu$ l of PBS and intranasally administered to mice ( $n = 6$ ) once weekly; 25  $\mu$ l per nare on days 64 and 71 of the 2-week treatment period [26].

AECs alone: AECs (from term placentas; pooled from 2–3 separate donors; and characterized previously [33]) were obtained and reconstituted overnight (once thawed from being stored in liquid nitrogen) before use in Dulbecco's modified Eagle's medium (DMEM)/F-12 medium containing 10% FBS.  $1 \times 10^6$  AECs were resuspended in 50  $\mu$ l of PBS and administered to a fourth sub-group of mice ( $n = 6$ ), on days 64 and 71, as detailed above for MSC treatment of mice.

Combination treatment: Two further sub-groups of mice ( $n = 6$ /group) received either intranasal administration of MSCs and RLX or AECs and RLX (as described above for each treatment) over the 2-week treatment period. RLX was administered approximately 15–20 min prior to MSC or AEC administration in each case.

#### Invasive plethysmography

On day 78 (24 h after the final intranasal administration of PBS or various treatments detailed), mice were anaesthetized with an i.p. injection of ketamine 10 mg/kg and xylazine 2 mg/kg BW (in 0.9% saline). Tracheostomy was then performed and anaesthetized mice were then positioned in the chamber of the Buxco Fine Pointe plethysmograph (Buxco, Research Systems). The airway resistance of each mouse was then measured (reflecting changes in AHR) in response to increasing doses of nebulized acetyl- $\beta$ -methacholine chloride (methacholine; Sigma–Aldrich), delivered intratracheally, from 3.125 to 50 mg/ml over 5 doses, to elicit bronchoconstriction. The change in airway resistance calculated by the maximal resistance after each dose minus baseline resistance (PBS alone) was plotted against each dose of methacholine evaluated.

#### Bronchoalveolar lavage and tissue collection

Following invasive plethysmography, bronchoalveolar lavage (BAL) fluid was collected by pooling 3  $\times$  0.5 ml lavages with ice-cold PBS and stored in 300  $\mu$ l of 5% FBS, at  $-80^\circ\text{C}$ . Eosinophils were identified by their morphology (horseshoe-shaped nuclei and eosinophilic cytoplasmic granules), as a measure of AI. Lung tissues were then isolated and rinsed in ice-cold PBS before being divided into four separate lobes. The largest lobe was fixed in 10% neutral buffered formaldehyde overnight and processed to be cut and embedded in paraffin wax. The remaining three lobes were snap-frozen in liquid nitrogen for various other assays.

#### Alu PCR

To determine if AECs were still present in the lung at the end of the 2-week treatment period, total genomic DNA (gDNA) was isolated from an equivalent lung lobe from OVA-injured mice treated with ( $n = 6$ ) or without ( $n = 6$ ) AECs alone, using the PureLink Genomic DNA kit (Thermo Fisher Scientific Australia). PCR for the detection of human Alu elements (used as a surrogate

marker of the presence of human AECs [13]) was performed as previously described [34]. Briefly PCRs were performed using 5 ng gDNA and GoTaq Green Mastermix (Promega). Primer sequences were as follows: forward: GTC AGG AGA TCG AGA CCA TCC C; reverse: TCC TGC CTC AGC CTC CCA AG. Cycling conditions were 10 min at  $95^\circ\text{C}$  followed by 35 cycles of  $95^\circ\text{C}$  for 15 s,  $60^\circ\text{C}$  for 30 s and  $72^\circ\text{C}$  for 30 s, and a final extension at  $72^\circ\text{C}$  for 5 min. Human placental gDNA was used as a positive control.

#### Lung histopathology

Once the largest lobe from each mouse had been processed and paraffin-embedded, each tissue block was serially-sectioned (3  $\mu$ m thickness) and placed on charged Mikro Glass slides (Gale Scientific) and subjected to various histological stains or immunohistochemistry (IHC). To assess inflammation score (as a measure of AI), epithelial thickness and sub-epithelial extracellular matrix (ECM) deposition (as measures of AWR), one slide from each mouse (total of 42) underwent Masson's trichrome staining. To assess goblet cell metaplasia (as another measure of AWR), a second set of slides underwent Alcian blue periodic acid Schiff (ABPAS) staining. The Masson trichrome and ABPAS-stained sections were morphometrically analysed, as detailed below.

#### Immunohistochemistry and Immunofluorescence

IHC was used to detect transforming growth factor- $\beta$ 1 (TGF- $\beta$ 1; using a polyclonal antibody; sc-146; Santa Cruz Biotechnology; 1:1000 dilution),  $\alpha$ -smooth muscle actin ( $\alpha$ -SMA; a marker of myofibroblast differentiation; using a monoclonal antibody; M0851; DAKO Antibodies, Glostrup, Denmark; 1:200 dilution) and thymic stromal lymphopoietin (TSLP; a marker for epithelial damage; using a polyclonal antibody; ABT330; EMD Millipore Corp.; 1:1000 dilution) – as additional measures of AWR. Primary antibody staining was detected using the DAKO EnVision anti-rabbit or anti-mouse kits and 3,3'-diaminobenzidine (DAB) chromogen, whereas negative controls, which were exposed to the EnVision kits in the absence of any primary antibody, were also included. All slides were then counter-stained with haematoxylin.

IF (immunofluorescence) was performed on AECs and human renal fibroblasts (hRFs; used as a positive control; kindly provided by Prof. Carol Pollock, Kolling Institute of Medical Research, University of Sydney, NSW, Australia) cultured on chamber slides to detect RXFP1 (using a polyclonal antibody to RXFP1; HPA027067; Sigma–Aldrich; 1:200 dilution). Primary antibody was detected using a goat anti-rabbit Alexa Fluor<sup>®</sup> 555 secondary antibody (Invitrogen). Nuclei was visualized with DAPI, whereas an isotype (negative) control was also included.

All IHC-stained slides were scanned by Monash Histology Services using ScanScope AT Turbo for morphometric analysis; whereas IF-stained slides were imaged using a HyD confocal microscope (Leica SP8 Confocal Invert, Monash Micro Imaging).

#### Morphometric analysis

Masson's trichrome-, ABPAS- and IHC-stained slides underwent morphometric analysis as follows. Five airways (of 150–300  $\mu$ m

in diameter) per slide were randomly selected and analysed using Aperio ImageScope software. Masson's trichrome-stained slides underwent semi-quantitative peri-bronchiolar inflammation scoring, where the experimenter was blinded and scored individual airways from 0 (no detectable inflammation surrounding the airway) to 4 (widespread and massive inflammatory cell aggregates, pooled size  $\sim 0.6 \text{ mm}^2$ ), as previously described [26]. Masson's trichrome-stained slides also underwent analysis for epithelial thickness and subepithelial ECM deposition by measuring the thickness of the epithelium and the subepithelial ECM layer (stained blue); which were expressed as  $\mu\text{m}^2/\mu\text{m}$  of basement membrane (BM) length.

ABPAS-,  $\alpha$ -SMA- and TSLP-stained slides were analysed for goblet cell metaplasia, myofibroblast number and damaged epithelial cells, respectively, by counting the number of positively stained goblet cells,  $\alpha$ -SMA-positive cells and TSLP-positive cells per  $100 \mu\text{m}$  of BM length. TGF- $\beta$ 1-stained slides were analysed for TGF- $\beta$ 1 protein expression by running an algorithm to assess strong positively-stained pixels within the airway epithelium. Results were expressed as the number of strong positive pixels per total area ( $\text{mm}^2$ ) of epithelium; and then relative to that of the saline-treated control group, which was expressed as 1.

#### Hydroxyproline assay

The second largest lung lobe from each mouse was processed as described before [23,24,26] for the measurement of hydroxyproline content, which was determined from a standard curve of purified *trans*-4-hydroxy-L-proline (Sigma-Aldrich). Hydroxyproline values were multiplied by a factor of 6.94 (based on hydroxyproline representing  $\sim 14.4\%$  of the amino acid composition of collagen in most mammalian tissues [35]) to extrapolate total collagen content, which in turn was divided by the dry weight of each corresponding tissue to yield percent collagen concentration (as a measure of AWR-induced fibrosis).

#### Effects of RLX on AEC proliferation

As RLX had previously been found to promote the proliferation and migration of MSCs *in vitro* [25], we also determined if RLX could directly promote the proliferation of AECs. AECs were seeded at  $2 \times 10^4$  cells per well in 48-well plates containing Dulbecco's Modified Eagle Medium and Hams F12 (DMEM/F12) medium, then were either left untreated or were treated with 1 ng/ml RLX (a concentration typically observed in human pregnancy; and which was found to stimulate MSC proliferation *in vitro* [25]) or 40 ng/ml RLX (the concentration of RLX found in the BAL fluid of mice after 14 days of daily i.n. administration [24]) for 48 h. Cell proliferation was then determined using the CellTiter 96 AQueous One Solution Proliferation Assay (Promega) according to manufacturer's instructions. Absorbance was read at 490 nm using a Molecular Devices Versamax microplate spectrophotometer. Results were expressed as a percentage of proliferation relative to the control (untreated AECs; which was expressed as 100%); from  $n = 3$  separate experiments conducted in triplicate.

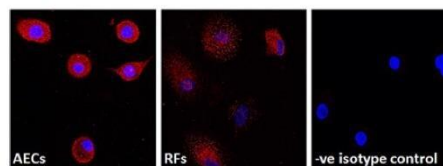


**Figure 1 Expression of RXFP1 on AECs**

AECs and hRFs (positive control) were stained for RXFP1 by IF and nuclear counterstained with DAPI. Both AECs and hRFs had diffuse cytoplasmic staining for RXFP1. Staining was absent from negative control cells where primary antibody was substituted with an isotype control.

#### Statistical analysis

All statistical analysis was performed using GraphPad Prism v6.0 (GraphPad Software) and expressed as the mean  $\pm$  S.E.M. AHR results were analysed by a two-way ANOVA with Bonferroni post-hoc test; the cell proliferation data analysed by an unpaired Student's *t* test; whereas the remaining data were analysed by a one-way ANOVA with Neuman-Keuls post-hoc test for multiple comparisons between groups. In each case, data were considered significant with a *P*-value less than 0.05.

## RESULTS

#### Expression of RXFP1 on AECs

AECs and hRFs (positive control) stained positively for RXFP1 by immunofluorescence (IF) and nuclear counterstaining with DAPI (Figure 1). Both AECs and hRFs had diffuse cytoplasmic staining for RXFP1, similar to the cytoplasmic localization of RXFP1 in other cells [36]. Staining was absent from negative control cells where primary antibody was substituted with an isotype control.

#### PCR analysis of human Alu from lung tissue

PCR analysis of lung tissue gDNA isolated from AEC-treated OVA-injured mice failed to detect the presence of human Alu (as a surrogate marker of the presence of AECs) 2 weeks after the initial AEC administration; whereas a positive signal was only detected from human placental gDNA (results not shown).

#### Effects of RLX, MSCs, AECs and combination treatments on AI

Peri-bronchial inflammation score from Masson's trichrome-stained images (Figures 2A and 2B) and eosinophil infiltration from the BAL fluid (Figure 2C) were used as measures of AI. The peri-bronchial inflammation score of OVA-treated mice ( $1.70 \pm 0.60$ ) was significantly increased compared with that of saline controls ( $0.15 \pm 0.40$ ;  $P < 0.001$  compared with Saline group; Figure 2B). This confirmed that the chronic model of AAD had been established in OVA-treated mice. RLX-treatment of animals did not significantly affect the OVA-induced increase in inflammation score ( $1.55 \pm 0.83$ ;  $P < 0.001$  compared with Saline group), whereas MSCs alone ( $1.30 \pm 0.20$ ;  $P < 0.05$  com-

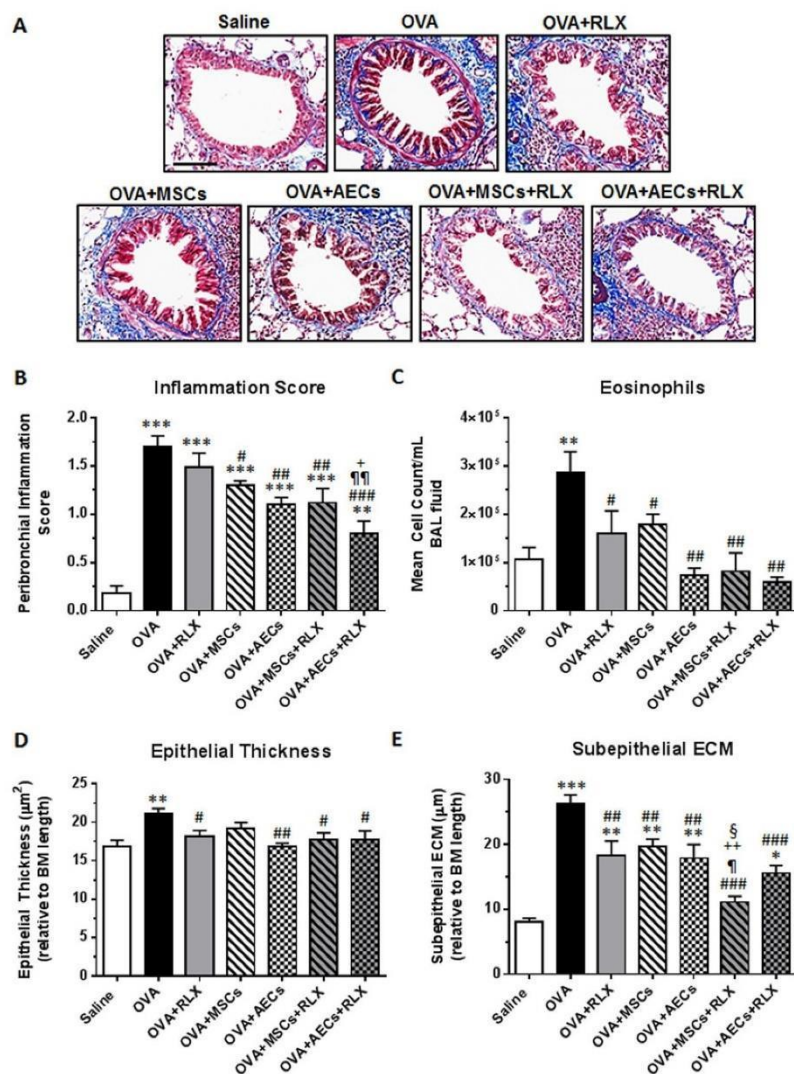


**Figure 2** Effects of RLX, MSCs, AECs and combination treatments on AI, epithelial thickness and subepithelial ECM (A) Representative images of Masson's trichrome-stained lung sections from each group studied demonstrating the extent of inflammatory cell infiltration within the bronchial wall. Scale bar = 100  $\mu$ m. Also shown is the median  $\pm$  interquartile range of peribronchial inflammation scores from 5 airways/mouse [where sections were scored based on the number and distribution of inflammatory cell aggregates on a scale of 0 (no visible inflammation) to 4 (severe inflammation)] (B;  $n = 6$ /group); the mean  $\pm$  S.E.M. eosinophil count per millilitre of BAL fluid (C;  $n = 6$  group); the mean  $\pm$  S.E.M. epithelial thickness ( $\mu$ m<sup>2</sup>) relative to BM length (D;  $n = 6$  group); and the mean  $\pm$  S.E.M. subepithelial ECM thickness ( $\mu$ m) relative to BM length (E;  $n = 6$ /group). \* $P < 0.05$ , \*\* $P < 0.01$ , \*\*\* $P < 0.001$  compared with Saline group; # $P < 0.05$ , ## $P < 0.01$ , ### $P < 0.001$  compared with OVA group; † $P < 0.05$ , †† $P < 0.01$  compared with OVA + RLX group; ‡ $P < 0.05$ , ‡‡ $P < 0.01$  compared with OVA + MSC group; § $P < 0.05$  compared with OVA + AEC group.

pared with OVA group;  $P < 0.001$  compared with Saline group) only modestly but significantly reduced peri-bronchial inflammation (Figure 2B). In comparison, AECs alone ( $1.05 \pm 0.28$ ), MSCs + RLX ( $1.00 \pm 0.40$ ) and AECs + RLX ( $0.90 \pm 0.70$ ) were able to significantly reduce OVA-induced inflammation score by ~40–50%; with the greatest effect observed with AECs + RLX ( $P < 0.001$  compared with OVA group;  $P < 0.01$  compared with OVA + RLX group;  $P < 0.05$  compared with OVA + MSC group). However, neither AECs alone or the combination treatments were able to reduce peri-bronchial inflammation to that seen in saline-treated controls (all  $P < 0.01$  compared with Saline group; Figure 2B).

OVA-treated mice also had significantly increased numbers of eosinophils ( $2.85 \pm 0.45 \text{ ml}^{-1}$  of BAL fluid) compared with that from saline-treated controls ( $1.06 \pm 0.25 \times 10^5 \text{ ml}^{-1}$  of BAL fluid;  $P < 0.01$  compared with Saline group; Figure 2C). RLX ( $1.60 \pm 0.47 \times 10^5 \text{ ml}^{-1}$  of BAL fluid) or MSCs alone ( $1.79 \pm 0.21 \times 10^5 \text{ ml}^{-1}$  of BAL fluid) partially, but significantly, decreased eosinophil infiltration to a similar degree (both  $P < 0.05$  compared with OVA alone), but to a level which did not differ from that measured in saline-treated controls (Figure 2C). In comparison, AECs alone ( $7.37 \pm 1.46 \times 10^4 \text{ ml}^{-1}$  of BAL fluid), and the combined effects of MSCs + RLX ( $8.19 \pm 3.79 \times 10^4 \text{ ml}^{-1}$  of BAL fluid) or AECs + RLX ( $5.92 \pm 1.05 \times 10^4 \text{ ml}^{-1}$  of BAL fluid) completely abrogated eosinophil infiltration (all  $P < 0.01$  compared with OVA group; no different to Saline group), again to a level which was no longer different to that measured in saline-treated controls (Figure 2C).

#### Effects of RLX, MSCs, AECs and combination treatments on epithelial thickness and damage

The epithelial thickness of OVA-treated mice ( $21.20 \pm 0.60 \mu\text{m}^2$ ) was significantly increased compared with that of saline-treated controls ( $16.89 \pm 0.76 \mu\text{m}^2$ ;  $P < 0.01$  compared with Saline group; Figure 2D). Treatment with MSCs alone ( $19.23 \pm 0.73 \mu\text{m}^2$ ) only induced a trend towards reducing the OVA-induced increase in epithelial thickness, although this value was not statistically different to that measured from saline-treated control mice. In comparison, RLX alone ( $18.19 \pm 0.74 \mu\text{m}^2$ ), AECs alone ( $16.90 \pm 0.39 \mu\text{m}^2$ ), MSCs + RLX ( $17.75 \pm 0.87 \mu\text{m}^2$ ) and AECs + RLX ( $18.21 \pm 2.19 \mu\text{m}^2$ ) all normalized the OVA-induced increase in epithelial thickness back to that seen in saline-treated control mice (all  $P < 0.05$  compared with OVA alone group; no different to Saline group; Figure 2D).

TSLP was used as a marker of epithelial damage and the number of TSLP-positive cells within the airway epithelium was significantly higher in OVA-treated mice ( $4.61 \pm 0.53$ ) compared with that in their saline-treated counterparts ( $1.00 \pm 0.30$ ;  $P < 0.001$  compared with Saline group). MSCs alone ( $4.50 \pm 0.42$ ) were unable to reduce the OVA-induced increase in TSLP expression. However, RLX alone ( $3.14 \pm 0.34$ ), AECs alone ( $3.50 \pm 0.19$ ) and the combined effects of MSCs + RLX ( $3.53 \pm 0.28$ ) or AECs + RLX ( $3.30 \pm 0.27$ ) all significantly reduced TSLP expression levels compared with that in the OVA alone group (all  $P < 0.05$  compared with OVA alone group); but not to levels measured

in saline-treated control mice (all  $P < 0.01$  compared with Saline Group) (Figure 3). Of note, RLX alone also reduced TSLP expression levels compared with the effects of MSCs alone ( $P < 0.05$  compared with OVA + MSC group; Figure 3).

#### Effects of RLX, MSCs, AECs and combination treatments on goblet cell metaplasia

Goblet cell metaplasia was analysed from ABPAS-stained lung sections and was significantly increased in OVA-treated mice ( $4.83 \pm 0.20$ ) compared with that measured from saline-treated counterparts ( $1.62 \pm 0.32$ ;  $P < 0.001$  compared with Saline group; Figure 4). Neither RLX alone ( $5.08 \pm 0.25$ ), MSCs alone ( $5.23 \pm 0.47$ ), AECs alone ( $5.00 \pm 0.16$ ) or MSCs + RLX ( $5.06 \pm 0.41$ ) affected the OVA-induced increase in goblet cell numbers (all  $P < 0.001$  compared with Saline group). In comparison, only the combined effects of AECs + RLX ( $4.39 \pm 0.28$ ) significantly reduced the OVA-induced increase in goblet cell numbers ( $P < 0.05$  compared with OVA alone; OVA + RLX; OVA + MSCs, OVA + AECs; and OVA + MSCs + RLX groups; Figure 4); but not fully back to levels measured from saline-treated controls ( $P < 0.01$  compared with Saline group).

#### Effects of RLX, MSCs, AECs and combination treatments on airway fibrosis

Airway fibrosis was measured by analysing subepithelial ECM deposition from Masson's trichrome-stained lung sections (Figure 2E) and hydroxyproline analysis of total lung collagen concentration (Figure 5). Subepithelial ECM deposition (relative to BM length) was significantly increased in OVA-treated mice ( $26.26 \pm 1.37 \mu\text{m}$ ) compared with that measured from saline-treated controls ( $8.07 \pm 0.58 \mu\text{m}$ ;  $P < 0.001$  compared with Saline group; Figure 2E). RLX alone ( $18.27 \pm 2.26 \mu\text{m}$ ), MSCs alone ( $19.67 \pm 1.17 \mu\text{m}$ ) or AECs alone ( $17.87 \pm 2.150 \mu\text{m}$ ) significantly reduced the OVA-induced aberrant increase in subepithelial ECM deposition to a similar extent (by ~35–45%; all  $P < 0.01$  compared with OVA alone group; Figure 2E). Mice treated with AECs + RLX had a further reduction in subepithelial ECM deposition ( $13.72 \pm 1.25 \mu\text{m}$ ) compared with that measured in OVA-injured mice (by ~70%;  $P < 0.001$  compared with OVA group;  $P < 0.05$  compared with Saline group), whereas the OVA-induced increase in subepithelial ECM deposition was normalized ( $11.12 \pm 0.93 \mu\text{m}$ ) by the combined effects of MSCs + RLX ( $P < 0.001$  compared with OVA group; no different to Saline group); and to a greater extent than either therapy alone ( $P < 0.05$  compared with RLX alone or AECs alone;  $P < 0.01$  compared with MSCs alone; Figure 2E).

Similar findings were observed with measurements of total lung collagen concentration, which was significantly increased in OVA-treated mice ( $3.82 \pm 0.10\%$ ) compared with corresponding measurements obtained from saline-treated controls ( $2.84 \pm 0.11\%$ ;  $P < 0.001$  compared with saline group); and significantly reduced by RLX alone ( $3.08 \pm 0.23\%$ ;  $P < 0.01$  compared with OVA alone group) or AECs alone ( $3.26 \pm 0.14\%$ ;  $P < 0.05$  compared with OVA alone group), but not MSCs alone ( $3.52 \pm 0.12\%$ ) (Figure 5). Strikingly, the combined effects of MSCs + RLX ( $2.75 \pm 0.11\%$ ;  $P < 0.001$  compared with OVA

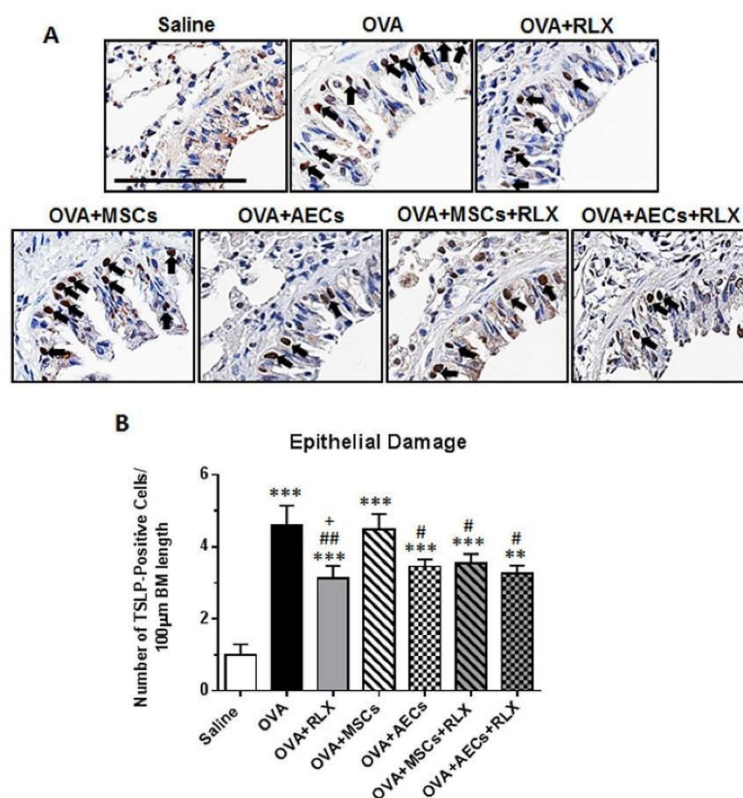


**Figure 3** Effects of RLX, MSCs, AECs and combination treatments on epithelial damage

(A) Representative images of TSLP-stained lung sections from each group studied demonstrating the extent of epithelial damage. Scale bar = 100  $\mu\text{m}$ . Also shown is the mean  $\pm$  S.E.M. number of TSLP-positive cells (indicated by arrows) within the epithelium/100  $\mu\text{m}$  of BM length from 5 airways/mouse is also shown (B;  $n = 6/\text{group}$ ). \*\* $P < 0.01$ , \*\*\* $P < 0.001$  compared with Saline group; # $P < 0.05$ , ## $P < 0.01$  compared with OVA group; + $P < 0.05$  compared with OVA + MSC group.

alone group) or AECs + RLX ( $2.90 \pm 0.04\%$ ;  $P < 0.01$  compared with OVA alone group) completely reversed the OVA-induced increase in lung collagen concentration, back to levels measured in saline-treated control animals (Figure 5). The combined effects of MSCs + RLX or AECs + RLX also reduced total lung collagen concentration to a greater extent than MSCs alone (both  $P < 0.01$  compared with OVA + MSC group; Figure 5).

#### Effects of RLX, MSCs, AECs and combination treatments on airway epithelial TGF- $\beta$ 1 expression

To elucidate the possible mechanisms by which the combined effects of RLX and MSCs or AECs were able to normalize the OVA-induced subepithelial and total lung collagen deposition, changes in airway epithelial TGF- $\beta$ 1 staining were assessed (Fig-

ures 6A and 6B). Epithelial TGF- $\beta$ 1 expression was significantly increased in OVA-treated mice ( $10.65 \pm 0.81$ ), compared with that in saline-treated controls ( $1.00 \pm 0.47$ ;  $P < 0.01$  compared with Saline group; Figure 6B). RLX alone ( $5.85 \pm 1.42$ ), but not MSCs alone ( $8.15 \pm 1.78$ ) was able to partially, but significantly, reduce the OVA-induced increase in aberrant epithelial TGF- $\beta$ 1 expression levels, as demonstrated previously in a separate study [26]. On the other hand, AECs alone ( $3.04 \pm 0.44$ ) and the combined effects of MSCs + RLX ( $1.47 \pm 0.45$ ) or AECs + RLX ( $2.63 \pm 0.060$ ) were able to markedly reduce airway epithelial TGF- $\beta$ 1 expression to that which was no longer different to the levels measured in saline-treated controls (all  $P < 0.001$  compared with OVA alone group; no difference to Saline group); and to a greater extent than the effects of MSCs alone (all  $P < 0.05$  compared with OVA + MSC group; Figure 6B).

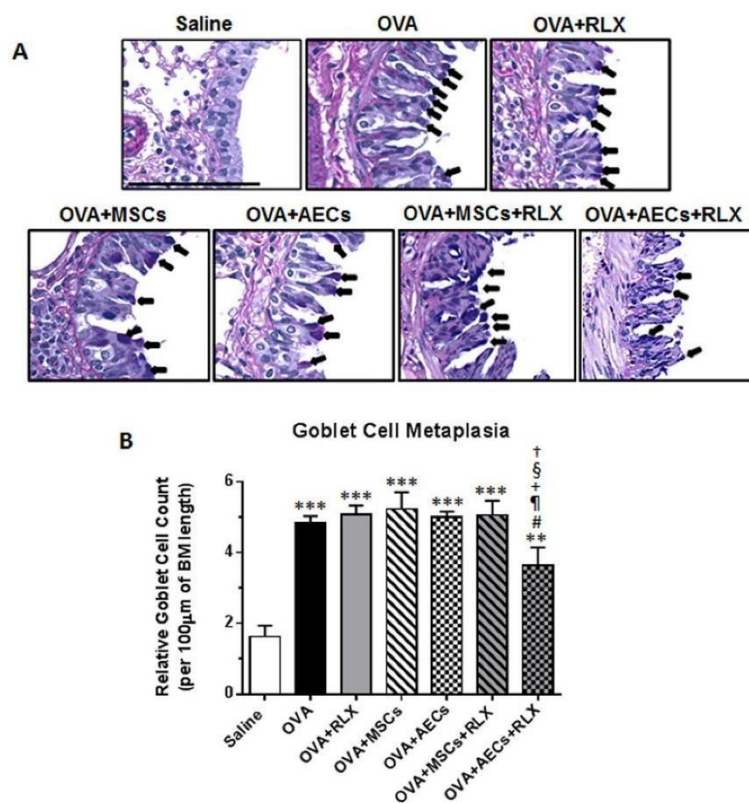


**Figure 4** Effects of RLX, MSCs, AECs and combination treatments on goblet cell metaplasia (A) Representative images of ABPAS-stained lung sections from each treatment group demonstrating the number of goblet cells (indicated by arrows) present within the airway epithelium. Scale bar = 100  $\mu$ m. Also shown is the mean  $\pm$  S.E.M. goblet cell count (represented as the number of goblet cells/100  $\mu$ m BM length) from 5 airways/mouse (B;  $n = 6$ /group). \*\*\* $P < 0.01$ , \*\*\*\* $P < 0.001$  compared with Saline group; \* $P < 0.05$  compared with OVA group; † $P < 0.05$  compared with OVA + RLX group; ‡ $P < 0.05$  compared with OVA + MSC group; § $P < 0.05$  compared with OVA + AEC group; ¶ $P < 0.05$  compared with OVA + MSC + RLX group.

#### Effects of RLX, MSCs, AECs and combination treatments on subepithelial myofibroblast accumulation

OVA-treatment of mice also resulted in a significantly increased number of  $\alpha$ -SMA-stained myofibroblasts per 100  $\mu$ m BM length, in the subepithelial layer of the airways ( $1.72 \pm 0.07$ ) compared with that measured from their saline-treated counterparts ( $0.44 \pm 0.13$ ;  $P < 0.001$  compared with Saline group; Figures 6C and 6D). All individual treatments including RLX alone ( $1.08 \pm 0.10$ ), MSCs alone ( $1.06 \pm 0.10$ ) or AECs alone ( $1.13 \pm 0.19$ ) significantly reduced the OVA-induced increase in subepithelial myofibroblast numbers to a similar extent (by ~45–50%; all  $P < 0.01$  compared with OVA alone group; all  $P < 0.05$

compared with Saline group); whereas the combined effects of MSCs + RLX ( $0.88 \pm 0.12$ ) or AECs + RLX ( $0.63 \pm 0.12$ ) further reduced the number of subepithelial myofibroblasts to numbers that were no longer different to that measured in saline-treated control animals (both  $P < 0.001$  compared with OVA alone group; no different to Saline group; Figure 6D).

#### Effects of RLX, MSCs, AECs and combination treatments on AHR

AHR was assessed via invasive plethysmography and was significantly increased in OVA-treated mice compared with that measured in saline controls (Figure 7). AHR was partially, but significantly decreased by RLX alone (by ~50%;  $P < 0.001$  com-

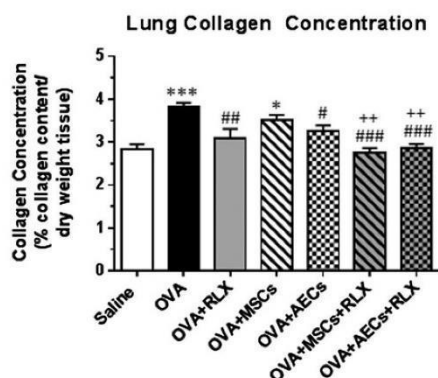


**Figure 5** Effects of RLX, MSCs, AECs and combination treatments on total lung collagen concentration

The total lung collagen content of each mouse was calculated via hydroxyproline analysis and then divided by the dry weight of the corresponding lung section analysed to yield % collagen concentration. Shown is the mean  $\pm$  S.E.M. % lung collagen concentration from each of the groups studied ( $n = 6$ /group). \* $P < 0.05$ , \*\*\* $P < 0.001$  compared with Saline group; # $P < 0.05$ , ## $P < 0.01$ , ### $P < 0.001$  compared with OVA group; ++ $P < 0.01$  compared with OVA + MSC group.

pared with OVA group;  $P < 0.01$  compared with Saline group) or AECs alone (by ~35–40%;  $P < 0.05$  compared with OVA group;  $P < 0.001$  compared with Saline group), but not MSCs alone ( $P < 0.001$  compared with Saline group); correlating with how effective these treatments were in reversing airway/lung fibrosis. In comparison, the combined effects of MSCs + RLX or AECs + RLX further reduced AHR to levels that were no longer significantly different to that measured from saline-treated control mice (both  $P < 0.001$  compared with OVA alone group; no different to Saline group; Figure 7). The combined effects of MSCs + RLX or AECs + RLX also reduced AHR to a significantly greater extent than MSCs alone (both  $P < 0.01$  compared with OVA + MSC group; Figure 7).

#### Effects of RLX on AEC proliferation *In vitro*

As RLX had previously been demonstrated to stimulate MSC proliferation to enhance the therapeutic effects of MSCs [25], we similarly determined if RLX could promote AEC proliferation *in vitro* as part of its ability to augment the effects of RXFP1-expressing AECs. RLX, at the same concentration used to stimulate MSC proliferation (1 ng/ml; [25]) or at an equivalent concentration to that found in the BAL fluid of mice daily i.n.-administered with RLX for 14 days (40 ng/ml; [24]) significantly increased AEC proliferation by ~24 and ~14%, respectively, after 48 h (both  $P < 0.05$  compared with untreated AEC proliferation alone; Figure 8).

## DISCUSSION

The aim of the present study was to compare the therapeutic effects of i.n.-administered AECs to that of MSCs, in the ab-

sence and presence of an anti-fibrotic agent (RLX), in the setting of chronic OVA-induced AAD. The main findings of the study were that: (1) AECs expressed RXFP1 and their proliferation could be directly promoted by RLX (at 1 or 40 ng/ml). (2) AECs alone demonstrated greater protection against the chronic AAD-induced increase in AI (as assessed by changes in peribronchial inflammation score and eosinophil counts), AWR (as assessed by changes in epithelial damage/thickness, total lung collagen concentration and epithelial TGF- $\beta$ 1 expression) and AHR, compared with the effects of the MSCs alone. However, AEC-treatment alone was not able to fully reverse the structural and functional changes associated with the model. (3) The presence of RLX was able to enhance the protection offered by MSCs or AECs, such that eosinophil counts, epithelial thickness, ECM/collagen deposition, epithelial TGF- $\beta$ 1 expression levels, subepithelial myofibroblast accumulation and AHR were all normalized in both combination treatment groups, returning to that measured in saline-treated control mice (Table 1). The superior anti-fibrotic effects of the combination treatments appeared to be explained by their greater ability to reverse aberrant TGF- $\beta$ 1 expression and myofibroblast differentiation, compared with the effects of the individual treatments. Hence, combining RLX with either MSCs or AECs appeared to effectively reverse several aspects of AWR (including airway/lung fibrosis), and the AWR-induced changes in AHR in the setting of chronic AAD.

Although we did not directly track the tissue site(s) of i.n.-administered stem cells, our previous studies [26] and that of others [37] demonstrating that MSCs [26] and other fluorescently-labelled factors [37] were detected in the lungs of inflamed mice following i.n.-delivery, suggested that these cells were likely homing to the inflamed lung post-chronic AAD. However, similar to previous findings showing that MSCs were found to have disappeared from murine models of kidney disease 7 days after administration regardless of the route of administration [25,38], our inability to detect AECs in the lungs of treated mice with chronic AAD after the 2-week treatment period suggested that these cells were also likely cleared from the lungs, but were able to induce long-term paracrine effects that persisted long after they had been cleared.

Although all treatments evaluated were able to markedly reduce or normalize eosinophil infiltration, RLX and MSCs alone were less effective in reversing peribronchial inflammation in general. In comparison, AECs alone demonstrated the most effective anti-inflammatory effects and also markedly reduced eosinophil counts to a level which was no longer different to that measured in saline-treated controls. Interestingly, the combined effects of AECs and RLX further reduced peribronchial inflammation score to a greater extent than RLX or MSCs alone. These differences in the anti-inflammatory effects of the various treatments evaluated may have been attributed to the individual treatments only being able to target smaller subsets of inflammatory cells whereas the combination treatments may have likely affected a wider range of inflammatory cells. In the chronic AAD model, intratracheal transplantation of MSCs was shown to decrease infiltration of eosinophils (consistent with the findings of the present study), neutrophils and monocytes within the BAL

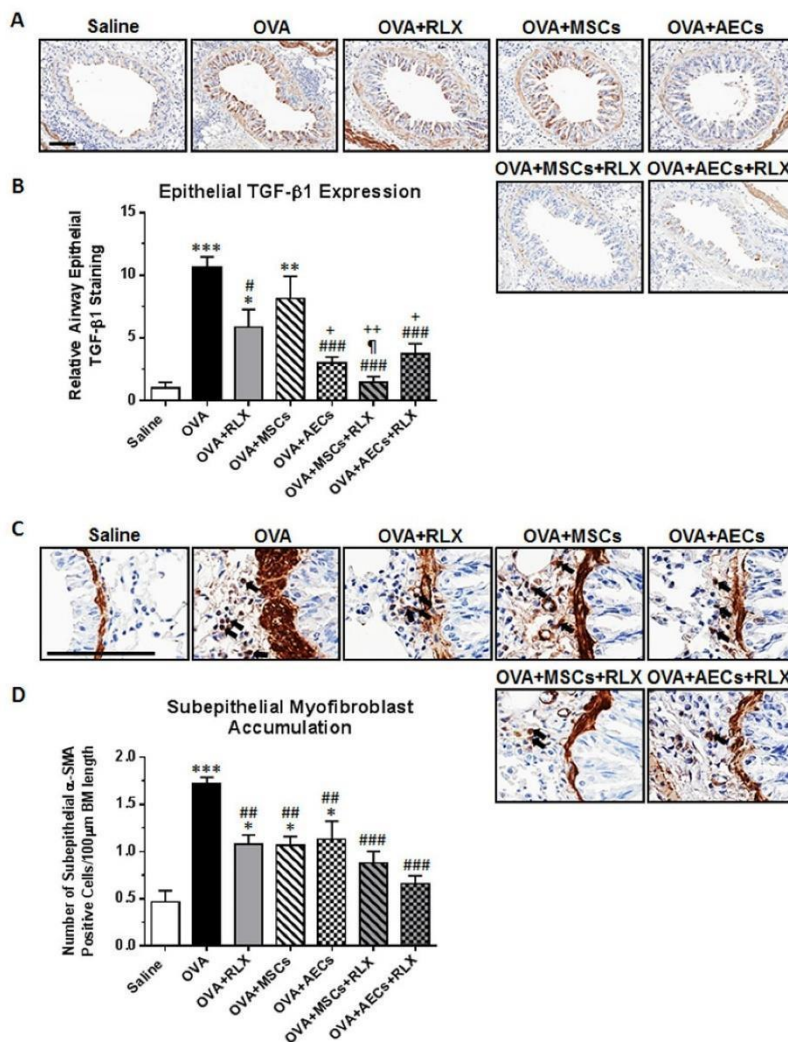


**Figure 6** Effects of RLX, MSCs, AECs and combination treatments on airway epithelial TGF-β1 expression and subepithelial myofibroblast accumulation

Representative images of IHC-stained lung sections from each treatment group demonstrating the level of epithelial TGF-β1 expression and distribution within the airway epithelium (A) and subepithelial myofibroblast accumulation (C). Scale bar = 100 μm (A and C). Also shown are the mean ± S.E.M. epithelial TGF-β1 staining (relative to that in the saline control group; which was expressed as 1) from 5 airways/mouse (B; n = 5-6/group); and mean ± S.E.M. subepithelial myofibroblast number per 100 μm BM length (D; n = 5-6/group) \*P < 0.05, \*\*P < 0.01, \*\*\*P < 0.001 compared with saline group; #P < 0.05, ##P < 0.01, ###P < 0.001 compared with OVA group; †P < 0.05 compared with OVA + RLX group; ‡P < 0.05, ††P < 0.01 compared with OVA + MSC group.

**Table 1 Summary of the individual compared with combined effects of RLX, MSCs and AECs in the chronic AAD model**

A summary of the individual compared with combined effects of RLX, MSCs or AECs on chronic AAD-induced AI, AWR, fibrosis and AHR. The arrows in the OVA column are reflective of changes to that measured in saline-treated mice, whereas the arrows in the various treatment groups are reflective of changes relative to that in the OVA alone group. '–' denotes no changes compared with the effects of OVA alone.

	Key features of human asthma	OVA	OVA + RLX	OVA + MSCs	OVA + AECs	OVA + RLX + MSCs	OVA + RLX + AECs
AI	Inflammatory score	↑↑↑	–	↓	↓	↓	↓↓
	Eosinophil count	↑↑	↓	↓	↓↓	↓	↓↓
AWR	Goblet cell count	↑↑↑	–	–	–	–	↓
	Epithelial damage	↑↑↑	↓	–	↓	↓	↓
	Epithelial thickness	↑↑	↓	–	↓↓	↓	↓
Fibrosis	Subepithelial ECM	↑↑↑	↓↓	↓↓	↓↓	↓↓↓	↓↓
	Total collagen	↑↑↑	↓↓	–	↓	↓↓↓	↓↓↓
	Epithelial TGF-β1	↑↑↑	↓	–	↓↓↓	↓↓↓	↓↓↓
	α-SMA	↑↑↑	↓↓	↓↓	↓	↓↓↓	↓↓↓
AHR		↑↑↑	↓	–	↓	↓↓↓	↓↓↓

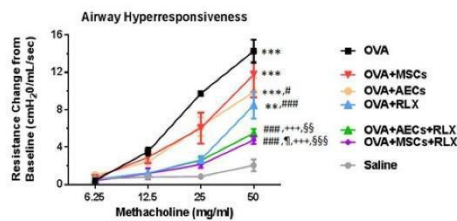


**Figure 7 Effects of RLX, MSCs, AECs and combination treatments on AHR**

AHR was assessed by measuring airway resistance (via invasive plethysmography) in response to increasing doses of the bronchoconstrictor methacholine, delivered by nebulization. Responses are expressed as the resistance change from the baseline response to saline. Shown is the mean ± S.E.M. of the airway resistance measured in response to each dose of methacholine, from each group studied (*n* = 6/group). \*\**P* < 0.01, \*\*\**P* < 0.001 compared with Saline group; #*P* < 0.01, ###*P* < 0.001 compared with OVA alone group; †*P* < 0.05 compared with OVA + RLX group; †††*P* < 0.001 compared with OVA + MSC group; ‡*P* < 0.01, ‡‡‡*P* < 0.001 compared with OVA + AEC group.

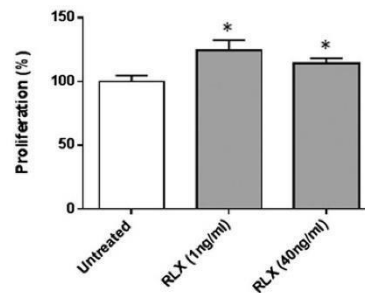


**Figure 8 Effects of RLX on AEC proliferation**

The effects of RLX (1 or 40 ng/ml) on AEC proliferation were measured after 48 h, using the CellTiter 96 Aqueous One Solution Proliferation Assay. Shown is the mean ± S.E.M. relative percentage proliferation from three independent experiments conducted in triplicate, and expressed as a ratio to that of untreated AEC proliferation alone (which was expressed as 100%). \**P* < 0.05 compared with untreated group.

fluid [8]. Although the effects of AECs have not been investigated before in the setting of chronic AAD, they have been shown to reduce the infiltration of macrophages and neutrophils in a bleomycin-induced murine model of interstitial lung disease, when administered i.p. [29]. Furthermore, AECs were shown to normalize the bleomycin-induced increase in total leucocyte infiltration when administered 2 weeks after bleomycin challenge [30]. These findings may suggest that AECs alone are able to target a broader subset of inflammatory cells and more effectively abrogate eosinophil infiltration in the setting of chronic AAD. Although RLX alone has not been effective in reducing the infiltration of monocytes [23,24] and lymphocytes [23,24] in the chronic mouse model of AAD, and macrophages in other models [16], this peptide has been demonstrated to reduce mast cell [39,40], neutrophil [41] and basophil [42] re-

cruitment. Therefore, the combined effects of RLX and MSCs, and in particular with AECs, appeared to have broader anti-inflammatory effects compared with the effects of each treatment alone.

The infiltration of these various inflammatory cells, as well as Th2 CD4<sup>+</sup> cells, is also associated with various structural changes that encompass AWR. During asthma, repeated cycles of injury and repair lead to aberrant structural changes in the airways which contribute to an irreversible loss of lung function [43]. In the current study, AWR was assessed via epithelial thickening, goblet cell metaplasia, airway ECM/collagen deposition (fibrosis) as well as epithelial TGF-β1 expression and subepithelial myofibroblast accumulation.

Epithelial thickening contributes to narrowing of the airways and hence, increased airway resistance, resulting in an increase

in asthma-induced breathing difficulties [44]. Epithelial thickening was exacerbated in the OVA-treated mice and was not significantly affected by MSC alone-treatment. This is consistent with previous results demonstrating an inability of intranasally [26] or intravenously (i.v.) [45]-delivered MSCs to inhibit epithelial thickening in the chronic AAD model. In contrast, RLX alone was able to reduce epithelial thickness, which is consistent with previous findings using chronic AAD-injured mice treated with RLX systemically [23] or intranasally [24]. Likewise, AECs alone and in combination with RLX or MSCs + RLX were found to normalize the OVA-induced increase in epithelial thickness; the latter being consistent with a recently published study [26]. These findings may suggest that treatments which can normalize aberrant epithelial thickening and the related fibrosis that ensues from epithelial damage to the airways/lung are more likely to protect from AAD-induced AWR and the contributions of AWR to AHR. Indeed another recent study demonstrated that the ability of RLX alone or in combination with an epithelial repair factor (trefoil factor-2; TFF2) or with TFF2 and the corticosteroid, dexamethasone, was able to completely reverse the OVA-induced loss of dynamic lung compliance, due to the ability of these treatments to significantly reduce both epithelial thickness and lung collagen concentration (the basis of fibrosis) [46].

Related to epithelial thickening, the present study evaluated a marker of lung damage (TSLP), which is markedly produced and secreted by airway epithelial cells (along with IL-25 and IL-33) in response to various stimuli of asthma-like symptoms [47]. Interestingly, all treatments that could significantly reverse epithelial thickening were found to also partially reduce the OVA-induced increase in airway epithelial TSLP expression. These findings imply that administration of RLX or AECs alone and the two sets of combination treatments evaluated were able to partially induce epithelial tissue repair. Consistent with the findings of the present study, RLX alone and in combination with MSCs was also found to significantly suppress epithelial injury molecule (KIM-1) expression in a ureteric obstruction-induced model of kidney disease/fibrosis [25]. This may have been due to the anti-apoptotic and/or angiogenic effects of these therapies [16,48].

Deposition of excessive ECM components, particularly collagens, occurs within the subepithelial and adventitia of airways in asthmatic individuals and contributes to the development of fibrosis [49]. In the current study, fibrosis was evaluated by examining subepithelial ECM and total collagen content, as well as two markers of collagen turnover, namely TGF- $\beta$ 1 and  $\alpha$ -SMA (a marker of myofibroblast differentiation). MSCs alone were able to partially reduce subepithelial ECM levels but only demonstrated a trend towards reducing total lung collagen concentration levels, which is somewhat inconsistent with previous studies [11,24] and suggestive that the effects of these cells may be patient- and/or batch-to-batch-dependent. In comparison, either RLX or AECs alone were able to significantly although not totally reverse the OVA-induced increase in both subepithelial ECM and total lung collagen. This is consistent with previous studies which have shown that RLX alone can reduce airway/lung fibrosis associated with chronic AAD [23,24,26];

and those showing that AECs alone [13,29] can reduce interstitial lung fibrosis following bleomycin-induced injury. More impressively, both combination treatments were able to further reduce and in fact normalize the OVA-induced increase in airway/lung fibrosis. This is consistent with previous findings from our group using the combination of MSCs and RLX to reduce both the renal fibrosis induced by unilateral ureteral obstruction [25] as well as airway/lung fibrosis induced by chronic AAD [26].

In the current study, the limited anti-fibrotic efficacy demonstrated by MSCs in the setting of chronic AAD was found to be associated with their lack of ability to affect airway epithelial TGF- $\beta$ 1 expression levels, while modestly reducing subepithelial myofibroblast accumulation.

These results support previous findings demonstrating that although MSCs showed reparative effects in acute models of fibrosis, their effectiveness was reduced in models of chronic fibrosis [50–52]. In contrast, the anti-fibrotic efficacy demonstrated by RLX or AECs alone was consistent with their ability to significantly reduce both airway epithelial TGF- $\beta$ 1 expression levels and subepithelial myofibroblast accumulation; and with the general TGF- $\beta$ 1-inhibitory effects of both RLX [19,21,46] and AECs [13,53] in the airways/lung. Of further significance, the enhanced anti-fibrotic efficacy of both combination therapies resulted in their ability to both normalize the aberrant increase in chronic AAD-induced epithelial TGF- $\beta$ 1 expression levels, while markedly lowering subepithelial myofibroblast differentiation; likely leading to the marked reversal, if not normalization of the chronic AAD-induced increase in aberrant subepithelial and total lung collagen deposition measured. These findings suggest that RLX can be combined with multiple stem cells types that express RXFP1, to treat the AWR and related AHR associated with asthma; either by creating a more favourable environment in which these transplanted cells can survive and execute their therapeutic/reparative effects and/or by directly promoting their viability, proliferation and migration [25].

Both AI and AWR contribute to the development of AHR [54,55]. The extent of AHR also relates to the severity of asthma [56,57]. Previous studies have demonstrated that an increase in BM thickness due to deposition of ECM components (subepithelial fibrosis) correlates with a decrease in distensibility of the airways [58], concurrent with an increase in AHR [59]. In the current study, AHR was evaluated using invasive plethysmography to determine airway resistance. The OVA-induced increase in AHR was proportionally reduced in line with how effective each of the treatments investigated reversed airway/lung fibrosis; with either of the combination treatments being able to completely reverse AHR back to levels measured from saline-treated control mice, based on their ability to normalize airway epithelial thickness, epithelial TGF- $\beta$ 1 expression levels and total lung collagen concentration. These findings are consistent with a recently published study [46] which also demonstrated that other therapies that could abrogate the chronic AAD-induced aberrant increase in epithelial thickness and/or damage as well as collagen concentration, was key to normalizing methacholine-induced AHR. However, the extent to which these treatments reduced air-

way/lung fibrosis appeared to correlate more with how effectively they could reverse AHR.

In conclusion, the current study found that combining RLX with either MSCs or AECs was able to significantly reduce AI, and completely abrogate airway epithelial thickening, airway epithelial TGF- $\beta$ 1 expression levels, airway/lung fibrosis and AHR associated with chronic AAD. The enhanced effects of these combination therapies (over either therapy alone) on these parameters may be partly explained by the fact that RLX could directly stimulate MSC [25] or AEC proliferation, resulting in more viable cells that could mediate their therapeutic effects. Hence, these combination therapies may offer a novel means to treat the three central components of asthma pathogenesis (AI, AWR and related AHR), particularly to patients who are resistant to corticosteroid therapy. Although AECs alone were more effective in reducing epithelial damage and fibrosis as well as improving AHR compared with MSCs alone, both types of stem cells in combination with RLX were as effective as each other in further reducing AI and AWR as well as improving AHR associated with asthma.

## CLINICAL PERSPECTIVES

- Despite the availability of corticosteroids and  $\beta$ -agonists, asthma remains a major health problem with many patients continuing to experience symptoms and AHR, likely due to progressive AWR. Cell-based therapies including MSCs and AECs hold promise in this area due to their anti-inflammatory and tissue repair capabilities which may prevent and slow the remodelling process. The anti-fibrotic hormone RLX has also been shown to have potent anti-fibrotic and other organ-protective effects in mouse models of chronic AAD displaying airway pathology reminiscent of chronic asthma.
- In the present study we compared and combined the therapeutic efficacy of MSCs and AECs, in the absence or presence of RLX, in the setting of chronic AAD.
- RLX or AECs alone, but not MSCs alone, normalized epithelial thickness and partially reversed OVA-induced fibrosis and AHR; with the extent of AHR being decreased in line with how effectively each therapy reduced epithelial thickness, TGF- $\beta$ 1 expression levels and total lung collagen concentration. Furthermore, the combination treatments normalized epithelial thickness and TGF- $\beta$ 1 expression levels, total lung collagen concentration and AHR to that in normal mice, and significantly decreased AI. Thus, the anti-fibrotic effects of RLX appear to provide an improved environment in which cell-based therapies can be introduced into, and enhance the therapeutic and regenerative capacity of stem cells expressing RXFP1.

## AUTHOR CONTRIBUTION

Simon Royce, Sharon Ricardo and Chrishan Samuel conceptualized and designed the experiments; Simon Royce, Anna Tominaga, Matthew Shen, Krupesh Patel, Brooke Huuskes, Rebecca Lim, Sharon Ricardo and Chrishan Samuel participated in the collection, ana-

lysis and interpretation of the data; Simon Royce, Anna Tominaga and Chrishan Samuel drafted the manuscript.

## FUNDING

This work was supported by the Monash University Postgraduate Discovery Scholarships (to M.S. and K.R.); the Australia Postgraduate Scholarship (to B.M.H.); and the National Health & Medical Research Council (NHMRC) of Australia Senior Research Fellowship [grant number GNT1041766 (to C.S.S.)].

## REFERENCES

- 1 Levy, M.L., Fletcher, M., Price, D.B., Hausen, T., Halbert, R.J. and Yawn, B.P. (2006) International primary care respiratory group (IPCRG) guidelines: diagnosis of respiratory diseases in primary care. *Prim. Care Respir. J.* **15**, 20–34 [CrossRef PubMed](#)
- 2 Myers, T.R. and Tomasiolo, L. (2011) Asthma: 2015 and beyond. *Respir. Care* **56**, 1389–1407 [CrossRef PubMed](#)
- 3 To, T., Stanojevic, S., Moores, G., Gershon, A.S., Bateman, E.D., Cruz, A.A. and Boulet, L.P. (2012) Global asthma prevalence in adults: findings from the cross-sectional world health survey. *BMC Public Health* **12**, 204 [CrossRef PubMed](#)
- 4 Braman, S.S. (2006) The global burden of asthma. *Chest* **130**, 4S–12S [CrossRef PubMed](#)
- 5 Marceau, C., Lemi re, C., Berbiche, D., Perreault, S. and Blais, L. (2006) Persistence, adherence, and effectiveness of combination therapy among adult patients with asthma. *J. Allergy Clin. Immunol.* **118**, 574–581 [CrossRef PubMed](#)
- 6 Holgate, S.T. (2008) Pathogenesis of asthma. *Clin. Exp. Allergy* **38**, 872–897 [CrossRef PubMed](#)
- 7 Royce, S.G. and Tang, M.L. (2009) The effects of current therapies on airway remodeling in asthma and new possibilities for treatment and prevention. *Curr. Mol. Pharmacol.* **2**, 169–181 [CrossRef PubMed](#)
- 8 Ge, X., Bai, C., Yang, J., Lou, G., Li, Q. and Chen, R. (2013) Effect of mesenchymal stem cells on inhibiting airway remodeling and airway inflammation in chronic asthma. *J. Cell. Biochem.* **114**, 1595–1605 [CrossRef PubMed](#)
- 9 Baraniak, P.R. and McDevitt, T.C. (2010) Stem cell paracrine actions and tissue regeneration. *Regen. Med.* **5**, 121–143 [CrossRef PubMed](#)
- 10 Weiss, D.J. (2014) Current status of stem cells and regenerative medicine in lung biology and diseases. *Stem Cells* **32**, 16–25 [CrossRef PubMed](#)
- 11 Royce, S.G., Moodley, Y. and Samuel, C.S. (2014) Novel therapeutic strategies for lung disorders associated with airway remodelling and fibrosis. *Pharm. Therap.* **141**, 250–260 [CrossRef](#)
- 12 Sun, Y.-Q., Deng, M.-X., He, J., Zeng, Q.-X., Wen, W., Wong, D.S.H., Tse, H.-F., Xu, G., Lian, Q., Shi, J. and Fu, Q.-L. (2012) Human pluripotent stem cell-derived mesenchymal stem cells prevent allergic airway inflammation in mice. *Stem Cells* **30**, 2692–2699 [CrossRef PubMed](#)
- 13 Moodley, Y., Ilancheran, S., Samuel, C., Vaghjiani, V., Atienza, D., Williams, E.D., Jenkin, G., Wallace, E., Trounson, A. and Manuelpillai, U. (2010) Human amnion epithelial cell transplantation abrogates lung fibrosis and augments repair. *Am. J. Respir. Crit. Care Med.* **182**, 643–651 [CrossRef PubMed](#)
- 14 Dolgachev, V.A., Ullénbruch, M.R., Lukacs, N.W. and Phan, S.H. (2009) Role of stem cell factor and bone marrow-derived fibroblasts in airway remodeling. *Am. J. Pathol.* **174**, 390–400 [CrossRef](#)

**S.G. Royce and others**

- 15 Knight, D.A. and Rossi, F.M. (2010) Mesenchymal stem cells for repair of the airway epithelium in asthma. *Expert Rev. Respir. Med.* **4**, 747–758 [CrossRef](#) [PubMed](#)
- 16 Samuel, C.S., Cendrawan, S., Gao, X.M., Ming, Z., Zhao, C., Kiriazis, H., Xu, Q., Tregear, G.W., Bathgate, R.A. and Du, X.J. (2011) Relaxin remodels fibrotic healing following myocardial infarction. *Lab. Invest.* **91**, 675–690 [CrossRef](#) [PubMed](#)
- 17 Teerlink, J.R., Cotter, G., Davison, B.A., Felker, G.M., Filippatos, G., Greenberg, B.H., Ponikowski, P., Unemori, E., Voors, A.A., Adams, Jr, K.F. et al. (2013) Serelaxin, recombinant relaxin-2, for treatment of acute heart failure (RELAX-AHF): a randomised, placebo-controlled trial. *Lancet* **381**, 29–39 [CrossRef](#) [PubMed](#)
- 18 Samuel, C.S., Hewitson, T.D., Unemori, E.N. and Tang, M.L. (2007) Drugs of the future: the hormone relaxin. *Cell. Mol. Life Sci.* **64**, 1539–1557 [CrossRef](#) [PubMed](#)
- 19 Unemori, E.N., Pickford, L.B., Salles, A.L., Piercy, C.E., Grove, B.H., Erikson, M.E. and Amento, E.P. (1996) Relaxin induces an extracellular matrix-degrading phenotype in human lung fibroblasts *in vitro* and inhibits lung fibrosis in a murine model *in vivo*. *J. Clin. Invest.* **98**, 2739–2745 [CrossRef](#) [PubMed](#)
- 20 Kenyon, N.J., Ward, R.W. and Last, J.A. (2003) Airway fibrosis in a mouse model of airway inflammation. *Toxicol. Appl. Pharmacol.* **186**, 90–100 [CrossRef](#) [PubMed](#)
- 21 Tozzi, C.A., Poiani, G.J., McHugh, N. A., Shakarjian, M.P., Grove, B.H., Samuel, C.S., Unemori, E.N. and Riley, D.J. (2005) Recombinant human relaxin reduces hypoxic pulmonary hypertension in the rat. *Pulm. Pharm. Therap.* **18**, 346–353 [CrossRef](#)
- 22 Huang, X., Gai, Y., Yang, N., Lu, B., Samuel, C.S., Thannickal, V.J. and Zhou, Y. (2011) Relaxin regulates myofibroblast contractility and protects against lung fibrosis. *Am. J. Path.* **179**, 2751–2765 [CrossRef](#)
- 23 Royce, S.G., Miao, Y.R., Lee, M., Samuel, C.S., Tregear, G.W. and Tang, M.L. (2009) Relaxin reverses airway remodeling and airway dysfunction in allergic airways disease. *Endocrinology* **150**, 2692–2699 [CrossRef](#) [PubMed](#)
- 24 Royce, S.G., Lim, C.X., Patel, K.P., Wang, B., Samuel, C.S. and Tang, M.L. (2014) Intranasally administered serelaxin abrogates airway remodelling and attenuates airway hyperresponsiveness in allergic airways disease. *Clin. Exp. Allergy* **44**, 1399–1408 [CrossRef](#) [PubMed](#)
- 25 Huuskas, B.M., Wise, A.F., Cox, A.J., Lim, E.X., Payne, N.L., Kelly, D.J., Samuel, C.S. and Ricardo, S.D. (2015) Combination therapy of mesenchymal stem cells and serelaxin effectively attenuates renal fibrosis in obstructive nephropathy. *FASEB J.* **29**, 540–553 [CrossRef](#) [PubMed](#)
- 26 Royce, S.G., Shen, M., Patel, K.P., Huuskas, B.M., Ricardo, S.D. and Samuel, C.S. (2015) Mesenchymal stem cells and serelaxin synergistically abrogate established airway fibrosis in an experimental model of chronic allergic airways disease. *Stem Cell Res* **15**, 495–505 [CrossRef](#) [PubMed](#)
- 27 Akle, C.A., Adinolfi, M., Welsh, K.L., Leibowitz, S. and McColl, I. (1981) Immunogenicity of human amniotic epithelial cells after transplantation into volunteers. *Lancet* **2**, 1003–1005 [CrossRef](#) [PubMed](#)
- 28 Miki, T., Lehmann, T., Cai, H., Stolz, D.B. and Strom, S.C. (2005) Stem cell characteristics of amniotic epithelial cells. *Stem Cells* **23**, 1549–1559 [CrossRef](#) [PubMed](#)
- 29 Murphy, S., Lim, R., Dickinson, H., Acharya, R., Rosli, S., Jenkin, G. and Wallace, E. (2011) Human amnion epithelial cells prevent bleomycin-induced lung injury and preserve lung function. *Cell Transplant* **20**, 909–923 [CrossRef](#) [PubMed](#)
- 30 Vosdoganes, P., Wallace, E.M., Chan, S.T., Acharya, R., Moss, T.J. and Lim, R. (2013) Human amnion epithelial cells repair established lung injury. *Cell Transplant.* **22**, 1337–1349 [CrossRef](#) [PubMed](#)
- 31 Temelkovski, J., Hogan, S.P., Shepherd, D.P., Foster, P.S. and Kumar, R.K. (1998) An improved murine model of asthma: selective airway inflammation, epithelial lesions and increased methacholine responsiveness following chronic exposure to aerosolised allergen. *Thorax* **53**, 849–856 [CrossRef](#) [PubMed](#)
- 32 Wise, A.F., Williams, T.M., Kiewiet, M.B., Payne, N.L., Siatskas, C., Samuel, C.S. and Ricardo, S.D. (2014) Human mesenchymal stem cells alter macrophage phenotype and promote regeneration via homing to the kidney following ischemia-reperfusion injury. *Am. J. Physiol. Renal Physiol.* **306**, F1222–F1235 [CrossRef](#) [PubMed](#)
- 33 Murphy, S., Rosli, S., Acharya, R., Mathias, L., Lim, R., Wallace, E. and Jenkin, G. (2010) Amnion epithelial cell isolation and characterization for clinical use. *Curr. Prot. Stem Cell Biol.* [CrossRef](#)
- 34 Schneider, T., Osl, F., Friess, T., Stockinger, H. and Scheuer, W.V. (2002) Quantification of human Alu sequences by real-time PCR—an improved method to measure therapeutic efficacy of anti-metastatic drugs in human xenotransplants. *Clin. Exp. Metastasis* **19**, 571–582 [CrossRef](#) [PubMed](#)
- 35 Gallop, P.M. and Paz, M.A. (1975) Posttranslational protein modifications, with special attention to collagen and elastin. *Physiol. Rev.* **55**, 418–487 [PubMed](#)
- 36 Giordano, N., Volpi, N., Franci, D., Corallo, C., Fioravanti, A., Papakostas, P., Montella, A., Biagioli, M., Fimiani, M., Grasso, G. et al. (2012) Expression of RFXP1 in skin of scleroderma patients and control subjects. *Scand. J. Rheum.* **41**, 391–395 [CrossRef](#)
- 37 Chen, H., Wu, S., Lu, R., Zhang, Y.G., Zheng, Y. and Sun, J. (2014) Pulmonary permeability assessed by fluorescent-labeled dextran instilled intranasally into mice with LPS-induced acute lung injury. *PLoS One* **9**, e101925 [CrossRef](#) [PubMed](#)
- 38 Bani, D., Ballati, L., Masini, E., Bigazzi, M. and Sacchi, T.B. (1997) Relaxin counteracts asthma-like reaction induced by inhaled antigen in sensitized guinea pigs. *Endocrinology* **138**, 1909–1915 [PubMed](#)
- 39 Masini, E., Bani, D., Bigazzi, M., Mannaioni, P. F. and Bani-Sacchi, T. (1994) Effects of relaxin on mast cells. *In vitro* and *in vivo* studies in rats and guinea pigs. *J. Clin. Invest.* **94**, 1974–1980 [CrossRef](#) [PubMed](#)
- 40 Masini, E., Nistri, S., Vannacci, A., Bani Sacchi, T., Novelli, A. and Bani, D. (2004) Relaxin inhibits the activation of human neutrophils: involvement of the nitric oxide pathway. *Endocrinology* **145**, 1106–1112 [CrossRef](#) [PubMed](#)
- 41 Bani, D., Baronti, R., Vannacci, A., Bigazzi, M., Sacchi, T.B., Mannaioni, P.F. and Masini, E. (2002) Inhibitory effects of relaxin on human basophils activated by stimulation of the Fc epsilon receptor. The role of nitric oxide. *Int. Immunopharmacol.* **2**, 1195–1204 [CrossRef](#) [PubMed](#)
- 42 Hirota, N. and Martin, J.G. (2013) Mechanisms of airway remodeling. *Chest* **144**, 1026–1032 [CrossRef](#) [PubMed](#)
- 43 Hogg, J.C. (1997) The pathology of asthma. *APMIS* **105**, 735–745 [CrossRef](#) [PubMed](#)
- 44 Firinci, F., Karaman, M., Baran, Y., Bagriyanik, A., Ayyildiz, Z.A., Kiray, M., Kozanoglu, I., Yilmaz, O., Uzuner, N. and Karaman, O. (2011) Mesenchymal stem cells ameliorate the histopathological changes in a murine model of chronic asthma. *Int. Immunopharmacol.* **11**, 1120–1126 [CrossRef](#) [PubMed](#)
- 45 Patel, K.P., Giraud, A.S., Samuel, C.S. and Royce, S.G. (2016) Combining an epithelial repair factor and anti-fibrotic with a corticosteroid offers optimal treatment for allergic airways disease. *Br. J. Pharmacol.* **173**, 2016–2029 [CrossRef](#) [PubMed](#)

- 46 Bartemes, K.R. and Kita, H. (2012) Dynamic role of epithelium-derived cytokines in asthma. *Clin. Immunol.* **143**, 222–235 [CrossRef](#) [PubMed](#)
- 47 Linthout, S.V., Spillmann, F., Schultheiss, H.P. and Tschöpe, C. (2011) Effects of mesenchymal stromal cells on diabetic cardiomyopathy. *Curr. Pharmaceut. Des.* **17**, 3341–3347 [CrossRef](#)
- 48 Gillis, H.L. and Lutchen, K.R. (1999) Airway remodeling in asthma amplifies heterogeneities in smooth muscle shortening causing hyperresponsiveness. *J. Appl. Physiol.* **86**, 2001–2012 [CrossRef](#) [PubMed](#)
- 49 Weiss, D.J., Bertoncello, I., Borok, Z., Kim, C., Panoskaltzis-Mortari, A., Reynolds, S., Rojas, M., Stripp, B., Warburton, D. and Prockop, D.J. (2011) Stem cells and cell therapies in lung biology and lung diseases. *Proc. Am. Thorac. Soc.* **8**, 223–272 [CrossRef](#) [PubMed](#)
- 50 Weiss, D.J., Bertoncello, I., Borok, Z., Kim, C., Panoskaltzis-Mortari, A., Reynolds, S., Rojas, M., Stripp, B., Warburton, D. and Prockop, D.J. (2011) Stem cells and cell therapies in lung biology and lung diseases. *Proc. Am. Thorac. Soc.* **8**, 223–272 [CrossRef](#) [PubMed](#)
- 51 Weiss, D.J., Berberich, M.A., Borok, Z., Gail, D.B., Kolls, J.K., Penland, C. and Prockop, D.J. (2006) Adult stem cells, lung biology, and lung disease. NHLBI/Cystic Fibrosis Foundation Workshop. *Proc. Am. Thorac. Soc.* **3**, 193–207 [CrossRef](#)
- 52 Zhang, W.-G., He, L., Shi, X.-M., Wu, S.-S., Zhang, B., Mei, L., Xu, Y.-J., Zhang, Z.-X., Zhao, J.-P. and Zhang, H.-L. (2014) Regulation of transplanted mesenchymal stem cells by the lung progenitor niche in rats with chronic obstructive pulmonary disease. *Respir. Res.* **15**, 33 [CrossRef](#) [PubMed](#)
- 53 Moodley, Y., Vaghjiani, V., Chan, J., Baltic, S., Ryan, M., Tchongue, J., Samuel, C.S., Murthi, P., Parolini, O. and Manuelpillai, U. (2013) Anti-inflammatory effects of adult stem cells in sustained lung injury: a comparative study. *PLoS One* **8**, e69299 [CrossRef](#) [PubMed](#)
- 54 Ober, C. and Hoffjan, S. (2006) Asthma genetics 2006: the long and winding road to gene discovery. *Genes Immun.* **7**, 95–100 [CrossRef](#) [PubMed](#)
- 55 Kariyawasam, H.H., Aizen, M., Barkans, J., Robinson, D.S. and Kay, A.B. (2007) Remodeling and airway hyperresponsiveness but not cellular inflammation persist after allergen challenge in asthma. *Am. J. Respir. Crit. Care Med.* **175**, 896–904 [CrossRef](#) [PubMed](#)
- 56 Boulet, L.P., Laviolette, M., Turcotte, H., Cartier, A., Dugas, M., Malo, J.L. and Boutet, M. (1997) Bronchial subepithelial fibrosis correlates with airway responsiveness to methacholine. *Chest* **112**, 45–52 [CrossRef](#) [PubMed](#)
- 57 Holgate, S.T., Holloway, J., Wilson, S., Bucchieri, F., Puddicombe, S. and Davies, D.E. (2004) Epithelial-mesenchymal communication in the pathogenesis of chronic asthma. *Proc. Am. Thorac. Soc.* **1**, 93–98 [CrossRef](#) [PubMed](#)
- 58 Ward, C., Johns, D.P., Bish, R., Pais, M., Reid, D.W., Ingram, C., Feltis, B. and Walters, E.H. (2001) Reduced airway distensibility, fixed airflow limitation, and airway wall remodeling in asthma. *Am. J. Respir. Crit. Care Med.* **164**, 1718–1721 [CrossRef](#) [PubMed](#)
- 59 Milanese, M., Crimi, E., Scordamaglia, A., Riccio, A., Pellegrino, R., Canonica, G.W. and Brusasco, V. (2001) On the functional consequences of bronchial basement membrane thickening. *J. Appl. Physiol.* **91**, 1035–1040 [PubMed](#)

Received 9 May 2016/24 August 2016; accepted 12 September 2016

Accepted Manuscript online 19 September 2016, doi: 10.1042/CS20160328